# รายงานวิจัยฉบับสมบูรณ์

## โครงการ การยับยั้งระบบต้านออกซิเดชันและป้องกันตัวในเซลล์เป็นยุทธวิธีการเพิ่มการตอบสนองยาเคมีบำบัดในมะเร็งท่อน้ำดี

## Interference of antioxidant and cytoprotective defense system in cholangiocarcinoma as the mean for enhancing chemotherapeutic drug response

โดย รองศาสตราจารย์ ดร. วีรพล คู่คงวิริยพันธุ์ และคณะ

โครงการวิจัยทุนวิจัยองค์ความรู้ใหม่ที่เป็นพื้นฐานต่อการพัฒนา

โครงการเลขที่ **BRG5480011**

ประจำปี **2554**

รายงาน มิถุนายน **2557**

สัญญาเลขที่ BRG5480011

# รายงานวิจัยฉบับสมบูรณ์

## โครงการ การยับยั้งระบบต้านออกซิเดชันและป้องกันตัวในเซลล์เป็นยุทธวิธีการเพิ่มการตอบสนองยาเคมีบำบัดในมะเร็งท่อน้ำดี

## Interference of antioxidant and cytoprotective defense system in cholangiocarcinoma as the mean for enhancing chemotherapeutic drug response


**คณะผู้วิจัย**

| | |
|---|---|
| **1. รองศาสตราจารย์ ดร. วีรพล คู่คงวิริยพันธุ์** | **ภาควิชาเภสัชวิทยา คณะแพทยศาสตร์ มหาวิทยาลัยขอนแก่น** |
| **2. ผู้ช่วยศาสตราจารย์ ดร. เอื้อมเดือน ประวาศ** | **ภาควิชาเภสัชวิทยา คณะแพทยศาสตร์ มหาวิทยาลัยขอนแก่น** |
| **3. ผู้ช่วยศาสตราจารย์ ดร.ลัดดาวัลย์ เส็งกันไพร** | **ภาควิชาเภสัชวิทยา คณะแพทยศาสตร์ มหาวิทยาลัยขอนแก่น** |
| **4. รองศาสตราจารย์ ดร. บรรจบ ศรีภา** | **ภาควิชาพยาธิวิทยา คณะแพทยศาสตร์ มหาวิทยาลัยขอนแก่น** |
| **5. ผู้ช่วยศาสตราจารย์ นพ.อนุชา พัวไพโรจน์** | **ภาควิชาพยาธิวิทยา คณะแพทยศาสตร์ มหาวิทยาลัยขอนแก่น** |



**สนับสนุนโดยสำนักงานกองทุนสนับสนุนการวิจัย**

**(ความเห็นในรายงานเป็นของผู้วิจัย สกว.ไม่จำเป็นต้องเห็นด้วยเสมอไป)**

# บทคัดย่อ

## โครงการ การยับยั้งระบบต้านออกซิเดชันและป้องกันตัวในเซลล์เป็นยุทธวิธีการเพิ่มการตอบสนองยาเคมีบำบัดในมะเร็งท่อน้ำดี


มะเร็งท่อน้ำดี (CCA) เป็นมะเร็งที่ร้ายแรงมากชนิดหนึ่งเนื่องจากผู้ป่วยมักไม่มีอาการแสดงปรากฏจนถึงระยะสุดท้ายทำให้การวินิจฉัยทำได้ยากลำบากมาก พยากรณ์โรคของมะเร็งชนิดนี้เลวร้ายมาก ความพยายามพัฒนาการรักษาที่ผ่านมาหลายสิบปีมีผลเปลี่ยนแปลงการอยู่รอดเพียงเล็กน้อย เนื่องจากผู้ป่วยส่วนใหญ่อยู่ในระยะสุดท้ายของโรค การรักษาที่เป็นไปได้จึงเหลือวิธีเคมีบำบัดและรังสีรักษา แต่การรักษาดังกล่าวยังไม่มีประสิทธิภาพ การศึกษาครั้งนี้จึงมีวัตถุประสงค์เพื่อหาข้อมูลสนับสนุนยุทธวิธีใหม่ในการรักษาเพื่อเพิ่มประสิทธิภาพของยาเคมีและรังสีรักษาโดยการยับยั้งการทำงานของเอนไซม์ต้านออกซิเดชัน/เอนไซม์ป้องกันตัว หรือการเพิ่มออกซิเดชันภายในเซลล์มะเร็ง

การศึกษาพบว่าการยับยั้งเอนไซม์ heme oxygenase-1 (HO-1) หรือ NADPH quinone-oxidoreductase-1 (NQO1) ทำให้เพิ่มภาวะออกซิเดชันภายในเซลล์และกระตุ้นให้เซลล์มะเร็งว่องไวต่อยาเคมีบำบัดมากยิ่งขึ้น การศึกษาได้ยืนยันด้วยการยับยั้ง HO-1 และ NQO1 ด้วยเทคนิค RNAi การยับยั้ง HO-1 ยังมีผลกระตุ้นให้มะเร็งไวต่อรังสีแกมมาโดยทำให้ความสามารถของ colony forming ลดลง ยับยั้งวัฏจักรเซลล์ที่ G2-M phase การใช้สารเคมียับยั้ง HO-1 ด้วย Zn-protoporophyrin (ZnPP) ร่วมกับยาเคมี gemcitabine (GEM) ชักนำให้สร้างอนุมูลอิสระออกซิเจนและมีผลยับยั้งการเติบโตของเซลล์ การศึกษาได้พิสูจน์ต่อในหนูทดลองที่รับการปลูกถ่ายมะเร็งท่อน้ำดี หนูที่ได้รับ ZnPP ร่วมกับ Gem มีก้อนมะเร็งที่เกือบหยุดการเติบโตโดยสิ้นเชิงเมื่อเปรียบเทียบกับการได้รับยาเดียว ๆที่ไม่มีผลเทียบเท่า ฤทธิ์ดังกล่าวสัมพันธ์กับฤทธิ์ยับยั้งการแบ่งเซลล์ การสร้างหลอดเลือดและการกระตุ้น p53 นอกจากนี้บทบาทของ NQO1 ในผู้ป่วยมะเร็งท่อน้ำดีได้รับการวิเคราะห์และพบว่าระดับการแสดงของ NQO1 ในเนื้อเยื่อมะเร็งสามารถพยากรณ์โรคได้ดี โดยที่ผู้ป่วยที่มีระดับการแสดงออกของ NQO สูงจะมีพยากรณ์โรคไม่ดี มีระยะการรอดชีพสั้น การศึกษาเกี่ยวกับสาร phenethyl isothiocyanate (PEITC) สารธรรมชาติในตระกูลกะหล่ำที่ทราบดีว่ามีฤทธิ์กระตุ้นเพิ่มภาวะออกซิเดชันภายในเซลล์ พบว่ามีฤทธิ์แรงมากสามารถฆ่าเซลล์มะเร็งท่อน้ำดีได้หลายชนิด ผลของ PEITC ต่อภาวะรีดอกซ์ภายในเซลล์มีหลายกลไกที่แตกต่างกันขึ้นกับชนิดของเซลล์มะเร็งซึ่งในที่สุดชักนำทำให้เซลล์ถูกทำลายผ่านวิถีของไมโตคอนเดรีย ดังนั้น PEITC จึงเป็นสารที่ได้ผลดี สามารถต่อต้านมะเร็งหลากหลายชนิดที่ดื้อยาได้

การศึกษาแสดงให้เห็นว่าแนวคิดการเพิ่มการตอบสนองการรักษาด้วยยาเคมี/รังสีรักษาสามารถเป็นไปได้ด้วยการยับยั้งระบบต้านออกซิเดชัน/ป้องกันตัว การยับยั้งเอนไซม์ HO-1 มีผลเพิ่มการตอบสนองต่อยาเคมีบำบัดและรังสีรักษาและในทำนองเดียวกับการยับยั้ง NQO1 ที่อาจมีผลเช่นกันจึงเป็นยุทธวิธีที่มีค่าควรแก่การศึกษาต่อไปเพื่อการรักษามะเร็งท่อน้ำดีที่ได้ผล



Keywords: cholangiocarcinoma, antioxidant, heme oxygenase-1, NQO1, phenethyl isothiocyanate, redox, mitochondrial death pathway

## Abstract

### Interference of antioxidant and cytoprotective defense system in cholangiocarcinoma as the mean for enhancing chemotherapeutic drug response

Cholangiocarcinoma (CCA) is one of the most devastating malignancies because the majority of cases develop without clinical symptoms, and thus making the diagnosis of CCA very difficult. Prognosis of CCA is extremely poor because treatment outcomes and survival of the patients have only slightly improved in the past several decades. Because most of patients are already in the advanced stage of the disease at diagnosis, chemotherapy and radiotherapy may be the options left for most patients. However, no effective chemotherapy is known for CCA. The study was to provide evidence น to support a new strategy for enhancing cancer cell killing by mean of inhibition of antioxidant/cytoprotective enzymes and increase of cellular oxidants in cancer cells.

The study reviewed that inhibition of heme oxygenase-1 (HO-1) or NADPH quinone-oxidoreductase-1 (NQO1) resulted increased cellular oxidant and conferred a strong sensitizing effect to CCA cells in response to chemotherapeutic agents. The study was verified by knockdown of HO-1 or NQO1 gene expression. Inhibition of HO-1 also sensitized CCA cells to gamma radiation, where colony forming ability was impaired and cell cycle was arrested at G2-M phase. The antiproliferation of Zn-protoporophyrin (ZnPP), a potent HO-1 inhibitor, in combination with gemcitabine (Gem) was causally associated with oxygen radical formation. The study was validated in nude mice xenografted with CCA cells. Treatment with ZnPP, in combination with (Gem) almost completely arrested the tumor growth, while single treatment did not. The effect was associated with suppression of tumor cell proliferation and angiogenesis, and with activation of p53. Moreover, the role of NQO1 in CCA patients was investigated and showed to be a good prognostic biomarker. As the level of NQO1 mRNA expression was inversely correlated with patient survival, the higher NQO1 expression, the shorter survival time found in the patients. The study of phenethyl isothiocyanate (PEITC), a phytochemical known for its inducer of cellular oxidants found in cruciferous vegetables, was shown that it potently inhibited growth of several CCA cells and induced apoptotic cell death. The effects of PEITC on the cellular redox are mediated via different ways in different CCA cells leading to cell killing through the mitochondrial pathway. The multiple effects of PEITC may be beneficial in overcoming the drug resistant cancer cells.

The study demonstrated a proof of concept of approach to enhanced chemo/radiotherapy response by interference with antioxidant/ cytoprotective system of the cancer. Our studies indicated the synergistic effect of HO-1 inhibition in chemotherapy and radiotherapy and it may be true for NQO1 inhibition. This worthy strategy warrants further investigation in the treatment of CCA.



Keywords: cholangiocarcinoma, antioxidant, heme oxygenase-1, NQO1, phenethyl isothiocyanate, redox, mitochondrial death pathway

# สารบัญ

**โครงการเลขที่ BRG5480011**

**ระยะเวลาโครงการ มิถุนายน 2554 –มิถุนายน 2557 งบประมาณโครงการ 1,500,000 บาท**

## 1. Executive Summary

Biliary tract cancer or cholangiocarcinoma (CCA) is the most fatal cancer and considered the important health burden in Thai people, as it is highly prevalent in northeastern Thailand and neighboring countries. Complete surgical resection of CCA tumor is the treatment of choice. However, most patients have advanced disease at presentation and no effective chemotherapy is known for CCA. The development of innovative approach for the treatment of CCA may be very important to improve survival and quality of life. Cancer cells are characterized by metabolic alteration with high oxidative status where its result drives cancer cells to growth and proliferation. This study was to prove a hypothesis of enhanced susceptibility of CCA to cancer therapy through manipulating cancer oxidative status. The strategy involves with inhibition of antioxidant/ cytoprotective enzymes, i.e. heme oxygenase-1 (HO-1) and NADPH quinone-oxidoreductase-1 (NQO1) to increase oxidative status, thereby rendering CCA cells to be susceptible to chemotherapeutic agent. Another strategy involved with treatment with agents, like phenethylisothiocyanate (PEITC) to induce oxidative stress in cancer cells which are already in high oxidative status resulting in cancer cell killing.

The study found that inhibition of HO-1 or NQO1 conferred a strong sensitizing effect to CCA cells in response to chemotherapeutic agents. The inhibition of the enzymes were performed by pharmacological inhibitors and validated by silencing HO-1 and NQO1 gene expression. Inhibition of HO-1 also sensitized CCA cells to gamma radiation, where colony forming ability was impaired and cell cycle was arrested at G2-M phase. The antiproliferation of Zn-protoporophyrin (ZnPP), a potent HO-1 inhibitor, in combination with gemcitabine (Gem) was causally associated with oxygen radical formation. The study was validated in nude mice xenografted with CCA cells. Treatment with ZnPP, in combination with (Gem) almost completely arrested the tumor growth, while single treatment did not. The effect was associated with suppression of tumor cell proliferation, angiogenesis, and activation of p53. Moreover, the role of NQO1 in CCA patients was investigated and showed to be a good prognostic biomarker, as the level of NQO1 mRNA expression was inversely correlated with patient survival, the higher NQO1 expression, the shorter survival time found in the patients. The study of PEITC, a phytochemical widely found in cruciferous vegetables, was shown that it potently inhibited growth of several CCA cells and induced apoptotic cell death. The effects of PEITC on the cellular redox are mediated via different ways in different CCA cells leading to cell killing through the mitochondrial pathway. The multiple effects of PEITC may be beneficial in overcoming the drug resistant cancer cells.

The study demonstrated a proof of concept of approach to enhanced chemo/radiotherapy response by interference with antioxidant/ cytoprotective system of the cancer. Our studies indicated the synergistic effect of HO-1 inhibition in chemotherapy and radiotherapy and it may be true for NQO1 inhibition. This worthy strategy warrants further investigation in the treatment of CCA.

Interference of antioxidant and cytoprotective defense system in cholangiocarcinoma as the mean for enhancing chemotherapeutic drug response

## Objectives

The study was to prove of concept that antioxidant and cytoprotective enzymes are essential for cholangiocarcinoma (CCA) cells in growth, proliferation and susceptible to cancer therapy, whereas suppression of these enzymes would render the cells to the sensitivity to chemotherapy and radiotherapy. Moreover, an induction of increase in cellular oxidants will drive cancer cells to redox stress and eventual cell death.

### Specific objectives

1. To investigate the critical roles of enzyme hemoxygenase-1 (HO-1) in proliferation, migration and cytoprotection against chemotherapy and radiotherapy

2. To evaluate whether inhibition of HO-1 could sensitize CCA cells to the sensitivity of chemotherapy and gamma radiation using HO-1 siRNA and pharmacological inhibitor

3. To verify that the increased sensitivity in *in vitro* by inhibiting HO-1 could be translated to animal model xenografted with cancer cells

4. To examine the role of NADPH quinone oxidoreductase-1 (NQO1), an antioxidant and xenobiotic metabolizing enzyme, in modulation of susceptibility of CCA to chemotherapeutic agents

5. To analyze the role of NQO1 as a possible prognostic biomarker of cholangiocarcinoma patients

6. To investigate the chemopreventive activity of phenethyl isothiocyanate (PEITC) in modulation of cellular oxidants and induction of cancer cell death

7. To evaluate mechanisms of PEITC in inhibition of various CCA cells in relation to cellular redox stress and mitochondrial cell death pathway

## Results

The study was organized into 5 sections in accordance with the objectives. The section 1 and 2 presented the study of HO-1 *in vitro* and *in vivo,* demonstrating the critical role of HO-1 in sensitivity to chemotherapeutic agents and elucidating the mechanism underlying the sensitizing effect. The study extended to gamma radiation where inhibition of HO-1 sensitized cancer cells to gamma irradiation in suppression of cell growth, invasion and cell cycle progression. The inhibition of HO-1 also showed to potentiated gemcitabine in suppression of tumor growth in xenografted mice. The section 3 demonstrated that expression of NQO1 in tumor tissue could be a prognostic biomarker in CCA patients where the high NQO1 expression was associated with poor prognosis. The last two sections (section 4 and 5) presented the study of PEITC which it showed the potent anticancer activity with different mechanisms in different CCA cells. PEITC induced cell death in either glutathione redox dependent and independent pathways in KKU-100 and M214 cells where activation of mitochondrial cell death signaling may be the common pathway in induction of cell death.

# Section 1

## Crucial Role of Heme Oxygenase-1 on the Sensitivity of Cholangiocarcinoma Cells to Chemotherapeutic Agents

### Introduction

Cholangiocarcinoma (CCA) is a malignant tumor of the bile duct, which originates from the bile duct epithelial cells (cholangiocytes). CCA is a devastating malignancy with poor prognosis. CCA is a rare type of cancer worldwide, however populations residing in the Southeast Asian region are at very high risk. The important risk factors are liver fluke infection and possible involvement from chronic infection with hepatitis B and C viruses [1,2]. Early diagnosis and extensive surgery offers the only chance for prolonged life. Unfortunately, most patients are diagnosed at the advanced stage of disease and current biomarkers are of limited value [3,4]. Chemotherapy is a remaining option. However, current chemotherapy has not been shown to substantially improve survival in patients with unresected CCA [3,5]. Many chemotherapeutic drugs as well as targeted chemotherapeutic agents have been tested as single agents or in combinations. Nevertheless, drug resistance or drug inefficacy remain major obstacles in the treatment of CCA [6]. It is apparent that a new strategy of chemotherapeutic treatment is urgently needed in management of the unresectable CCA.

Heme oxygenase-1 (HO-1) is one of the powerful cytoprotective enzymes. HO-1 plays critical roles in physiological iron homeostasis, antioxidant defense, anti-inflammatory and anti-apoptotic effect[7]. It is induced by various stimuli such as hypoxia, UV-radiation, heavy metals, chemotherapeutic drugs and oxidative stress [8,9]. HO-1 catalyzes the first and rate-limiting step in the degradation of heme to biliverdin, carbonmonoxide (CO) and ferrous iron. Biliverdin is further converted to bilirubin by biliverdin reductase. Biliverdin and bilirubin are the most potent endogenous reactive oxygen species (ROS) scavengers [7]. CO is also an efficient anti-inflammatory mediator in several models of inflammation and tissue injury [10,11]. The increased expression of HO-1 has been observed in several cancers including brain tumor, melanoma, chronic myeloid leukemia, and lymphosarcoma [12], suggesting possible contribution of HO-1 to tumor progression through promotion of angiogenesis, metastases and pro-proliferation [13]. HO-1 expression may contribute to resistance to chemotherapeutic agents such as cisplatin, doxorubicin and gemcitabine in some human cancers [9,14,15]. Thus, some studies revealed that suppression of HO-1 activity or HO-1 knockdown by siRNA increased the chemosensitivity of AML cells, pancreatic and lung cancer cells [9,14,16], but was not effective in other cancer cells [17]. The inhibition of HO-1 by zinc protoporphyrin IX (ZnPP) induced apoptotic cell death and this may be associated with the increase in ROS production. Similarly, HO-1 gene silencing by specific siRNA also induced ROS generation [17]. However, the exact mechanism of the sensitizing effect to chemotherapeutic agents confered by suppression of HO-1 is largely unknown. Mitochondria may be a primary target of HO-1 inhibition, as ZnPP and triiodothyronine induced the opening of the mitochondrial permeability transition (MPT) pore leading to liver injury [18].

In the present study, we investigated whether HO-1 in CCA cells plays a critical role in cytoprotection against chemotherapeutic agents. The results show that inhibition of HO-1 induced the sensitization of CCA cells to gemcitabine (Gem) and doxorubicin (Dox). Inhibition of HO-1 could be a strategy to enhance the response of CCA to chemotherapeutic drugs.

## Materials and methods

### Cell lines and cell cultures.

The human cholangiocarcinoma (CCA) cell lines; KKU-100 and KKU-M214 used in this study were kindly provided by Dr. Banchob Sripa of Department of Pathology, Faculty of Medicine, Khon Kaen University. Both cell lines were cultured in complete media consisting of Ham's F12 media, supplemented with 10% fetal calf serum, 12.5 mM HEPES, pH 7.3, 100 U/ml penicillin G and 100 µg/ml gentamicin. The cells were subcultured every 3 days using 0.25% trypsin-EDTA and the medium was renewed after an overnight incubation. The cultured cells were changed to incubate in serum-free defined Ham's F12 medium immediately before further treatment.

### Cytotoxicity assay.

Cytotoxicity was determined by fluorescent staining using acridine orange and ethidium bromide (AO/EB) as described previously [19]. KKU-100 (7,500 cells/well) and KKU-M214 (5,000 cells/well) cells were cultured in 96 well-plate and allowed to attach overnight. On the next day, the medium was removed and gemcitabine (Gemzar®, Eli Lilly, IN, USA: Gem) dissolved in phosphate-buffered saline (PBS: 137 mM NaCl, 2.7 mM KCl, 10 mM $Na_2HPO_4$, 2 mM $KH_2PO_4$, pH 7.4), doxorubicin HCl (Boryung Pharm, Seoul, South Korea: Dox) dissolved in DMSO (100 mM) and further diluted with PBS, 4-hydroxy-2,2,6,6-tetramethylpiperidine-1-oxyl (Tempol), dissolved in PBS, zinc protoporphyrin IX (ZnPP; HO-1 inhibitor), dissolved in DMSO (50 mM) and further diluted with PBS or stannous chloride ($SnCl_2$; HO-1 inducer) dissolved in PBS, or combinations of them were added to the media culture to final concentrations as indicated in results section and incubated for a designated period of time. Then, cells were washed once with PBS and stained with AO/EB. The cells were examined using a Nikon Eclipse TS100 inverted microscope with excitation and long–pass emission filters of 480 and 535 nm, respectively. The fluorescent images were taken at predetermined areas with a Nikon Coolpix digital camera. The numbers of viable, apoptotic and necrotic cells which were stained with green fluorescence, bright orange fluorescence and green fluorescence with appearance of cell shrinkage, condensation and fragmentation of the nuclei, respectively, were enumerated. The cytotoxicity value was calculated as = (number of viable cells in treatment wells)/ (number of viable cells in control cells) × 100.

### HO-1 small interfering RNA transfection.

The transfection of HO-1 siRNA was performed using siGENOME SMARTpool (M-006372-02-0005: Dharmacon, CO, USA) at a final concentration of 200 nM and lipofectamine 2000 (Invitrogen, CA, USA) according to the manufacturers' instructions. HO-1 expression was specifically suppressed by introduction of siRNA against human HMOX1 (Gene Id: 3162). - In brief, cells were grown in a 6-well plate to reach a confluence of 70%. For each well, 100 pmoles of HO-1 siRNA were mixed with 2 µL of lipofectamine 2000 and 500 µL of serum- and antibiotic-free Ham's F12 medium was added. Cells were exposed to the transfection mixture for 6 h. At the end of incubation period, 1.5 mL of antibiotic-free Ham's F12 complete medium was added and the cells were cultured for an additional 18 h. The siGENOME non-targeting siRNA (D-001210-02-05: Dharmacon), as a negative control was introduced to the cells using the same protocol. Total RNA and protein were extracted from cells 24 h after transfection using previously described methods [20,21]. Efficiency of the transient transfection was determined by real-time polymerase chain reaction (PCR) using specific primers and Western blotting.

Cytotoxicity of Gem to HO-1 knock-down CCA cells was performed. KKU-100 cells (7,500 Cells/well) were grown in 96-well plate to reach the confluence of 70%. For each well, cells were transfected with 3 ρmoles of HO-1 siRNA reagent mixed with 0.06 μL of lipofectamine 2000 in serum- and antibiotic-free Ham's F12 medium. Cells were kept in the transfection mixture for 6 h. Then, 100 μL of antibiotic-free Ham's F12 complete medium was added and the cells were kept for an additional 18 hours. Then, cells were treated with varied concentrations of Gem for further 24 h and cytotoxicity assay was performed as described as above.

**Real-time polymerase chain reaction**.

KKU-100 and KKU-M214 cells were seeded at the density of $1.5x10^5$ cells/well in 6 well-plates and allowed to growth for 24 h. Total RNA was isolated using a previously described method [20]. Total RNA (1 μg) was then reverse transcribed to single-stranded cDNA by the ImProm-II™ reverse transcription system (Promega, WI, USA) at conditions of 42ºC for 60 min. The reverse transcription products served as a template for real-time PCR. The primer sequences were as follows: HO-1: forward, 5'-CTG ACC CAT GAC ACC AAG GAC-3' and HO-1 reverse: 5'-AAA GCC CTA CAG CAA CTG TCG-3', β-actin: forward 5'-AGT GTA GCC CAG GAT GCC CTT-3' and β-actin: reverse, 5'-GCC AAG GTC ATC CAT GAC AAC-3'. The PCR was performed in a final volume of 15 μL containing cDNA template, 5 μM of each HO-1 primer or 2.5 μM of each β-actin primer in SsoFast™ EvaGreen Supermix with low Rox (Bio-Rad, CA, USA). After an initial denaturation step at 95°C for 10 min, 40 cycles for HO-1 and β-actin were performed as follows: denaturating for 15 sec at 95°C, annealing for 30 sec at 55°C and extension for 45 sec at 72°C. To verify the purity of the products, a melting curve analysis was performed after each run. To quantify the relative expression of genes, the relative quantitation using standard curve method was used. The amount of HO-1 mRNA was expressed as a ratio to β-actin mRNA.

**Western blot analysis.**

Western blot analysis was used to determine the expression levels of HO-1, $p21^{Cip/WAF1}$, cytochrome C, and β-actin. KKU-100 ($7.5x10^5$) and KKU-M214 ($6x10^5$) cells were cultured in 100 $mm^3$ dishes and treated with drug or drug combinations. The cultured cells were washed with PBS, lysed with RIPA buffer [150 mM NaCl, 1% NP-40, 0.5% sodium deoxycholate, 0.1% SDS, 50mM Tris–HCl (pH 7.4), 50 mM glycerophosphate, 20 mM NaF, 20 mM EGTA, 1 mM DTT, 1 mM $Na_3VO_4$ and protease inhibitor cocktail (M221: Amresco, OH, USA) at 4◦ C for 15 min and transferred into a microtube. After vigorous vortex mixing, the suspension was centrifuged at 12,000×g for 20 min and supernatant was collected and stored at −70◦C until use. The protein samples were mixed with SDS loading buffer and subjected to separation by electrophoresis in 8-10% SDS-polyacrylamide gel. The bands were blotted onto a PVDF membrane. The membranes were blocked for 1 h at room temperature with 5% (w/v) skimmed milk powder in Tris buffered saline (TBS) containing 0.1% Tween-20. The PVDF membrane was incubated overnight at 4°C with primary antibodies of rabbit polyclonal anti-human HO-1 (1:1000) (ADI-SPA-895: Enzo Life Sciences, Switzerland), rabbit monoclonal anti-human $p21^{Cip/WAF1}$ (1:500) (#2947: Cell Signaling Technology, MA, USA), mouse monoclonal anti-human cytochrome c (1:1000) (sc-13560) and horseradish peroxidase (HRP)-goat polyclonal anti-human β-actin (1:2500) (sc-1616 HRP) in TBS. After washing with TBS the blots were incubated for 1 h at room temperature with the HRP-conjugated secondary antibodies (anti-rabbit IgG-HRP sc-2004, anti-mouse IgG-HRP sc-2005, anti-goat IgG-HRP sc-2354). After removal of the secondary antibody and TBS buffer washes, the blots were incubated in ECL substrate solution (SuperSignal West Pico Chemiluminescent Substrate: Thermoscientific, IL, USA). The densities of the specific protein bands were visualized and captured by ImageQuant™ 400.

**Measurement of intracellular ROS accumulation.**

To monitor the intracellular accumulation of ROS, the lucigenin-enhanced chemiluminescence method was used for detecting superoxide anion according to the previously described method [20]. Briefly, KKU-100 cells were cultured in 35-mm dishes overnight. After treatment with compounds for 3 h, cultured cells were rinsed, incubated in PBS containing lucigenin and measured for luminescent signal in a 20/20n Luminometer (Turner Biosystem, CA, USA).

**Measurement of mitochondrial transmembrane potential.**

To analyze the mitochondrial transmembrane potential ($\Delta\psi_m$), the lipophilic cationic fluorescent probe; JC-1 (Cayman Chemical, MI, USA) was used as previously described [21]. KKU-100 cells were seeded in a 96-well plate for an overnight before treatment with compounds for 6 or 24 h. Cultured cells in the plate were centrifuged at 1,500 rpm 25◦ C for 5 min and were loaded with JC-1 dye for 30 min at 37◦C. Then, cultured cells were rinsed, incubated in JC-1 assay buffer and $\Delta\psi_m$ was analysed in a fluorescent microscope. JC-1 forms J-aggregates in cells with healthy mitochondria, which can be detected with fluorescent settings of excitation and emission wavelengths at 560 and 595 nm, respectively. Cells with depolarized mitochondria, JC-1 existed as J monomers can be detected with excitation and emission wavelengths at 485 and 535 nm, respectively. The change of the orange fluorescence in healthy cultured cells to green fluorescence is an indicative of depolarization of $\Delta\psi_m$.

**Statistical analysis.**

Data are expressed as mean ± SEM of three separated experiments. An analysis of variance was used to determine significant differences between each experimental group. The level of significance was set at $P < 0.05$.

**Results**

**Basal HO-1 expression and inducible expression by anticancer agents**

The two cholangiocarcinoma cells, KKU-100 and KKU-M214, were used to determine the basal expression levels of HO-1. The mRNA and protein expressions of HO-1 were determined by real-time PCR and Western blot analysis. At basal condition, KKU-100 showed the higher HO-1 mRNA and protein levels than KKU-M214 cells (Fig. 1A-B). To examine whether anticancer agent could induce HO-1 in CCA cells, two lines of cells were incubated with 1 μM of Gem and the time-course of HO-1 protein expression was examined. Both KKU-100 and KKU-M214 cells treated with Gem showed a rapid increased HO-1 protein expression within 3 h when compared with concurrent controls and returned to control level by 24 h (Fig. 2).

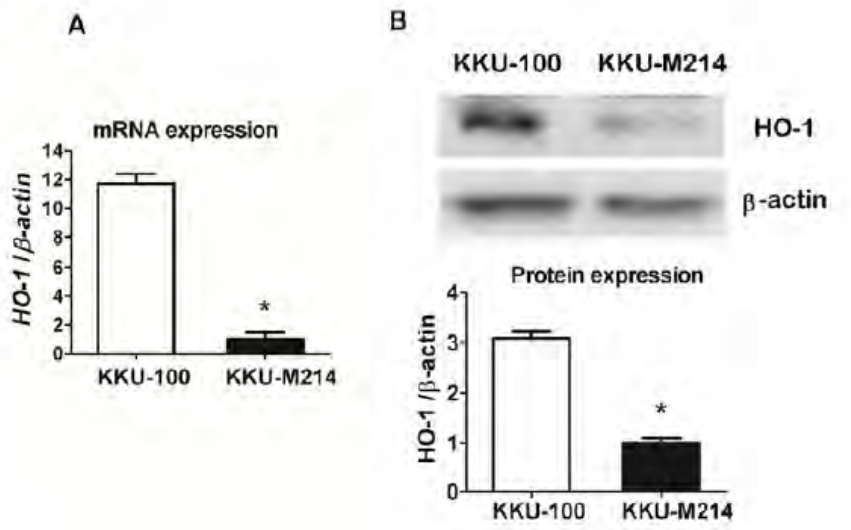


**Figure 1 HO-1 mRNA and protein expressions in CCA cells**. **(A)** The basal mRNA expression of HO-1 in CCA cells; KKU-100 and KKU-M214 cells. Total RNA of cells were collected and analysed by real-time RT-PCR. The bars represent relative expression of HO-1 normalized with β -actin. The expression of HO-1 in KKU-100 cells is much higher than that of KKU-M214 cells, $p<0.05$. **(B)** The basal protein expression of HO-1 in KKU-100 and KKU-M214 cells. Total cell lysates were prepared and subjected to Western blot analysis using β-actin as a loading control. Image samples of HO-1 and β -actin are shown in the top panel of the figure. HO-1 protein in KKU-100 cells is relatively higher than that of KKU-M214 cells. The bars represent mean±SEM, each from three separated experiments. *, $p<0.05$ vs KKU-100 group.

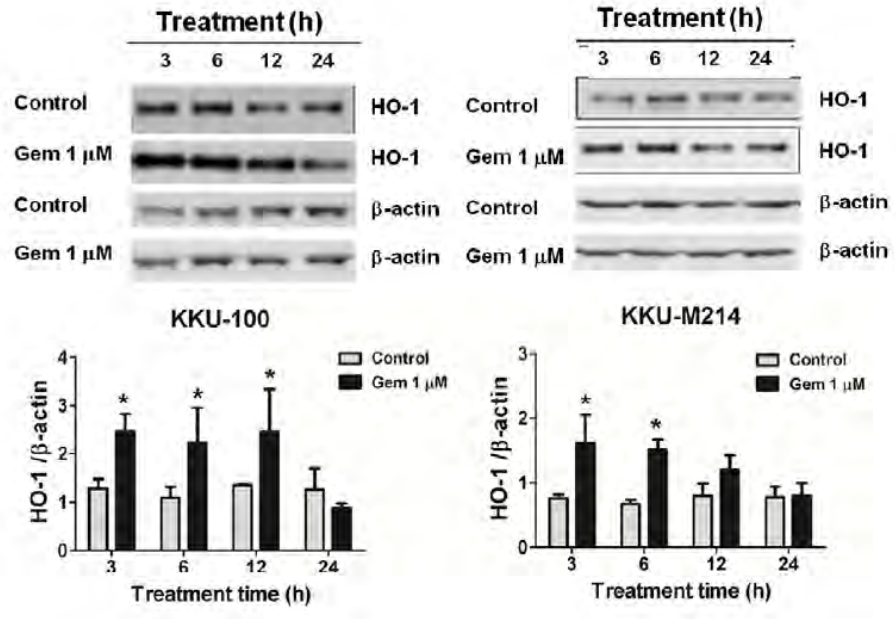


**Figure 2 Time-course of HO-1 protein induction by Gem.** (**A**) KKU-100 cells and (**B**) KKU-M214 cells were cultured for overnight and exposed to Gem (1 μM) for 3, 6, 12 and 24 h. The cultured cells exposed to vehicle only were performed as concurrent control groups. Total cell lysates were collected at the indicated time points and subjected to Western blot analysis using β-actin as a loading control. The relative expression of HO-1 was normalized with β actin. The bars show the HO-1 expression in Gem-treated group and concurrent control group. The bars represent mean±SEM, each from three separated experiments. *,$p<0.05$ vs concurrent controls.

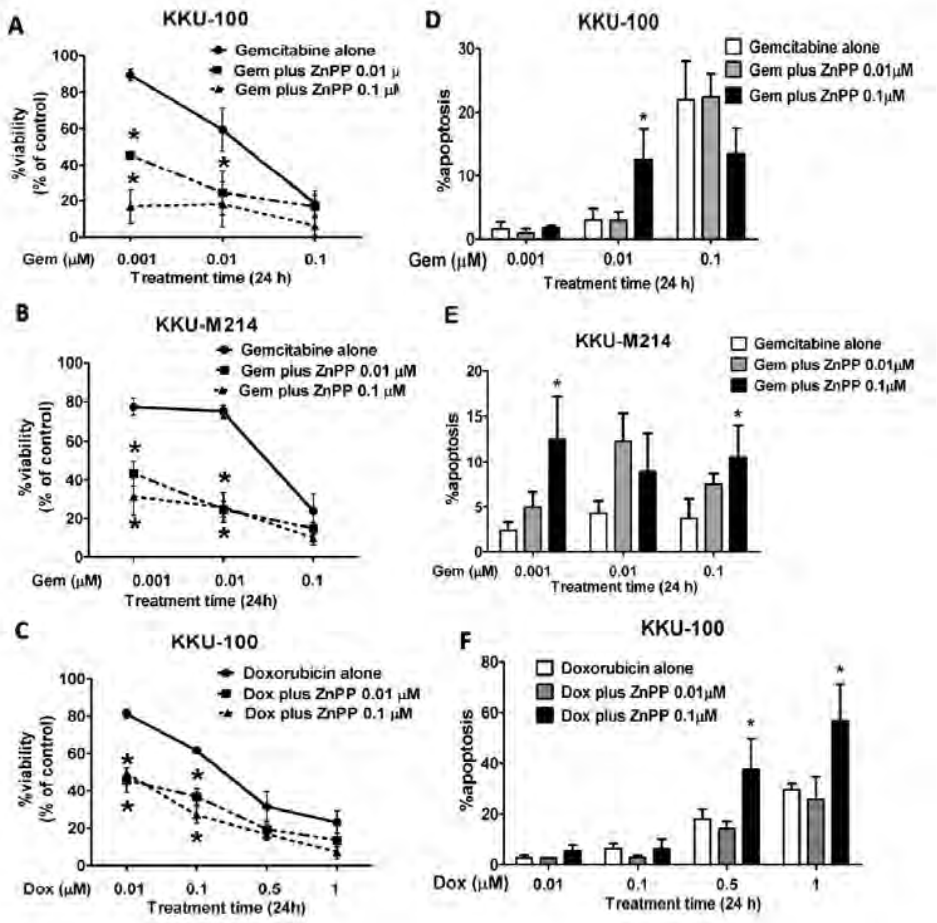


**Figure 3 Inhibition of HO-1 activity enhances the cytotoxic effect of Gem**. KKU-100 and KKU-M214 cells were treated with the varied concentrations (0.001, 0.01 and 0.1 μM) of Gem (A,B,D and E) and (0.01, 0.1, 0.5 and 1 μM) of Dox (C and F) with or without 0.01 and 0.1 μM of ZnPP (HO-1 inhibitor) for 24 h. KKU-100 and KKU-M214 cells were evaluated for cytotoxicity (A,B and C) and apoptosis (D,E and F) by fluorescent dye staining. The cytotoxicity of the drugs are in concentration-response manner, whereas in co-treatment of drug and ZnPP, the concentration-response curves are shifted downward, indicating enhancement of the response to drug combinations. The bars at the right panel show percent of apoptotic cell death when cells were treated with anticancer drugs in combination with various concentrations of ZnPP (0.001-0.1 μM). The bars represent mean±SEM, each from three separated experiments. *, $p<0.05$ vs drug alone (Gem and Dox).

**Effect of HO-1 inhibition on the sensitivity of CCA cells to anticancer agents**

The cytoprotective effects of HO-1 in CCA cells to anticancer agents were explored using high and low HO-1 expressing KKU-100 and KKU-M214 cells cultured with HO-1 inhibitor. Both cells were exposed to Gem (0.001- 0.1 μM) in the presence of HO-1 inhibitor, ZnPP (0.01 and 0.1 μM) for 24 h. As shown in Fig. 3A and 3B, ZnPP rendered both CCA cells to be highly susceptible to cytotoxic effect of Gem, which can be seen as the downward shift of the dose-response curves of Gem in the presence of ZnPP. Similar downward shift of the dose-response curves in the presence of ZnPP was observed in KKU-100 cells to another chemotherapeutic agent, Dox (Fig. 3C). The presence of ZnPP augmented significantly Gem- or Dox-induced cell growth inhibition and induction of apoptotic cell death in both cell lines (Fig. 3D, E and F). ZnPP itself showed only a slight cytotoxicity at the concentrations used in this study (data not shown).

**HO-1 induction enhanced resistance of CCA cells to anticancer agents.**

To validate the cytoprotective roles of HO-1, $SnCl_2$, a HO-1 inducer, was used in combination with Gem or Dox**.** KKU-100 and KKU-M214 cells were exposed to $SnCl_2$ and changes in HO-1 protein was evaluated by Western blot analysis. $SnCl_2$ (10 μM) induced HO-1 protein expression with a similar pattern in both cell types with maximal induction observed during 6-24 h (Fig. 4A). KKU-100 and KKU-M214 cells were treated with Gem (0.1 μM) or Dox (0.5 μM) with or without $SnCl_2$ for 24 h. Induction of HO-1 was associated with increased cell viability more than 2 fold after treatment with Gem or Dox (Fig. 4B). Induction of HO-1 by $SnCl_2$ decreased the apoptotic and necrotic cell death induced by Gem and Dox in both CCA cells (Fig. 4C). $SnCl_2$ alone was slightly toxic at the concentrations used in this study (data not shown).

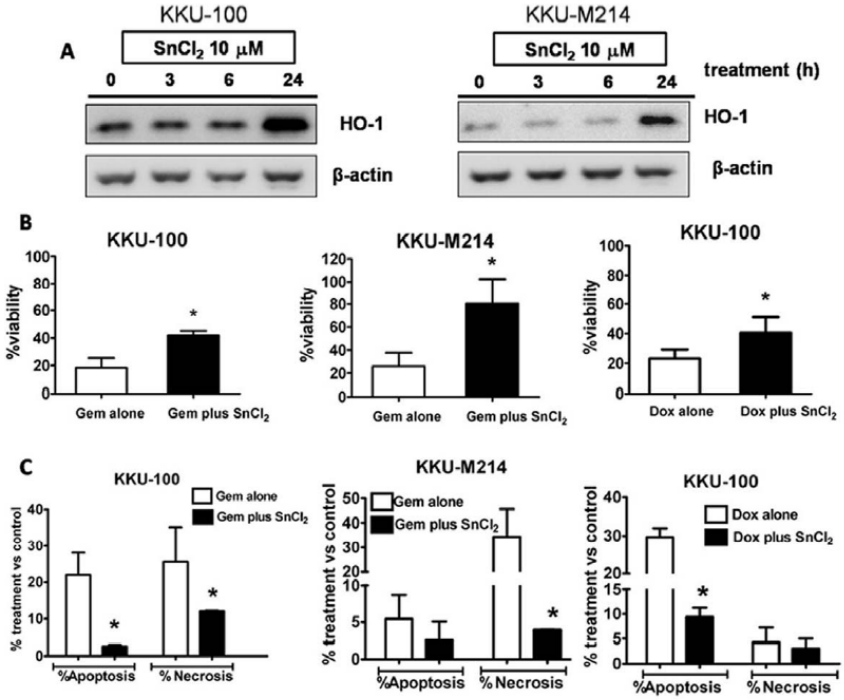


**Figure 4 Induction of HO-1 suppressed the cytotoxicity of Gem and Dox.** (**A**) The time-course of HO-1 induction by $SnCl_2$ (10 μM) in KKU-100 and KKU-M214 cells. The cells were cultured for overnight and exposed to $SnCl_2$ for 3, 6 and 24 h before whole cell lysates were collected and HO-1 protein was determined by the Western blotting, using β-actin; as loading control. The HO-1 protein expression in KKU-100 and KKU-M214 cells is relative stable during the first 6 h of exposure to $SnCl_2$, whereas high HO-1 expression is evident during 6 to 24 h. The cytotoxicity of Gem (0.1 μM) and Dox (0.5 μM) with or without $SnCl_2$ (10 μM) was determined in both cell lines after incubation for 24 h. The cell viability (**B**), apoptotic and necrotic cells (**C**) were evaluated by fluorescent dye staining. Data represent mean±SEM, each from three separated experiments. *****, $p<0.05$ vs drug alone.

**HO-1 gene silencing sensitized CCA cells to chemotherapeutic agents.**

To further validate that HO-1 inhibition indeed induced sensitization of CCA cells to anticancer agents, the effects of HO-1 gene silencing to Gem was examined. Since both KKU-100 and KKU-M214 cells showed similar responses to HO-1 inhibitor and inducer, KKU-100 cells were employed as a representative of CCA cells. The levels of HO-1 mRNA (Fig. 5A) and immunoreactive HO-1 protein (Fig. 5B) were dramatically decreased 24 h after transfection of HO-1 siRNA. Then, HO-1 knocked-down KKU-100 cells were exposed to various concentrations of Gem (0.001-0.1 μM) for further 24 h. The $IC_{50}$ concentration of Gem in non-targeting control was 0.0360±0.0042 μM,

whereas that in HO-1 knockdown cells was 0.0005±0.0001 μM (Fig. 5C) ($p$ <0.001), showing that the inhibition of HO-1 sensitizes KKU-100 cells to be highly susceptible to Gem.

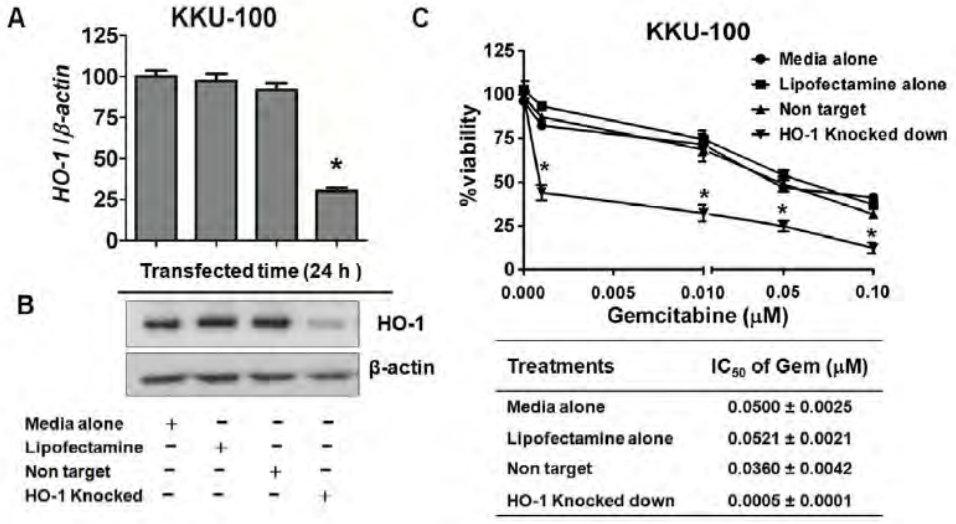


| Treatments | $IC_{50}$ of Gem (μM) |
|---|---|
| Media alone | 0.0500 ± 0.0025 |
| Lipofectamine alone | 0.0521 ± 0.0021 |
| Non target | 0.0360 ± 0.0042 |
| HO-1 Knocked down | 0.0005 ± 0.0001 |

**Figure 5 Knockdown of HO-1 by siRNA sensitized KKU-100 cells to Gem.** The mRNA (A) and protein (B) levels of HO-1expression in KKU-100 cells are shown. KKU-100 cells were transfected with siRNA against HO-1 for 24 h and total RNA was prepared and analyzed by reverse transcription-PCR. In similar experiments, cell lysates were collected and HO-1 was determined by the Western blotting in KKU-100 cells, using β-actin, as loading control. (**C**) The cytotoxicity and IC50 of Gem in knocked down KKU-100 cells was determined. After transfection for 24 h, KKU-100 cells were treated with varied concentrations of Gem (0.001, 0.01, 0.05 and 0.1 μM) for another 24 h. The cell viability was evaluated by fluorescent dye staining. Data represent mean±SEM, each from three separated experiments. ***,** $p$<0.05 vs non target knocked down cells.

**ZnPP induced intracellular ROS formation and mitochondrial dysfunction**

From the above experiments, HO-1 inhibition by ZnPP enhanced the susceptibility of CCA cells to the cytotoxic effect of Gem. To explore the underlying mechanisms of enhanced cytotoxicity by the combination of Gem and ZnPP, the intracellular ROS formation was assessed. Treatment with ZnPP alone caused a remarkable increase in ROS formation as early as 3 h. The combination of ZnPP and Gem showed further increase in ROS levels (Fig. 6A). Gem alone showed no effect on ROS formation. To test whether the ROS was indeed responsible to enhance the cytotoxicity of Gem, the superoxide dismutase (SOD)-mimetic compound, Tempol, was used to scavenge $O_2^{\bullet-}$ induced by combined ZnPP and Gem treatment. The concentrations of Tempol to be used in studies were evaluated in a previous experiment which had shown to inhibit ROS formation and produce minimal toxicity. Moreover, it is verified that Tempol (500 μM) does not inhibit HO-1 activity. ZnPP-enhanced cytotoxicity of Gem was abolished by the presence of Tempol (Fig. 6B). Tempol alone has little cytotoxicity to the cells. Since ROS formation is thought to be involved in induction of cell killing in association with mitochondrial pathway, KKU-100 cells were treated with the combination of ZnPP and Gem and the $\Delta\psi_m$ were evaluated using JC-1 assay. Gem treatment alone had no effect on the $\Delta\psi_m$ (Fig. 6 C, inset b & f), whereas ZnPP and the combination of ZnPP with Gem induced the depolarization of $\Delta\psi_m$ as evident by the change of red fluorescent staining in healthy mitochondria (Fig. 6C, inset a & e) to green fluorescent staining in depolarized mitochondria (Fig. 6C, inset c, d, g & h).

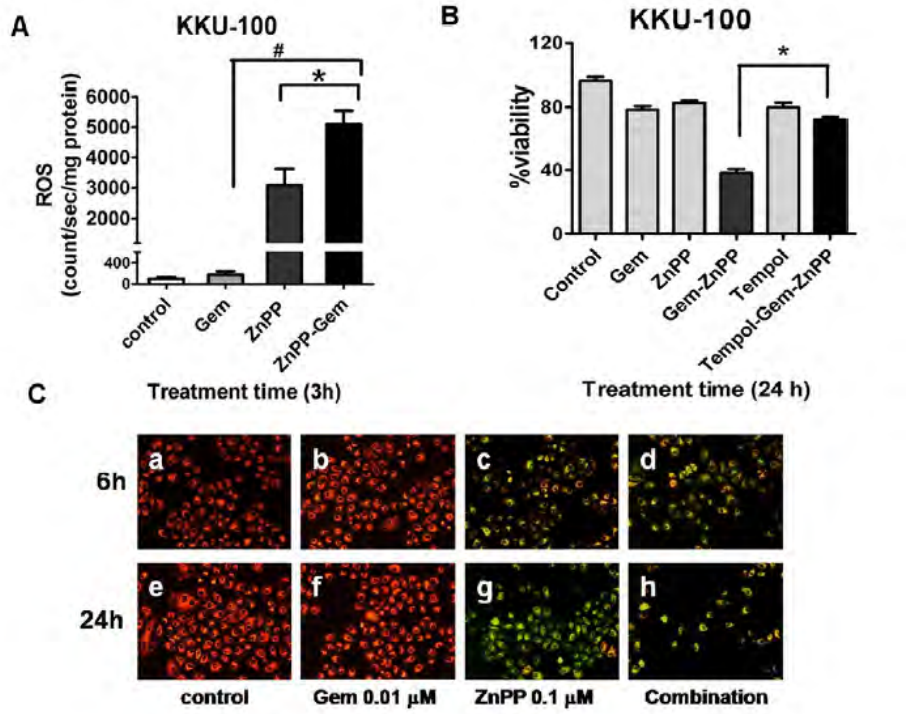


**Figure 6 ZnPP induced the intracellular reactive oxygen generation, depolarization of mitochondrial transmembrane potential and cytotoxcity.** (**A**) The generation of ROS induced by ZnPP (0.1 μM) and combination of ZnPP and Gem (0.01 μM) for 3 h in KKU-100 cells as measured by lucigenin-enhanced chemiluminescent method. *, p<0.05 vs ZnPP alone and #, vs Gem alone. (**B**) The ROS scavenger, Tempol (500 μM), inhibited cytotoxicity of the combination of ZnPP (0.1 μM) and Gem (0.01 μM) in KKU-100 cells The cell viability was evaluated by fluorescent dye staining. *****, *p*<0.05 vs the combination of ZnPP and Gem. Data represent mean±S.E.M., each from three independent experiments. (**C**) The induction of depolarization of the mitochondrial transmembrane potential ($\Delta\psi_m$) using JC-1 fluorescent probe, in KKU-100 cells after treatment with Gem +/- ZnPP for 6 h (a,b,c, &d) and 24 h (e,f,g & h). The healthy mitochondria, JC-1 forms J-aggregates and display strong red fluorescent signal, whereas the depolarized mitochondria, JC-1 exists as monomers and show green fluorescent signal.

**Combination of ZnPP and Gem altered the expression of proteins related to cell proliferation and apoptosis.**

To investigate further the effects of combined Gem and ZnPP if it was mediated via mitochondrial pathway, cytochrome c, release from the mitochondria in response to pro-apoptotic stimuli, was determined. The combined drug treatment exerted significant increase in levels of cytochrome c protein when compared with the controls. ZnPP or Gem alone did not induce the release (Fig. 7). Since the combined Gem and ZnPP suppressed the tumor cell growth, a protein related to cell proliferation; the $p21^{Cip/WAF1}$ was analyzed by Western blotting. Gem or ZnPP alone did not affect the $p21^{Cip/WAF1}$ protein expression, whereas the combination of Gem and ZnPP caused marked induction of $p21^{Cip/WAF1}$ and was associated with marked antiproliferative effect.

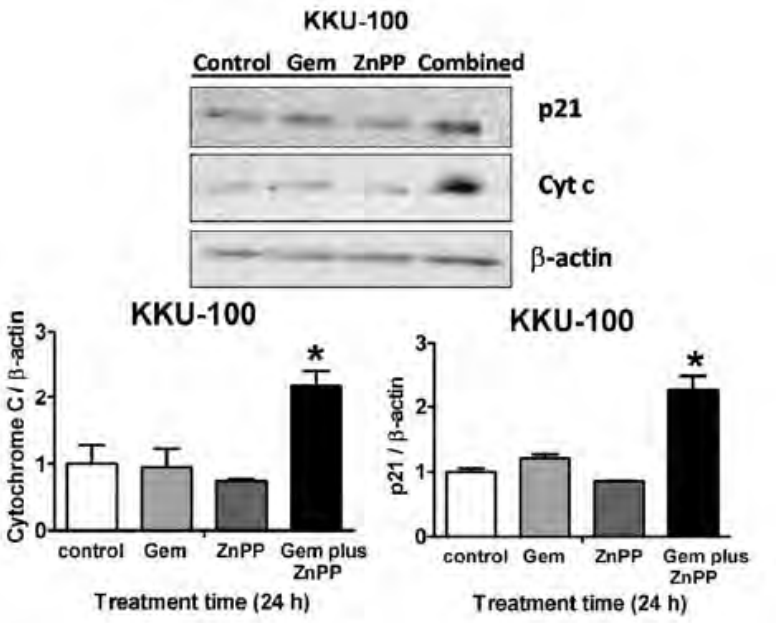


**Figure 7 Alteration of expression of proteins related to cell proliferation and apoptosis.** The Western blots of p21 and cytochrome c protein expression in KKU-100 cells after treatment with Gem (0.01 μM) +/- ZnPP (0.1 μM) for 24 h. The levels of p21 and cytochrome c were normalized with β-actin as a loading control. The bars are mean±SEM, each from three independent experiments. *$p < 0.05$ vs untreated controls.

## Discussion

HO-1 has a potent cytoprotective activity against noxious stimuli in inflammatory diseases such as sepsis, inflammatory bowel disease, or in various oxidative injuries [7]. Moreover, HO-1 plays a protective role in normal tissues as well as in cancer cells [22,23]. Our study demonstrated that HO-1 plays a critical role in CCA cells in cytoprotection against anticancer agents, regardless of the basal HO-1 expression levels of the cells. Inhibition of HO-1 by ZnPP or HO-1 siRNA could sensitize CCA cells to the cytotoxicity of anticancer agents, whereas the induction of HO-1 exerted a cytoprotective and drug resistant effects. The sensitization of CCA cells by HO-1 inhibition is probably involved with generation of ROS, which leads to the loss of $\Delta\Psi m$, and initiates apoptotic cell death processes.

Altered expression of drug metabolizing enzymes, such as *UGT1A, UGT2B, SULT1C* [24], *NAT2* [25] and *GSTO* [26] have been reportedly associated with intrahepatic cholangiocarcinoma in endemic area of liver fluke infection. However, there is still no evidence to establish their roles in protecting cancer cells. Elevated expression of HO-1 has been reported in various human tumors including renal cell carcinoma, prostate tumors, bladder and pancreatic cancers [15,27,28,29], with close association to the disease states. In the present study, HO-1 induction by $SnCl_2$ caused a significant cytoprotection against chemotherapeutic agents regardless of basal HO-1 expression. On the other hand, treatment with anticancer agent also strongly up-regulated HO-1 expression, implying that adaptive defense response in CCA cells is induced to endure the drugs. These results suggest that role of HO-1 in cytoprotection is very critical even in low basal level of HO-1 expression. It should be noted that cytoprotective effect conferred by HO-1 is not specific to Gem but also to Dox and perhaps to some others, in spite of the different mechanisms of actions of these anticancer agents.

These results also suggest that the resistance of CCA cells to anticancer agents is, at least in part, due to induction of HO-1. Overall, the inhibition of HO-1 may overcome the intrinsic as well as acquired resistance to chemotherapeutic agents.

Subsequently in this study, we investigated further as to how HO-1 inhibition induces the sensitization in CCA cells to anticancer agents. HO-1 possesses an indirect antioxidant effects probably via generation of biliverdin/bilirubin, carbon monoxide, and other oxidative stress responses [11,30]. Bilirubin is a potent antioxidant by recycling between biliverdin and bilirubin during the catalytic cycle of oxidation and reduction [11]. Inhibition of HO-1 by ZnPP resulted in significant increase in ROS formation [17,23,29]. Our results showed that ZnPP caused marked increase in ROS levels in KKU-100 cells, whereas Gem treatment alone did not induce ROS. Moreover, combination of ZnPP and Gem enhanced more ROS production than ZnPP alone. Our study further verified that ROS is essential for the chemosensitizing effect, as scavenging of ROS by Tempol virtually abolished the sensitizing effect of ZnPP. Moreover, these results imply that inhibition of HO-1 increases the oxidative stress, where ROS may be derived from the metabolism of the cells themselves [7,30].

The loss of $\Delta\psi_m$ is regarded as an early event of mitochondrial dysfunction. It is apparent that a small change in mitochondrial permeability transition (MPT) could depolarize the mitochondria, whilst increasing number of MPT leads to necrosis and apoptosis [31]. The increase of ROS production in ZnPP treated groups was associated with the loss of $\Delta\psi_m$. Our recent study on chemopreventive effect of curcumin has demonstrated a temporal relationship of ROS formation, depolarization of mitochondria and induction of apoptosis [32]. An inducer such as ROS may attack and modify membrane proteins of MPT pores leading to the aggregation of misfolded proteins creating regulated PT pores [31]. In this circumstance, the cells are in a state of highly susceptible to further attack by inducers of MPT. Role of ROS induced by ZnPP in relation to mitochondrial function and induction of apoptotic cell death is needed further clarification.

Alternatively, inhibition of HO-1 activity results in an increase accumulation of protoporphyrin in mitochondria [33] and this lead to depolarization of $\Delta\psi_m$ and sensitize MPT to cytotoxic agents. Protoporphyrin IX has been suggested to be a ligand of peripheral benzodiazepine receptor, a component of MPT pores, thereby sensitizes MPT [34,35]. The present study showed that only the combination of ZnPP and Gem enhanced cell killing effect, whilst ZnPP alone at sub-micromolar concentrations caused the release of ROS in association with loss of $\Delta\psi_m$, but this was still insufficient to induce cell death. Our study is in agreement with recent reports, ZnPP alone shows no effect on MPT, however ZnPP in combination with triiodothyronine induced oxidative stress, MPT opening and apoptotic cell death [18]. Furthermore, effect of protoporphyrin IX at nanomolar range in enhanced rotenone-induced cytotoxicity is demonstrated to be due to MPT opening, because the effects were inhibited by cyclosporine A, an inhibitor of MPT [35].

The sensitizing effect is consistent with present experiment in that no increased release of cytochrome c by ZnPP or Gem alone, whereas the drug combination increased release of cytochrome c. It is noted that Gem alone may not exert cytotoxic effect via mitochondrial pathway, as Gem did not induce changes of $\Delta\psi_m$ and cytochrome c levels. Gem is known to induce cell cycle arrest and apoptosis by p53-dependent and independent pathways.[36]. Our study observed that combination of ZnPP and Gem induced an increased level of the protein p21, which is a p53-dependent downstream gene product, and a potent cyclin-dependent kinase inhibitor. Gem or ZnPP alone did not exert any significant changes in p21. It is probable that induction of mitochondrial dysfunction induces p21 accumulation [37]. This is consistent with a strong antiproliferation effect of Gem and ZnPP combination.

In summary, HO-1 plays an important role in cytoprotection in both low and high HO-1 expressing CCA cells. Inhibition of HO-1 induced ROS formation, which may initiate the loss of $\Delta\psi_m$ and sensitizes CCA cells to a cytotoxic effect of anticancer agents. Thus, targeted suppression of HO-1 may be a strategy to overcome drug resistance in cholangiocarcinoma chemotherapy.

**References**


1. Sripa B, Pairojkul C (2008) Cholangiocarcinoma: lessons from Thailand. Curr Opin Gastroenterol 24: 349-56.
2. Shin HR, Oh JK, Masuyer E, Curado MP, Bouvard V, et al. (2010) Epidemiology of cholangiocarcinoma: an update focusing on risk factors. Cancer Sci 101: 579-85.
3. Blechacz B, Gores GJ (2008) Cholangiocarcinoma: advances in pathogenesis, diagnosis, and treatment. Hepatology 48: 308-21.
4. Patel T (2011) Cholangiocarcinoma--controversies and challenges. Nat Rev Gastroenterol Hepatol 8: 189-200.
5. Malhi H, Gores GJ (2006) Cholangiocarcinoma: Modern advances in understanding a deadly old disease. Journal of Hepatology 45: 856-67.
6. Hezel AF, Zhu AX (2008) Systemic therapy for biliary tract cancers. Oncologist 13: 415-23.
7. Ryter SW, Alam J, Choi AM (2006) Heme oxygenase-1/carbon monoxide: from basic science to therapeutic applications. Physiol Rev 86: 583-650.
8. Doi K, Akaike T, Fujii S, Tanaka S, Ikebe N, et al. (1999) Induction of haem oxygenase-1 nitric oxide and ischaemia in experimental solid tumours and implications for tumour growth. Br J Cancer 80: 1945-54.
9. Nuhn P, Kunzli BM, Hennig R, Mitkus T, Ramanauskas T, et al. (2009) Heme oxygenase-1 and its metabolites affect pancreatic tumor growth in vivo. Mol Cancer 8: 37.
10. Boutros C, Zegdi R, Lila N, Cambillau M, Fornes P, et al. (2007) Carbon monoxide can prevent acute lung injury observed after ischemia reperfusion of the lower extremities. J Surg Res 143: 437-42.
11. Ryter SW, Kim HP, Nakahira K, Zuckerbraun BS, Morse D, et al. (2007) Protective functions of heme oxygenase-1 and carbon monoxide in the respiratory system. Antioxid Redox Signal 9: 2157-73.
12. Jozkowicz A, Was H, Dulak J (2007) Heme oxygenase-1 in tumors: is it a false friend? Antioxid Redox Signal 9: 2099-117.
13. Was H, Cichon T, Smolarczyk R, Rudnicka D, Stopa M, et al. (2006) Overexpression of heme oxygenase-1 in murine melanoma: increased proliferation and viability of tumor cells, decreased survival of mice. Am J Pathol 169: 2181-98.
14. Kuroda H, Takeno M, Murakami S, Miyazawa N, Kaneko T, et al. (2010) Inhibition of heme oxygenase-1 with an epidermal growth factor receptor inhibitor and cisplatin decreases proliferation of lung cancer A549 cells. Lung Cancer 67: 31-6.
15. Miyake M, Fujimoto K, Anai S, Ohnishi S, Nakai Y, et al. (2010) Clinical significance of heme oxygenase-1 expression in non-muscle-invasive bladder cancer. Urol Int 85: 355-63.
16. Miyazaki T, Kirino Y, Takeno M, Samukawa S, Hama M, et al. (2010) Expression of heme oxygenase-1 in human leukemic cells and its regulation by transcriptional repressor Bach1. Cancer Sci 101: 1409-16.

17. Nowis D, Bugajski M, Winiarska M, Bil J, Szokalska A, et al. (2008) Zinc protoporphyrin IX, a heme oxygenase-1 inhibitor, demonstrates potent antitumor effects but is unable to potentiate antitumor effects of chemotherapeutics in mice. BMC Cancer 8: 197.
18. Giris M, Erbil Y, Depboylu B, Mete O, Turkoglu U, et al. (2010) Heme oxygenase-1 prevents hyperthyroidism induced hepatic damage via an antioxidant and antiapoptotic pathway. J Surg Res 164: 266-75.
19. Buranrat B, Prawan A, Kukongviriyapan U, Kongpetch S, Kukongviriyapan V (2010) Dicoumarol enhances gemcitabine-induced cytotoxicity in high NQO1-expressing cholangiocarcinoma cells. World J Gastroenterol 16: 2362-70.
20. Buranrat B, Prawan A, Sripa B, Kukongviriyapan V (2007) Inflammatory cytokines suppress arylamine N-acetyltransferase 1 in cholangiocarcinoma cells. World J Gastroenterol 16: 6219-25.
21. Buranrat B, Prawan A, Kukongviriyapan U, Kongpetch S, Kukongviriyapan V (2010) Dicoumarol enhances gemcitabine-induced cytotoxicity in high NQO1-expressing cholangiocarcinoma cells. World J Gastroenterol 16: 2362-70.
22. Correa-Costa M, Semedo P, Monteiro AP, Silva RC, Pereira RL, et al. (2010) Induction of heme oxygenase-1 can halt and even reverse renal tubule-interstitial fibrosis. PLoS One 5: e14298.
23. Fang J, Sawa T, Akaike T, Akuta T, Sahoo SK, et al. (2003) In vivo antitumor activity of pegylated zinc protoporphyrin: targeted inhibition of heme oxygenase in solid tumor. Cancer Res 63: 3567-74.
24. Jinawath N, Chamgramol Y, Furukawa Y, Obama K, Tsunoda T, et al. (2006) Comparison of gene expression profiles between Opisthorchis viverrini and non-Opisthorchis viverrini associated human intrahepatic cholangiocarcinoma. Hepatology 44: 1025-38.
25. Prawan A, Kukongviriyapan V, Tassaneeyakul W, Pairojkul C, Bhudhisawasdi V (2005) Association between genetic polymorphisms of CYP1A2, arylamine N-acetyltransferase 1 and 2 and susceptibility to cholangiocarcinoma. Eur J Cancer Prev 14: 245-50.
26. Marahatta SB, Punyarit P, Bhudisawasdi V, Paupairoj A, Wongkham S, et al. (2006) Polymorphism of glutathione S-transferase omega gene and risk of cancer. Cancer Lett 236: 276-81.
27. Goodman AI, Choudhury M, da Silva JL, Schwartzman ML, Abraham NG (1997) Overexpression of the heme oxygenase gene in renal cell carcinoma. Proc Soc Exp Biol Med 214: 54-61.
28. Maines MD, Abrahamsson PA (1996) Expression of heme oxygenase-1 (HSP32) in human prostate: normal, hyperplastic, and tumor tissue distribution. Urology 47: 727-33.
29. Berberat PO, Dambrauskas Z, Gulbinas A, Giese T, Giese N, et al. (2005) Inhibition of heme oxygenase-1 increases responsiveness of pancreatic cancer cells to anticancer treatment. Clin Cancer Res 11: 3790-8.
30. Gozzelino R, Jeney V, Soares MP (2010) Mechanisms of cell protection by heme oxygenase-1. Annu Rev Pharmacol Toxicol 50: 323-54.
31. Kim JS, He L, Lemasters JJ (2003) Mitochondrial permeability transition: a common pathway to necrosis and apoptosis. Biochem Biophys Res Commun 304: 463-70.
32. Suphim B, Prawan A, Kukongviriyapan U, Kongpetch S, Buranrat B, et al. (2010) Redox modulation and human bile duct cancer inhibition by curcumin. Food Chem Toxicol 48: 2265-72.
33. Ohgari Y, Miyata Y, Chau TT, Kitajima S, Adachi Y, et al. (2011) Quinolone compounds enhance delta-aminolevulinic acid-induced accumulation of protoporphyrin IX and photosensitivity of tumour cells. J Biochem 149: 153-60.
34. Azarashvili T, Grachev D, Krestinina O, Evtodienko Y, Yurkov I, et al. (2007) The peripheral-type benzodiazepine receptor is involved in control of Ca2+-induced permeability transition pore opening in rat brain mitochondria. Cell Calcium 42: 27-39.

35. Pastorino JG, Simbula G, Gilfor E, Hoek JB, Farber JL (1994) Protoporphyrin IX, an endogenous ligand of the peripheral benzodiazepine receptor, potentiates induction of the mitochondrial permeability transition and the killing of cultured hepatocytes by rotenone. J Biol Chem 269: 31041-6.
36. Tolis C, Peters GJ, Ferreira CG, Pinedo HM, Giaccone G (1999) Cell cycle disturbances and apoptosis induced by topotecan and gemcitabine on human lung cancer cell lines. Eur J Cancer 35: 796-807.
37. Li CH, Tzeng SL, Cheng YW, Kang JJ (2005) Chloramphenicol-induced mitochondrial stress increases p21 expression and prevents cell apoptosis through a p21-dependent pathway. J Biol Chem 280: 26193-9.

## Section 2

### Modulation of heme oxygenase-1 increases sensitivity of cholangiocarcinoma cells to radiation and chemotherapy

#### Introduction

**C**holangiocarcinoma (CCA) is one of the most devastating malignancies, because the majority of cases develop without clinical symptoms, and thus making the diagnosis of CCA very difficult. Prognosis of CCA is extremely poor because treatment outcomes and survival of the patients have only slightly improved in the past several decades [1]. The complete tumor resection with negative pathological margins (R0 resection) is the only effective option to prolong survival with the five-year survival rate of 20-44%, but the recurrence of cancer is common which can occur in up to 63% within 2 year [2-3]. Nonetheless, most of patients are already in the advanced stage of the disease at diagnosis thus making radical surgery not possible and prognosis of the unresectable or incomplete (R1) resection is extremely poor [3]. Chemotherapy and radiotherapy may be the options left for most patients [4]. The most accepted chemotherapy with gemcitabine-base has documented a median overall survival of only 11 months. Experiences in radiotherapy of CCA in adjuvant and neoadjuvant settings are very limited and there is currently no evidence to support the routine use of radiotherapy for unresectable disease [2, 4]. It is, therefore, there is an urgent need for a more effective treatment approach to improve survival and quality of life of these patients [5-6]. Targeting the prosurvival mechanisms in cancer cells could be a strategy to overcome resistance to chemotherapy and radiotherapy. Antioxidant and cytoprotective proteins such as HO-1 and NQO1 could be such targets [7-9].

Heme oxygenase-1 (HO-1) is a microsomal enzyme catalyzing the first rate-limiting step in degradation of heme, leading to equimolar production of biliverdin, carbon monoxide (CO) and free iron. HO-1 can be induced in response to cellular stress, oxidative stimuli, hypoxia and during tumor growth [10]. More importantly, HO-1 is found to be over-expressed in various cancer types including prostate cancer, hepatoma, pancreatic cancer and lymphosarcoma [11]. These cancers express a high level of HO-1 and the over-expression of this enzyme may provide growth advantages and render resistance to chemotherapeutic agents such as cisplatin, doxorubicin and gemcitabine [12-14]. HO-1 plays a role in tumor growth, neoangiogenesis and cytoprotection of tumors against the attack of oxidative insults from chemotherapy and radiotherapy, probably due to its anti-oxidative and anti-apoptotic activities [15-17]. Thus, suppression of HO-1 activity may be a strategy to increase the chemosensitivity and radiosensitivity of tumors. We recently have shown that the inhibition of HO-1 in CCA cell lines by HO-1 siRNA or by pharmacological inhibitor, zinc protoporphyrin IX (ZnPP) resulted in an remarkable reduction of the IC50 of CCA cells to gemcitabine [17]. Moreover, ellagic acid inhibits prostate cancer cells in association with downregulation of HO-1 [18].

In the present study, the effects of HO-1 suppression on tumor cell growth, cell cycle progression and sensitivity to radiation and chemotherapeutic agents were examined by using HO-1 knockdown CCA cells with high and low basal HO-1 levels. We further evaluated and examined the effects of combined therapy of gemcitabine and ZnPP using an *in vivo* model.

#### Materials and methods

**Cell lines and cell cultures**

The human cholangiocarcinoma (CCA) cell lines; KKU-100, KKU-M055, KKU-M214, KKU-M213, and KKU-M139 were kindly provided by Dr. Banchob Sripa, Department of Pathology, Faculty of Medicine, Khon Kaen University. Cell lines were established, characterized, and derived from CCA tissues which are classified histologically as follows: poorly differentiated adenocarcinom (KKU-100, M055), well differentiated adenocarcinoma (M214, M213), aquamous cell carcinoma (KKU-M139) [19-20]. All cell lines were routinely cultured in complete media consisting of Ham's F12 media, supplemented with 10% fetal calf serum, 12.5 mM HEPES, pH 7.3, 100 U/ml penicillin G and 100 μg/ml gentamicin [21].

**Cytotoxicity assay**

KKU-100 cells were seeded onto 96-well plate at density of 7,500 cells/well for overnight. The cells were treated with varied concentration of ZnPP and gemcitabine (GEM) from 1- 1000 nM for 24 h. For the combination treatment, KKU-100 cells were pretreated with ZnPP for 4 h prior GEM, and incubation was continued for 24 h. The cytotoxicity assay was performed by sulforhodamine B (SRB) assay as previously described [21].

**Cell motility, wound healing and clonogenic assays**

KKU-100 and M213 cells with HO-1 knockdown were used in the cell motility and wound healing assays. KKU-100 and M213 cells were transfected with HO-1 siRNA (method as below) for 24 h, then seeded onto a transwell insert in 300 μL of medium. After incubation for 6 h, the filter membrane was cut and placed on the glass slide, covered with the mounting medium with DAPI, and then covered with a cover-slip. The cells migrated across the membrane were enumerated using a fluorescence microscope; Nikon Eclipse Ti.

For wound healing assay, after transfection with HO-1 siRNA for 24 h, KKU-100 and M213 cells were seeded into 24-well plate with density of 150,000 per well in full cultured media to obtain cell confluence of 80-90% on the experimental day. On the next day, cultured cells were scratched with a sterile 200 μL-pipette tip making straight line of wounds. The width of wound outline was recorded under a phase-contrast microscope at 0, 6, 12 and 24 h after scratching the cultured cells.

The clonogenic survival of CCA cells following gamma irradiation was determined by clonogenic assay. The stable knockdown of HO-1, KKU-100 and M214 cells in suspensions at the density of 12,500 cells/mL were irradiated over the dose range of 0-10 Gy. Immediately after irradiation, the cells were seeded at 300 and 200 cells of KKU-100 and M214, respectively, onto a 6-well plate. After 14 days of incubation with renewal of cultured media every other day, the cells were fixed in absolute methanol and stained with 0.25% crystal violet in 2% ethanol. The number of colonies in each well was counted under a Nikon Eclipse Ti microscope (10X).

**Irradiation-induced antiproliferation**

The five CCA cells; KKU-100, M213, M214, M055 and M139 cells were employed to assay of the sensitivity to radiation. Cells in suspensions at the density of 12,500 cells/mL were irradiated at room temperature over the dose range of 0–10 Gy using a Gammacell® 40 Exactor (Nordion Gamma Irradiator®). The cells were seeded at density of 625-1250 cells/well in 96-well plate and incubated for 4 days. Cell proliferation was determined by MTS assay, performed according to the instruction guideline of CellTiter 96® (Promega)

**HO-1 small interfering RNA transfection**

The transfection of HO-1 siRNA was performed using siGENOME SMARTpool of four sequences of siRNA (M-006372-02-0005: Dharmacon) at a final concentration of 200 nM and lipofectamine 2000 (Invitrogen) according to the manufacturers' instructions. The siGENOME non-targeting siRNA (D-001210-02-05), as a negative control was introduced to the cells using the same protocol as previously described method [17].

**Generation of HO-1 stable knocked down by Lentivirus-mediated shRNA transfection**

To generate the lentivirus for transduction, ps-ShRNA-ControlA and ps-ShRNA -HO-1 plasmids were purchased from Santa Cruz and packaged using the ViraPower™ Lentiviral Packaging Mix (Invitrogen) as described by manufacturer. Briefly, 293FT cells were plated at 90% confluence in 10-cm plates and transfected with 3µg of ps-ShRNA-ControlA, or ps-ShRNA -HO-1, 36µL lipofectamine and 9 µg ViraPower™Packaging mixed in 1.5 mL Opti-MEM medium for an overnight. On the third day, medium with specific viral conjugated with ps-ShRNA-controlA or -HO-1, was collected and kept at -80°C before use. To generate stable control and HO-1 knockdown cell, 30,000 cells/well in 12-well plate of KKU-100 and M214 cells were transduced with 1µL of ps-ShRNA-ControlA or ps-ShRNA-HO-1 lentivirus. Positively transduced cells were selected by culturing in media containing 2 µg/ml puromycin B for 3 weeks.

**Reverse transcription real-time polymerase chain reaction**

The five CCA cells; KKU-100, M213, M214, M055 and M139 cells were seeded at the density of $1.5x10^4$ cells/well in 6 well-plates and allowed to grow for 24 h. Total RNA was isolated and the PCR products were generated using a previously described method [22]. The primer sequences were as follows: HO-1: forward, 5'-CTG ACC CAT GAC ACC AAG GAC-3' and HO-1 reverse: 5'-AAA GCC CTA CAG CAA CTG TCG-3', Gen Bank accession number.NM_002133.2, β-actin: forward 5'-AGT GTA GCC CAG GAT GCC CTT-3' and β-actin: reverse, 5'-GCC AAG GTC ATC CAT GAC AAC-3', Gen Bank accession number NM_00246.5. To quantify the relative expression of genes, the relative quantitation was performed by using standard curve method. The amount of HO-1 mRNA was expressed as a ratio to β-actin mRNA.

**Western blot analysis**

Western blot analysis was used to determine the expression levels of HO-1, cyclin A, cyclin B1, cdc2, and β-actin. Cultured cells were washed with PBS, lysed with RIPA buffer containing protease inhibitor cocktail. The protein samples were mixed with SDS loading buffer and subject to separation by electrophoresis in 8-10% SDS-polyacrylamide gel. The protein bands were blotted onto a PVDF membrane. After blocking with skimmed milk in phosphate buffer saline (PBS), the membrane was incubated overnight at 4°C with primary antibodies of HO-1 (ADI-SPA-895: Enzo Life Sciences), cdc2 p34 (sc-8395: Santa Cruz), cyclinA (sc-751), cyclinB1 (sc-752) and β-actin (A1978: Sigma-Aldrich) in PBS. After washing with PBS containing 0.05% Tween-20, the blots were incubated with the secondary antibodies (170-6515 or 170-6516: Biorad). The protein bands were detected by using an ECL kit (Pierce Biotechnology).

**Immunocytofluorescence for γ- H2AX**

To analyze the irradiation-induced phosphorylated histone protein, γ- H2AX foci in CCA cells were examined by the immunocytofluorescence technique after irradiation as described previously [23]. KKU-100 cells (30,000 cells/well) were seeded on polystyrene treated glass slide, irradiated with gamma ray at the doses of 5 Gy for KKU-100, and incubated for 15 min. Cells were fixed in 3.7% paraformaldehyde in PBS and permeabilized with 0.2% Triton X-100 in PBS. The cultured cells on slides were blocked, stained with anti- γ- H2AX (ab11174: ABCAM) in 0.2% BSA, followed by anti-rabbit IgG conjugated to Alexa-fluor 594 (Molecular Probe: Eugene). The cultured slides were covered with DAPI mounting medium (H1200: VECTASHIELD®, Vector Lab) and examined under a fluorescence microscope (TE-2000E: Nikon). γ-H2AX foci were measured under a 60X -objective lens.

**Flow cytometry for cell cycle analysis**

After the transfection with HO-1 siRNA, cells were irradiated with 5 Gy for KKU-100 and 8 Gy for M214. Then, at the designated times post-irradiation, cells were fixed by resuspending the cells in 3 mL of ice-cold 70% ethanol. The cell pellets were resuspended in 1 mL of PBS containing 0.1% Triton X-100, 20 µg/mL of propidium iodide and 20 µg/mL of RNase incubated at 4°C for 60 minutes in dark chamber, and then analyzed in a FACSCalibur flow cytometer (BD Biosciences).

**Antitumor activity in animal model**

All experimental procedures were performed according to the experimental animal handling standards and study protocol was approved by the Institutional Animal Care and Use Committee (IACUC) (application #2011/SHS/650) SingHealth, Singapore. KKU-100 cells ($2x10^6$) in 200 µL Ham-F12 medium were injected subcutaneously into the dorsal skin of 6-week-old female Balb/c nude mice (Animal Resource Center, Western Australia) and housed under a specific pathogen-free condition. When tumor grew to the volume about 200 $mm^3$, mice were randomly divided into four groups; control, gemcitabine (Gemzar®, Eli Lilly), ZnPP (Enzo Life Sciences) and the combination of both agents. ZnPP was dissolved in DMSO at the concentration of 100 mg/mL and diluted further in PBS immediately before use. Gem was dissolved in PBS as previously described to the concentration of 10 mg/mL and diluted further in PBS. ZnPP (12.5 mg/kg) and GEM (60 mg/kg) were administered intraperitonially once a week for three weeks (day 0, 7 and 14). In the combined drug treated group, ZnPP was injected 1 hour before Gem injection. Control group was treated with vehicle with the same schedule. Xenograft tumor volume was measured twice a week using electronic calipers and the tumor volume was calculated by the equation; $[L \times W^2]/2$ ($mm^3$), where L = length and W = width. The weight of mice was measured twice a week. The mice were terminated on day 17, and the tumor mass were collected for further analysis.

**Immunohistochemical analysis of tumor tissues**

The tumor tissues from xenografted mice were dissected, weighted and fixed in 10% formaldehyde solution and embedded in paraffin. The sections (3-µm-thick) were deparaffinised, followed by antigen retrieval with autoclave treatment for 10 min in 0.01 M citrate buffer (pH 6.0). Immunohistochemical staining for Ki67, CD31, mdm2, p53 and p21 was performed with a streptavidin-biotin (SAB) complex method using R.T.U. VECTORSTAIN® Universal Quick Kit (PK-7800: VECTOR) according to the manufacturer's instruction. The tissue-sections were incubated with primary antibodies, anti-Ki- 67 (clone MIB-1; Dako) at room temperature for 30 min, anti-CD31 (ab 28364: ABCAM), anti mdm2 (sc-965: Santa Cruz), anti p53 (sc-98) and anti p21 (2946: Cell Signaling Technology) at 4˚C overnight. The IHC-sections were counterstained with haematoxylin

and with eosin for H&E staining, and then mounted with DPX Mounting Medium (UN 1866: CellPath). CD31-stained vessels were detected under a Zeiss Axio ScopeA.1 microscope with original magnification 200X. The mean value of the vessel numbers in tumors, were calculated from 10 fields of the three most vascularized areas according to previously described. The areas of mdm2, p21 and p53 positive cell staining were captured under a Nikon DS-Ri1 microscope with original magnification 400X and using Image Pro-plus program to count positive cells. The staining levels of p53 were calculated by the grading of numbers of positive-cells multiply with the levels of intensity (positive-cell numbers were graded as 0-30=1, 31-60=2, 61-90=3 and 91-120=4 and levels of intensity ranges by 0-4)

**Statistical analysis**

Data were expressed as the mean ± SD. An analysis of variance was used to determine significant differences between each experimental group with Student-Newmann-Keuls post-hoc test. The level of significance was set at $P < 0.05$.

## Results

### HO-1 expression in CCA cells and contribution to cell migration

The expression levels of HO-1 were determined in five CCA cell lines using reverse transcription RT-PCR. KKU-100 cells showed high level of HO-1 mRNA expression, while others cell lines including M213, M214, M139 and M055 have much lower expression levels (Fig. 1A). KKU-100, and M213 and M214 which are representative of high, and low HO-1 expressing cell lines, respectively, were used for further functional studies. To investigate the functional role of HO-1 in CCA, HO-1 knockdown cells using siRNA were subjected to transwell and wound healing assays. The siRNA effectively reduced the HO-1 transcripts in KKU-100 and M213 cells by about 70% and 60%, respectively compared to control (Fig. 1B). HO-1 knockdown CCA cells showed a reduced number of cells migrated through the membrane in transwell chamber compared to control cells (Fig. 1C and 1D). The suppression of cell motility was further supported by wound healing assay, where the HO-1 knockdown CCA cells migrate much slower than the control cells, resulting in almost no closure of the wounds (Fig. 1E). This result suggested HO-1 plays role in cell migration in CCA cells regardless of basal HO-1 expression.

### HO-1 conferred cytoprotection to gamma radiation and DNA repair

HO-1 has been shown to exert prosurvival effect in cancer cells against chemotherapeutic agents [17]. However, the effect against radiation is not certain. Firstly, we determine the sensitivity of CCA cell lines to gamma irradiation by establishing the median effective dose (IC50) of radiation in antiproliferation (Fig. 2A). There was no clear relationship between the basal levels of HO-1 expression and IC50 doses, although the two lowest HO-1 expression cell lines were the most sensitive cell lines to radiation. Next we studied KKU-100 and M214 cells with stable HO-1 knockdown by transduction with lentiviral-mediated HO-1 shRNA. The knockdown clones were selected where the efficiency of HO-1 knockdown in KKU-100 and M214 cells were about 60% and almost 100%, respectively (Fig. 2B). The control cells and HO-1 knockdown cells of KKU-100 and M214 were exposed to 2.5 or 5.0 Gys of gamma radiation, respectively, and subject to clonogenic assay. The non-irradiated, HO-1 knockdown KKU-100 cells showed a decrease in their ability to form colonies when compared with shRNA control cells, but not observed in M214 cells (Fig. 2C & 2D, left bar groups). The role of HO-1 in colony forming became significant when CCA cells were exposed to gamma irradiation. The irradiated cells with HO-1 knockdown diminished significantly in their ability to form cancer cell colony, compared to the relevant control cells ($p<0.05$), suggesting that inhibiting of HO-1 sensitize CCA cells to gamma radiation (Fig. 2C & 2D, right bar groups).

To further evaluate the role of HO-1 in the maintenance of genomic stability, the level of phosphorylated histone H2AX (γ-H2AX) formation, a surrogate marker for unrepaired DNA double-strand breaks (DSBs) was determined in HO-1 knockdown and control CCA cells subjected to gamma irradiation. More γ- H2AX foci were observed in HO-1 knockdown KKU-100 cells compared to control, even before exposure to radiation (Fig. 2E) suggesting that HO-1 is associated with genome stability. Moreover, the number of γ- H2AX foci was significantly greater in HO-1 knocked down cells with exposure to gamma radiation when compared to the non-target siRNA control cells (Fig. 2F). The result indicated the suppression of HO-1 is associated with suppression of DNA DSBs repair mechanism.

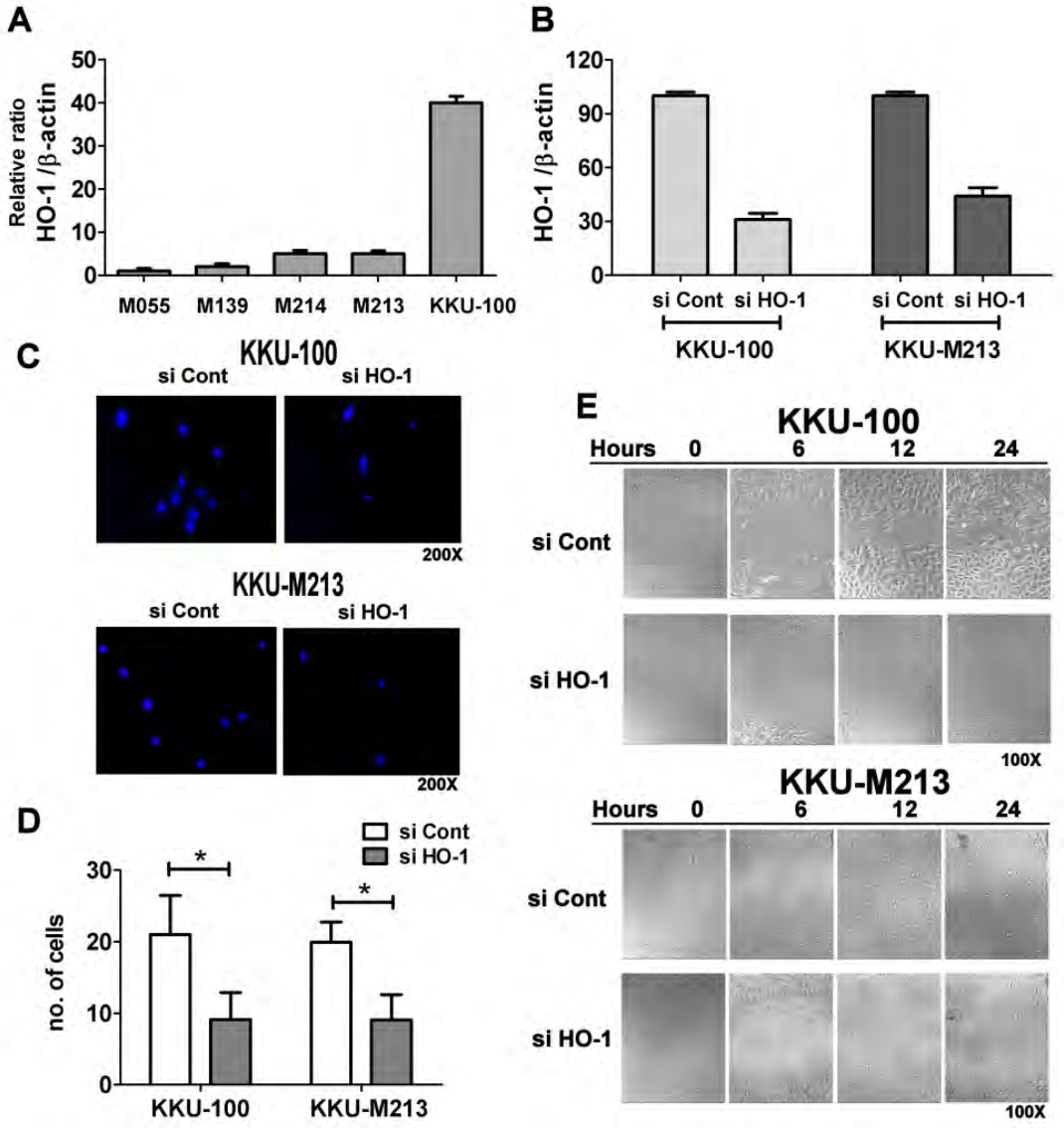


**Fig. 1 Expression of HO-1 in CCA cells and effect of HO-1 knockdown on cell migration.** **(a)** The basal HO-1 mRNA expression in CCA cells. Total RNA of CCA cells: KKU-100, M213, M214, M055 and M139, were collected and analyzed by real-time PCR. Each bar represents the relative expression of HO-1 normalized with β-actin. **(b)** KKU-100 and M213 were knocked down of HO-1 expression by HO-1 siRNA (si HO-1) or control transfection (si Cont). The efficiency was validated by using real-time PCR**. (c & d)** Cell migration of KKU-100 and M213 cells was performed using a transwell inserts. Representatives of DAPI-staining images of migrated cells, were captured under fluorescence microscope (original magnification 200X). **(d)** The number of colonies of KKU-100 and M213 cells was counted for four fields from each insert (original magnification 100X). Each bar represents the mean±SD of 12 fields from at least three independent experiments. * $p<0.05$ vs controls). **(e)** Wound-healing assay in KKU-100 and M213 cells. Cells were grown into confluence in 24-well plate. Images of four fields from each well were captured (original magnification 100X) and distance of the closing wound was measured.

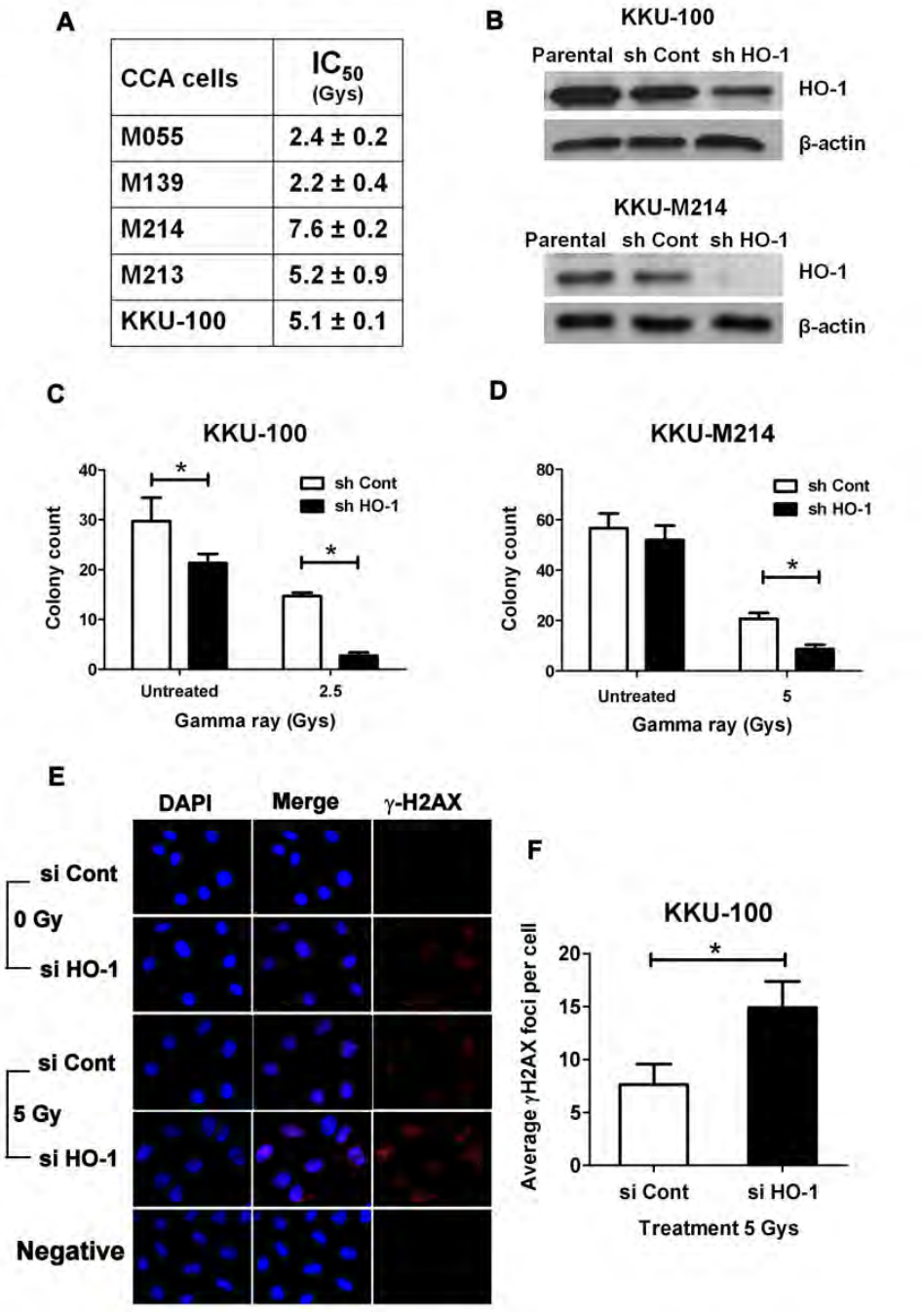


**Fig. 2 HO-1 knockdown enhanced the DNA damage of gamma radiation and formation of γ-H2AX foci.** **(a)** The sensitivity (IC50) of five CCA cell lines to gamma irradiation. The IC50 values represent mean±SD. **(b)** KKU-100 and M214 were stably knocked down HO-1 expression by transduction with HO-1 shRNA (sh HO-1) or control vector (sh Cont). The efficiency was validated by using Western blot analysis**. (c & d)** The clonogenic assay of CCA cells with or without irradiation. KKU-100 and M214 cells were irradiated by gamma radiation at the doses of 2.5 Gy and 5 Gy, respectively. Each bar represents the mean±SD, each from three separated experiments. * $p<0.05$ vs controls. **(e)** The representative fluorescent images of γ- H2AX foci (original magnification 600X). KKU-100 cells were transfected with HO-1 siRNA for 24 hr, then the cells were irradiated with gamma ray at 5 Gy. Left panel shows the DAPI staining to the nucleus, the right panel shows the γ- H2AX foci (red), and the merged images in the middle. Presented images are representatives of two independent experiments conducted in duplicate chambers. **(f)** Each bar represents the mean±SD of γ- H2AX foci per cell, each from two separated experiments. *$p<0.05$ vs control knockdown.

**Inhibition of HO-1 promoted G2-M arrest in CCA cells after irradiation**

HO-1 is known to regulate cell proliferation and migration, and the silencing of HO-1 expression suppresses cell growth [12, 15]. In this study, knockdown of HO-1 in both KKU-100 and M214 cells resulted in significant accumulation of cells (~10%) at G2-M phase (Fig. 3A and 3B) suggesting its role in cell cycle progression. However, dramatic G2-M arrest was observed in HO-1 knockdown CCA cells exposed to gamma irradiation (Fig. 3B). The proportion of cells in the G2-M phase in HO-1 knockdown KKU-100 cells was increased from 20% before irradiation to 48 % after the irradiation and that in M214 cells increased from 16% to 56% (Fig. 3B). It was noted that the effects on cell cycle progression by radiation were similar in KKU-100 and M214 cells regardless of their significant difference in basal HO-1 expression.

To characterize the influence of HO-1 in cell cycle progression, proteins of cell cycle regulators involved in G2-M transition were examined by Western immunoblotting. The basal expression levels of cyclin A, B1, and its positive regulator, cdc2, were higher in HO-1 knockdown cells of KKU-100 and M214 cells than in their corresponding control cells. These protein expression was even increased higher when the HO-1 knockdown cells were irradiated (Fig. 3C), supporting the functional role of HO-1 in cell cycle progression.

**Suppression of HO-1 enhanced antitumor response to GEM in vitro and in vivo**

The effect of HO-1 inhibition in relation to GEM-induced cytotoxicity was evaluated *in vitro* and *in vivo*. In the *in vitro* study, the toxicity of ZnPP, as a HO-1 inhibitor, and GEM alone was evaluated in KKU-100 cells. The cytotoxicity of ZnPP and GEM was dose-dependent (Fig. 4A). ZnPP at 10 nM induced cytotoxicity of less than 10%, which was then used in combination with GEM. The drug combination enhanced cytotoxicity, particularly at low concentrations of GEM (Fig. 4B).

The enhanced cytotoxic effect of GEM by ZnPP was further evaluated in nude mice xenografted with KKU-100 cells. The mice were treated with ZnPP or GEM or both in combination. Tumor mass in control mice grew exponentially during the study (Fig. 4C). Treatment with GEM or ZnPP alone for 3 cycles resulted in a partial suppression of tumor growth when compared with non-treatment controls. In contrast, the combination of ZnPP and GEM caused almost complete arrest of tumor growth (Fig. 4C). The treatment with individual agent or in combination for 3 cycles did not cause overt toxicity, as indicated by absence of significant changes in body weight (Fig. 4D). The mean tumor weight (mg) on day 17, three days after the last cycle of treatment, was 772, 427, 300 and 110 mg, for control, ZnPP, GEM and the combination group, respectively (Fig. 4E and 4F).

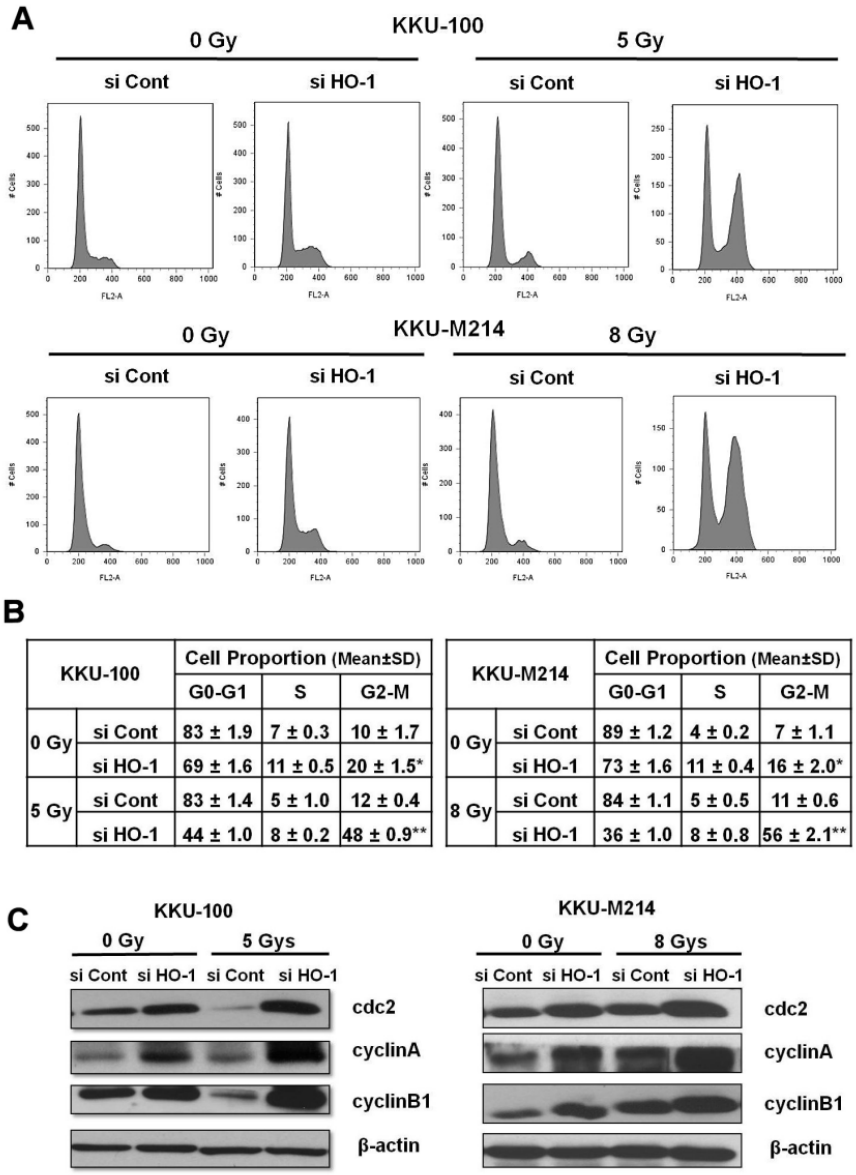


**B**

| KKU-100 | | Cell Proportion (Mean±SD) | | |
|---|---|---|---|---|
| | | G0-G1 | S | G2-M |
| 0 Gy | si Cont | 83 ± 1.9 | 7 ± 0.3 | 10 ± 1.7 |
| | si HO-1 | 69 ± 1.6 | 11 ± 0.5 | 20 ± 1.5* |
| 5 Gy | si Cont | 83 ± 1.4 | 5 ± 1.0 | 12 ± 0.4 |
| | si HO-1 | 44 ± 1.0 | 8 ± 0.2 | 48 ± 0.9** |

| KKU-M214 | | Cell Proportion (Mean±SD) | | |
|---|---|---|---|---|
| | | G0-G1 | S | G2-M |
| 0 Gy | si Cont | 89 ± 1.2 | 4 ± 0.2 | 7 ± 1.1 |
| | si HO-1 | 73 ± 1.6 | 11 ± 0.4 | 16 ± 2.0* |
| 8 Gy | si Cont | 84 ± 1.1 | 5 ± 0.5 | 11 ± 0.6 |
| | si HO-1 | 36 ± 1.0 | 8 ± 0.8 | 56 ± 2.1** |




**Fig. 3 Effect of HO-1 knockdown and irradiation on cell cycle distribution and regulatory proteins in cell cycle.** **(a)** The cell cycle histograms represent DNA content using FACS analysis. KKU-100 and M214 cells were transfected with HO-1 siRNA (si HO-1) or control (si Cont) with or without gamma irradiation at 5 and 8 Gy, respectively. Cells were collected and stained with propidium iodide for flow analysis. **(b)** The tables present the percentage of cells in cell cycle. Each value represents the mean±SD, each from three separated experiments. *$p$<0.05 HO-1 knockdown vs control knockdown, **$p$<0.05 irradiated HO-1 knockdown vs nonirradiated HO-1 knockdown. (**c)** Immunoblots of regulatory proteins in cell cycle. Following the irradiation on wild type or HO-1 knockdown KKU-100 and M214 cells, cell lysates were prepared and analyzed by Western immunobloting for cdc2, cyclin A, cyclin B1 and β-actin as a loading control. The experiment was done twice with similar results, and representative bands from one experiment are shown.

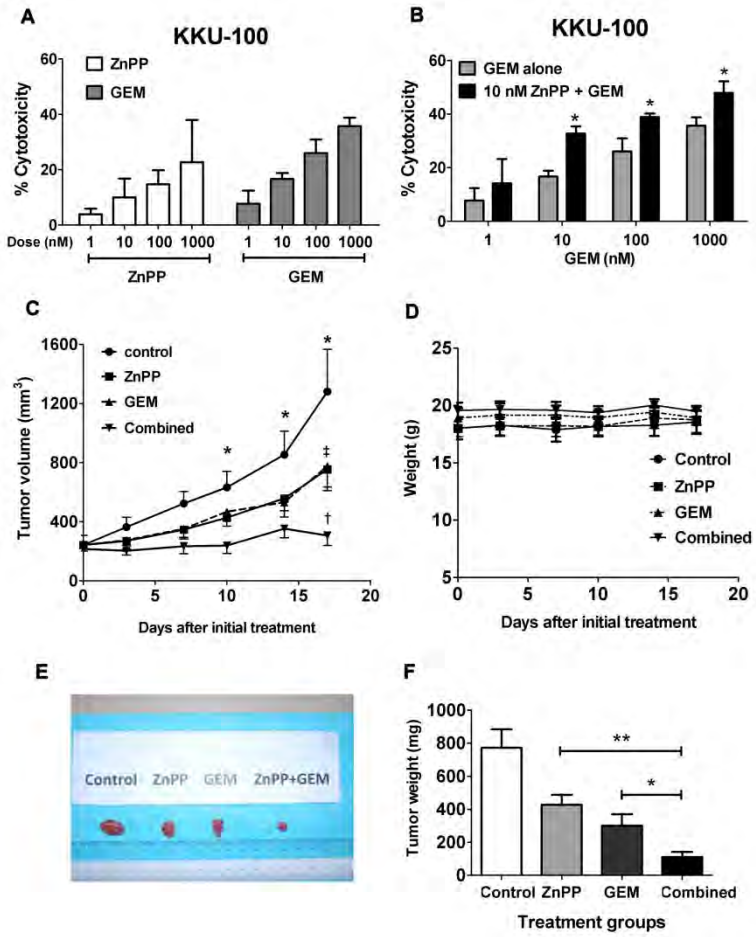


**Fig. 4 Inhibition of HO-1 by ZnPP enhances the antitumor effect of GEM *in vitro* and *in vivo*.** (**a**) The dose-response cytotoxicity of ZnPP and GEM in KKU-100 cells after incubation for 24 h. **(b)** Enhanced cytotoxicity of GEM by ZnPP. KKU-100 cells with or without pretreatment with ZnPP for 4 h were exposure to GEM for another 24 h. Each bar represents the mean±SD from each three independent experiment. * $p$<0.05 vs GEM alone. **(c)** Time-course of tumor growth on nude mice transplanted with KKU-100 cells. ZnPP, GEM, combination of ZnPP and GEM and saline as vehicle control were administered intraperitoneally on days 0, 7 and 14, when the tumor mass grew to have at least 200 $mm^3$. Each value represents the mean±SEM, each from 7 mice per group. * $p$<0.05 the combination group vs control group; † $p$<0.05 the combination vs ZnPP alone, and ‡ $p$<0.05 the combination vs GEM alone. **(d)** Time-course of body weights of mice during the drug treatments. **(e)** The representative of tumors resected from mice on day 17. **(f)** The tumor weights from each group of treatment on day 17. Each bar represents the mean±SEM each from 7 mice in the group. * $p$<0.05 drug combination vs GEM alone, and ** $p$<0.05 drug combination vs ZnPP alone.

### Combined GEM and ZnPP treatment suppressed tumor growth via activation of p53 pathway

We further investigated whether suppression of tumor growth was associated with the inhibition of cell proliferation and angiogenesis of tumor tissues. Tumor tissues extracted from 4 groups of animals were analyzed for the expression of Ki-67 and CD31 by immunohistochemistry. The monotherapy of GEM or ZnPP significantly suppressed the nuclear expression of Ki-67 compared to control group (Fig. 5A). The drug combination further decreased the expression of Ki-67 more than the monotherapy. For the CD31 staining, a representative of microvascular density, tumor tissues from control group showed the highest density of the blood vessels, followed by the ZnPP-alone and GEM-alone groups. Tumors from drug combination group showed the lowest density (Fig. 5B). These results indicated that the drug combination enhanced anti-proliferation and anti-angiogenesis in CCA.

Since the suppression of HO-1 activity by ZnPP enhanced GEM-induced antiproliferation and inhibition of neoangiogenesis, the underlying mechanism was explored. The p53 and its negative regulator, mdm2, and p21 protein expression in tumor tissues were evaluated. The immunohistochemistry showed that the drug combination induced p53 at a higher level than that of single drug treatment (Fig. 6A & 6C). On the other hand, mdm2 was highly expressed in control tissues and was decreased in GEM or ZnPP group and most remarkably decreased in drug combination group (Fig. 6B). Expression of p21 or cyclin-dependent kinase inhibitor 1, was highly expressed in the combination treatment group followed by the single drug treatment groups with the lowest in the control (Fig. 6D). The results demonstrated the effect of ZnPP-enhanced GEM-induced tumor suppression was associated with p53 and downstream protein expression.

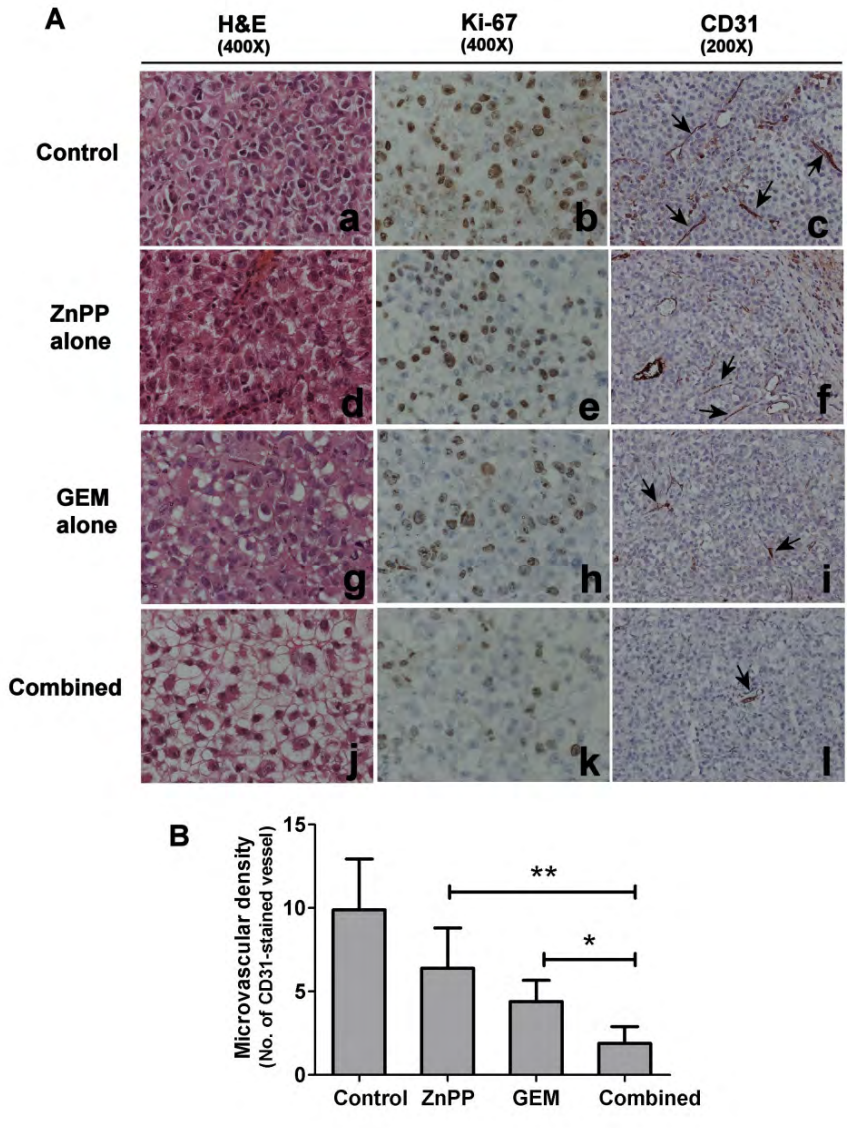


**Fig. 5 Immunohistochemistry of Ki-67 and CD31 staining in tumor tissues.** **(a)** The tumor tissues from mice treated with various drug regimens were analyzed by H&E staining and immunohistochemical staining for Ki-67 and CD31. Panels a-c: control; d-f: ZnPP alone, g-i: GEM alone; j-l: combination of GEM and ZnPP. Panels a, d, g, j; H&E staining; b, e, h, k for Ki-67 staining; c, f, i,l for CD31 staining (the arrows indicate microvessels). **(b)** Microvascular density as assessed by CD31 staining (original magnification 200X). Each bar represents the mean±SD, each from 7 mice * $p<0.05$ drug combination vs GEM alone, and ** $p<0.05$ drug combination vs ZnPP alone.

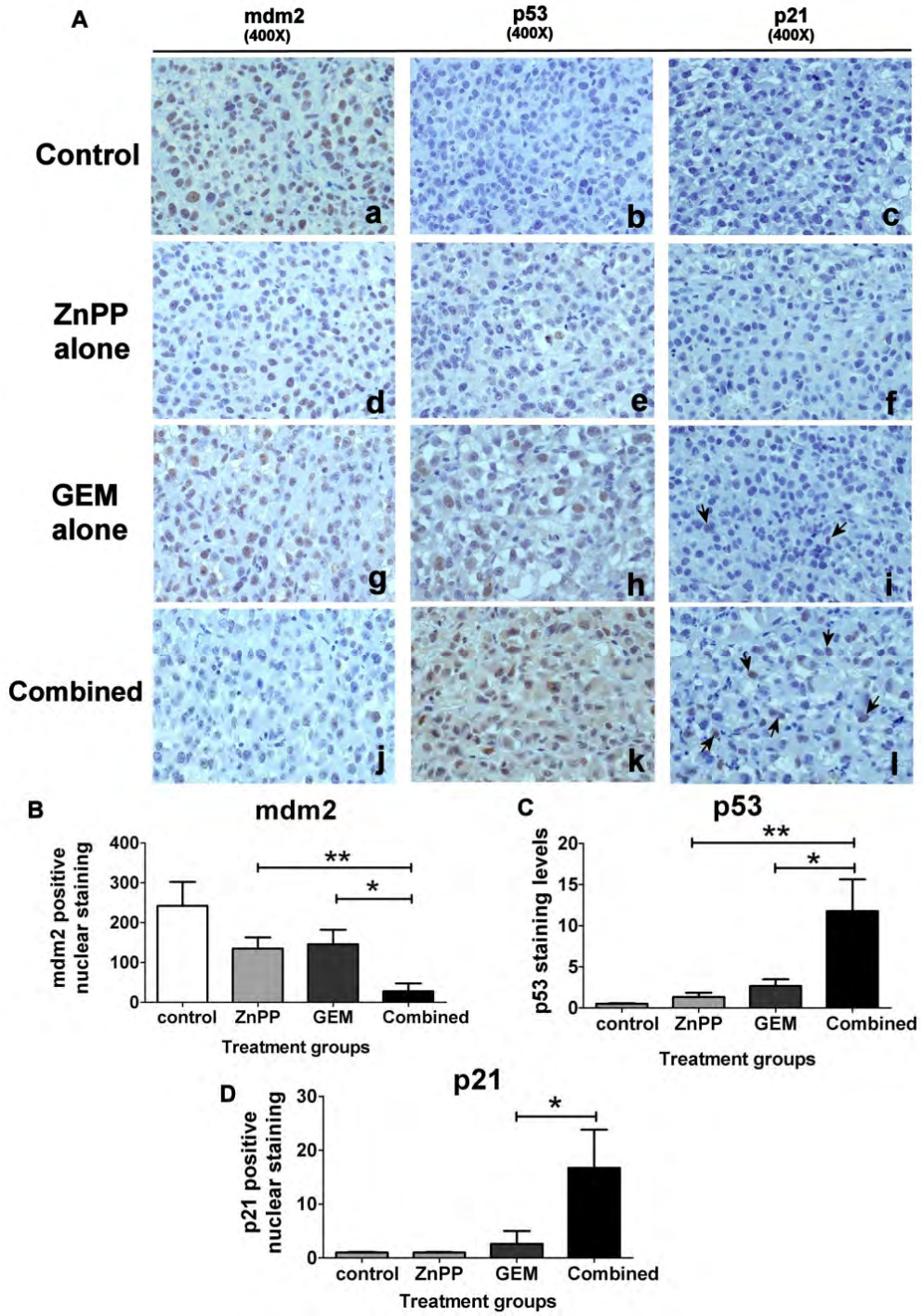


**Fig. 6 Immunohistochemistry of mdm2, p53 and p21 staining in tumor tissues.** **(a)** The tumor tissues from mice treatment with various drug regimens were analyzed by immunohistochemical staining for mdm2, p53 and p21. Panels a-c: control; d-f: ZnPP alone, g-i: GEM alone; j-l: combination of GEM and ZnPP. Panels a, d, g and j for mdm2 staining; b, e, h and k for p53 staining; c, f, i, and l for p21staining. (original magnification 400X). **(b)** The numbers of mdm2 positive-nuclear staining, **(c)** levels of p53 staining, assessed from the intensity and area of staining and **(d)** the numbers of p21 positive-nuclear staining were shown. Each bar represents the mean±SD, each from 7 mice * $p<0.05$ drug combination vs GEM alone, and ** $p<0.05$ drug combination vs ZnPP alone.

**Discussion**

HO-1 confers a powerful cytoprotective effect against various insults in normal tissues [24-25]. Several lines of evidences have demonstrated that HO-1 plays an important role in tumor growth, anti-apoptosis, angiogenesis, metastasis, and DNA repair response following chemotherapeutic or radiotherapy treatment [11]. In this study, we showed the crucial role of HO-1 in radiotherapy and chemotherapy in cholangiocarcinoma that, regardless of it basal expression level.

HO-1 plays an important role in cell proliferation, and the hyperplastic and malignant tissues showed pronounced increase in HO-1 expression [13] which was associated with cell migration and invasion [12]. Role of HO-1 in cancer may be mediated via the Nrf2-HO-1 axis, where it is activated in some cancers [8]. The present works were consistent with these findings in that HO-1 is necessary for CCA cells proliferation and migration. HO-1 knockdown in both high and low HO-1 expressing cells, i.e. KKU-100 or M213 cells showed diminished ability of migration in transwell and wound healing assays.

The role of HO-1 in cell proliferation under genotoxic stress by gamma irradiation is even more important. In non-radiation condition, knockdown of HO-1 in only the high HO-1 expressing KKU-100 cells could impair the clonogenic survival. However, with gamma radiation, both KKU-100 and M214 cells require HO-1 for colony forming ability. This suggests that HO-1 plays an important role in proliferative ability especially at severe stress condition in CCA cells. Our study is consistent with recent studies in that HO-1 inhibition enhanced the X-ray irradiation in reducing clonogenic survival in A549 cells [26].

The role of HO-1 may be extended to DNA repair system in some cancers [24] and probably including CCA cells. γ-H2AX is a phosphorylated form of the histone H2AX by action of ATM, ATR and other kinases in the chromatin microenvironment marking the accommodation of adaptor proteins for DNA repair process [27]. γ-H2AX foci are therefore used as markers of DNA damage and vanishing of the γ-H2AX foci reflects efficiency of the DNA repair of cells [24, 28]. In HO-1 knockdown CCA cells, there was an increased level of γH2AX foci and when cells were irradiated, the foci were markedly increased as compared with control cells (Figure 2E & 2F). Our results were consistent with recent studies that several organs from $Hmox1^{-/-}$ mice had increased γH2AX foci [24]. HO-1 may be important in DNA repair, as HO-1 knockdown resulted in increase in γH2AX foci in association with marked cell cycle derangement, suggesting the role of HO-1 in the interplay of DNA repair mechanism and cell cycle progression in CCA cells.

The antiproliferative effect in CCA cells is associated with cell cycle arrest in that HO-1 knockdown caused a cell cycle arrest at G2-M phase. Gamma irradiation further potentiated the cell cycle arrest. It suggests the important role of HO-1 in regulation of cell cycle progression and DNA repair mechanism, as unrepaired chromosome will result in cell cycle arrest or apoptosis [29]. Our study is consistent with the role of HO-1 in cell cycle progression and is even more obvious in cells treated with gamma irradiation. Together these results explained the enhanced antiproliferation of irradiation in HO-1 knockdown cells.

The deregulation of cell cycle was found to be related to the expression of cell cycle related proteins in HO-1 knockdown cells. Western immunoblotting revealed a marked increase in cyclin A and B1 and cdc2 protein expression in both cell lines. Cyclin A is synthesized in late G1 and accumulates during S and G2 phase. Expression of cyclin B, a major activator of cdc2 [30], is normally maximal during the G2 to M phase transition and controls passage through the M phase. In

normal cells, the mitosis phase is initiated by the cdc2/Cyclin B1 complex, however, in cancer cells, these proteins are deregulated [31]. In contrast to our results, pectenotoxin-2-induced G2-M arrest was associated with the reduced levels of cdc2, cylcin B1 and cdc25C in MDA-MB-231 cells [32]. It is, therefore, the alteration of these checkpoint proteins could be variable depending on inducing agents [33].

In previous reports showed that ZnPP, a HO-1 inhibitor, enhanced the sensitivity of CCA cells to chemotherapeutic agents *in vitro* [17]. In the present study, we demonstrated that the inhibition of HO-1 activity by ZnPP significantly potentiated the chemotherapeutic effect of GEM *in vivo* using CCA xenograft model. This result was consistent with recent studies using xenografted urothelial tumor, LL/2 lung cancer and pancreatic tumor in mice, where treatment with GEM plus ZnPP resulted in inhibition of tumor growth [14, 34]. The drug combination probably inhibits cancer proliferation by interrupting the cell cycle and inhibiting neovascularization by suppression the levels of vascular endothelial growth factor in tumors [16]. *In vivo* with mice study, ZnPP or GEM alone suppressed tumor growth with decrease in Ki-67; the regulatory protein for cell cycle and CD31 or PECAM-1which represents microvascular density. The combination of HO-1 inhibitor and GEM strongly decreased of Ki-67 and CD31 expression more than monotherapy. This suggests the enhanced tumor suppression may be from inhibition of cell proliferation and neovascularization.

The mechanism of CCA growth suppression by the drug combination is associated markedly with increased levels of p53 and p21expression in tumor tissues where the monotherapy of ZnPP or GEM did not affect these levels. p21 has been reported as a p53-dependent downstream transcriptional control, and a potent cyclin-dependent kinase inhibitor, inhibiting cell cycle progression and growth [35]. It is noted that GEM or ZnPP alone could only slow down tumor growth, as both treatment did not significantly induce p53 and p21 levels. These present results were consistent with our previous *in vitro* studies , which found increased p21 and cytochrome c expression in the drug combination group compared to drug alone [17]. The p53 can also cause cell death through the Bcl2 proteins which can induce the intrinsic mitochondrial apoptotic pathway [36]. Our previous studies showed that the drug combination could induce a massive formation of reactive oxygen species which was associated with mitochondrial dysfunction triggering cell death in CCA cells [17].

It should be noted that animals in ZnPP group or combination group did not show any overt signs of toxicity, because body weight loss, generally a sensitive index of toxicity, was unchanged in all animals. Therefore, it probably allow further optimization of the dosage regimen to maximize the antitumor activity. The strong sensitizing effect of HO-1 inhibition to chemotherapeutic agents may be of relevance in clinical setting where drug resistance is the main cause of failure in cancer chemotherapy.

In summary, inhibition of HO-1 resulted in antiproliferation, and suppression of cytoprotection when it is in combination with anticancer agent (eg. gemcitabine) or gamma radiation in CCA cells. The antiproliferation of HO-1 knockdown is associated with cell cycle arrest. The animal experiment showed the potential tumor suppression effect by using combination of ZnPP plus GEM. This study may provide a novel treatment strategy for CCA by combining HO-1 inhibitor with chemotherapy and radiotherapy.

**References**


1. Khan SA, Thomas HC, Davidson BR, Taylor-Robinson SD: **Cholangiocarcinoma**. *Lancet* 2005, **366**:1303-1314.
2. Skipworth JR, Olde Damink SW, Imber C, Bridgewater J, Pereira SP, Malago M: **Review article: surgical, neo-adjuvant and adjuvant management strategies in biliary tract cancer**. *Aliment Pharmacol Ther* 2011, **34**:1063-1078.
3. Farges O, Fuks D, Boleslawski E, Le Treut YP, Castaing D, Laurent A, Ducerf C, Rivoire M, Bachellier P, Chiche L *et al*: **Influence of surgical margins on outcome in patients with intrahepatic cholangiocarcinoma: a multicenter study by the AFC-IHCC-2009 study group**. *Ann Surg* 2011, **254**:824-829; discussion 830.
4. Khan SA, Davidson BR, Goldin RD, Heaton N, Karani J, Pereira SP, Rosenberg WM, Tait P, Taylor-Robinson SD, Thillainayagam AV *et al*: **Guidelines for the diagnosis and treatment of cholangiocarcinoma: an update**. *Gut* 2012, **61**:1657-1669.
5. Butthongkomvong K, Sirachainan E, Jhankumpha S, Kumdang S, Sukhontharot OU: **Treatment outcome of palliative chemotherapy in inoperable cholangiocarcinoma in Thailand**. *Asian Pac J Cancer Prev* 2013, **14**:3565-3568.
6. Patel T: **Cholangiocarcinoma--controversies and challenges**. *Nat Rev Gastroenterol Hepatol* 2011, **8**:189-200.
7. Buranrat B, Prawan A, Kukongviriyapan U, Kongpetch S, Kukongviriyapan V: **Dicoumarol enhances gemcitabine-induced cytotoxicity in high NQO1-expressing cholangiocarcinoma cells**. *World J Gastroenterol* 2010, **16**:2362-2370.
8. Na HK, Surh YJ: **Oncogenic potential of Nrf2 and its principal target protein heme oxygenase-1**. *Free Radic Biol Med* 2014, **67**:353-365.
9. Zeekpudsa P, Kukongviriyapan V, Senggunprai L, Sripa B, Prawan A: **Suppression of NAD(P)H-quinone oxidoreductase 1 enhanced the susceptibility of cholangiocarcinoma cells to chemotherapeutic agents**. *J Exp Clin Cancer Res* 2014, **33**:11.
10. Prawan A, Kundu JK, Surh YJ: **Molecular basis of heme oxygenase-1 induction: implications for chemoprevention and chemoprotection**. *Antioxid Redox Signal* 2005, **7**:1688-1703.
11. Jozkowicz A, Was H, Dulak J: **Heme oxygenase-1 in tumors: is it a false friend?** *Antioxid Redox Signal* 2007, **9**:2099-2117.
12. Gueron G, De Siervi A, Ferrando M, Salierno M, De Luca P, Elguero B, Meiss R, Navone N, Vazquez ES: **Critical role of endogenous heme oxygenase 1 as a tuner of the invasive potential of prostate cancer cells**. *Mol Cancer Res* 2009, **7**:1745-1755.
13. Maines MD, Abrahamsson PA: **Expression of heme oxygenase-1 (HSP32) in human prostate: normal, hyperplastic, and tumor tissue distribution**. *Urology* 1996, **47**:727-733.
14. Nuhn P, Kunzli BM, Hennig R, Mitkus T, Ramanauskas T, Nobiling R, Meuer SC, Friess H, Berberat PO: **Heme oxygenase-1 and its metabolites affect pancreatic tumor growth in vivo**. *Mol Cancer* 2009, **8**:37.
15. Berberat PO, Dambrauskas Z, Gulbinas A, Giese T, Giese N, Kunzli B, Autschbach F, Meuer S, Buchler MW, Friess H: **Inhibition of heme oxygenase-1 increases responsiveness of pancreatic cancer cells to anticancer treatment**. *Clin Cancer Res* 2005, **11**:3790-3798.
16. Hirai K, Sasahira T, Ohmori H, Fujii K, Kuniyasu H: **Inhibition of heme oxygenase-1 by zinc protoporphyrin IX reduces tumor growth of LL/2 lung cancer in C57BL mice**. *Int J Cancer* 2007, **120**:500-505.
17. Kongpetch S, Kukongviriyapan V, Prawan A, Senggunprai L, Kukongviriyapan U, Buranrat B: **Crucial Role of Heme Oxygenase-1 on the Sensitivity of Cholangiocarcinoma Cells to Chemotherapeutic Agents**. *PLoS ONE* 2012, **7**:e34994.

18. Vanella L, Di Giacomo C, Acquaviva R, Barbagallo I, Cardile V, Kim DH, Abraham NG, Sorrenti V: **Apoptotic markers in a prostate cancer cell line: effect of ellagic acid**. *Oncol Rep* 2013, **30**:2804-2810.
19. Sripa B, Leungwattanawanit S, Nitta T, Wongkham C, Bhudhisawasdi V, Puapairoj A, Sripa C, Miwa M: **Establishment and characterization of an opisthorchiasis-associated cholangiocarcinoma cell line (KKU-100)**. *World J Gastroenterol* 2005, **11**:3392-3397.
20. Yonglitthipagon P, Pairojkul C, Chamgramol Y, Loukas A, Mulvenna J, Bethony J, Bhudhisawasdi V, Sripa B: **Prognostic significance of peroxiredoxin 1 and ezrin-radixin-moesin-binding phosphoprotein 50 in cholangiocarcinoma**. *Hum Pathol* 2012, **43**:1719-1730.
21. Tusskorn O, Prawan A, Senggunprai L, Kukongviriyapan U, Kukongviriyapan V: **Phenethyl isothiocyanate induces apoptosis of cholangiocarcinoma cells through interruption of glutathione and mitochondrial pathway**. *Naunyn Schmiedebergs Arch Pharmacol* 2013, **386**:1009-1016.
22. Buranrat B, Prawan A, Sripa B, Kukongviriyapan V: **Inflammatory cytokines suppress arylamine N-acetyltransferase 1 in cholangiocarcinoma cells**. *World J Gastroenterol* 2007, **13**:6219-6225.
23. Chan-On W, Kuwahara K, Kobayashi N, Ohta K, Shimasaki T, Sripa B, Leelayuwat C, Sakaguchi N: **Cholangiocarcinomas associated with long-term inflammation express the activation-induced cytidine deaminase and germinal center-associated nuclear protein involved in immunoglobulin V-region diversification**. *Int J Oncol* 2009, **35**:287-295.
24. Otterbein LE, Hedblom A, Harris C, Csizmadia E, Gallo D, Wegiel B: **Heme oxygenase-1 and carbon monoxide modulate DNA repair through ataxia-telangiectasia mutated (ATM) protein**. *Proc Natl Acad Sci U S A* 2011, **108**:14491-14496.
25. Tsuchihashi S, Zhai Y, Bo Q, Busuttil RW, Kupiec-Weglinski JW: **Heme oxygenase-1 mediated cytoprotection against liver ischemia and reperfusion injury: inhibition of type-1 interferon signaling**. *Transplantation* 2007, **83**:1628-1634.
26. Zhang W, Qiao T, Zha L: **Inhibition of heme oxygenase-1 enhances the radiosensitivity in human nonsmall cell lung cancer a549 cells**. *Cancer Biother Radiopharm* 2011, **26**:639-645.
27. Celeste A, Fernandez-Capetillo O, Kruhlak MJ, Pilch DR, Staudt DW, Lee A, Bonner RF, Bonner WM, Nussenzweig A: **Histone H2AX phosphorylation is dispensable for the initial recognition of DNA breaks**. *Nat Cell Biol* 2003, **5**:675-679.
28. Ivashkevich A, Redon CE, Nakamura AJ, Martin RF, Martin OA: **Use of the gamma-H2AX assay to monitor DNA damage and repair in translational cancer research**. *Cancer Lett* 2012, **327**:123-133.
29. Jackson SP: **Detecting, signalling and repairing DNA double-strand breaks**. *Biochem Soc Trans* 2001, **29**:655-661.
30. Vermeulen K, Van Bockstaele DR, Berneman ZN: **The cell cycle: a review of regulation, deregulation and therapeutic targets in cancer**. *Cell Prolif* 2003, **36**:131-149.
31. Evan GI, Vousden KH: **Proliferation, cell cycle and apoptosis in cancer**. *Nature* 2001, **411**:342-348.
32. Moon DO, Kim MO, Nam TJ, Kim SK, Choi YH, Kim GY: **Pectenotoxin-2 induces G2/M phase cell cycle arrest in human breast cancer cells via ATM and Chk1/2-mediated phosphorylation of cdc25C**. *Oncol Rep* 2010, **24**:271-276.
33. DiPaola RS: **To arrest or not to G(2)-M Cell-cycle arrest : commentary re: A. K. Tyagi et al., Silibinin strongly synergizes human prostate carcinoma DU145 cells to doxorubicin-induced growth inhibition, G(2)-M arrest, and apoptosis**. *Clin Cancer Res* 2002, **8**:3311-3314.

34. Miyake M, Fujimoto K, Anai S, Ohnishi S, Nakai Y, Inoue T, Matsumura Y, Tomioka A, Ikeda T, Okajima E *et al*: **Inhibition of heme oxygenase-1 enhances the cytotoxic effect of gemcitabine in urothelial cancer cells**. *Anticancer Res* 2010, **30**:2145-2152.
35. Li CH, Tzeng SL, Cheng YW, Kang JJ: **Chloramphenicol-induced mitochondrial stress increases p21 expression and prevents cell apoptosis through a p21-dependent pathway**. *J Biol Chem* 2005, **280**:26193-26199.
36. Galluzzi L, Blomgren K, Kroemer G: **Mitochondrial membrane permeabilization in neuronal injury**. *Nat Rev Neurosci* 2009, **10**:481-494.

# Section 3

## NQO1 Expression is Correlated with the Prognosis of Cholangiocarcinoma

### Introduction

Cholangiocarcinoma (CCA) is a malignant neoplasm originating from the bile duct epithelium. Although CCA is a rare cancer worldwide, the incidence and mortality rates have grown up in the US, United Kingdom, Japan and Australia [1]. The incidence of this cancer is very high in regions of northeast Thailand, Cambodia, and Laos, where the prevalence of liver fluke infection is very high [2-3]. *Opisthorchis viverrini* infection is one of the important risk factors of CCA probably through chronic inflammation-induced oxidative stress and nitrosative stress [4-5], since chronic inflammation predisposes to several types of cancers. Activated inflammatory cells release a variety of inflammatory cytokines such as IL-1β, IFN–γ, TNF-α and inflammatory mediators, including nitric oxide and prostaglandin E2 which act as tumor promoters [6-7]. CCA is an aggressive malignancy characterized by the resistance to the current chemotherapy and radiotherapy in vast majority of cases [1]. Diagnosis of CCA is very difficult because of the nonspecific clinical manifestations and the lack of appropriate biomarkers [1, 8]. Complete surgical excision with negative tumor margin, solitary lesion, absence of lymph node involvement, and lack of vascular invasion are the best predictors for long term survival [8]. However, current predictors of pathological and operative staging strategies do not accurately predict long-term prognosis of CCA patients. The other markers for diagnosis or treatment such as serum markers of CA 19-9 and CEA are of very limited value [1].

NAD(P)H:quinone oxidoreductase-1 (NQO1) is a ubiquitous flavoprotein that functions as an antioxidant enzyme [9]. The enzyme catalyzes two electron reduction of quinones to hydroquinones, thus avoids a one electron reduction and associated redox cycling which generates reactive oxygen species (ROS) (Dinkova-Kostova, 2010). Functions of NQO1 include xenobiotic detoxification, superoxide scavenger and the maintenance of endogenous antioxidant vitamins [9]. The antioxidant role of NQO1 was suggested by evidences such that the disruption of NQO1 gene [10] or genetic polymorphism increased the risk of chemical-induced toxicity and cancers [11-12]. Several lines of evidences indicate that cancer chemoprevention afforded by regular intake of dietary phytochemicals involves with induction of the phase II enzymes including NQO1 [13]. It is conceivable that NQO1 plays an important role in protecting normal cells against oxidative injury and carcinogenesis.

Over-expression of NQO1 mRNA in tumor tissue compared to the surrounding normal tissue was reported in liver cancer [14], lung cancer [15], pancreatic cancer [16], and over-expression of NQO1 detected by immunohistochemistry in breast, ovary, thyroid, adrenal, colorectal and bladder was also observed [17]. These circumstantial evidences suggest that over-expression of NQO1 may confer cytoprotection for tumor cells against oxidative stress and cause cells resistant to anticancer agents [18]. The treatment of CCA based on targeting NQO1 has been shown to be a potential strategy to overcome the resistance in CCA [19]. In this study we analyzed NQO1 expression in CCA tumor and apparently normal adjacent tissues and examined whether NQO1 expression could be a prognostic marker of CCA in association with the overall survival.

## Materials and Methods

### Subjects

Subjects were patients admitted at Sringarind Hospital, Khon Kaen University for the treatment of cholangiocarcinoma. All patients have been diagnosed and confirmed by histopathological examination. Their average age was (mean ± SD) 56.1 ± 9.4 years, with 27 males and 16 females. Their survival time ranged from 36 days to 1,120 days, at which time the subjects were still alive. In this study, nine patients (22.5%) received adjuvant chemotherapy after surgery. Tumor tissues were collected from surgical resection of tumor mass for histopathological examination and other tissue samples were kept in liquid nitrogen before uses for extraction of RNA and enzymatic assay.

### Tissue samples

Forty-three tissue sections from the specimen bank of the Liver Fluke and Cholangiocarcinoma Research Center, Faculty of Medicine, Khon Kaen University. The study protocol was approved by the Khon Kaen University Ethics Committee for Human Research. Written informed consent was obtained from all patients. Among forty three samples, thirty samples were available as the pair of tumorous and non-tumorous tissues. Samples of the same tissue section were used for assays of NQO1 activity and total mRNA. Patients who died within 2 weeks after operation were excluded from this study.

### Immunohistochemistry

CCA tissue sections were cut from archival paraffin blocks. Sections were deparaffinized in xylene and rehydrated through descending alcohol series to distilled water. Endogenous peroxidase activity was eliminated by placing sections in 3% hydrogen peroxide for 30 min. Sections were rinsed in PBS for 10 min and then blocked in 5% milk in PBST for 20 min. Immunohistochemistry analysis of NQO1 was performed using mouse monoclonal IgG against NQO1 (sc-32793, Santa Cruz, CA, USA) 1:100 dilution for an overnight at 4°C, followed by Immunodetection with Envision system-HRP labeled polymer anti-mouse (Dako) for 1 hr. Sections were counterstained with hematoxylin, and photographed.

### NQO1 activity in tissues.

Tissues was thawed, cut into small pieces in ice-cold 1.15% (w/v) KCl in 0.1 M phosphate buffer pH 7.4 and homogenized with Utra-Turrax homogenizer. Homogenates were centrifuged at 100,000 g at 4°C for 6 min. Finally, supernatant was collected for the cytosol fraction and the microsomal pellet was resuspended by homogenizing the pellet in the same buffer. Cytosol and microsomal fractions were preserved with 20% (v/v) glycerol. Aliquots of samples were stored at -70°C until use.

NQO1 activity was measured according to the previously described method [20] with slight modifications [21]. Cytosol samples were assayed by coupling reaction using menadione and MTT (3-(4,5-dmethylthiazol-2-yl)-2,5-diphenyltetrazolium bromide, a tetrazole) as the substrate. Tissue cytosol was added to reaction mixture containing with Tris 25 mM, pH 7.4, bovine serum albumin 67 mg/mL, 0.015% tween-20, 50 µM FAD, 1 mM glucose-6-phosphate (G6P), 30 □M NADP, 2 unit/mL G6P-dehydrogenase, 0.03 mg/mL MTT and 0.24 µM menadione. The assay was performed in the presence and absence of 50 µM dicoumarol. The enzyme activity was measured as a

rate-kinetics at a wavelength of 620 nm, and the readings were made at 30 sec intervals for 5 min. The initial velocity of dicoumarol-suppressible kinetics was calculated as the NQO1 activity using the extinction coefficient of formazan of MTT of 11,300 $M^{-1}$ $cm^{-1}$.

**RNA preparation and reverse transcription-polymerase chain reaction**

Total RNA was extracted from tumor tissues using Trizol reagent following the manufacturer's instruction. Total RNA (1 µg) was reverse-transcribed in 20 µL containing 0.5 µg of oligo$(dT)_{15}$ primer, 20 U of RNasin® ribonuclease inhibitor and 200 U of ImProm-II ™ reverse trancriptase in 10 x PCR buffer, 3 mmol/L $MgCl_2$, and 1 mmol/L dNTPs. The first-strand cDNA was synthesized at condition of 42°C for 60 min. The reverse transcription products were served as a template for real-time PCR. PCR amplification was performed using specific primers for the NQO1 using beta-actin as an internal control. The PCR primer sequences were: NQO1; forward primer: 5' GGC AGA AGA GCA CTG ATC GTA 3', NQO1; reverse primer: 5' TGA TGG GAT TGA AGT TCA TGG C 3', GenBank accession number BC007659.2, with the expected amplicon size of 159 bp, beta-actin; forward primer: 5' TGC CAT CCT AAA AGC CAC 3', beta-actin; reverse primer: 5' TCA ACT GGT CTC AAG TCA GTG 3', GenBank accession number NM_001101.3 with amplicon size of 290 bp. The real-time PCR, based on SYBR Green, was carried out in a final volume of 20 µL containing 1x SYBR Green master mix, 0.5 µmol/L of each NQO1 or beta-actin primers. Thermal cycling was performed for each gene in duplicate on cDNA samples in 96-wells reaction plate using the ABI 7500 Sequence Detection system (Applied Biosystems). The negative control, set up by substituting the template with deionized $H_2O$ and that routinely had a high Ct value which represented the lower detection limit, was included in the experimental runs. Real-time PCR was conducted with the following cycling conditions: 95°C for 10 min, followed by 40 cycles of 95°C for 15 s, 55°C for 30 s and 72°C for 45 s. Assay was performed in triplicate. The relative expression ratio (R) of the target genes was calculated based on the efficiency (E) and CT deviation and expressed as the ratio to the reference gene. The corresponding real time PCR efficiencies were calculated according to the equation $E = 10^{[-1/slope]}$. All data were analyzed using Sequence Detector Software Version 1.4 (Applied Biosystems).

**Statistical analysis**

Data are expressed as mean ±SD. Student's *t*-test was used to determine significant differences between tumor and normal tissues. The level of significance was preset at $P<0.05$. Cross tabulations were analyzed with the chi-square test for association of NQO1 mRNA expression and the pathological features of patients. The Kaplan-Meier survival curves were generated for patients who having high and low expression of NQO1 mRNA, histological types of papillary type and other. Hazard ratios and p-values for comparisons of patients having high and low NQO1 expression were calculated based on multivariate Cox proportional hazards model, adjusting for their age, sex, histological types, tumor residue and metastasis. The analyses were conducted by using Stata software version 7.0

**Results**

**Characteristics of patients**

Characteristics of subjects are shown in Table 1. There were 8 long survivors, and 6 out of 8 patients had a papillary type CCA by histopathology. Patients in this series were initially evaluated as the candidates for complete excision. However, only 18 (42%) patients were proven to have been achieved complete resection with negative margin (R0) by histopathology, while all the others have extensive invasion and tumor residue at the surgical margin.

**Table 2** Multivariate analysis by COX proportional hazards

| Variable | | Hazard ratio | 95% CI | p-value |
|---|---|---|---|---|
| Age | | | | |
| | <57 | 1 | | |
| | >=57 | 2.74 | 1.23 – 6.07 | 0.013 |
| Gender | | | | |
| | Female | 1 | | |
| | Male | 1.02 | 0.49 – 2.42 | 0.84 |
| Histological types | | | | |
| | Papillary | 1 | | |
| | Non-papillary | 2.99 | 1.39 – 6.42 | 0.005 |
| Metastasis | | | | |
| | Presence | 1 | | |
| | No evidences | 1.25 | 0.56 – 2.79 | 0.58 |
| Surgical margin | | | | |
| | R0 | 1 | | |
| | Not R0 | 2.61 | 1.11 – 6.14 | 0.027 |
| NQO1 mRNA expression | | | | |
| | Low | 1 | | |
| | High | 2.43 | 1.12 – 5.28 | 0.025 |

**NQO1 activity and immunohistochemical localization in CCA tissue**

NQO1 activity in tumor tissues was much higher than that in non-tumor adjacent tissues ($p < 0.001$) (Fig. 1). The median and 25% and 75% percentiles of NQO1 activities were 14.9, 1.0 and 20.8 nmol/min/mg protein for tumor tissues and 0.81, 0.44 and 1.21 nmol/min/mg protein for normal tissues. There was no association between NQO1 activity and survival time or NQO1 mRNA expression. The immunohistochemical staining in tumor and non-tumor areas are shown in Fig.2. The normal issue showed liver parenchyma and small bile ducts only weakly stained with NQO1 in cytosol (Fig.2B). NQO1 is strongly stained in tumors with tubular type as well as papillary type of adenocarcinoma (Fig 2 C and D).

**NQO1 expression and association with clinicopathologic variables**

Expression levels of NQO1 mRNA were measured by reverse-transcription real-time PCR. Subjects at the forth quartile of NQO1 expression were assigned to high expression group (13 subjects) and the rest were low expression group (30 subjects). There was no significant correlation

between the level of NQO1 and the histological type of tumors, and evidence of metastasis (Table 1). The age of patients between NQO1 high and low groups was also of no difference.

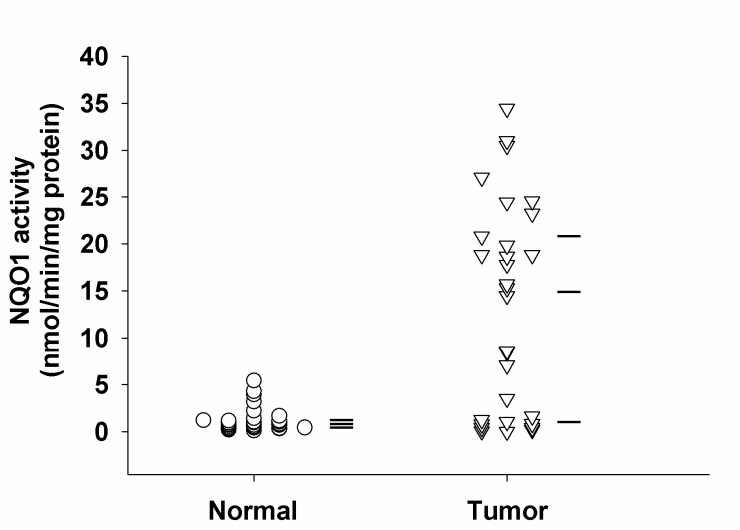


**Figure 1. Activity of NQO1 in tissues from normal and tumor sections of CCA patients.** Surgical liver specimens from CCA patients were sectioned for tumor and adjacent normal tissues. Tissues were homogenized for preparation of cytosolic fraction to determine NQO1 activity by the enzymatic coupling assay. All samples were performed in triplicate assay. Small horizontal bars on the right side of the plots represent the percentiles of 25$^{th}$, 50$^{th}$ and 75$^{th}$.

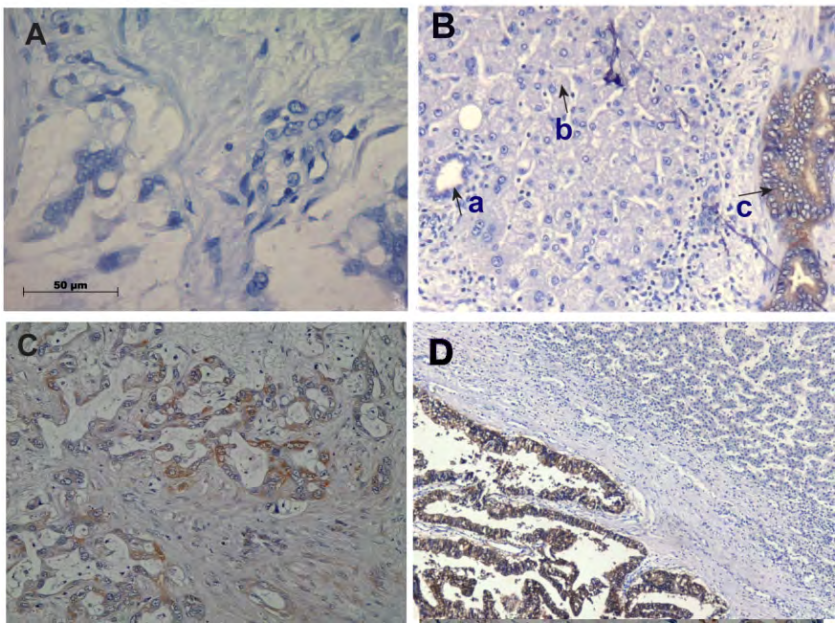


**Figure 2 Immunohistochemical staining of NQO1 in CCA sections.** A. The negative control of NQO staining. B. The non-tumor tissue stained very weakly with NQO1, a: non-tumor bile duct, b: liver parenchyma, and c: bile duct tumor stained strongly with NQO1. C. The well-differentiated adenocarcinoma type. D. The papillary type. (Original magnification of x40 for A & C, and 10X for B & D)

**Survival time analysis**

The median survival time of the patients in this series was 267 days with 95% CI of 131 to 403 days. Using Kaplan-Meier and log-rank analysis, the median survival time of CCA patients with the high and low expression of NQO1were of 149.0 days (95%CI: 102-196 days) and 342.0 days (95%CI: 228 to 456 days), respectively. The median survival time of the patients having papillary and non-papillary types by histology were 297 (95%CI: 219-375 days) and 157 day (95%CI: 98-352 days), respectively. In the univariate analysis, none of variables was a significant predictor for survival.

The multivariate Cox proportional hazard analysis was performed in patients to explore the impact of NQO1 expression after adjusting for age, gender, histological type, metastasis and presence of tumor residue. The levels of NQO1 expression, histological type, gender and tumor residue at surgical margin were significant predictors of the survival time of CCA patients (Fig. 3). CCA patients with low expression of NQO1 have longer survival than who have high expression, with the hazard ratio of 2.43 ($p< 0.05$) (Table 2). The prognosis of patients having papillary adenocarcinoma was better than the patients having other histological types of CCA with the hazard ratio of over 2.99 (Table 2). The patients with residual tumor (surgical margin positive) were at risk with the hazard ratio of 2.61 when compared with complete excision of tumor.

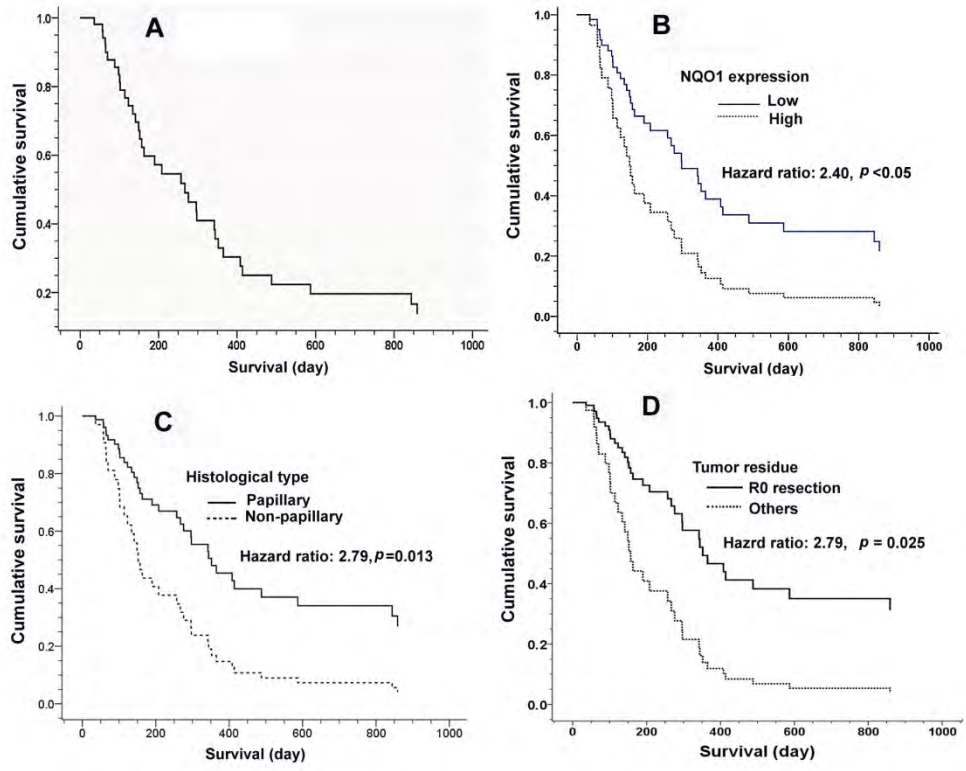


**Figure 3 Cumulative survival curves for intrahepatic cholangiocarcinoma**. A. The survival function at mean of covariates. B. Survival function stratified by the levels of NQO1 mRNA expression. C. Survival function stratified by histological. D. Survival function type stratified by surgical margin. Tumor tissues from surgical sections of cholangiocarcinoma patients were prepared for total RNA and analyzed for NQO1 mRNA by reverse-transcription and real-time PCR.

All samples were performed in triplicate assay. Patients with high NQO1 mRNA expression group or histology of non-papillary type or surgical margin showing tumor residue had worse overall survival.

**Discussion**

NQO1 functions as xenobiotic metabolizing and antioxidant in normal cells. NQO1 gene is one of the down-stream genes regulated by Nrf2 - antioxidant-response-element (Nrf2-ARE) signaling pathway, which is an important target for cancer chemoprevention of various phytochemicals [13]. However, in certain circumstances, NQO1 also functions to protect tumor cells, as it is over-expressed in some cancers [14-15, 18]. Our results revealed that NQO1 expression by immunohistochemical staining and NQO1 activity in tumor tissues were significantly higher than the normal adjacent tissues. NQO1 mRNA expression in tumor tissue can be an independent predictor of long-term survival.

In this study, NQO1 activity was very high in CCA tumor tissues compared to the normal liver tissue. There was a wide variation in the activity of tumors, whereas there was much less in normal tissues. However, there was lack of correlation between the activity and mRNA expression of NQO1. The high expression might not directly represent the activity observed. Alternatively, NQO1 expression may represent the activity of Nrf2-ARE signaling system, where the pathway could regulate a number of downstream genes including NQO1 and other antioxidant genes where they provide cytoprotection and resistance to stress [22].

In a previous study, Strassburg et al [23] reported the expression of NQO1 and NQO2 in bile duct tumor was comparable to that of normal bile duct tissues. In contrast to our study, high NQO1 immunohistochemical staining was observed in CCA tissues, whereas surrounding tissues including normal bile ducts and liver parenchyma were very weakly stained. Since Strassburg et al. [23] observed in only four CCA patients and use of gall bladder as the representative normal biliary tissues. The small sample size with different control specimen might cause the differences in results.

Recently Wakai et al. [24] reported that the loss of NQO1 expression evaluated by immunohistochemical technique was associated with the poor prognosis of intrahepatic CCA. This report is in contrast with our finding where low NQO1 expression is associated with longer survival than the high expression. The discrepancy of findings may be due to the different study populations. CCA patients in our report were from the Northeast region of Thailand where liver fluke infection is probably the most important causative agent of CCA [25-26]. On the other hand, Wakai et al. studied on Japanese patients where opisthorchiasis is not a risk factor. Related to this, Jinawath et al [27] reported that liver fluke-associated and non-liver fluke associated intrahepatic CCA showed significantly different gene expression profiles in such that, xenobiotic metabolizing enzyme genes were over-expressed in Thai CCA patients, whereas growth factor signaling genes were over expressed in Japanese patients [27]. A larger population is deemed necessary to clarify an association of NQO1 and the prognosis of CCA. It also highlights the need to evaluate the biomarkers under relevant circumstances.

Apart from NQO1, the present results revealed that histological type of CCA tissue could be a significant and independent predictor associated with prognosis of the patients; i.e. the patients having papillary type have better prognosis than those having non-papillary type. Our result is in agreement with the previous report in CCA patients of Thailand [28]. Histological type and NQO1 expression are independent parameters of patients' survival, as the histological type is not correlated with NQO1 expression level (Table 1). Residual tumor after surgical operation is usually regarded as the

predictor of poor survival after surgery. The complete excision of tumor with surgical margin negative (R0) is associated with long-term survival [29]. Our study is consistent with the concept of patients without R0 excision are at higher risk than those with R0 operation.

In summary, NQO1 acting as xenobiotic metabolizing and antioxidant enzyme was over-expressed in the majority of CCA. Since NQO1 is over-expressed in some other tumors, this enzyme may provide protection to cancer cells. The high expression of NQO1 was associated with poor prognosis. Histology of tumors of papillary type and complete surgical removal of tumor mass were significantly associated with good prognosis. Further study with larger population is necessary to clarify the inconsistency among the reports.

**References**


1. Patel T: **Cholangiocarcinoma--controversies and challenges**. *Nat Rev Gastroenterol Hepatol* 2011, **8**:189-200.
2. Kamsa-ard S, Wiangnon S, Suwanrungruang K, Promthet S, Khuntikeo N, Mahaweerawat S: **Trends in liver cancer incidence between 1985 and 2009, Khon Kaen, Thailand: cholangiocarcinoma**. *Asian Pac J Cancer Prev* 2011, **12**:2209-2213.
3. Sripa B, Pairojkul C: **Cholangiocarcinoma: lessons from Thailand**. *Curr Opin Gastroenterol* 2008, **24**:349-356.
4. Coussens LM, Werb Z: **Inflammation and cancer**. *Nature* 2002, **420**:860-867.
5. Pinlaor S, Hiraku Y, Ma N, Yongvanit P, Semba R, Oikawa S, Murata M, Sripa B, Sithithaworn P, Kawanishi S: **Mechanism of NO-mediated oxidative and nitrative DNA damage in hamsters infected with Opisthorchis viverrini: a model of inflammation-mediated carcinogenesis**. *Nitric Oxide* 2004, **11**:175-183.
6. Dijkstra G, Blokzijl H, Bok L, Homan M, van Goor H, Faber KN, Jansen PL, Moshage H: **Opposite effect of oxidative stress on inducible nitric oxide synthase and haem oxygenase-1 expression in intestinal inflammation: anti-inflammatory effect of carbon monoxide**. *J Pathol* 2004, **204**:296-303.
7. Ohshima H, Tazawa H, Sylla BS, Sawa T: **Prevention of human cancer by modulation of chronic inflammatory processes**. *Mutat Res* 2005, **591**:110-122.
8. Khan SA, Thomas HC, Davidson BR, Taylor-Robinson SD: **Cholangiocarcinoma**. *Lancet* 2005, **366**:1303-1314.
9. Siegel D, Gustafson DL, Dehn DL, Han JY, Boonchoong P, Berliner LJ, Ross D: **NAD(P)H:quinone oxidoreductase 1: role as a superoxide scavenger**. *Mol Pharmacol* 2004, **65**:1238-1247.
10. Radjendirane V, Joseph P, Lee YH, Kimura S, Klein-Szanto AJ, Gonzalez FJ, Jaiswal AK: **Disruption of the DT diaphorase (NQO1) gene in mice leads to increased menadione toxicity**. *J Biol Chem* 1998, **273**:7382-7389.
11. Saldivar SJ, Wang Y, Zhao H, Shao L, Lin J, Spitz MR, Wu X: **An association between a NQO1 genetic polymorphism and risk of lung cancer**. *Mutat Res* 2005, **582**:71-78.
12. Yang FY, Guan QK, Cui YH, Zhao ZQ, Rao W, Xi Z: **NAD(P)H quinone oxidoreductase 1 (NQO1) genetic C609T polymorphism is associated with the risk of digestive tract cancer: a meta-analysis based on 21 case-control studies**. *Eur J Cancer Prev* 2012.
13. Surh YJ, Kundu JK, Na HK: **Nrf2 as a master redox switch in turning on the cellular signaling involved in the induction of cytoprotective genes by some chemopreventive phytochemicals**. *Planta Med* 2008, **74**:1526-1539.

14. Cresteil T, Jaiswal AK: **High levels of expression of the NAD(P)H:quinone oxidoreductase (NQO1) gene in tumor cells compared to normal cells of the same origin**. *Biochem Pharmacol* 1991, **42**:1021-1027.
15. Kolesar JM, Pritchard SC, Kerr KM, Kim K, Nicolson MC, McLeod H: **Evaluation of NQO1 gene expression and variant allele in human NSCLC tumors and matched normal lung tissue**. *Int J Oncol* 2002, **21**:1119-1124.
16. Logsdon CD, Simeone DM, Binkley C, Arumugam T, Greenson JK, Giordano TJ, Misek DE, Kuick R, Hanash S: **Molecular profiling of pancreatic adenocarcinoma and chronic pancreatitis identifies multiple genes differentially regulated in pancreatic cancer**. *Cancer Res* 2003, **63**:2649-2657.
17. Siegel D, Ross D: **Immunodetection of NAD(P)H:quinone oxidoreductase 1 (NQO1) in human tissues**. *Free Radic Biol Med* 2000, **29**:246-253.
18. Danson S, Ward TH, Butler J, Ranson M: **DT-diaphorase: a target for new anticancer drugs**. *Cancer Treat Rev* 2004, **30**:437-449.
19. Buranrat B, Prawan A, Kukongviriyapan U, Kongpetch S, Kukongviriyapan V: **Dicoumarol enhances gemcitabine-induced cytotoxicity in high NQO1-expressing cholangiocarcinoma cells**. *World J Gastroenterol* 2010, **16**:2362-2370.
20. Prochaska HJ, Santamaria AB: **Direct measurement of NAD(P)H:quinone reductase from cells cultured in microtiter wells: a screening assay for anticarcinogenic enzyme inducers**. *Anal Biochem* 1988, **169**:328-336.
21. Prawan A, Buranrat B, Kukongviriyapan U, Sripa B, Kukongviriyapan V: **Inflammatory cytokines suppress NAD(P)H:quinone oxidoreductase-1 and induce oxidative stress in cholangiocarcinoma cells**. *J Cancer Res Clin Oncol* 2008.
22. Kensler TW, Wakabayashi N: **Nrf2: friend or foe for chemoprevention?** *Carcinogenesis* 2010, **31**:90-99.
23. Strassburg A, Strassburg CP, Manns MP, Tukey RH: **Differential gene expression of NAD(P)H:quinone oxidoreductase and NRH:quinone oxidoreductase in human hepatocellular and biliary tissue**. *Mol Pharmacol* 2002, **61**:320-325.
24. Wakai T, Shirai Y, Sakata J, Matsuda Y, Korita PV, Takamura M, Ajioka Y, Hatakeyama K: **Prognostic significance of NQO1 expression in intrahepatic cholangiocarcinoma**. *Int J Clin Exp Pathol* 2011, **4**:363-370.
25. Green A, Uttaravichien T, Bhudhisawasdi V, Chartbanchachai W, Elkins DB, Marieng EO, Pairqjkul C, Dhiensiri T, Kanteekaew N, Haswell-Elkins MR: **Cholangiocarcinoma in north east Thailand. A hospital-based study**. *Trop Geogr Med* 1991, **43**:193-198.
26. IARC: **Infection with liver flukes (Opisthorchis viverrini, Opisthorchis felineus and Clonorchis sinensis)**. *IARC Monogr Eval Carcinog Risks Hum* 1994, **61**:121-175.
27. Jinawath N, Chamgramol Y, Furukawa Y, Obama K, Tsunoda T, Sripa B, Pairojkul C, Nakamura Y: **Comparison of gene expression profiles between Opisthorchis viverrini and non-Opisthorchis viverrini associated human intrahepatic cholangiocarcinoma**. *Hepatology* 2006, **44**:1025-1038.
28. Subimerb C, Pinlaor S, Khuntikeo N, Leelayuwat C, Morris A, McGrath MS, Wongkham S: **Tissue invasive macrophage density is correlated with prognosis in cholangiocarcinoma**. *Mol Med Report* 2010, **3**:597-605.
29. Guglielmi A, Ruzzenente A, Campagnaro T, Pachera S, Valdegamberi A, Nicoli P, Cappellani A, Malfermoni G, Iacono C: **Intrahepatic cholangiocarcinoma: prognostic factors after surgical resection**. *World J Surg* 2009, **33**:1247-1254.

## Section 4

## Phenethyl isothiocyanate induces apoptosis of cholangiocarcinoma cells through interruption of glutathione and mitochondrial pathway

### Introduction

Isothiocyanates (ITCs) are hydrolysis products of a group of naturally occurring thioglucoside and glucosinolate compounds which are found in cruciferous vegetables and others including broccoli, cauliflower, cabbage, brassicas, watercress, and kale [1]. The ITCs rather than their parent compounds, the glycosinolates, are highly active. The ITCs including phenethyl isothiocyanate (PEITC), sulforaphane and allyl isothiocyanate are very effective antioxidants and potent suppressors of tumor growth [2]. The compounds possess dual effects of antioxidant activity and also generation oxidative stress. The antioxidant is demonstrated by radical scavenging activity and indirectly by induction the expression of antioxidant and cytoprotective enzymes, whereas the oxidative stress is generated via several cellular mechanisms [1]. The antitumor activities *in vitro* and *in vivo* confer a collective activity so-called cancer chemoprevention [3-5]. Several epidemiological studies have suggested that dietary intake of cruciferous vegetables is inversely related to the development of cancer [6]. PEITC, an isothiocyanate, found abundantly in cruciferous vegetables has been shown effectively inhibit the growth of cancers of prostate, colon, lung, and leukemic cells [7-9]. Clinical trials of PEITC on the treatment of lung cancer and leukemia are currently undertaken (www.clinicaltrials.gov).

The cancer chemopreventive effects of PEITC are expressed via several cell signaling pathways at multiple levels. The induction of reactive oxygen species (ROS) formation plays a pivotal role in oxidation of cellular redox-sensitive molecules and disruption of the mitochondrial function leading to the death of leukemic and prostate cancer cells [5, 10]. However, PEITC mediated apoptosis of HepG2 or multiple myeloma cells were suggested to be independent of ROS formation [11-12]. It is interesting to note that PEITC mediates apoptotic cell death of various drug-resistant cancer cells including imatinib-, gleevec- and fludarabine-resistant leukemic cells, and prostate cancer [10, 13-14]. Moreover, the effects of PEITC on multiple steps of cancer growth make this compound highly versatile and promising candidate for cancer chemoprevention and chemotherapy.

Bile duct cancer or cholangiocarcinoma (CCA) is a highly malignant adenocarcinoma originating from the cholangiocytes [15]. CCA is a rare type of cancer world-wide, however CCA is the most common type of liver cancer in some regions in Asia, particularly the Mekong Basin sub-region, where the incidence of CCA is highest in the world [16]. In the Western countries, the incidence and the mortality rate of intrahepatic CCA are reportedly increasing at an alarming rate [15, 17]. The prognosis of CCA patients is very poor, because most patients are already in the advanced stage at diagnosis. Chemotherapy and radiotherapy shows modest benefit for prolonged overall survival in patients with unresected CCA [18]. Currently, there is no standard regimen of chemotherapy for CCA [15]. Despite of many recent advances in cancer chemotherapy, management of CCA is still an immense challenge and several strategies in sensitizing resistant CCA cells to respond to chemotherapeutic drugs have been attempted [19-20].

The cancer chemopreventive effect of PEITC in CCA is still unknown. In this study, we examined the inhibitory effect of PEITC on KKU-100, a CCA cell-line derived from human tumor

tissue with poorly differentiated adenocarcinoma. To elucidate the possible mechanisms of the effects of PEITC on CCA cells, ROS formation, GSH redox stress and mitochondrial function were evaluated for PEITC-treated CCA cells. The results show that the PEITC-mediated killing of CCA cells was not associated with the generation of superoxide anion. The disruption of GSH redox may be an important step eliciting mitochondrial dysfunction, a common pathway leading to cell death.

## Materials and methods

### Chemicals and reagents

Phenethyl isothiocyanate (PEITC), 4-hydroxy-TEMPO (TEMPOL), *N*-acetyl-L-cysteine (NAC), dihydroethidium (DHE), sulphorhodamine B (SRB) and buthionine sulfoximine (BSO), were obtained from Sigma Chemical Co. (St. Louis, MO, USA). 1-Methyl-2 vinyl-pyridinium trifate (M2VP) was obtained from Fluka Chemical (Buch, Switzerland). 5,5',6,'-tetrachloro-1,1',3,3'tetraethylbenzimidazolyl carbocyanine iodide (JC-1) was obtained from Clayman Chemical (Ann Arbor, MI, USA). Caspase 9 substrate I (Ac-LEHD-AFC), granzyme B substrate II caspase 8 (Z-IETD-AFC) and glutathione monoethylester (GSH-MEE) were purchased from Calbiochem (EMD Millipore, Billerica, MA, USA). EnzCheck® Caspase-3 Assay kit#1 was purchased from Molecular Probes (Eugene, OR, USA). Antibodies used for immunoblotting were from Santa Cruz Biotechnology (Sandiego, CA, USA).

### Cell cultures

A human CCA cell line, KKU-100 established in our institute [21], were grown in Ham's F12 medium supplemented with 4 mM L-glutamine, 1 mM sodium pyruvate, 12.5 mM *N*-2-hydroxyethylpiperazine-*N*0-2-ethanesulfonic acid (HEPES; pH 7.3), 100 U/mL penicillin, 100 µg/mL streptomycin sulfate and 10% fetal calf serum and maintained under 5% $CO_2$ in air at 37°C. The cells were subcultured every 2-3 days before cultured cell confluence using 0.25% trypsin–EDTA, and the medium was changed after overnight incubation.

### Cytotoxicity assay

CCA cells were seeded onto 96-well culture plates at a density of 7,500 cells/well. After an overnight culture, the serum-free medium was replaced with an addition of PEITC, and the cells were cultured for various time intervals. The cytotoxicity was examined by the SRB assay. In brief, cultured cells were fixed with ice-cold trichloroacetic acid and stained with 0.4% SRB in 1% acetic acid for 30 min. Excess dye was removed by rinsing several times with 1% acetic acid, and protein-bound dye was dissolved with 10 mM Tris base solution for determination of absorbance with a microplate reader with filter wavelength of 570 nm.

To determine cells undergone apoptosis, cultured cells were stained with fluorescent dyes as previously described [19, 22]. In brief, the cells were washed once with phosphate-buffered saline (PBS) and stained with acridine orange and ethidium bromide (AO/EB) in PBS with the trace amount of hemoglobin. The cells were examined using a Nikon Eclipse TS100 inverted microscope with the excitation and emission filters of 480 nm and 535 nm, respectively. The number of viable, apoptotic, and necrotic cells which were stained with green fluorescence with intact nuclei, green fluorescence with the appearance of cell shrinkage, nuclear condensation and fragmentation, and bright orange fluorescence, respectively, were enumerated. The apoptotic cells were calculated as the percent apoptotic cells over a total number of cells in the same area.

**Assays for ROS and glutathione**

Intracellular ROS generation was measured by cell-permeable fluorescent probe, DHE, staining, which is specific for superoxide anion. Briefly, $5\times10^4$ cells were seeded in 96 black well plates and cultured overnight. Then, the medium was removed and the cells were washed with PBS, and were treated with PEITC, 25 μM DHE with or without 2 mM NAC or 0.5 mM TEMPOL in serum-free medium and kept under an atmosphere of 5% $CO_2$ at 37°C for 90 min. The fluorescence intensity was read and quantified in a Gemini XPS fluorescent plate reader with excitation and emission wavelength of 518 nm and 605 nm, respectively.

Glutathione was assayed by the method previously described [22] using 1-methyl-2-vinylpyridinium trifate (M2VP) as a glutathione scavenger. In brief, cell lines were trypsinized and washed three times with cold PBS and cell suspensions were reacted with M2VP (1 mM) for determination of GSSG. Another aliquot of cell suspension was used for the assay of total GSH. The cultured media were collected, centrifuged, and supernatants were saved for total GSH assay.

**Measurement of mitochondrial transmembrane potential**

The dissipation of the mitochondrial electrochemical potential gradient is known as an early event in apoptosis. The assay of mitochondrial transmembrane potential ($\Delta\Psi_m$) was performed according to the previously described method [20] using the cationic, lipophilic dye, 5,5',6,'-tetrachloro- 1,1',3,3' tetraethylbenzimidazolyl carbocyanine iodide (JC-1) staining. The cells were seeded in 96 black well plates at the density of $1\times10^4$ cells/well and cultured overnight before treatment with PEITC at varied concentrations for 3 and 24 h. Images were captured by a fluorescence microscope with excitation wavelength of 485 nm and long-pass emission wavelength of 535 nm. JC-1 forms J-aggregates in healthy mitochondrial matrix, which can be visualized as red fluorescence. In depolarized mitochondria, JC-1 effluxes to the cytoplasm and exists as monomers with green fluorescence. The shift of red to green fluorescence is an indicative of depolarization of $\Delta\Psi_m$.

**Western blot analysis**

Whole cell lysates were prepared as described previously [19]. The protein was electrophoretically separated on 10% SDS–polyacrylamide gel and was transferred to polyvinylidene difluoride (PVDF) membranes by semi-dry blotting. The PVDF membranes were blocked with 5% (w/v) skimmed milk powder in PBS and incubated overnight at 4 °C with primary antibodies including rabbit polyclonal IgG against cytochrome c (sc-13560), Bax (sc-493) and AIF (sc-5586), and mouse monoclonal IgG against Bcl-XL (sc-8392) and β-actin (sc-1616). The primary antibody was removed and the blots were incubated with the respective horseradish peroxidase-conjugated secondary antibodies (goat anti-mouse or anti-rabbit IgG). The blots were incubated with ECL substrate solution. The densities of bands of specific cytochrome c, Bcl-XL, Bax, AIF and β-actin were visualized and captured by Imagequant™ 400.

**Measurements of caspase activities**

After treatment with PEITC for 3 and 6 h, the cultured cells were trypsinized, washed in PBS and adjusted to $10^6$ cells for each reaction. Cell pellets were stored frozen at -80°C for analysis at a later time. Cell pellet was lysed with the cell lysis buffer and incubated on ice for 10 min. After

centrifugation to pellet the cellular debris, the supernatant was transferred to individual microplate wells and processed according to the manufacturers' instructions using Ac-LEHD-AFC as caspase 9 substrate, Z-IETD-AFC as caspase 8 substrate and Z-DEVD-AMC as caspase 3 substrate. The fluorescent signals were read using Gemini XPS fluorescent plate reader with the excitation and emission wavelengths of 400 and 505 nm, respectively, to assess caspase 9 and 8 activities, and 340 and 440 nm, respectively to caspase 3 activity.

**Statistical analysis**

All results were presented as the mean ± S.E.M. Comparison between control and treated group was performed with Student's t-test or ANOVA with Student-Newman-Keuls test, where appropriate. The level of significance was set at $p<0.05$.

## Results

**PEITC induced cytotoxicity and depletion of GSH**

To examine the cytotoxic effect of PEITC, KKU-100 cells were exposed to various concentrations (0.3, 1, 3, 10 and 30 μM) of PEITC for 24 and 48 h (Figure 1a). The viability of CCA cells reduced rapidly after exposure to PEITC in a dose-response manner and the % cytotoxicity at 48 h was not significantly different from that at 24 h. The IC50 values were not different between 24 and 48 h of incubation (inset, Fig. 1a). Moreover, PEITC induced apoptosis very rapidly within the first 3 h and in a dose dependent manner (Fig.1b). In contrast, PEITC induced only few number of necrotic cell death at every time points (data not shown).

As cellular GSH is the major cellular redox buffer, the mechanism of PEITC-induced cytotoxicity was suggested to be associated with disturbance of GSH [14]. GSH in KKU-100 cells was decreased rapidly within first 3 h and continuously suppressed through 24 h of incubation (Fig. 1c). The efflux of total GSH from the cells into the medium was also determined to observe how oxidative stress was handled by CCA cells. Total GSH levels in the medium were increased with time of incubation and concordant with the decrease of cellular GSH levels (Fig. 1c).

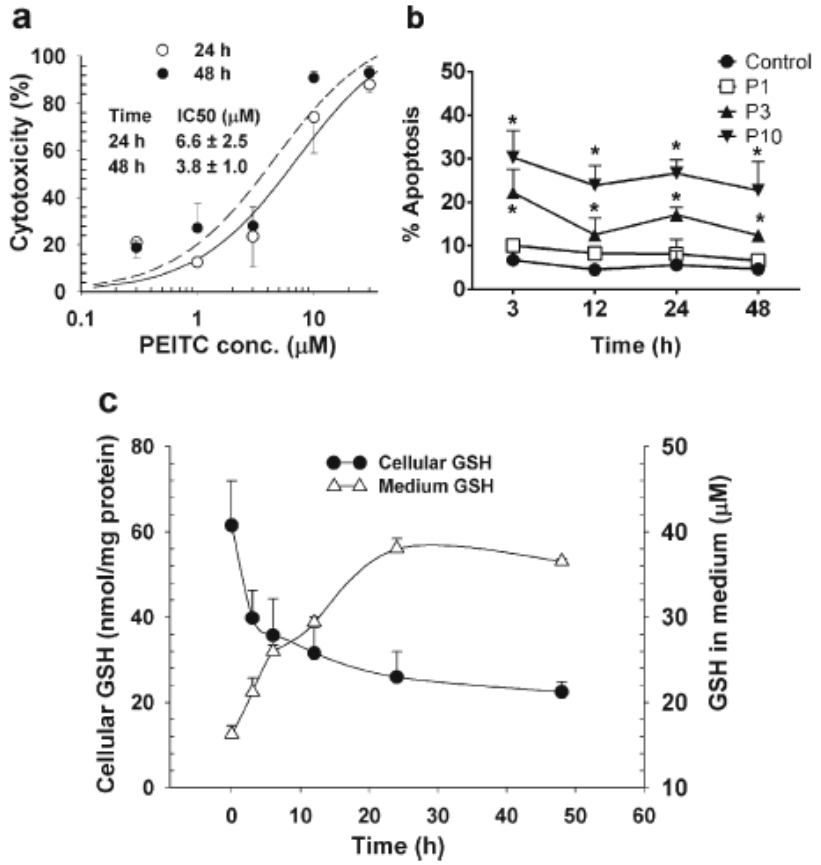


**Fig 1. PEITC induced cytotoxicity and GSH depletion.** KKU-100 cells were incubated with various concentrations (0.3, 1, 3, 10, 30 μM) of PEITC for 24 and 48 h before the cytotoxicity of the cells was determined by SRB assay (a) and the number of apoptotic cells was assessed by AO/EB method at 24 h of incubation (b). GSH levels were measured in cell pellet as intracellular GSH (c) and in the medium as efflux from the cells. Each value represents the mean ± SEM of three experiments. *Significantly different from controls, $p<0.05$.

**Effects of Antioxidants on PEITC-induced ROS formation and GSH depletion**

As PEITC suppressed cell growth and induced cell death in association with oxidative stress manifested as GSH depletion, we evaluated whether the GSH redox stress was causally related with the formation of superoxide anion by using TEMPOL, a superoxide scavenging agent and NAC, a thiol antioxidant and redox reagent. Treatment of 3 or 10 μM of PEITC rapidly induced an increase of fluorescent signals of superoxide formation within 90 min (Fig. 2a). Co-treatment of the cells with PEITC and 0.5 mM TEMPOL or 2 mM NAC almost completely suppressed PEITC-induced ROS formation in the cells. Treatment with NAC or TEMPOL alone did not change the basal ROS levels when compared with controls. GSH in the cells was determined after concurrent treatment of PEITC with TEMPOL or NAC. The PEITC (10 μM) suppressed the cellular GSH after incubation for 3 h. It was only NAC that could completely stabilize GSH levels when cells were treated with PEITC (Fig. 2b). The treatment of TEMPOL could not protect losses of cellular GSH and even induced loss at low concentration of PEITC.

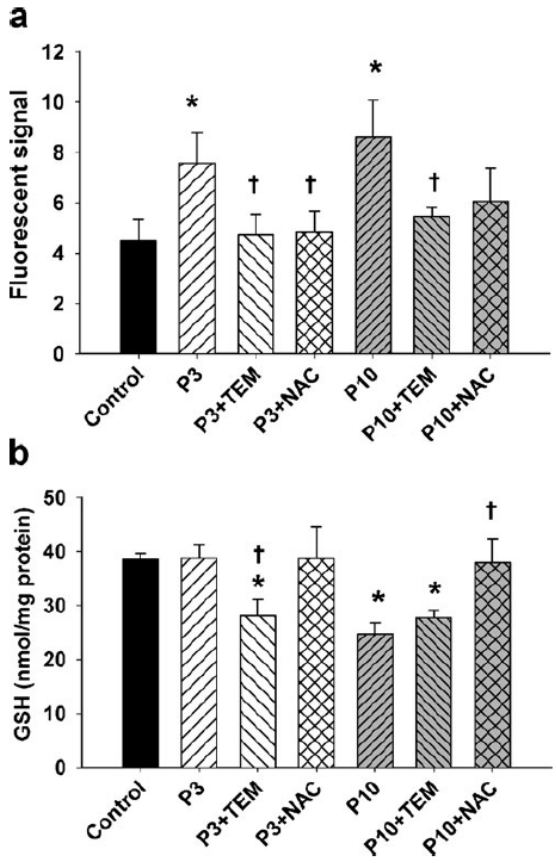


**Fig. 2. Effect of antioxidants on superoxide formation and GSH levels** KKU-100 cells were incubated with PEITC at indicated concentrations [ 3 and 10 μM, shown as P3 and P10] with or without TEMPOL (TEM, 0.5 mM) or N-acetylcystein (NAC, 2 mM) for 90 min. Superoxide formation was quantified by dihydroethidium fluorescent method (a). The effects of TEM and NAC on PEITC-induced reduction of cellular GSH were determined after incubation for 3 h (b). Each bar represents the mean± SEM of three experiments. *Significantly different from controls, $p<0.05$, † significantly different from PEITC treatment, $p<0.05$.

**Protective effect of TEMPOL and NAC on PEITC-induced cytotoxicity**

To evaluate whether the cytotoxicity of PEITC was associated with the superoxide and GSH redox stress, KKU-100 cell were concurrently treated with PEITC and TEMPOL or NAC. The presence of TEMPOL could not suppress the cytotoxic effects of PEITC at any incubation periods, i.e. 3, 24 and 48 h. Rather, the concurrent treatment with TEMPOL tended to exacerbate the cytotoxic effect of PEITC at 24-48 h of incubation (Fig. 3 upper panel). On the other hand, NAC significantly prevented the cytotoxicity of PEITC (Fig. 3 upper panel) in association with the protection of cellular GSH (Fig. 2b).

PEITC-induced depolarization of mitochondrial transmembrane potential

To elucidate the underlying mechanisms of PEITC-induced cytotoxicity in relation to oxidative stress, the effect of PEITC treatment on mitochondrial function was investigated. The mitochondrial transmembrane potential ($\Delta\Psi_m$) was determined by JC-1 assay in cells treated PEITC for 3 and 24 h. In control cells, mitochondria predominantly exhibited red fluorescence indicating the intact $\Delta\Psi_m$ (Fig

3A, lower panel). PEITC rapidly depolarized $\Delta\Psi_m$ as revealed by green fluorescence staining. The depolarization of $\Delta\Psi_m$ was apparent within the first 3 h of PEITC treatment and persisted up to 24 h. When cells were concurrently treated with PEITC and antioxidants, NAC but not TEMPOL, showed protective effect on the $\Delta\Psi_m$ (Fig. 3c & d). Treatment with TEMPOL or NAC alone did not affect $\Delta\Psi_m$ (data not shown). The changes in $\Delta\Psi_m$ were correlated well with the cytotoxicity of PEITC.

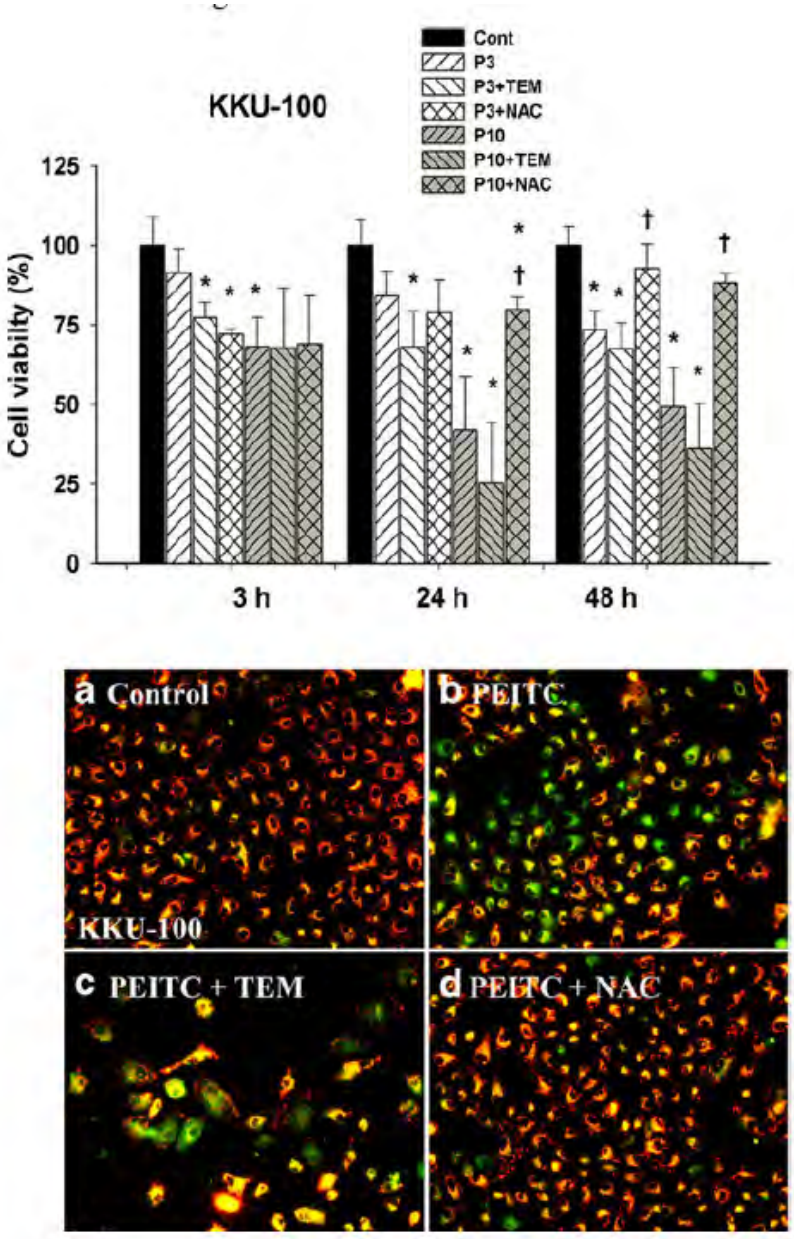


**Fig. 3. Effects of antioxidants on cytotoxicity and changes in mitochondrial transmembrane potential** KKU-100 cells were incubated with PEITC at indicated concentrations [P3 and P10 (μM)] with or without TEMPOL (TEM, 0.5 mM) or N-acetylcystein (NAC, 2 mM) for 3, 24 and 48 h. The cytotoxicity was assayed by SRB method (bar graph in upper panel). Each bar represents the mean ± SEM of three experiments. *Significantly different from control, $p<0.05$, † significantly different from PEITC treated group, $p<0.05$. The $\Delta\Psi_m$ was assessed using JC-1 staining method after the cells were treated with PEITC for 24 h. Fluorescent images were captured by a fluorescence microscope. The experiment was done twice with similar results. The representative images from one experiment are shown (images in lower panel).

**Effects of GSH replenishment and GSH depletion**

Since there was a relationship between GSH depletion and cell death, we further evaluated whether depletion of GSH by PEITC was an important cause of cell death. For this purpose, the cultured cells were treated with BSO (0.5 mM), an inhibitor of GSH synthesis. Treatment with BSO caused a rapid depletion of cellular GSH (data not shown), but did not induce any cytotoxic effect after incubation for 24 h (Fig. 4 a). However, BSO strongly potentiated PEITC-induced cytotoxicity. The result indicates that GSH depletion alone is insufficient to cause cell death. To demonstrate the protective effect of NAC is related to GSH redox regulation, the cells were treated with GSH-MEE, a cell permeable GSH concurrent with high concentration of PEITC to cause massive cell death. Treatment with GSH-MEE could almost completely prevent cell death (Fig. 4b).

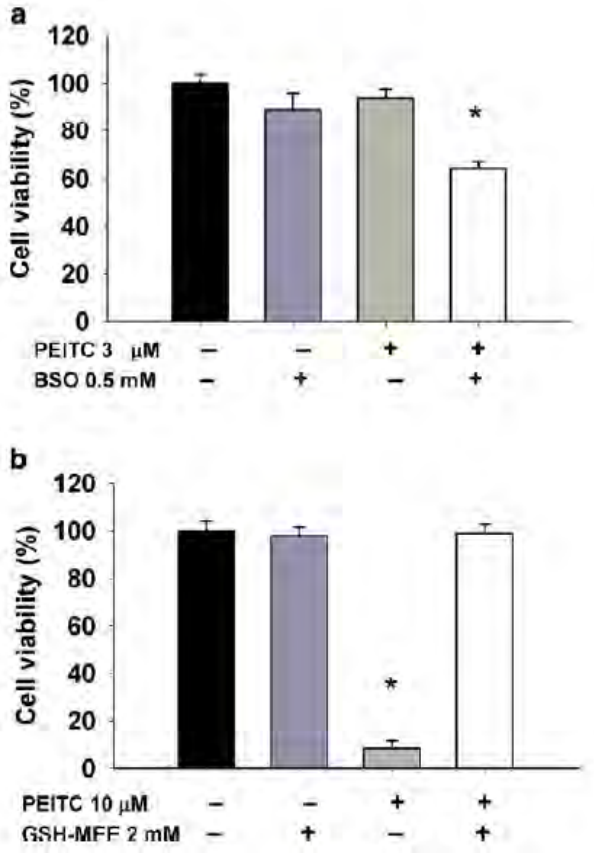


**Fig. 4 Effects of GSH replenishment and GSH depletion on PEITC-induced cytotoxicity** Cultured cells of KKU-100 cells were treated with combination of PEITC and buthionine sulfoximine (BSO) for 24 h for 24 h (a) or PEITC with glutathione monoethylester (GSH-MEE) (b). Analysis of cell death was performed by fluorescent staining method. Each bar represents the mean ± SE of three experiments. *Significantly different from controls, $p<0.05$

**Effects of PEITC on cytochrome c, Bcl-2 proteins and caspase activity**

The involvement of mitochondria in PEITC-induced cytotoxicity was examined further. After PEITC treatment for 3 and 6 h, the remarkable release of cytochrome c was observed (Fig.5, left panel) along with increases in AIF and Bax levels, while Bcl-xl expression was suppressed.

Along with the cytochrome c release, the activation of caspases was observed. PEITC treatment activated caspase-9 and -3, but not caspase 8, in KKU-100 cells (Fig.5, right panel).

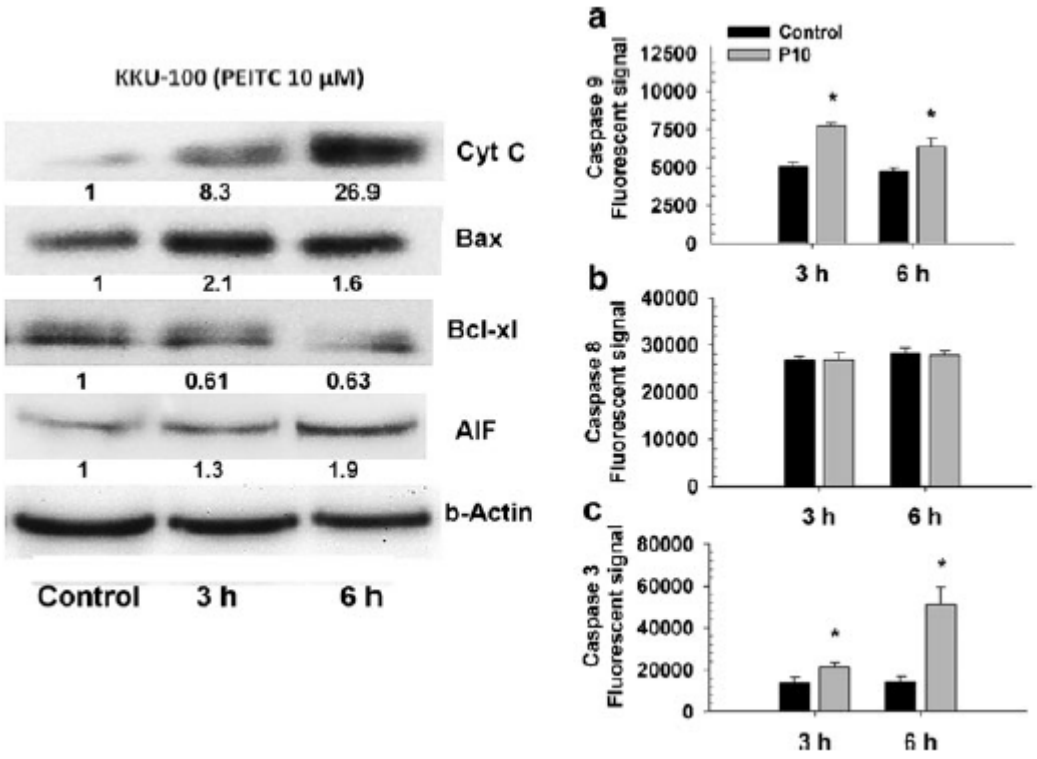


**Fig. 5. PEITC induced the release of cytochrome c and Bcl2 proteins, and activation of caspases**
KKU-100 cells were treated with PEITC (10 µM) for 3 and 6 hours. The cytosol protein was analyzed for cytochrome c, Bax, Bcl-xl and AIF by Western immunoblotting using β-actin as loading control. Values beneath images indicated the relative protein intensity as a ratio of the treatment to the corresponding vehicle-treated control. Each experiment was done at least twice with similar results, and the representative bands from one experiment are shown (images at left panel). The total cell lysates were assayed for caspase activities using specific fluorogenic substrates (bar graph at right panel), caspase-3 (a), caspase-8 (b) and caspase-9 (c). Each bar represents the mean ± SE of three experiments. *Significantly different from corresponding controls, $p<0.05$.

## Discussion

PEITC is a natural compound of isothiocyanate group. It has been advocated as a chemopreventive agent for leukemia, pancreatic, prostate and lung cancers [2, 5, 14, 23]. The mechanism of actions of PEITC is multifaceted, including ROS formation, interacting with redox-signaling and mitochondrial proteins, leading to oxidative stress and mitochondrial damage [7, 9-10]. Although CCA is a malignant tumor highly resistant to chemotherapy [18, 24], PEITC potently inhibited CCA cell growth and induced apoptosis. The ROS was generated by PEITC, but it does not seem to play a critical role in induction of cell death. On the other hand, GSH depletion and oxidative stress seems to increase cellular redox stress and alter expression of Bcl-XL and Bax protein expressions with subsequently initiating an intrinsic mitochondrial cell death pathway leading to the release of cytochorome c, activation of caspase enzymes and ensuing cell death.

PEITC-induced GSH depletion in association with cell death is consistently observed in various tumor cells [2, 14, 25]. GSH depletion might be caused by the increased ROS formation.

Alternatively, GSH depletion by PEITC may be caused by rapid adduction of GSH. The PEITC adducts efflux from the cells via multi-drug resistance associated protein 2 (MRP2), whereas PEITC could reversibly be hydrolyzed and re-taken up into the cells to generate a wasting cycle of GSH [2]. This was consistent with the observed rapid increase of GSH efflux into the medium. However, GSH depletion itself could not induce cell death, as BSO, which could deplete GSH by large, did not induce cell death. However, depletion of GSH may sensitize the cells to the other concurrent effect of PEITC leading to cell death. This is consistent with our results in that NAC and GSH-MEE can almost completely abolish cytotoxicity of PEITC. Because, NAC is not an efficient radical scavenging agent [26], it serves as a precursor for GSH synthesis. More importantly, GSH and NAC have been shown to play critical roles in modulating a number of redox-sensitive enzyme, where these proteins involve in cellular signaling for survival and cell death [27]. It is probable that PEITC may exert multiple effects probably via redox stress in induction of cell death.

In these studies, TEMPOL, a superoxide scavenger [28], abolished superoxide anion without cytoprotective effect. The role of ROS in PEITC-induced cell death may be cell type-specific, because PEITC caused cell death of chronic lymphocytic and chronic myelogenous leukemic cells in a ROS dependent manner [5, 14]. On the other hand, PEITC and its electrophilic adducts may cause oxidative stress by interacting with an active cysteine thiol moiety of vital cellular molecules, particularly redox regulating and signaling regulating proteins such as thioredoxin, 14-3-3 protein, and HSP where those proteins are ultimately involved in the regulation of cell death [9]. Our results suggested a mechanistic dissociation between superoxide production and cellular redox disturbance, in the regulation of cell death.

Cellular GSH redox plays important roles in the complex process of apoptosis involving with Bcl2 family proteins where Bcl2 proteins modulate the mitochondrial permeability transition (MPT) and the activity of mitochondrial complexes [5]. The mode of action of PEITC to CCA cells, which is common to some tumor cells, may be an induction of mitochondrial damage [5, 10]. The mitochondrial dysfunction is evidenced by the loss of $\Delta\Psi_m$ which is closely related to the cytotoxic effect of PEITC. The MPT pore is a protein pore that is formed in the inner membrane of mitochondria under certain stimuli. The opening of the MPT pores lead to the loss of proton gradient across the membrane rendering mitochondria into a depolarized state, whilst increasing the number of MPT pores leads to apoptosis and necrosis [29]. As NAC prevented the loss of $\Delta\Psi_m$ and protected cell death, this suggests redox stress may an early event leading to mitochondrial damage, whereas NAC may alleviate the redox stress.

In the present study, the release of cytochrome c and AIF via mitochondrial outer membrane paralleled with the altered levels of Bax and Bcl-xl. Bax is a multidomain proapoptotic Bcl2 family protein which forms the MOMP upon activation [30]. The release of cytochrome c resulted in the activation of caspase enzymes in KKU-100 cells. AIF, a caspase-independent effector of apoptosis, is located in the inner membrane of mitochondria and released upon induction of apoptosis [31]. AIF is activated by oxidative modifications and proteolysis. The release of AIF from mitochondria is regulated by Bcl2 proteins including Bcl-xl and Bax to form MOMP [31]. It is noted that, caspase 8 activity remained unchanged, suggesting that the induction of apoptosis of KKU-100 cells by PEITC may be primarily mediated through the intrinsic mitochondrial pathway.

In summary, PEITC induced ROS-independent oxidative stress, GSH depletion, alteration of Bcl2 proteins leading to mitochondrial dysfunction and cell death. The exact mechanism of alteration of GSH affecting the changes in Bcl2 proteins remains to be elucidated. PEITC is an useful chemopreventive agent where it provides multiple modes of actions to inhibit CCA cells.

**References**


1. Cheung KL, Kong AN: **Molecular targets of dietary phenethyl isothiocyanate and sulforaphane for cancer chemoprevention**. *AAPS J* 2010, **12**:87-97.
2. Hayes JD, Kelleher MO, Eggleston IM: **The cancer chemopreventive actions of phytochemicals derived from glucosinolates**. *Eur J Nutr* 2008, **47 Suppl 2**:73-88.
3. Keum YS, Owuor ED, Kim BR, Hu R, Kong AN: **Involvement of Nrf2 and JNK1 in the activation of antioxidant responsive element (ARE) by chemopreventive agent phenethyl isothiocyanate (PEITC)**. *Pharm Res* 2003, **20**:1351-1356.
4. Khor TO, Cheung WK, Prawan A, Reddy BS, Kong AN: **Chemoprevention of familial adenomatous polyposis in Apc(Min/+) mice by phenethyl isothiocyanate (PEITC)**. *Mol Carcinog* 2008, **47**:321-325.
5. Xiao D, Powolny AA, Moura MB, Kelley EE, Bommareddy A, Kim SH, Hahm ER, Normolle D, Van Houten B, Singh SV: **Phenethyl isothiocyanate inhibits oxidative phosphorylation to trigger reactive oxygen species-mediated death of human prostate cancer cells**. *J Biol Chem* 2010, **285**:26558-26569.
6. Chan JM, Wang F, Holly EA: **Vegetable and fruit intake and pancreatic cancer in a population-based case-control study in the San Francisco bay area**. *Cancer Epidemiol Biomarkers Prev* 2005, **14**:2093-2097.
7. Cheung KL, Khor TO, Yu S, Kong AN: **PEITC induces G1 cell cycle arrest on HT-29 cells through the activation of p38 MAPK signaling pathway**. *AAPS J* 2008, **10**:277-281.
8. Chiao JW, Wu H, Ramaswamy G, Conaway CC, Chung FL, Wang L, Liu D: **Ingestion of an isothiocyanate metabolite from cruciferous vegetables inhibits growth of human prostate cancer cell xenografts by apoptosis and cell cycle arrest**. *Carcinogenesis* 2004, **25**:1403-1408.
9. Mi L, Hood BL, Stewart NA, Xiao Z, Govind S, Wang X, Conrads TP, Veenstra TD, Chung FL: **Identification of potential protein targets of isothiocyanates by proteomics**. *Chem Res Toxicol* 2011, **24**:1735-1743.
10. Kluza J, Jendoubi M, Ballot C, Dammak A, Jonneaux A, Idziorek T, Joha S, Dauphin V, Malet-Martino M, Balayssac S *et al*: **Exploiting mitochondrial dysfunction for effective elimination of imatinib-resistant leukemic cells**. *PLoS One* 2011, **6**:e21924.
11. Mi L, Gan N, Chung FL: **Isothiocyanates inhibit proteasome activity and proliferation of multiple myeloma cells**. *Carcinogenesis* 2011, **32**:216-223.
12. Rose P, Whiteman M, Huang SH, Halliwell B, Ong CN: **beta-Phenylethyl isothiocyanate-mediated apoptosis in hepatoma HepG2 cells**. *Cell Mol Life Sci* 2003, **60**:1489-1503.
13. Mukherjee S, Bhattacharya RK, Roy M: **Targeting protein kinase C (PKC) and telomerase by phenethyl isothiocyanate (PEITC) sensitizes PC-3 cells towards chemotherapeutic drug-induced apoptosis**. *J Environ Pathol Toxicol Oncol* 2009, **28**:269-282.
14. Trachootham D, Zhang H, Zhang W, Feng L, Du M, Zhou Y, Chen Z, Pelicano H, Plunkett W, Wierda WG *et al*: **Effective elimination of fludarabine-resistant CLL cells by PEITC through a redox-mediated mechanism**. *Blood* 2008, **112**:1912-1922.
15. Patel T: **Cholangiocarcinoma--controversies and challenges**. *Nat Rev Gastroenterol Hepatol* 2011, **8**:189-200.
16. Sripa B, Brindley PJ, Mulvenna J, Laha T, Smout MJ, Mairiang E, Bethony JM, Loukas A: **The tumorigenic liver fluke Opisthorchis viverrini--multiple pathways to cancer**. *Trends Parasitol* 2012, **28**:395-407.
17. Khan SA, Thomas HC, Davidson BR, Taylor-Robinson SD: **Cholangiocarcinoma**. *Lancet* 2005, **366**:1303-1314.
18. Hezel AF, Zhu AX: **Systemic therapy for biliary tract cancers**. *Oncologist* 2008, **13**:415-423.

19. Buranrat B, Prawan A, Kukongviriyapan U, Kongpetch S, Kukongviriyapan V: **Dicoumarol enhances gemcitabine-induced cytotoxicity in high NQO1-expressing cholangiocarcinoma cells**. *World J Gastroenterol* 2010, **16**:2362-2370.
20. Kongpetch S, Kukongviriyapan V, Prawan A, Senggunprai L, Kukongviriyapan U, Buranrat B: **Crucial role of heme oxygenase-1 on the sensitivity of cholangiocarcinoma cells to chemotherapeutic agents**. *PLoS One* 2012, **7**:e34994.
21. Sripa B, Leungwattanawanit S, Nitta T, Wongkham C, Bhudhisawasdi V, Puapairoj A, Sripa C, Miwa M: **Establishment and characterization of an opisthorchiasis-associated cholangiocarcinoma cell line (KKU-100)**. *World J Gastroenterol* 2005, **11**:3392-3397.
22. Suphim B, Prawan A, Kukongviriyapan U, Kongpetch S, Buranrat B, Kukongviriyapan V: **Redox modulation and human bile duct cancer inhibition by curcumin**. *Food Chem Toxicol* 2010, **48**:2265-2272.
23. Mi L, Wang X, Govind S, Hood BL, Veenstra TD, Conrads TP, Saha DT, Goldman R, Chung FL: **The role of protein binding in induction of apoptosis by phenethyl isothiocyanate and sulforaphane in human non-small lung cancer cells**. *Cancer Res* 2007, **67**:6409-6416.
24. Eckel F, Schmid RM: **Chemotherapy in advanced biliary tract carcinoma: a pooled analysis of clinical trials**. *Br J Cancer* 2007, **96**:896-902.
25. Lee S, Kim WH, Jung HY, Yang MH, Kang GH: **Aberrant CpG island methylation of multiple genes in intrahepatic cholangiocarcinoma**. *Am J Pathol* 2002, **161**:1015-1022.
26. Parasassi T, Brunelli R, Costa G, De Spirito M, Krasnowska E, Lundeberg T, Pittaluga E, Ursini F: **Thiol redox transitions in cell signaling: a lesson from N-acetylcysteine**. *ScientificWorldJournal* 2010, **10**:1192-1202.
27. Lee Y, Kim YJ, Choi YJ, Lee JW, Lee S, Chung HW: **Enhancement of cisplatin cytotoxicity by benzyl isothiocyanate in HL-60 cells**. *Food Chem Toxicol* 2012.
28. Krishna MC, Russo A, Mitchell JB, Goldstein S, Dafni H, Samuni A: **Do nitroxide antioxidants act as scavengers of O2-. or as SOD mimics?** *J Biol Chem* 1996, **271**:26026-26031.
29. Kim JS, He L, Lemasters JJ: **Mitochondrial permeability transition: a common pathway to necrosis and apoptosis**. *Biochem Biophys Res Commun* 2003, **304**:463-470.
30. Chipuk JE, Green DR: **How do BCL-2 proteins induce mitochondrial outer membrane permeabilization?** *Trends Cell Biol* 2008, **18**:157-164.
31. Norberg E, Gogvadze V, Vakifahmetoglu H, Orrenius S, Zhivotovsky B: **Oxidative modification sensitizes mitochondrial apoptosis-inducing factor to calpain-mediated processing**. *Free Radic Biol Med* 2010, **48**:791-797.

## Section 5
## Phenethyl isothiocyanate induces calcium mobilization and mitochondrial cell death pathway in cholangiocarcinoma KKU-M214 cells

### Background

Cholangiocarcinoma (CCA) is a malignancy originating from the bile ducts, usually adenocarcinomatous, and is the second common primary liver cancer [1]. CCA is a rare cancer worldwide, but the most common form of liver cancer in Mekong subregion countries, including northeastern Thailand, Cambodia, Vietnam and Laos [2]. In the Western countries, the incidence and the mortality rate of intrahepatic CCA have risen steeply and steadily over the last decades [3]. In spite of tremendous efforts to improve the treatment, CCA is still notoriously difficult in diagnosis and treatment [3]. Most of CCA patients are already in the advanced stage at diagnosis, and the radical surgery is not feasible. Chemotherapy and radiotherapy could not improve the survival of patients with unresectable CCA [3]. Despite of recent advances in chemotherapy for many cancers, management of CCA with chemotherapeutic drugs and biologic agents has so far been unsatisfied. The development of appropriate new chemotherapeutic drugs and new approaches for the treatment of chemo-resistant cancer like CCA should be of the high priority.

Isothiocyanates (ITCs) are the hydrolysis products of a group of naturally occurring thioglucoside and glucosinolate compounds found in cruciferous vegetables [4]. Among ITCs, phenethyl isothiocyanate (PEITC), sulforaphane and benzyl isothiocyanate are known to have potent biological activities. Recent epidemiological studies showed that intake of ITCs reduced the risk of certain cancers, such as pancreatic and lung cancers [5-6]. PEITC can suppress tumor cells growth, and induce apoptosis and cell cycle arrest [7]. Dietary intake of PEITC strongly inhibited tumorigenesis in various animal models such as a prostate cancer xenografted model [8], colon and lung tumors in transgenic mice models [9-10]. The effects of PEITC on tumor cells are multifaceted including induction of reactive oxygen species (ROS) formation, depolarization of mitochondrial transmembrane potential ($\Delta\Psi_m$) [11-12], activation of c-Jun N-terminal kinase (JNK) and p38 kinase-mediated apoptotic pathway [7, 13], and induction of hyper-expression of death receptor-5 mediated caspase 8 activation [14]. PEITC also can depress pro-survival signaling pathways of NF-κB and PI3K/Akt [15], as PEITC inhibits IKK, IκB and Akt phosphorylation leading to inhibit cell proliferation and apoptosis.

The selective cytotoxic effects of ITCs on various cell types have less frequently been reported. PEITC, benzyl ITC and sulforaphane showed the same ranges of IC50 values to MCF-7 breast cancer cells and MCF-12A, the non-cancer mammary epithelial cells, and also to HK-2 kidney cells [16]. The selective toxicity of anticancer agents on the major organs may be the primary concern in cancer chemotherapy. Although some functional distinction between cancer and normal cells such as oxidative status have been suggested [17-18], it is yet to be translated into an effective strategy to eliminate cancer cells while spare normal cells.

The effects of PEITC on multiple steps of cancer growth make this compound highly versatile and promising candidate in cancer chemoprevention and chemotherapy. However, the exact mechanisms of its chemopreventive effects are not fully understood. For the better understanding of the anticancer mechanisms of PEITC, we evaluated the effects of PEITC on a bile duct cancer cell line, KKU-M214 in relation to GSH redox stress and mitochondrial function. In this study, HeLa [Chang liver] cells were used as the reference because our previous study showed that oxidative stress caused the suppression of glutathione (GSH) redox in this cell line [19].

## Methods

### Cell cultures

Human CCA cell line, KKU-M214 established in our institute and human HeLa [Chang liver] cells were both kindly provided by Prof. Banchob Sripa, Department of Pathology, Faculty of Medicine, Khon Kaen University. Cells were grown in Ham's F12 medium supplemented with 12.5 mM N-2-hydroxyethylpiperazine-N'-2-ethanesulfonic acid (HEPES; pH 7.3), 100 U/mL penicillin, 100 µg/mL streptomycin sulfate and 10% fetal calf serum and maintained under 5% $CO_2$ in air at 37°C as described previously [20]. The cells were subcultured every 2-3 days before confluence of the cells using 0.25% trypsin–EDTA, and the medium was changed after an overnight incubation.

### Cytotoxicity assay

KKU-M214 and Chang liver cells were seeded onto 96-well culture plates at a density of 7,500 cells/well. After an overnight culture, the serum-free medium was replaced with the media containing PEITC, and the cells were cultured for various time intervals. The cytotoxicity was examined by the sulphorhodamine B (SRB) assay. In brief, cultured cells were washed once with phosphate-buffered saline (PBS), fixed with 100 µl of ice-cold trichloroacetic acid for 1h, and stained with 50 µl of 0.4% SRB in 1% acetic acid for 30 min. The cells were then rinsed several times with 1% acetic acid, and protein-bound dye was dissolved with 200 µl of 10 mM Tris base solution. The absorbance was determined using a microplate reader with the filter wavelength of 540 nm.

To determine cells undergone apoptosis, cultured cells were stained with fluorescent dyes as previously described with modifications [20-21]. In brief, the media was removed after PEITC treatment and the cells were stained with acridine orange and ethidium bromide (AO/EB) in PBS. The cells were examined using a Nikon Eclipse TS100 inverted microscope with the excitation and long-pass emission filters of 480 nm and 535 nm, respectively. The fluorescent images were taken at 2 predetermined areas in each well with triplicate wells per concentration using a Nikon Coolpix digital camera. The number of viable, apoptotic, and necrotic cells, which were stained with green fluorescence with intact nuclei, green fluorescence with the appearance of cell shrinkage, nuclear condensation and fragmentation, and bright orange fluorescence, respectively, were enumerated. The apoptotic cells were calculated as the percent apoptotic cells over a total number of cells in the same area.

### Measurement of ROS

Intracellular ROS generation was measured using a cell-permeable fluorescent probe, dihydroethidium (DHE). Briefly, $5\times10^4$ cells were seeded in 96 black well plates and cultured overnight. Then, the medium was removed and the cells were washed with phosphate buffered saline (PBS). They were then treated with PEITC and 25 µM DHE with or without 2 mM *N*-acetyl-L-cysteine (NAC) or 0.5 mM 4-hydroxy-TEMPO (TEMPOL), in serum-free medium and kept in 5% $CO_2$ atmosphere at 37°C for 90 min. The fluorescence intensity was read and quantified in a Gemini XPS fluorescent plate reader with the excitation and emission wavelength of 518 nm and 605 nm, respectively.

### Glutathione Assay

Total glutathione was measured essentially according to Tietze's method [22]. Glutathione disulfide (GSSG) was assayed by the method previously described [21] using 1-methyl-2 vinyl-pyridinium trifate (M2VP) as a glutathione scavenger. Cultured cells were trypsinized and washed three times with cold PBS. Cell suspensions were reacted with M2VP (1 mM) to determine GSSG. Aliquots of untreated cell suspensions were used for the assay of total GSH. Protein concentration was assayed using the Bradford's dye binding method.

**Calcium mobilization assay**

Intracellular calcium level was measured using an assay kit (Fluofort® Calcium Assay, Enzo Life Sciences, PA, USA). In brief, KKU-M214 and Chang cells were grown on 96 well plates at the density of 10,000 cells/well and treated with 3 and 10 μM PEITC with/without 2 mM of NAC for 1 h. Then, the media were removed and FluoForte® dye-loading solution was added according to the manufacturer's instruction. The plate was incubated at 37°C for 30 min and the fluorescent staining was analyzed under a fluorescent microscope with the excitation and emission wavelengths of 485 nm and 535 nm, respectively. Images of the cultured cells were captured and the integrated optical density (IOD) of each image was analyzed by using the Image-Pro Plus (Media Cybernetics) software.

**Measurement of mitochondrial transmembrane potential**

The dissipation of the mitochondrial electrochemical potential gradient is known as an early event leading to apoptosis. To measure the change in mitochondrial transmembrane potential ($\Delta\Psi_m$), cells were seeded in 96 black well plates at the density of $1\times10^4$ cells/well and cultured overnight before treatment with various concentrations of PEITC for 3 and 24 h. The assay was performed according to the method described previously [23] using the cationic, lipophilic dye, 5,5',6,'-tetrachloro-1,1',3,3'tetraethylbenzimidazolyl carbocyanine iodide (JC-1) (Clayman Chemical) staining with some modifications. The cultured plate was centrifuged at 1,000 rpm for 5 min at room temperature and the cultured media was removed, loaded with JC-1 dye for 20 min, washed by centrifugation, incubated in the assay buffer and $\Delta\Psi$m was analyzed under a fluorescent microscope with the excitation wavelength of 485 nm and emission wavelength of 535 nm. JC-1 forms J-aggregates in healthy mitochondrial matrix, which can be visualized as red fluorescence. In depolarized mitochondria, JC-1 effluxes to the cytoplasm and exists as monomers with green fluorescence. The shift of red to green fluorescence is an indicative of the depolarization of $\Delta\Psi_m$.

**Western blot analysis**

Whole cell lysates were prepared as described previously [21]. PEITC-treated and control cells were washed with PBS, collected, and lysed with cell lysis buffer at 4°C with vigorous shaking. After centrifugation at 12,000 g for 30 min, the supernatant was collected and stored at -80°C until use. The protein samples (30 μg protein/sample) were electrophoretically separated on 10% SDS–polyacrylamide gel (SDS-PAGE). The proteins were transferred to polyvinylidene difluoride (PVDF) membranes by semi-dry blotting at 10 V for 40 min. The PVDF membranes were blocked for 2 h at 4°C with 5% (w/v) skimmed milk powder in PBS containing 0.1% Tween-20. The PVDF membrane was incubated overnight at 4°C with primary antibodies including rabbit polyclonal IgG against cytochrome c (sc-13560, Santa Cruz BioTechnology, 1:1000 dilution,), mouse monoclonal IgG against Bcl-xl (sc-8392, 1:500 dilution), rabbit polyclonal IgG against Bax (sc-493,1:1000 dilution), rabbit polyclonal IgG against AIF (sc-5586, 1:500 dilution), rabbit polyclonal IgG against p53 (sc-6243, 1:500 dilution), goat polyclonal IgG against β-actin (sc-1616 HRP, 1:2500 dilution), in PBS containing 0.1% Tween-20. The primary antibody was removed and the membranes were extensively washed with PBS/Tween-20. The membranes were then incubated for 2 h at 4°C with 1:5,000 dilution of respective horseradish peroxidase-conjugated secondary antibodies (goat anti-mouse or anti-rabbit

IgG). After removal of the secondary antibody and PBS buffer washings, the blotted membranes were incubated with ECL substrate solution (ECL™ Prime Western Blotting Detection Reagent). The densities of the specific cytochrome c, Bcl-xl, Bax, AIF, p53 and β-actin bands were visualized and captured using ImageQuant™ 400 (GE Healthcare).

**Measurements of caspase activities**

**Caspase 8 and 9**

After treatment with PEITC for 3 and 6 h, the cultured cells were trypsinized, and adjusted to $10^6$ cells for each reaction. Cell pellet was lysed with cell lysis buffer on ice for 10 min, centrifuged, and then 50µl of the supernatant was transferred to individual black microplate wells. The sample in each well was mixed with 50 µl of 2x reaction buffer (containing 10% glycerol; 0.5 mM EDTA; 20 mM Hepes, pH 7.0; DTT 10 mM) and fluorogenic Ac-LEHD-AFC, a caspase 9 substrate (50µM) or Z-IETD-AFC (EMD Millipore), a caspase 8 substrate (50µM). Reaction mixtures were incubated for 8 h at 37°C in dark and fluorescent signals were read using the Gemini XPS fluorescent plate reader with the excitation and emission wavelengths of 400 and 505 nm, respectively.

**Caspase 3**

Cell lysates were prepared as above and mixed with the reaction buffer (containing 0.2% CHAPS; 4 mM EDTA; 20 mM PIPES, pH 7.4; DTT 10 mM and 0.2 mM Z-DEVD-AMC), EnzCheck® Caspase-3 Assay kit#1, (Molecular Probe). Reaction mixtures were incubated for 1 h at 30°C in dark and fluorescent signals were read using the Gemini XPS fluorescent plate reader with the excitation and emission wavelengths of 342 and 441 nm, respectively.

**Statistical analysis**

All the results were presented as the mean ± SEM. Statistical comparison between control and treated group was performed using Student's t-test or *One-way ANOVA with Student-Newmann-Keuls post-hoc* test, where appropriate. The level of significance was set at $p<0.05$.

**Results**

**Cytotoxic effects of PEITC on CCA and Chang cells**

KKU-M214 and Chang cells were exposed to PEITC at the indicated concentrations and the cytotoxicity of PEITC was assessed at 24 and 48 h. Viability of both cell lines was reduced rapidly after exposure to PEITC and the percent cytotoxicity remained similar level after 24 and 48 h incubation (Fig. 1). The IC50 values were not different between 24 and 48 h of incubation (2.99 ± 0.87 and 3.25 ± 0.19 µM), respectively, for KKU-M214 (Figure 1A), and (3.46 ± 0.20 and 3.39 ± 0.75 µM) for Chang cells (Figure 1B). KKU-M214 was apparently more sensitive to PEITC than Chang cells, especially at 24 h of incubation.

**PEITC-induced apoptosis in relation to apoptosis-associated proteins expression**

Induction of apoptotic cell death by PEITC was examined for KKU-M214 and Chang cells. PEITC induced apoptosis of both cell lines very rapidly within 3 h in a dose dependent manner (Figure 2A & B). In contrast, PEITC did not induce necrotic cell death at any time points examined (data not shown). The induction of apoptotic cell death was associated with changes in apoptotic proteins, *i.e.*, decrease of Bcl-xl and increase of Bax protein expression within 3 h. PEITC induced cytochrome c release in Chang cells but not in KKU-M214 cells. Conversely, AIF was markedly increased in KKU-M214 cells but not in Chang cells. Bcl-2 protein expression is known to be regulated partly by p53,

but, in this study, no significant changes in p53 protein expression were observed at 3 h (Figure 2C) in spite of significant changes in Bcl-xl, Bax and other apoptogenic proteins in both cells.

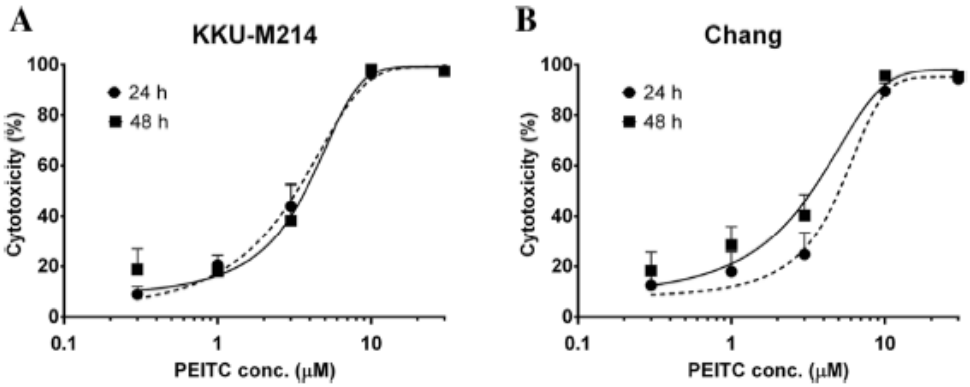


**Figure 1. Cytotoxic effects of PEITC on KKU-M214 and Chang cells**. Cells were incubated with various concentrations from 0.3 to 30 μM PEITC for 24 and 48 h. The cytotoxicity of PEITC in KKU-M214 (A) and Chang cells (B) was examined by SRB assay. Each value represents the mean ± SEM of three experiments.

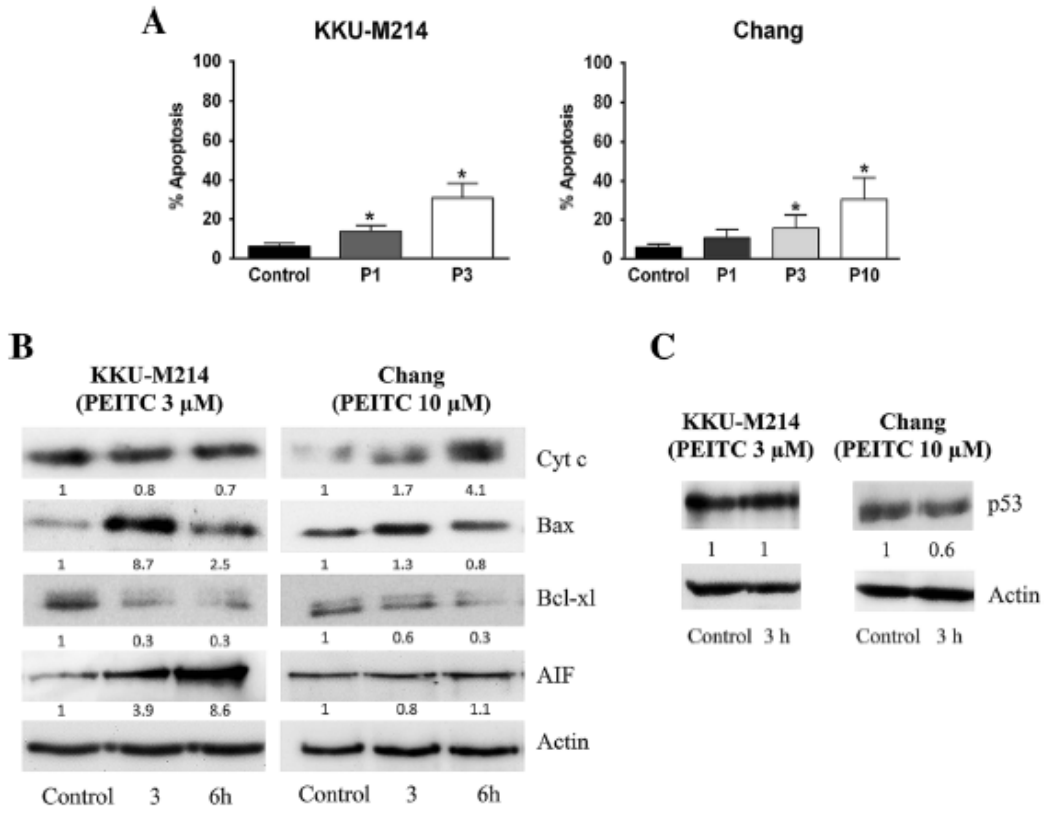


**Figure 2 PEITC-induced apoptosis and release of proapoptogenic proteins**. Chang and KKU-M214 cells were treated with PEITC 1, 3 or 10 μM (P1, P3 or P10, respectively) for 3 or 6 h. The number of apoptotic cells was assessed by AO/EB method at 3 h of incubation (A). Each bar represents the mean ± SEM of three experiments. Significantly different from control, $*p<0.05$. Immunoblot analysis was performed using 30 μg of protein and cytochrome c, Bax, Bcl-xl, AIF and p53 were detected by specific antibodies. β-actin was used as loading control (B & C). Value indicates the relative protein intensity as a ratio to the corresponding vehicle-treated control. Each experiment was done at least twice with similar results, and the representative bands from one experiment are shown

**PEITC-induced cell death via caspase -dependent and -independent pathways**

As the increase of AIF and cytochrome c levels are known to be involved in the intrinsic death pathway, their downstream caspase activities in mitochondrial pathway were evaluated along with caspase-8 extrinsic pathways. The effects of PEITC on caspase 3, 8 and 9 activities in both cell lines were measured at 3 and 6 h after treatment. Caspase-8 activity was unaltered in both cell lines (Figure 3A & B). While caspase-3 and -9 activities in KKU-M214 cells were unchanged after PEITC treatment, they were significantly increased in PEITC-treated Chang cells (Figure 3C-F).

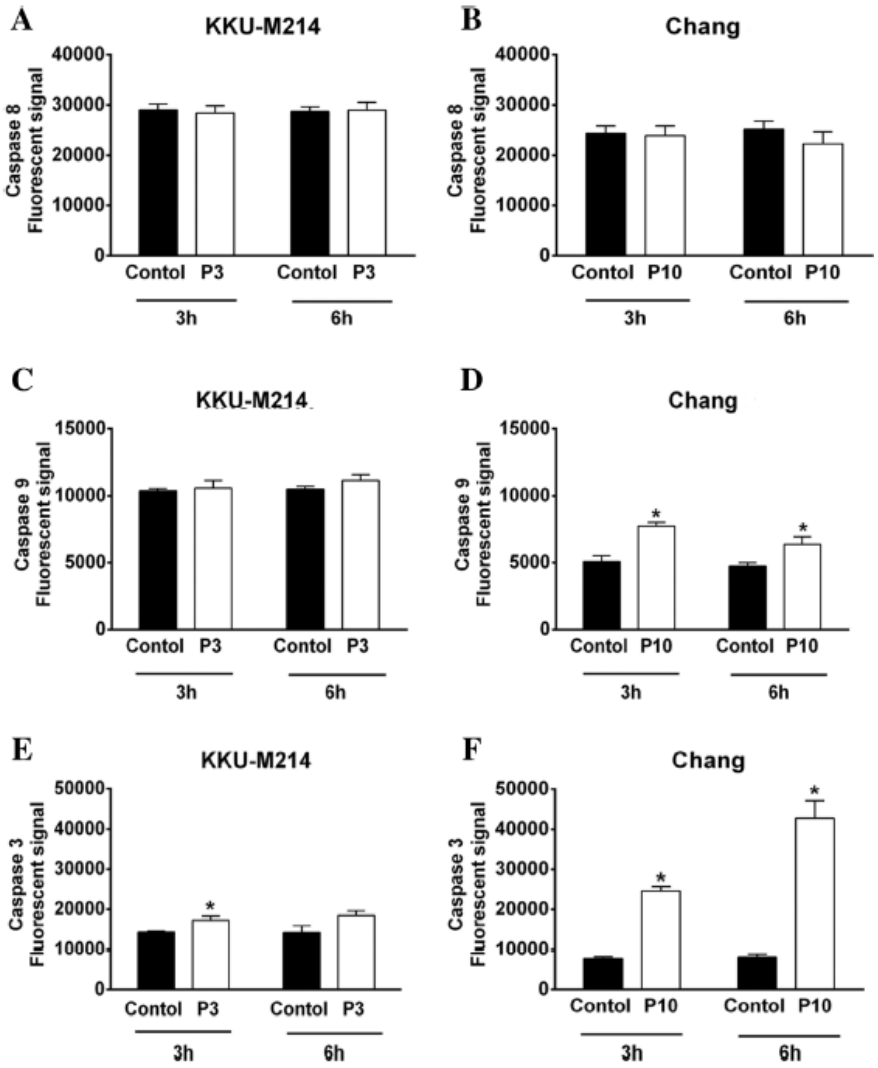


**Figure 3 Activation of caspases by PEITC**. Cells were treated with 3 or 10 μM of PEITC (P3, P10), for 3 and 6 h. Caspase-3 (E & F), caspase-8 (A & B) and caspase-9 (C & D) activities were determined by incubating the cell lysates with fluorogenic substrates specific for each caspase enzyme. Each bar represents the mean± SEM of three experiments. Significantly different from corresponding controls, *$p$<0.05.

**PEITC-induced glutathione depletion**

Previous reports [11-12] suggested that cytotoxicity of PEITC is related to oxidative stress. As GSH is a major cellular antioxidant, we investigated the effect of PEITC on cellular GSH levels. After

exposure to PEITC, both KKU-M214 and Chang cells rapidly lost cellular GSH in a dose-dependent manner as early as 3 h of incubation (Figure 4A & C). In KKU-M214 cells, GSH levels returned to, or rose up even higher than, the control level at 24 h. GSH /GSSG ratio in KKU-M214 cells was initially reduced and then returned to the control level by 24 h (Figure 4B). After treatment with 10 μM PEITC, only very few KKU-M214 cells were left alive at 24 h, then it was not possible to determine the levels of GSH. In contrast to the rapid recovery of KKU-M214 cells, PEITC-mediated depletion of GSH levels and depressed GSH redox ratios in Chang cells persisted even at 24 h of incubation (Figure 4C & D).

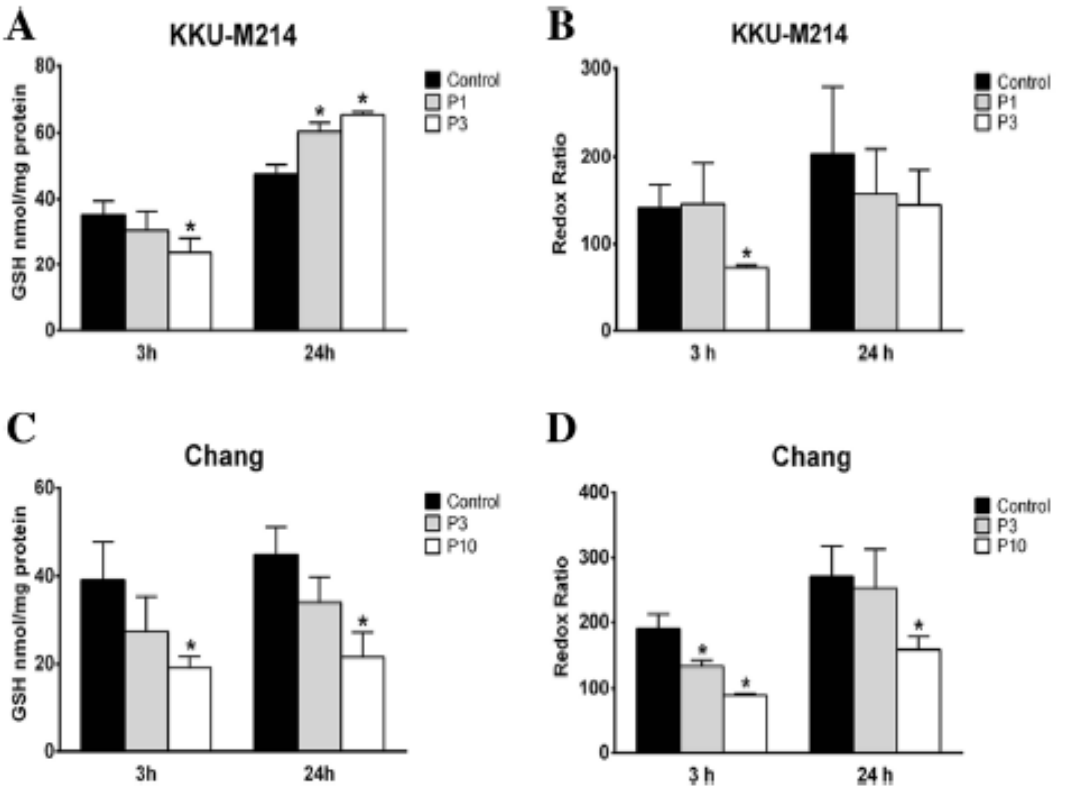


**Figure 4 Effect of PEITC on intracellular GSH and redox ratio.** KKU-M214 (A & B) and Chang cells (C & D) were incubated with PEITC 1, 3 or 10 μM (P1, P3 or P10, respectively) for 3 and 24 h. Total GSH contents were measured from cell pellets as intracellular GSH (A & C), and GSH and GSSG ratios (B & D) were determined for GSH redox ratio. Each bar represents the mean ± SEM of three experiments. Significantly different from control, *$p$<0.05.

**Effects of antioxidants on PEITC-induced oxidative stress**

Since the results given above, PEITC treatment induced GSH depletion in both cell lines, we examined whether this depletion was associated with the formation of reactive oxygen species (ROS). We examined also the role of antioxidants on GSH depletion and ROS formation. For this purpose, we used TEMPOL, a ROS scavenging agent, and NAC, a thiol modifier. As shown in Figure 5A and B, the basal level of superoxide in KKU-M214 cells was approximately 2-fold higher than that in Chang cells. Treatment of the cells with 3 and 10 μM PEITC caused significant increase of ROS in Chang cells, but only slight increase in KKU-M214 cells. Co-treatment of the cells with PEITC and 0.5 mM TEMPOL or 2 mM NAC completely normalized the ROS levels in both cell lines (Figure 5A & B). Moreover, treatment of NAC also largely prevented PEITC-induced losses of GSH in both cell

lines at 3 h (Figure 5C & D) and this protective effect persisted up to 48 h of incubation (data not shown). However, TEMPOL, which could completely neutralize ROS, could only partially prevented GSH depletion in both cell lines.

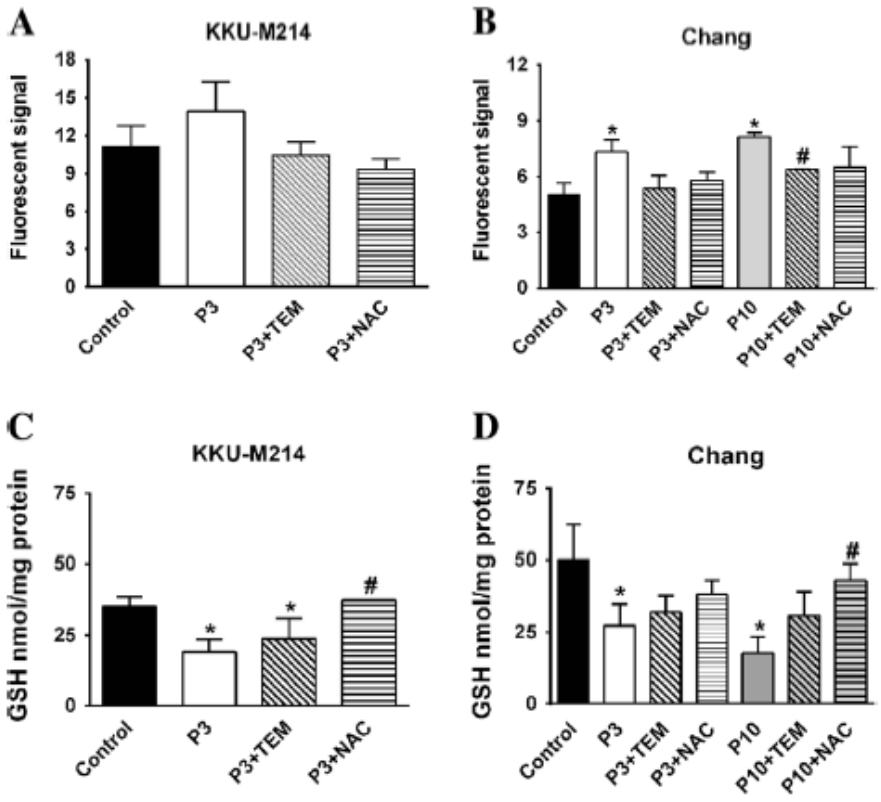


**Figure 5 Effect of PEITC on ROS production and GSH depletion**. KKU-M214 (A & C) and Chang cells (B & D) were incubated with PEITC at indicated concentrations 3 and 10 µM (P3 & P10) with or without TEMPOL (0.5 mM TEM) or NAC (2 mM). ROS formation was quantified by dihydroethidium method after incubation for 90 min (A & B) and cellular GSH (C & D) was assayed at 3 h after incubation. Each bar represents the mean ± SEM of three experiments. Significantly different from control, *$p$<0.05, and significantly different from PEITC treated group, #$p$<0.05.

**PEITC-induced intracellular calcium mobilization**

Oxidative stress is known to trigger the release of $Ca^{2+}$ from some intracellular $Ca^{2+}$ storages, particularly from the endoplasmic reticulum, resulting in the increase of cytosolic and mitochondrial $Ca^{2+}$, which initiates cell death [24]. We examined the effects of PEITC on intracellular $Ca^{2+}$ mobilization in KKU-M214 and Chang cells. As shown in Figures 6A & B, PEITC induced rapid $Ca^{2+}$ mobilization into cytosol within the first 1 hour of incubation, which was visualized by $Ca^{2+}$ fluorescent probe in KKU-M214 and Chang cells. NAC, a thiol modifier, could not inhibit $Ca^{2+}$ flux into cytosol in KKU-M214 cells (Figure 6 C), but could completely inhibit $Ca^{2+}$ flux into cytosol in Chang cells (Figure 6 D). This underlines the causal relationship between calcium flux and oxidative stress.

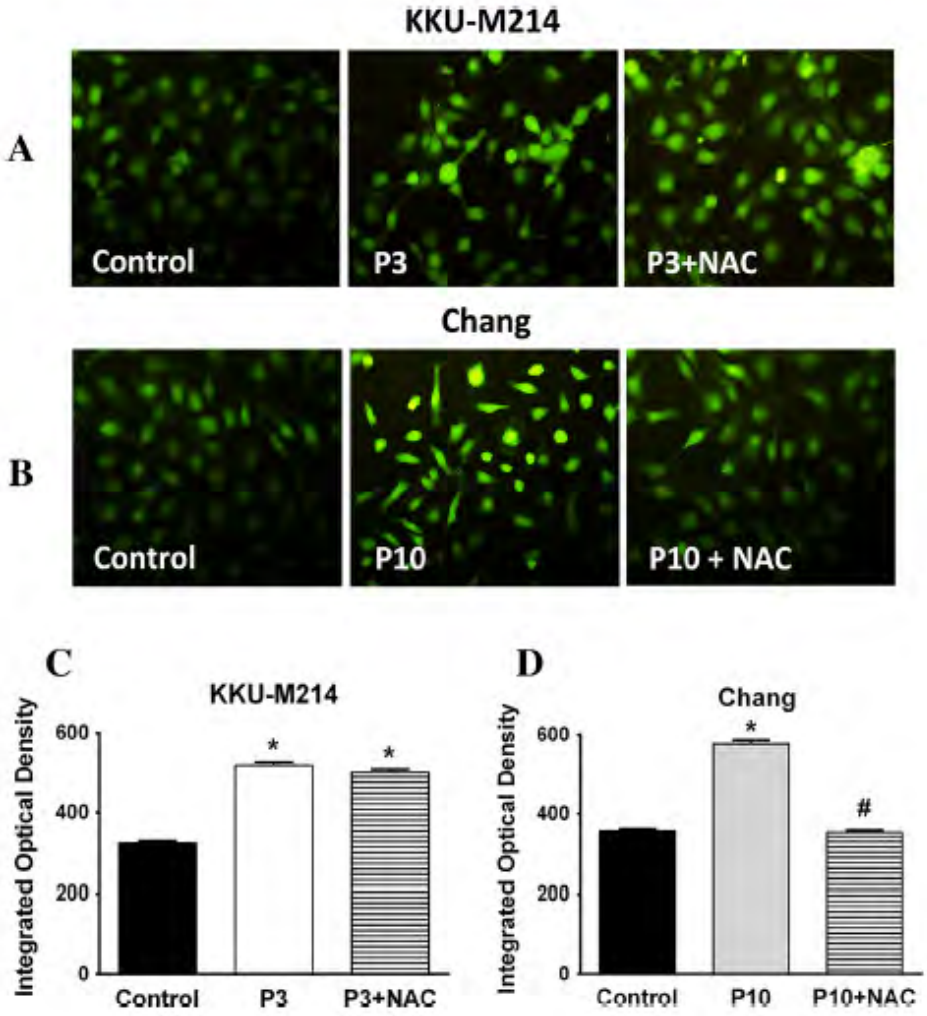


**Figure 6 PEITC induced the mobilization of intracellular $Ca^{2+}$** Cultured cells were treated with 3 or 10 µM of PEITC (P3 or P10) with NAC (2 mM) for 1 h. The mobilization of $Ca^{2+}$ into cytosol was analyzed by fluorescence staining using Fluoforte dye with excitation and emission wavelength of 485 and 535 nm, respectively. Representatives of images in each condition are shown (A & B). The integrated optical density (IOD) of fluorescence in each condition was analyzed (C & D) from 10 images of two experiments. Each bar represents the mean ± SEM. Significantly different from control, *p<0.05 and significantly different from PEITC treated group, # p <0.05.

**PEITC-induced depolarization of the mitochondrial transmembrane potential**

Since PEITC induced apoptotic cell death via Bcl2 protein family and other apoptogenic proteins, it is likely that the cytotoxicity of PEITC would be associated with the mitochondrial pathway. We examined the effect of PEITC on mitochondrial integrity by measuring the $\Delta\Psi_m$ using JC-1 fluorescent assay. In untreated control cells, mitochondria predominantly exhibited red fluorescence due to accumulation of J-aggregates representing the intact $\Delta\Psi_m$. PEITC treatment rapidly depolarized $\Delta\Psi_m$ as shown by the green fluorescence of JC-1 monomeric forms present in the cytosol (Figure 7). The effect was apparent within the first 1 hour of incubation and sustained up to 24 h in both cells. The images of the cells treated with PEITC for 3 h are shown in Figure 7. The effects of TEMPOL and NAC on the PEITC-induced $\Delta\Psi_m$ changes were evaluated. As is expected, TEMPOL did not prevent the depolarization of $\Delta\Psi_m$ in both cell lines. In contrast, NAC completely protected

PEITC-induced mitochondrial depolarization in Chang cells, but this protective effect was not apparent in KKU-M214 cells, despite that GSH in KKU-M214 cells was well maintained by NAC.

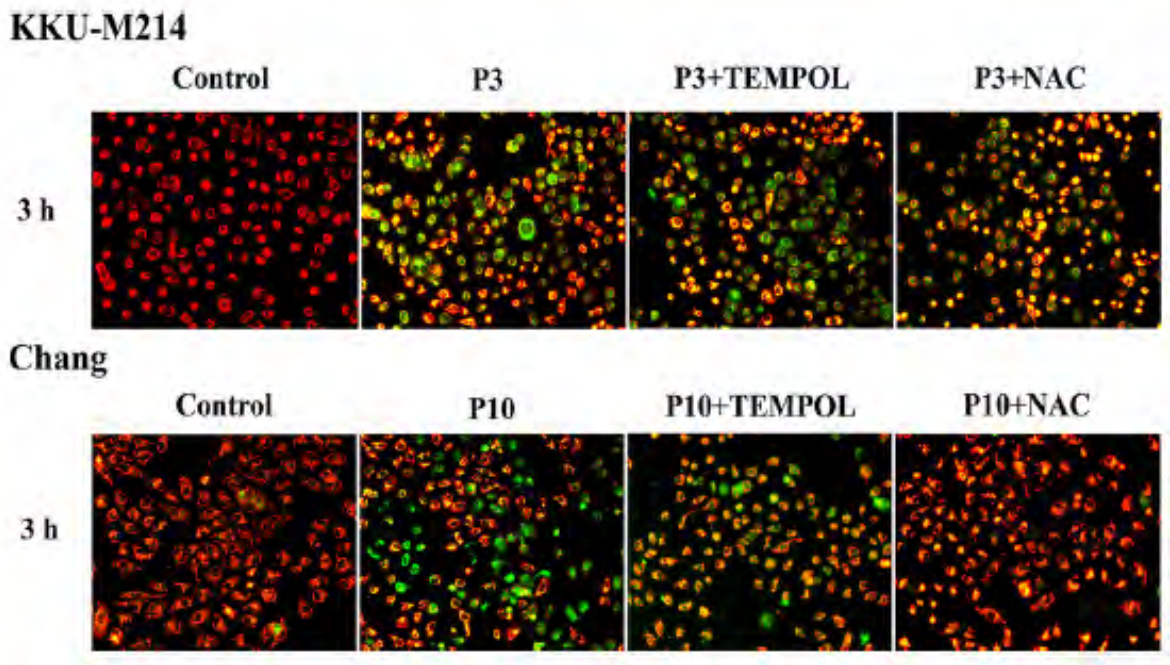


**Figure 7 PEITC induced depolarization of the mitochondrial transmembrane potential**. Cells were treated with 3 or 10 μM (P3 or P10) of PEITC with TEMPOL (0.5 mM TEM) or NAC (2 mM NAC) for 3 h. The change in $\Delta\Psi_m$ was examined using JC-1 staining method. Fluorescent images were captured by fluorescence microscopy with the excitation wavelength of 485 nm and the emission wavelength of 535 nm. The experiments were performed twice with similar results, representative images from one experiment were shown.

**Effect of cyclosporine on PEITC-induced cell death**

Since the depolarization of $\Delta\Psi_m$ may be resulted from the opening of the mitochondrial permeability transition (MPT) pores, we examined whether the opening of MPT was the primary effect of PEITC to induce cell death. The results show that cyclosporine (Cs) (Sandimmune, Novartis), a potent MPT inhibitor, could prevent the losses of $\Delta\Psi_m$ (data not shown), but could not prevent cell death in both cell types (Figure 8 A & B). These results suggested that the loss of $\Delta\Psi_m$ was not a critical event and might be secondary to the recruitment of Bcl2 protein members (Figure 2).

**Effect of antioxidants on PEITC-induced cytotoxicity**

It is apparent from the results given above that PEITC affected differently on KKU-M214 and Chang cells over the induction of GSH redox stress, protection of $Ca^{2+}$ efflux into cytosol and the protection to the loss of $\Delta\Psi_m$ by NAC. Therefore, the protective effects of antioxidants, TEMPOL or NAC, on PEITC-induced cytotoxicity were assessed. Figure 8 (C & D) shows that, co-treatment of the cells with PEITC and TEMPOL apparently could not protect cell death in both cell types, which was consistent with the results of the inefficacy of TEMPOL to prevent depolarization of $\Delta\Psi_m$ changes.

Rather, treatment with TEMPOL exacerbated cell death in KKU-M214 cells (Figure 8 C). NAC, which was unable to prevent the loss of $\Delta\Psi_m$ nor the $Ca^{2+}$ mobilization in cytosol in KKU-M214 cells, also could not protect PEITC-induced cell death. In contrast to the inefficacy to KKU-M214 cells, NAC almost fully protected Chang cells from the cytotoxic effect of PEITC at any time points examined after incubation (Figure 8 D).

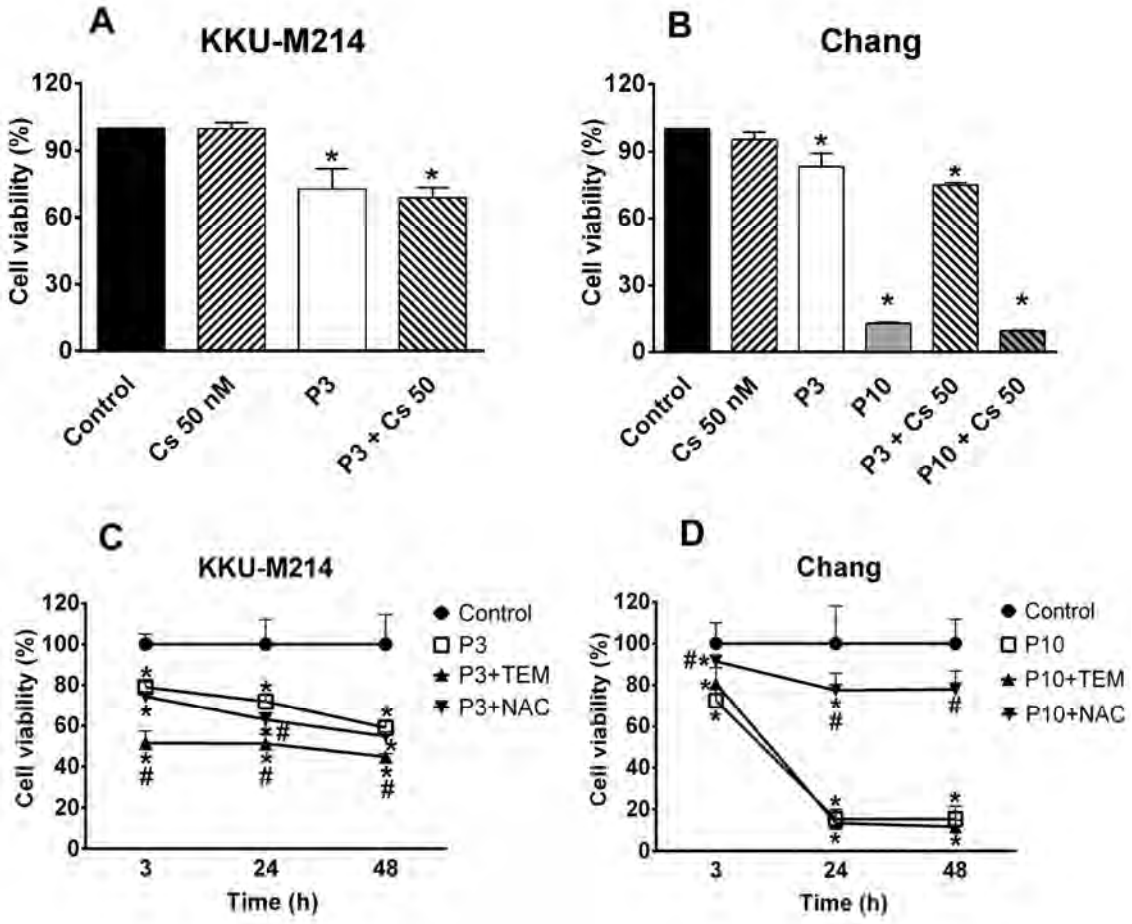


**Figure 8 Effects of Cs, NAC and TEMPOL on PEITC-induced cell death**. Cells were treated with 3 or 10 μM of PEITC (P3 or P10) in combination with Cs (cyclosporine) (50 nM) for 24h (A and B). Another experiments, cells were treated with NAC (2 mM) or TEMPOL (0.5 mM, TEM) for 3, 24 and 48 h (C and D). Cell viability was assayed. Each bar or each value represents the mean ± SEM of from three experiments. Significantly different from control group, *p<0.05. and significantly different from PEITC treated group, #p <0.05.

**Discussion**

The chemopreventive properties of dietary cruciferous vegetables are well recognized from the results of epidemiological and experimental studies [5-6, 9]. PEITC, one of the most promising ITCs, has been extensively studied *in vivo* and *in vitro*, information of its effects on CCA cells is lacking. Many strategies to enhance therapeutic outcomes in CCA treatment have been studied. For example, addition of biologic agents to block various kinase enzymes, or to suppress cytoprotective enzymes; NQO1 and HO-1 in CCA cells could increase the susceptibility of CCA to chemotherapeutic drugs [1, 20, 23]. In the present study, we demonstrated that PEITC could inhibit CCA cell growth and rapidly induce apoptosis. PEITC exerts different effects on KKU-M214 and Chang liver cells over cellular GSH redox and the release of mitochondrial apoptogenic molecules. The different cytoprotective effect of NAC on PEITC-induced cell death of the two cell types may reflect that the intracellular targets of PEITC are different in KKU-M214 and Chang liver cells.

Previous studies showed that PEITC induced cell death via several different mechanisms depending on cell types. Induction of cell death was associated with activation of c-Jun-N-terminal kinase (JNK) in DU145 but not in LnCaP cells [13] or with formation of ROS in PC3 and LnCaP, but was independent of ROS in HepG2 and multiple myeloma cells [12, 25-26]. In this study, cytotoxic effects of PEITC were explored using a CCA cell line, KKU-M214 cells and Chang liver cells, since most chemotherapeutic agents have little selectivity over cancer cells from normal host cells. Our findings of the lack of selective toxicity of PEITC over CCA and Chang cells is consistent with the previous reports that various ITC killed cancer cells and non-cancer cells at the same order of concentration [16].

Present study showed that PEITC could induce apoptosis of both KKU-M214 and Chang liver cell lines in association with the decreased Bcl-xl and increased Bax expressions. It is known that p53 plays an important role in physically and functionally interacting with Bcl-2 family members for their translocation to mitochondria [27]. However, in the present study, the changes of the Bcl-2 protein members were not associated with p53 expression. This may imply that the apoptotic signal from PEITC to mitochondria is not transmitted via p53 pathway. Alternatively, stress signals provoked by PEITC may induce Bcl-2 family proteins via TNF family receptors, endoplasmic reticulum stress pathway or others [14, 28]. It has been shown that PEITC sensitized HN22 oral carcinoma cells to DR5-mediated extrinsic death pathway [14]. We measured caspase 8 and 9 activities, which represent the initiator caspases of the extrinsic and intrinsic death signaling pathways, respectively. From the results of this study, PEITC-induced cell death appeared to be associated only with the intrinsic mitochondrial pathway, as there was no change in the caspase 8 activity after PEITC treatment.

In the present study, the cytotoxicity of PEITC was mediated via caspase-independent and caspase-dependent pathways for KKU-M214 and Chang cells, respectively. AIF is released from mitochondria and translocated to the nucleus where it fulfills the lethal function. Similar to cytochrome c, AIF play an important role in mitochondrial respiratory chain and is required for cell survival [29]. However, AIF is not a widespread cell death effector and its contribution to the execution of cell death is dependent upon the cell type, as well as the insulting signals [29]. PEITC induced AIF release in U2 OS sarcoma [11] and KKU-M214 cells in the present study. On the other hand, PEITC induced cytochrome c release in many cancer cells including MCF7, a breast cancer cell line [30], HT29, a colon cancer cell line [30], PC3, a prostate cancer cell line [12] and Chang cells in the present study. Our results showed that PEITC exerts its effects via AIF or cytochrome c depending on the cell types.

One of the prominent effects of PEITC is the induction of oxidative stress in cancer cells, which is characterized by ROS formation, GSH depletion and protein oxidation [11-12]. Our results only partially concurred with those previous reports. In the present study, PEITC induced GSH depletion in both KKU-M214 and Chang cells. However, PEITC induced ROS formation and GSH redox stress only in Chang cells but not in KKU-M214 cells (at least at 24 h of incubation). PEITC-induced cytotoxicity on Chang cells was associated with the depression of cellular GSH redox, as the replenishment of GSH by NAC could protect from cell killing by PEITC. This suggests PEITC-induced cell death of Chang cells may be via GSH redox stress. On the other hand, KKU-M214 cells seemed to handle PEITC-induced GSH redox stress rather well, because GSH levels were restored to the control level, or overshoot higher than controls at 24 h. Moreover, the treatment with NAC did not prevent PEITC-induced cell death of KKU-M214 cells. It is, therefore, the main mechanism of PEITC-induced cytotoxicity in KKU-M214 may be not by GSH redox stress. Although the cytotoxicity of PEITC against KKU-M214 and Chang cells was not much different in terms of the potency and efficacy, the underlining mechanism of the expression of cytotoxicity of PEITC on those two cells was obviously different because of the opposing results of the protective effect of NAC. It is, therefore, important to investigate further whether CCA tissues in the patients have the similar characteristics as the tumor cell responses to PEITC, before implementing NAC as an adjuvant.

PEITC is known to induce ROS formation, which is assumed to be a main mechanism of cell killing action of PEITC on some tumor cells [11-12, 17]. However, in this study, ROS was not causally related to GSH depletion or induction of cell death of KKU-M214 and Chang cells. Treatment with TEMPOL, which could completely normalize the superoxide to the background level, could not prevent cell death of both types of cells. Our results were consistent with the previous report of the failure of using various radical scavengers to prevent PEITC-induced cell death [26]. These results suggest that the mechanism of PEITC to induce cell death may be unique. As the possible mechanisms of PEITC, modifications of redox-sensitive proteins to form electrophiles attracting some critical proteins should be considered [31].

Oxidative stress can trigger the mobilization of $Ca^{2+}$ into cytosol, where endoplasmic reticulum is the important $Ca^{2+}$ storage [24]. We observed a rapid flux of $Ca^{2+}$ into cytosol shortly after PEITC treatment. The rapid increase of cytosolic $Ca^{2+}$ may cause elevation of mitochondrial $Ca^{2+}$ and decrease of $Ca^{2+}$ in endoplasmic reticulum, and such imbalance of $Ca^{2+}$ may trigger a variety of cascades leading to cell death. The lack of protective effect of NAC on cytosol $Ca^{2+}$ flux in KKU-M214 cells suggests that PEITC may exert the effect on the release of $Ca^{2+}$ by cellular stress other than the GSH redox system. On the other hand, in Chang cells, GSH redox disturbance may be primarily involved in cytosolic $Ca^{2+}$ flux.

In the present study, an increase of cytosolic $Ca^{2+}$ was accompanied with the rapid loss of $\Delta\Psi_m$. The depolarization of $\Delta\Psi_m$ is resulted from the opening of MPT pores, which is formed in the inner membrane of mitochondria [32]. The opening of MPT pores leads to diminish of ATP synthesis and ensuing cell death. However, present study showed that cyclosporine, a MPT pore inhibitor could not prevent PEITC-induced cell death, although it could prevent losses of the $\Delta\Psi_m$. This may imply that the depolarization of $\Delta\Psi_m$ is probably an associated event of PEITC treatment, but is not a direct effect leading to cell death. Taken all these together, mitochondria may not be a primary target of the increase of cytosolic $Ca^{2+}$ flux for initiation of cell death. Instead, the increased cytosol $Ca^{2+}$ may initiate the death signals in the cytosol by activation of a variety of $Ca^{2+}$-sensitive enzymes, such as calpain, leading to the cleavage and targeting of Bax to mitochondria [24] to activate the mitochondrial cell death pathway.

Our study revealed that PEITC induces up-regulation of Bax and down regulation of Bcl-XL. The formation of Bax pore and mitochondrial outer membrane permeabilization (MOMP) upon activation may be the critical event leading to the release of proapoptogenic proteins, cytochrome c and AIF, and ensuing cell death [33]. The mechanisms of the induction of cytosol $Ca^{2+}$ mobilization and activation of Bcl-2 proteins by PEITC remain to be elucidated. Since the precise mechanisms of PEITC-induced cell death of KKU-M214 cells remain unclear, further study is needed to explore novel mechanisms of the expression of cytotoxicity of PEITC.

## Conclusion

In conclusion, the present results show that PEITC induced apoptosis of CCA cells and Chang cells. This process may involve induction of oxidative stress and triggering of $Ca^{2+}$ flux, which leads to mitochondrial cell death mechanisms. Effect of PEITC on redox status of GSH may be not important for cell killing for CCA cells but it is important for maintaining cell functions in Chang cells. The different effect of PEITC on different cell types was clearly shown by the cytoprotection response to antioxidant, NAC. More study is needed using several CCA cell lines over the response to PEITC. Taken together, the present results highlighted different responses of the cells to PEITC, which may facilitate the new approaches in the study of PEITC for drug development for the treatment of CCA.

## References


1. Patel T: **Cholangiocarcinoma--controversies and challenges**. *Nat Rev Gastroenterol Hepatol* 2011, **8**:189-200.
2. Sripa B, Pairojkul C: **Cholangiocarcinoma: lessons from Thailand**. *Curr Opin Gastroenterol* 2008, **24**:349-356.
3. Khan SA, Davidson BR, Goldin RD, Heaton N, Karani J, Pereira SP, Rosenberg WM, Tait P, Taylor-Robinson SD, Thillainayagam AV *et al*: **Guidelines for the diagnosis and treatment of cholangiocarcinoma: an update**. *Gut* 2012, **61**:1657-1669.
4. Cheung KL, Kong AN: **Molecular targets of dietary phenethyl isothiocyanate and sulforaphane for cancer chemoprevention**. *AAPS J* 2010, **12**:87-97.
5. Chan JM, Wang F, Holly EA: **Vegetable and fruit intake and pancreatic cancer in a population-based case-control study in the San Francisco bay area**. *Cancer Epidemiol Biomarkers Prev* 2005, **14**:2093-2097.
6. Lam TK, Ruczinski I, Helzlsouer KJ, Shugart YY, Caulfield LE, Alberg AJ: **Cruciferous vegetable intake and lung cancer risk: a nested case-control study matched on cigarette smoking**. *Cancer Epidemiol Biomarkers Prev* 2010, **19**:2534-2540.
7. Cheung KL, Khor TO, Yu S, Kong AN: **PEITC induces G1 cell cycle arrest on HT-29 cells through the activation of p38 MAPK signaling pathway**. *AAPS J* 2008, **10**:277-281.
8. Chiao JW, Wu H, Ramaswamy G, Conaway CC, Chung FL, Wang L, Liu D: **Ingestion of an isothiocyanate metabolite from cruciferous vegetables inhibits growth of human prostate cancer cell xenografts by apoptosis and cell cycle arrest**. *Carcinogenesis* 2004, **25**:1403-1408.
9. Khor TO, Cheung WK, Prawan A, Reddy BS, Kong AN: **Chemoprevention of familial adenomatous polyposis in Apc(Min/+) mice by phenethyl isothiocyanate (PEITC)**. *Mol Carcinog* 2008, **47**:321-325.
10. Yang YM, Conaway CC, Chiao JW, Wang CX, Amin S, Whysner J, Dai W, Reinhardt J, Chung FL: **Inhibition of benzo(a)pyrene-induced lung tumorigenesis in A/J mice by dietary N-acetylcysteine conjugates of benzyl and phenethyl isothiocyanates during the postinitiation**

**phase is associated with activation of mitogen-activated protein kinases and p53 activity and induction of apoptosis**. *Cancer Res* 2002, **62**:2-7.

11. Wu CL, Huang AC, Yang JS, Liao CL, Lu HF, Chou ST, Ma CY, Hsia TC, Ko YC, Chung JG: **Benzyl isothiocyanate (BITC) and phenethyl isothiocyanate (PEITC)-mediated generation of reactive oxygen species causes cell cycle arrest and induces apoptosis via activation of caspase-3, mitochondria dysfunction and nitric oxide (NO) in human osteogenic sarcoma U-2 OS cells**. *J Orthop Res* 2011, **29**:1199-1209.
12. Xiao D, Powolny AA, Moura MB, Kelley EE, Bommareddy A, Kim SH, Hahm ER, Normolle D, Van Houten B, Singh SV: **Phenethyl isothiocyanate inhibits oxidative phosphorylation to trigger reactive oxygen species-mediated death of human prostate cancer cells**. *J Biol Chem* 2010, **285**:26558-26569.
13. Xiao D, Choi S, Lee YJ, Singh SV: **Role of mitogen-activated protein kinases in phenethyl isothiocyanate-induced apoptosis in human prostate cancer cells**. *Mol Carcinog* 2005, **43**:130-140.
14. Huong LD, Shin JA, Choi ES, Cho NP, Kim HM, Leem DH, Cho SD: **beta-Phenethyl isothiocyanate induces death receptor 5 to induce apoptosis in human oral cancer cells via p38**. *Oral Dis* 2012, **18**:513-519.
15. Kim JH, Xu C, Keum YS, Reddy B, Conney A, Kong AN: **Inhibition of EGFR signaling in human prostate cancer PC-3 cells by combination treatment with beta-phenylethyl isothiocyanate and curcumin**. *Carcinogenesis* 2006, **27**:475-482.
16. Tseng E, Scott-Ramsay EA, Morris ME: **Dietary organic isothiocyanates are cytotoxic in human breast cancer MCF-7 and mammary epithelial MCF-12A cell lines**. *Exp Biol Med (Maywood)* 2004, **229**:835-842.
17. Trachootham D, Alexandre J, Huang P: **Targeting cancer cells by ROS-mediated mechanisms: a radical therapeutic approach?** *Nat Rev Drug Discov* 2009, **8**:579-591.
18. Chaiswing L, Zhong W, Oberley TD: **Distinct Redox Profiles of Selected Human Prostate Carcinoma Cell Lines: Implications for Rational Design of Redox Therapy**. *Cancers (Basel)* 2011, **3**:3557-3584.
19. Prawan A, Buranrat B, Kukongviriyapan U, Sripa B, Kukongviriyapan V: **Inflammatory cytokines suppress NAD(P)H:quinone oxidoreductase-1 and induce oxidative stress in cholangiocarcinoma cells**. *J Cancer Res Clin Oncol* 2009, **135**:515-522.
20. Buranrat B, Prawan A, Kukongviriyapan U, Kongpetch S, Kukongviriyapan V: **Dicoumarol enhances gemcitabine-induced cytotoxicity in high NQO1-expressing cholangiocarcinoma cells**. *World J Gastroenterol* 2010, **16**:2362-2370.
21. Suphim B, Prawan A, Kukongviriyapan U, Kongpetch S, Buranrat B, Kukongviriyapan V: **Redox modulation and human bile duct cancer inhibition by curcumin**. *Food Chem Toxicol* 2010, **48**:2265-2272.
22. Tietze F: **Enzymic method for quantitative determination of nanogram amounts of total and oxidized glutathione: applications to mammalian blood and other tissues**. *Anal Biochem* 1969, **27**:502-522.
23. Kongpetch S, Kukongviriyapan V, Prawan A, Senggunprai L, Kukongviriyapan U, Buranrat B: **Crucial role of heme oxygenase-1 on the sensitivity of cholangiocarcinoma cells to chemotherapeutic agents**. *PLoS One* 2012, **7**:e34994.
24. Hajnoczky G, Csordas G, Das S, Garcia-Perez C, Saotome M, Sinha Roy S, Yi M: **Mitochondrial calcium signalling and cell death: approaches for assessing the role of mitochondrial Ca2+ uptake in apoptosis**. *Cell Calcium* 2006, **40**:553-560.
25. Mi L, Gan N, Chung FL: **Isothiocyanates inhibit proteasome activity and proliferation of multiple myeloma cells**. *Carcinogenesis* 2011, **32**:216-223.

26. Rose P, Whiteman M, Huang SH, Halliwell B, Ong CN: **beta-Phenylethyl isothiocyanate-mediated apoptosis in hepatoma HepG2 cells**. *Cell Mol Life Sci* 2003, **60**:1489-1503.
27. Vaseva AV, Moll UM: **The mitochondrial p53 pathway**. *Biochim Biophys Acta* 2009, **1787**:414-420.
28. Rong Y, Distelhorst CW: **Bcl-2 protein family members: versatile regulators of calcium signaling in cell survival and apoptosis**. *Annu Rev Physiol* 2008, **70**:73-91.
29. Hangen E, Blomgren K, Benit P, Kroemer G, Modjtahedi N: **Life with or without AIF**. *Trends Biochem Sci* 2010, **35**:278-287.
30. Lee JW, Cho MK: **Phenethyl isothiocyanate induced apoptosis via down regulation of Bcl-2/XIAP and triggering of the mitochondrial pathway in MCF-7 cells**. *Arch Pharm Res* 2008, **31**:1604-1612.
31. Mi L, Hood BL, Stewart NA, Xiao Z, Govind S, Wang X, Conrads TP, Veenstra TD, Chung FL: **Identification of potential protein targets of isothiocyanates by proteomics**. *Chem Res Toxicol* 2011, **24**:1735-1743.
32. Kim JS, He L, Lemasters JJ: **Mitochondrial permeability transition: a common pathway to necrosis and apoptosis**. *Biochem Biophys Res Commun* 2003, **304**:463-470.
33. Chipuk JE, Green DR: **How do BCL-2 proteins induce mitochondrial outer membrane permeabilization?** *Trends Cell Biol* 2008, **18**:157-164.

## Output จากโครงการวิจัย

### International publication

#### Original article

1. Kongpetch S, Kukongviriyapan V, Prawan A, Senggunprai L, Kukongviriyapan U, Buranrat B: Crucial role of heme oxygenase-1 on the sensitivity of cholangiocarcinoma cells to chemotherapeutic agents. *PLoS One* 2012, 7(4):e34994. (impact factor 3.73) (as principal investigator)
2. Buranrat B, Chau-In S, Prawan A, Puapairoj A, Zeekpudsa P and Kukongviriyapan V (2012) NQO1 Expression Correlates with Cholangiocarcinoma Prognosis. *Asian Pac J Cancer Prev* 13 Suppl:131-136. (impact factor 1.271) (as principal investigator)
3. Tusskorn O, Prawan A, Senggunprai L, Kukongviriyapan U, Kukongviriyapan V: Phenethyl isothiocyanate induces apoptosis of cholangiocarcinoma cells through interruption of glutathione and mitochondrial pathway. *Naunyn Schmiedebergs Arch Pharmacol* 2013, 386(11):1009-1016. (impact factor 2.147) (as principal investigator)
4. Tusskorn O, Senggunprai L, Prawan A, Kukongviriyapan U, Kukongviriyapan V: Phenethyl isothiocyanate induces calcium mobilization and mitochondrial cell death pathway in cholangiocarcinoma KKU-M214 cells. *BMC Cancer* 2013, 13(1):571. (impact factor 3.333) (as principal investigator)
5. Zeekpudsa P, Kukongviriyapan V, Senggunprai L, Sripa B, Prawan A: Suppression of NAD(P)H-quinone oxidoreductase 1 enhanced the susceptibility of cholangiocarcinoma cells to chemotherapeutic agents. *J Exp Clin Cancer Res* 2014, 33:11. (impact factor 3.066) (as co-principal investigator)

#### Review article (invited)

1. Kukongviriyapan V: Genetic polymorphism of drug metabolizing enzymes in association with risk of bile duct cancer. *Asian Pac J Cancer Prev* 2012, 13 Suppl:7-15. (impact factor 1.271) (as principal investigator)

#### Manuscript submission

1. Kongpetch S, Ong CH, Chan-On W, Siew EY, Prawan A, Senggunprai L, Kukongviriyapan U, Teh BT, Kukongviriyapan V. Modulation of heme oxygenase-1 enhances sensitivity of cholangiocarcinoma cells to radiation and chemotherapy. (as principal investigator)

### Presentation (International conference)

1. Kukongviriyapan V, Kongpetch S, Prawan A, Senggunprai L, Kukongviriyapan U. Critical role of heme oxygenase-1 in cytoprotection of cholangiocarcinoma cells against anticancer agents. SFRR-Europe 2011 Meeting, Istanbul, Turkey, September 7-10, 2011.

2. Senggunprai L, Tusskorn O, Kukongviriyapan V, Prawan A, Kukongviriyapan U. Mitochondria are the critical target in phenethylisothiocyanate-induced cell-killing in human bile duct cancer cells. SFRR-Europe 2011 Meeting, Istanbul, Turkey, , September 7-10, 2011

3. Prawan P, Zeekpudsa P, Kukongviriyapan V, Senggunprai L. RNAi-mediated silencing of NAD(P)H: quinone oxidoreductase-1 gene enhances chemosensitivity of cholangiocarcinoma. SFRR-Europe 2011 Meeting, Istanbul, Turkey, September 7-10, 2011.

4. Tusskorn O, Kukongviriyapan V, Prawan A, Senggunprai L, Kukongviriyapan U. The effects of phenethyl isothiocyanate on redox regulation of mitochondrial dysfunction in cholangiocarcinoma cell lines. The 7th Princess Chulabhorn International Science Congress, Chulabhorn Research Institute, Bangkok, 29 Nov-3 Dec 2012.

5. Zeekpudsa P, Prawan A, Kukongviriyapan V, Senggunprai L. Suppression of NAD(P)H-quinone oxidpreductase 1 enhances chemosensitivity by p53 mediated response. Biennial Meeting of Society for Free Radical Research Asia: Oxidative Stress and Mitochondrial Alterations in Ageing and Disease. The Second Medicine Building, Chang Gung University, Tao-Yuan, Taiwan, October 16-19, 2013

6. Somparn N, Kukongviriyapan V, Kukongviriyapan U, Senggunprai L, Prawan A, Khunluck T. Protective effects of tetrahydrocurcumin on doxorubicin induced apoptosis in cholangiocyte cell lines. The 5th International Conference on Natural Product for Health and Beauty (NATPRO 5), Phuket, Thailand, May 6-8, 2014,

7. Senggunprai L, Kukongviriyapan V, Prawan A, and Kukongviriyapan U. Chemopreventive effects of EGCG and quercetin against cholangiocarcinoma cells by targeting JAK/STAT pathway. 5th Asia Pacific ISSX Meeting 2014, Tianjin, People Republic of China, May 8-13 2014.

## การนำเสนอผลงานวิชาการระดับชาติ เรื่อง

1. Samatiwat P, Kukongviriyapan V, Prawan A, Senggunprai L, Kukongviriyapan U. Nrf2-mediated antioxidant responses to anticancer drugs in cholangiocarcinoma cells. Precongress Symposium 2012 การวิจัยและพัฒนาเพื่อกำจัดพยาธิใบไม้ตับและมะเร็งท่อน้ำดี การประชุมวิชาการประจำปีครั้งที่ 28 คณะแพทยศาสตร์ มหาวิทยาลัยขอนแก่น 9 -12 ตุลาคม 2555 คณะแพทยศาสตร์ มหาวิทยาลัยขอนแก่น
2. Tusskorn O, Kukongviriyapan V, Prawan A, Senggunprai L, Kukongviriyapan U. Phenethyl isothiocynate exerts distinct chemopreventive effects on mitochondria in cholangiocarcinoma cell lines. การประชุม Commission on Higher Education Congress IV University Staff Development Consortium, พัทยา 14-16 September, 2011.
3. Tusskorn O, Kukongviriyapan O, Prawan A, Senggunprai L, Kukongviriyapan U. Modulation of cytotoxic effect by inhibition of phenethylisothiocyanate metabolism in cholangiocarcinoma

cells. การประชุมวิชาการประจำปีครั้งที่ 28 คณะแพทยศาสตร์ มหาวิทยาลัยขอนแก่น 9 -12 ตุลาคม 2555 คณะแพทยศาสตร์ มหาวิทยาลัยขอนแก่น (รางวัลชมเชยการนำเสนอโปสเตอร์ )

4. Zeekpudsa P, Prawan A, Kukongviriyapan V, Senggunprai L. Suppression of NAD(P)H quinine oxidoreductase 1 (NQO1) sensitizes cholangiocarcinoma cells to anticancer agents by p53-related mechanism. การประชุมวิชาการประจำปีครั้งที่ 35 สมาคมเภสัชวิทยาแห่งประเทศไทย พิษณุโลก 20-22 มีนาคม 2556
5. Aneknan P, Senggunprai L, Prawan A, Kukongviriyapan V. Inhibitory effects of luteolin and silibinin on cholangiocarcinoma cell migration via JAK/STAT3 signaling pathway ประชุมวิชาการ The Second symposium of health cluster, National research university project "Specific health problem in Greater Mekong Sub-region (Shep-GMS) วันที่ 29 มีนาคม 2556 ณ คณะแพทยศาสตร์ มหาวิทยาลัยขอนแก่น
6. Zeekpudsal P, Prawan A, Kukongviriyapan V, Senggunprai L. Suppression of NAD(P)H Quinone Oxidoreductase 1 (NQO 1) Sensitizes Cholangiocarcinoma Cells to Anticancer Agents by P53-Related Mechanismใ การประชุมวิชาการสมาคมเภสัชวิทยาแห่งประเทศไทย ครั้งที่ 35 ณ ห้องประชุมคอนเวนชั่น 2 โรงแรมท็อปแลนด์ อำเภอเมือง จังหวัดพิษณุโลก ระหว่างวันที่ 20-22 มีนาคม 2556.
7. Samatiwat P, Kukongviriyapan V, Prawan A, and Senggunprai L. Knockdown of Nrf2 - Mediated Antioxidant Defense System by siRNA Sensitizes Cholangiocarcinoma Cells to Cisplatin. การประชุมวิชาการประจำปี ครั้งที่ 36 สมาคมเภสัชวิทยาแห่งประเทศไทย ในระหว่างวันที่ 27-28 มีนาคม 2557 ณ ห้องบรรยาย อวย เกตุสิงห์ อาคารศรีวรินทิรา ชั้น 3 คณะแพทยศาสตร์ศิริราชพยาบาล
8. Thammaniwit W, Kukongviriyapan V, Prawan A, Kigpetch S, Senggunprai L. Cytotoxic Effect of Cratoxylum formosum Dyer (Teaw) Leaf Extracts Against Cholangiocarcinoma Cells. การประชุมวิชาการประจำปี ครั้งที่ 36 สมาคมเภสัชวิทยาแห่งประเทศไทย ในระหว่างวันที่ 27-28 มีนาคม 2557 ณ ห้องบรรยาย อวย เกตุสิงห์ อาคารศรีวรินทิรา ชั้น 3 คณะแพทยศาสตร์ศิริราชพยาบาล

**Reviewer for international journals**

Reviewer:_Title: High antipsychotic maintenance dose among patients with schizophrenia, Journal ; Current Clinical Pharmacology (04/01/2556)

Reviewer:_Effect of hyperbaric oxygen treatment and gemcitabine on apoptosis in pancreatic ductal adenocarcinoma cells. Journal; Clinical & Experimental Pharmacology & Physiology (04/02/2556)

Reviewer_DNA damage and cell cycle arrest induced by protoporphyrin IX on sarcoma 180 cells. Journal: Cellular Physiology & Biochemistry (04/02/2556)

Reviewer_Title: First-line erlotinib and fixed dose-rate gemcitabine for advanced pancreatic cancer. Journal: World Journal of Gastroenterology (15/02/2556)

Reviewer: Modulation of intracellular redox state and induction of apoptosis by the Medium Chain Length Fatty acid, Lauric Acid, in the Caco-2 and IEC-6 cell line. Journal: Chemotherapy (15/02/2556)

Reviewer: Association between the CYP1A2-164 A/C polymorphism and colorectal cancer susceptibility. Journal: Tumor Biology (08/05/2556)

Reviewer: Esomeprazole induced irritability bowel syndrome Jurnal: World Journal of Gastrointestinal Pharmacology and Therapeutics (21/05/2556)

Reviewer: Association between the CYP1A2-164 A/C polymorphism and colorectal cancer susceptibility. Journal: Tumor Biology (08/05/2556)

Reviewer: he Possible Genotoxicity Of Metformin On Cultured Human Lymphocytes Journal: Current Clinical Pharmacology (20/10/2556)

Reviewer: In vitro and in vivo effecfs of Sysygium aromaticum seeds on hair dermal papilla cells. Current Clinical Pharmacology (20/10/2556)

Reviewer: A novel predictive equation for potential diagnosis of cholangiocarcinoma Journal: Plos One (08/11/2556)

Reviewer: Locally advanced rectal cancer. Journal: World Journal of Gastroenterology (20/12/2556)

Reviewer: Phenethyl isothiocyanate induced DNA damage-associated G2/M arrest and subsequent apoptosis in oral cancer cells with varying p53 mutations. Journal: Free Radical Biology & Medicine (29/01/2557)

Reviewer: The redox-active triphenylmethane dyes, Gentian Violet and Brilliant Green, and nitroxide Tempol inhibit IKKepsilon oncogenic kinase expression in MCF-7 and ZR75.1 breast cancer cells. Journal: BMC Cancer (13/04/2557)

Reviewer: α-Mangostin (AM) from Cratoxylum arborescens demonstrates apoptogenesis in human mammary adenocarcinoma cells (MCF-7): involvement of NF-KB and HSP70 signaling pathways. Journal: Drug Design, Development and Therapy (01/05/2557

Reviewer: Clinical Outcomes for Patients with Resected Hilar Cholangiocarcinoma). Journal World Journal of Gastroenterology (26/04/2557)

**Invited lecture**

1. Kukongviriyapan V. Association of Vascular Function, Arterial Stiffness and Antioxidative Responses in Pediatric Patients with Thalassemia Major. International Conference: Oxidative Stress Congenital & Acquired Hemolytic Anemia. March 22-23, 2012, Pattaya, Cholburi.

2. วีรพล คู่คงวิริยพันธุ์ Mechanisms of enzymatic and non-enzymatic antioxidants, vitamins and biological substances ในการประชุมเชิงปฏิบัติการ เทคนิคการตรวจวัดอนุมูลอิสระ สารต้านอนุมูลอิสระ และดัชนีภาวะเครียดออกซิเดชัน 14-15 พฤษภาคม 2555 ณ คณะวิทยาศาสตร์การแพทย์ มหาวิทยาลัยพะเยา

3. Kukongviriyapan V. Implication of drug metabolizing enzyme gene polymorphism in risk of cancer of the bile duct. Precongress Symposium 2012 การวิจัยและพัฒนาเพื่อกำจัดพยาธิใบไม้ตับและมะเร็ง

ท่อน้ำดี การประชุมวิชาการประจำปีครั้งที่ 28 คณะแพทยศาสตร์ มหาวิทยาลัยขอนแก่น 9 -12 ตุลาคม 2555 คณะแพทยศาสตร์ มหาวิทยาลัยขอนแก่น

**Award รางวัลที่ได้รับ**

-ได้รับรางวัลนักวิจัยดีเด่น ระดับเหรียญเงิน ปี 2554 จากมหาวิทยาลัยขอนแก่น
-รับการเสนอชื่อเพื่อรับรางวัลนักวิจัยดีเด่น ระดับเหรียญทอง ประจำปี 2557 จากมหาวิทยาลัยขอนแก่น

**การเชื่อมโยงทางวิชาการกับนักวิชาการอื่น ๆ ทั้งในและต่างประเทศ**

ได้มีความร่วมมือการวิจัยกับ Prof. Teh Bin Tean จาก National Cancer Centre –Van Andel Research Institute (NCC-VARI) Translational lab, National Cancer Centre of Singapore ในความร่วมมือวิจัย โดยได้เชิญมาเยี่ยมที่คณะแพทยศาสตร์ มหาวิทยาลัยขอนแก่น และคณะวิจัยของมะเร็งท่อน้ำดีได้เยี่ยมที่ห้องปฏิบัติการที่สิงคโปร์แล้ว โดยความตกลงแลกเปลี่ยนนักวิจัยที่เป็นอาจารย์ใหม่ และนักศึกษาบัณฑิตปริญญาเอก

ได้มีความร่วมมือการวิจัยกับ Prof. Choon He Chung จาก Departments of Internal Medicine and Microbiology, Wonju College of Medicine, Yonsei University, Korea ได้เชิญ Prof. Chung เป็นแขกของภาควิชาเภสัชวิทยา ได้มีความตกลงในความร่วมมือแลกเปลี่ยนนักศึกษา อาจารย์ในการวิจัยเกี่ยวกับภาวะเครียดออกซิเดชันและภาวะแทรกซ้อนของเบาหวาน กำลังจะส่งนักศึกษาระดับปริญญาเอกไปทำงานวิจัยที่ Yonsei University ภายใต้ทุนสนับสนุนจาก โครงการปริญญาเอกกาญจนาภิเศก (คปก) และการสนับสนุนจาก Wonju College of Medicine

**ภาคผนวก**

**- Reprint ผลงานตีพิมพ์**


1. Kongpetch S, Kukongviriyapan V, Prawan A, Senggunprai L, Kukongviriyapan U, Buranrat B: Crucial role of heme oxygenase-1 on the sensitivity of cholangiocarcinoma cells to chemotherapeutic agents. *PLoS One* 2012, 7(4):e34994.
2. Buranrat B, Chau-In S, Prawan A, Puapairoj A, Zeekpudsa P and Kukongviriyapan V (2012) NQO1 Expression Correlates with Cholangiocarcinoma Prognosis. *Asian Pac J Cancer Prev* 13 Suppl:131-136.
3. Tusskorn O, Prawan A, Senggunprai L, Kukongviriyapan U, Kukongviriyapan V: Phenethyl isothiocyanate induces apoptosis of cholangiocarcinoma cells through interruption of glutathione and mitochondrial pathway. *Naunyn Schmiedebergs Arch Pharmacol* 2013, 386(11):1009-1016.
4. Tusskorn O, Senggunprai L, Prawan A, Kukongviriyapan U, Kukongviriyapan V: Phenethyl isothiocyanate induces calcium mobilization and mitochondrial cell death pathway in cholangiocarcinoma KKU-M214 cells. *BMC Cancer* 2013, 13(1):571.
5. Kukongviriyapan V: Genetic polymorphism of drug metabolizing enzymes in association with risk of bile duct cancer. *Asian Pac J Cancer Prev* 2012, 13 Suppl:7-15.
6. Zeekpudsa P, Kukongviriyapan V, Senggunprai L, Sripa B, Prawan A: Suppression of NAD(P)H-quinone oxidoreductase 1 enhanced the susceptibility of cholangiocarcinoma cells to chemotherapeutic agents. *J Exp Clin Cancer Res* 2014, 33:11.


**- Manuscript submission**


1. Kongpetch S, Ong CH, Chan-On W, Siew EY, Prawan A, Senggunprai L, Kukongviriyapan U, Teh BT, Kukongviriyapan V. Modulation of heme oxygenase-1 enhances sensitivity of cholangiocarcinoma cells to radiation and chemotherapy.

OPEN ACCESS Freely available online

PLoS one

# Crucial Role of Heme Oxygenase-1 on the Sensitivity of Cholangiocarcinoma Cells to Chemotherapeutic Agents

**Sarinya Kongpetch[1], Veerapol Kukongviriyapan[1,3]*, Auemduan Prawan[1,3], Laddawan Senggunprai[1,3], Upa Kukongviriyapan[2], Benjaporn Buranrat[4]**

**1** Department of Pharmacology, Faculty of Medicine, Khon Kaen University, Khon Kaen, Thailand, **2** Department of Physiology, Faculty of Medicine, Khon Kaen University, Khon Kaen, Thailand, **3** Liver Fluke and Cholangiocarcinoma Research Center, Khon Kaen University, Khon Kaen, Thailand, **4** Faculty of Pharmaceutical Sciences, University of Phayao, Phayao, Thailand

## Abstract

Cancer cells acquire drug resistance via various mechanisms including enhanced cellular cytoprotective and antioxidant activities. Heme oxygenase-1 (HO-1) is a key enzyme exerting potent cytoprotection, cell proliferation and drug resistance. We aimed to investigate roles of HO-1 in human cholangiocarcinoma (CCA) cells for cytoprotection against chemotherapeutic agents. KKU-100 and KKU-M214 CCA cell lines with high and low HO-1 expression levels, respectively, were used to evaluate the sensitivity to chemotherapeutic agents, gemcitabine (Gem) and doxorubicin. Inhibition of HO-1 by zinc protoporphyrin IX (ZnPP) sensitized both cell types to the cytotoxicity of chemotherapeutic agents. HO-1 gene silencing by siRNA validated the cytoprotective effect of HO-1 on CCA cells against Gem. Induction of HO-1 protein expression by stannous chloride enhanced the cytoprotection and suppression of apoptosis caused by anticancer agents. The sensitizing effect of ZnPP was associated with increased ROS formation and loss of mitochondrial transmembrane potential, while Gem alone did not show any effects. A ROS scavenger, Tempol, abolished the sensitizing effect of ZnPP on Gem. Combination of ZnPP and Gem enhanced the release of cytochrome c and increased p21 levels. The results show that HO-1 played a critical role in cytoprotection in CCA cells against chemotherapeutic agents. Targeted inhibition of HO-1 may be a strategy to overcome drug resistance in chemotherapy of bile duct cancer.

**Citation:** Kongpetch S, Kukongviriyapan V, Prawan A, Senggunprai L, Kukongviriyapan U, et al. (2012) Crucial Role of Heme Oxygenase-1 on the Sensitivity of Cholangiocarcinoma Cells to Chemotherapeutic Agents. PLoS ONE 7(4): e34994. doi:10.1371/journal.pone.0034994

**Editor:** Robert B. Sim, Oxford University, United Kingdom

**Received** October 11, 2011; **Accepted** March 9, 2012; **Published** April 13, 2012

**Copyright:** © 2012 Kongpetch et al. This is an open-access article distributed under the terms of the Creative Commons Attribution License, which permits unrestricted use, distribution, and reproduction in any medium, provided the original author and source are credited.

**Funding:** This study was supported by Thailand Research Fund, Office of the Higher Education Commission through SHeP-GMS of Khon Kaen University, a grant-in-aid from Faculty of Medicine, Khon Kaen University and a scholarship from the Royal Golden Jubilee Ph.D. Programme. The funders had no role in study design, data collection and analysis, decision to publish, or preparation of the manuscript.

**Competing Interests:** The authors have declared that no competing interests exist.

* E-mail: veerapol@kku.ac.th

## Introduction

Cholangiocarcinoma (CCA) is a malignant tumor of the bile duct, which originates from the bile duct epithelial cells (cholangiocytes). CCA is a devastating malignancy with poor prognosis. CCA is a rare type of cancer worldwide, however populations residing in the Southeast Asian region are at very high risk. The important risk factors are liver fluke infection and possible involvement from chronic infection with hepatitis B and C viruses [1,2]. Early diagnosis and extensive surgery offers the only chance for prolonged life. Unfortunately, most patients are diagnosed at the advanced stage of disease and current biomarkers are of limited value [3,4]. Chemotherapy is a remaining option. However, current chemotherapy has not been shown to substantially improve survival in patients with unresected CCA [3,5]. Many chemotherapeutic drugs as well as targeted chemotherapeutic agents have been tested as single agents or in combinations. Nevertheless, drug resistance or drug inefficacy remain major obstacles in the treatment of CCA [6]. It is apparent that a new strategy of chemotherapeutic treatment is urgently needed in management of the unresectable CCA.

Heme oxygenase-1 (HO-1) is one of the powerful cytoprotective enzymes. HO-1 plays critical roles in physiological iron homeostasis, antioxidant defense, anti-inflammatory and anti-apoptotic effect [7]. It is induced by various stimuli such as hypoxia, UV-radiation, heavy metals, chemotherapeutic drugs and oxidative stress [8,9]. HO-1 catalyzes the first and rate-limiting step in the degradation of heme to biliverdin, carbonmonoxide (CO) and ferrous iron. Biliverdin is further converted to bilirubin by biliverdin reductase. Biliverdin and bilirubin are the most potent endogenous reactive oxygen species (ROS) scavengers [7]. CO is also an efficient anti-inflammatory mediator in several models of inflammation and tissue injury [10,11]. The increased expression of HO-1 has been observed in several cancers including brain tumor, melanoma, chronic myeloid leukemia, and lymphosarcoma [12], suggesting possible contribution of HO-1 to tumor progression through promotion of angiogenesis, metastases and pro-proliferation [13]. HO-1 expression may contribute to resistance to chemotherapeutic agents such as cisplatin, doxorubicin and gemcitabine in some human cancers [9,14,15]. Thus, some studies revealed that suppression of HO-1 activity or HO-1 knockdown by siRNA increased the chemosensitivity of AML cells, pancreatic and lung cancer cells [9,14,16], but was not effective in other cancer cells [17]. The inhibition of HO-1 by zinc protoporphyrin IX (ZnPP) induced apoptotic cell death and this may be associated with the increase in ROS production. Similarly, HO-1 gene silencing by specific siRNA also induced ROS

generation [17]. However, the exact mechanism of the sensitizing effect to chemotherapeutic agents confered by suppression of HO-1 is largely unknown. Mitochondria may be a primary target of HO-1 inhibition, as ZnPP and triiodothyronine induced the opening of the mitochondrial permeability transition (MPT) pore leading to liver injury [18].

In the present study, we investigated whether HO-1 in CCA cells plays a critical role in cytoprotection against chemotherapeutic agents. The results show that inhibition of HO-1 induced the sensitization of CCA cells to gemcitabine (Gem) and doxorubicin (Dox). Inhibition of HO-1 could be a strategy to enhance the response of CCA to chemotherapeutic drugs.

## Materials and Methods

### Cell lines and cell cultures

The human cholangiocarcinoma (CCA) cell lines; KKU-100 and KKU-M214 used in this study were kindly provided by Dr. Banchob Sripa of Department of Pathology, Faculty of Medicine, Khon Kaen University. Both cell lines were cultured in complete media consisting of Ham's F12 media, supplemented with 10% fetal calf serum, 12.5 mM HEPES, pH 7.3, 100 U/ml penicillin G and 100 µg/ml gentamicin. The cells were subcultured every 3 days using 0.25% trypsin-EDTA and the medium was renewed after an overnight incubation. The cultured cells were changed to incubate in serum-free defined Ham's F12 medium immediately before further treatment.

### Cytotoxicity assay

Cytotoxicity was determined by fluorescent staining using acridine orange and ethidium bromide (AO/EB) as described previously [19]. KKU-100 (7,500 cells/well) and KKU-M214 (5,000 cells/well) cells were cultured in 96 well-plate and allowed to attach overnight. On the next day, the medium was removed and gemcitabine (Gemzar®, Eli Lilly, IN, USA: Gem) dissolved in phosphate-buffered saline (PBS: 137 mM NaCl, 2.7 mM KCl, 10 mM $Na_2HPO_4$, 2 mM $KH_2PO_4$, pH 7.4), doxorubicin HCl (Boryung Pharm, Seoul, South Korea: Dox) dissolved in DMSO (100 mM) and further diluted with PBS, 4-hydroxy-2,2,6,6-tetramethylpiperidine-1-oxyl (Tempol), dissolved in PBS, zinc protoporphyrin IX (ZnPP; HO-1 inhibitor), dissolved in DMSO (50 mM) and further diluted with PBS or stannous chloride ($SnCl_2$; HO-1 inducer) dissolved in PBS, or combinations of them were added to the media culture to final concentrations as indicated in results section and incubated for a designated period of time. Then, cells were washed once with PBS and stained with AO/EB. The cells were examined using a Nikon Eclipse TS100 inverted microscope with excitation and long–pass emission filters of 480 and 535 nm, respectively. The fluorescent images were taken at predetermined areas with a Nikon Coolpix digital camera. The numbers of viable, apoptotic and necrotic cells which were stained with green fluorescence, bright orange fluorescence and green fluorescence with appearance of cell shrinkage, condensation and fragmentation of the nuclei, respectively, were enumerated. The cytotoxicity value was calculated as = (number of viable cells in treatment wells)/(number of viable cells in control cells)×100.

### HO-1 small interfering RNA transfection

The transfection of HO-1 siRNA was performed using siGENOME SMARTpool (M-006372-02-0005: Dharmacon, CO, USA) at a final concentration of 200 nM and lipofectamine 2000 (Invitrogen, CA, USA) according to the manufacturers' instructions. HO-1 expression was specifically suppressed by introduction of siRNA against human HMOX1 (Gene Id: 3162). - In brief, cells were grown in a 6-well plate to reach a confluence of 70%. For each well, 100 pmoles of HO-1 siRNA were mixed with 2 µL of lipofectamine 2000 and 500 µL of serum- and antibiotic-free Ham's F12 medium was added. Cells were exposed to the transfection mixture for 6 h. At the end of incubation period, 1.5 mL of antibiotic-free Ham's F12 complete medium was added and the cells were cultured for an additional 18 h. The siGENOME non-targeting siRNA (D-001210-02-05: Dharmacon), as a negative control was introduced to the cells using the same protocol. Total RNA and protein were extracted from cells 24 h after transfection using previously described methods [20,21]. Efficiency of the transient transfection was determined by real-time polymerase chain reaction (PCR) using specific primers and Western blotting.

Cytotoxicity of Gem to HO-1 knock-down CCA cells was performed. KKU-100 cells (7,500 Cells/well) were grown in 96-well plate to reach the confluence of 70%. For each well, cells were transfected with 3 ρmoles of HO-1 siRNA reagent mixed with 0.06 µL of lipofectamine 2000 in serum- and antibiotic-free Ham's F12 medium. Cells were kept in the transfection mixture for 6 h. Then, 100 µL of antibiotic-free Ham's F12 complete medium was added and the cells were kept for an additional 18 hours. Then, cells were treated with varied concentrations of Gem for further 24 h and cytotoxicity assay was performed as described as above.

### Real-time polymerase chain reaction

KKU-100 and KKU-M214 cells were seeded at the density of $1.5\times10^5$ cells/well in 6 well-plates and allowed to growth for 24 h. Total RNA was isolated using a previously described method [20]. Total RNA (1 µg) was then reverse transcribed to single-stranded cDNA by the ImProm-II$^{TM}$ reverse transcription system (Promega, WI, USA) at conditions of 42°C for 60 min. The reverse transcription products served as a template for real-time PCR. The primer sequences were as follows: HO-1: forward, 5′-CTG ACC CAT GAC ACC AAG GAC-3′ and HO-1 reverse: 5′-AAA GCC CTA CAG CAA CTG TCG-3′, β-actin: forward 5′-AGT GTA GCC CAG GAT GCC CTT-3′ and β-actin: reverse, 5′-GCC AAG GTC ATC CAT GAC AAC-3′. The PCR was performed in a final volume of 15 µL containing cDNA template, 5 µM of each HO-1 primer or 2.5 µM of each β-actin primer in SsoFast$^{TM}$ EvaGreen Supermix with low Rox (Bio-Rad, CA, USA). After an initial denaturation step at 95°C for 10 min, 40 cycles for HO-1 and β-actin were performed as follows: denaturating for 15 sec at 95°C, annealing for 30 sec at 55°C and extension for 45 sec at 72°C. To verify the purity of the products, a melting curve analysis was performed after each run. To quantify the relative expression of genes, the relative quantitation using standard curve method was used. The amount of HO-1 mRNA was expressed as a ratio to β-actin mRNA.

### Western blot analysis

Western blot analysis was used to determine the expression levels of HO-1, $p21^{Cip/WAF1}$, cytochrome C, and β-actin. KKU-100 ($7.5\times10^5$) and KKU-M214 ($6\times10^5$) cells were cultured in 100 $mm^3$ dishes and treated with drug or drug combinations. The cultured cells were washed with PBS, lysed with RIPA buffer [150 mM NaCl, 1% NP-40, 0.5% sodium deoxycholate, 0.1% SDS, 50 mM Tris–HCl (pH 7.4), 50 mM glycerophosphate, 20 mM NaF, 20 mM EGTA, 1 mM DTT, 1 mM $Na_3VO_4$ and protease inhibitor cocktail (M221: Amresco, OH, USA) at 4°C for 15 min and transferred into a microtube. After vigorous vortex mixing, the suspension was centrifuged at 12,000×g for 20 min and supernatant was collected and stored at −70°C until use. The

protein samples were mixed with SDS loading buffer and subjected to separation by electrophoresis in 8–10% SDS-polyacrylamide gel. The bands were blotted onto a PVDF membrane. The membranes were blocked for 1 h at room temperature with 5% (w/v) skimmed milk powder in Tris buffered saline (TBS) containing 0.1% Tween-20. The PVDF membrane was incubated overnight at 4°C with primary antibodies of rabbit polyclonal anti-human HO-1 (1:1000) (ADI-SPA-895: Enzo Life Sciences, Switzerland), rabbit monoclonal anti-human $p21^{Cip/WAF1}$ (1:500) (#2947: Cell Signaling Technology, MA, USA), mouse monoclonal anti-human cytochrome c (1:1000) (sc-13560) and horseradish peroxidase (HRP)-goat polyclonal anti-human β-actin (1:2500) (sc-1616 HRP) in TBS. After washing with TBS the blots were incubated for 1 h at room temperature with the HRP-conjugated secondary antibodies (anti-rabbit IgG-HRP sc-2004, anti-mouse IgG-HRP sc-2005, anti-goat IgG-HRP sc-2354). After removal of the secondary antibody and TBS buffer washes, the blots were incubated in ECL substrate solution (SuperSignal West Pico Chemiluminescent Substrate: Thermoscientific, IL, USA). The densities of the specific protein bands were visualized and captured by ImageQuant™ 400.

### Measurement of intracellular ROS accumulation

To monitor the intracellular accumulation of ROS, the lucigenin-enhanced chemiluminescence method was used for detecting superoxide anion according to the previously described method [20]. Briefly, KKU-100 cells were cultured in 35-mm dishes overnight. After treatment with compounds for 3 h, cultured cells were rinsed, incubated in PBS containing lucigenin and measured for luminescent signal in a 20/20 n Luminometer (Turner Biosystem, CA, USA).

### Measurement of mitochondrial transmembrane potential

To analyze the mitochondrial transmembrane potential ($\Delta\psi_m$), the lipophilic cationic fluorescent probe; JC-1 (Cayman Chemical, MI, USA) was used as previously described [21]. KKU-100 cells were seeded in a 96-well plate for an overnight before treatment with compounds for 6 or 24 h. Cultured cells in the plate were centrifuged at 1,500 rpm 25°C for 5 min and were loaded with JC-1 dye for 30 min at 37°C. Then, cultured cells were rinsed, incubated in JC-1 assay buffer and $\Delta\psi_m$ was analysed in a fluorescent microscope. JC-1 forms J-aggregates in cells with healthy mitochondria, which can be detected with fluorescent settings of excitation and emission wavelengths at 560 and 595 nm, respectively. Cells with depolarized mitochondria, JC-1 existed as J monomers can be detected with excitation and emission wavelengths at 485 and 535 nm, respectively. The change of the orange fluorescence in healthy cultured cells to green fluorescence is an indicative of depolarization of $\Delta\psi_m$.

### Statistical analysis

Data are expressed as mean ± SEM of three separated experiments. An analysis of variance was used to determine significant differences between each experimental group. The level of significance was set at $P<0.05$.

## Results

### Basal HO-1 expression and inducible expression by anticancer agents

The two cholangiocarcinoma cells, KKU-100 and KKU-M214, were used to determine the basal expression levels of HO-1. The mRNA and protein expressions of HO-1 were determined by real-time PCR and Western blot analysis. At basal condition, KKU-100 showed the higher HO-1 mRNA and protein levels than KKU-M214 cells (Fig. 1A–B). To examine whether anticancer agent could induce HO-1 in CCA cells, two lines of cells were incubated with 1 μM of Gem and the time-course of HO-1 protein expression was examined. Both KKU-100 and KKU-M214 cells treated with Gem showed a rapid increased HO-1 protein expression within 3 h when compared with concurrent controls and returned to control level by 24 h (Fig. 2).

### Effect of HO-1 inhibition on the sensitivity of CCA cells to anticancer agents

The cytoprotective effects of HO-1 in CCA cells to anticancer agents were explored using high and low HO-1 expressing KKU-100 and KKU-M214 cells cultured with HO-1 inhibitor. Both cells were exposed to Gem (0.001–0.1 μM) in the presence of HO-1 inhibitor, ZnPP (0.01 and 0.1 μM) for 24 h. As shown in Fig. 3A and 3B, ZnPP rendered both CCA cells to be highly susceptible to cytotoxic effect of Gem, which can be seen as the downward shift of the dose-response curves of Gem in the presence of ZnPP. Similar downward shift of the dose-response curves in the presence of ZnPP was observed in KKU-100 cells to another chemotherapeutic agent, Dox (Fig. 3C). The presence of ZnPP augmented significantly Gem- or Dox-induced cell growth inhibition and induction of apoptotic cell death in both cell lines (Fig. 3D, E and F). ZnPP itself showed only a slight cytotoxicity at the concentrations used in this study (data not shown).

### HO-1 induction enhanced resistance of CCA cells to anticancer agents

To validate the cytoprotective roles of HO-1, $SnCl_2$, a HO-1 inducer, was used in combination with Gem or Dox. KKU-100 and KKU-M214 cells were exposed to $SnCl_2$ and changes in HO-1 protein was evaluated by Western blot analysis. $SnCl_2$ (10 μM) induced HO-1 protein expression with a similar pattern in both cell types with maximal induction observed during 6–24 h

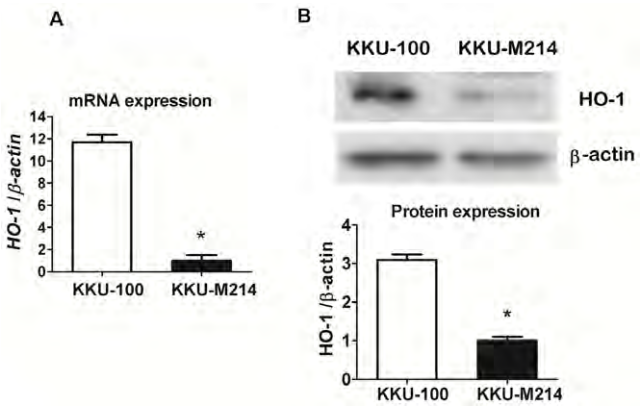


**Figure 1. HO-1 mRNA and protein expressions in CCA cells.** (**A**) The basal mRNA expression of HO-1 in CCA cells; KKU-100 and KKU-M214 cells. Total RNA of cells were collected and analysed by real-time RT-PCR. The bars represent relative expression of HO-1 normalized with β -actin. The expression of HO-1 in KKU-100 cells is much higher than that of KKU-M214 cells, $p<0.05$. (**B**) The basal protein expression of HO-1 in KKU-100 and KKU-M214 cells. Total cell lysates were prepared and subjected to Western blot analysis using β-actin as a loading control. Image samples of HO-1 and β -actin are shown in the top panel of the figure. HO-1 protein in KKU-100 cells is relatively higher than that of KKU-M214 cells. The bars represent mean±SEM, each from three separated experiments. *, $p<0.05$ vs KKU-100 group.
doi:10.1371/journal.pone.0034994.g001

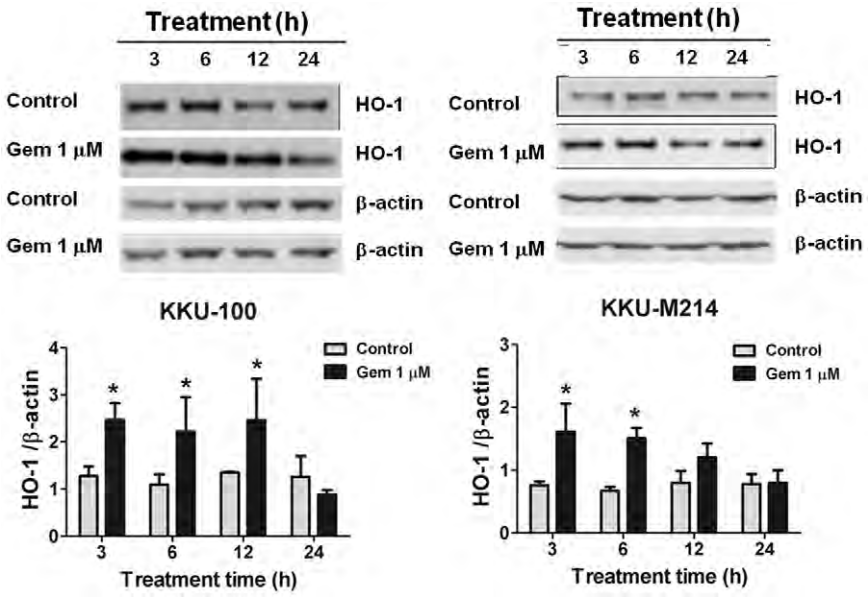


**Figure 2. Time-course of HO-1 protein induction by Gem.** (**A**) KKU-100 cells and (**B**) KKU-M214 cells were cultured for overnight and exposed to Gem (1 μM) for 3, 6, 12 and 24 h. The cultured cells exposed to vehicle only were performed as concurrent control groups. Total cell lysates were collected at the indicated time points and subjected to Western blot analysis using β-actin as a loading control. The relative expression of HO-1 was normalized with β actin. The bars show the HO-1 expression in Gem-treated group and concurrent control group. The bars represent mean±SEM, each from three separated experiments. *,$p<0.05$ vs concurrent controls.
doi:10.1371/journal.pone.0034994.g002

(Fig. 4A). KKU-100 and KKU-M214 cells were treated with Gem (0.1 μM) or Dox (0.5 μM) with or without $SnCl_2$ for 24 h. Induction of HO-1 was associated with increased cell viability more than 2 fold after treatment with Gem or Dox (Fig. 4B). Induction of HO-1 by $SnCl_2$ decreased the apoptotic and necrotic cell death induced by Gem and Dox in both CCA cells (Fig. 4C). $SnCl_2$ alone was slightly toxic at the concentrations used in this study (data not shown).

## HO-1 gene silencing sensitized CCA cells to chemotherapeutic agents

To further validate that HO-1 inhibition indeed induced sensitization of CCA cells to anticancer agents, the effects of HO-1 gene silencing to Gem was examined. Since both KKU-100 and KKU-M214 cells showed similar responses to HO-1 inhibitor and inducer, KKU-100 cells were employed as a representative of CCA cells. The levels of HO-1 mRNA (Fig. 5A) and immunoreactive HO-1 protein (Fig. 5B) were dramatically decreased 24 h after transfection of HO-1 siRNA. Then, HO-1 knocked-down KKU-100 cells were exposed to various concentrations of Gem (0.001–0.1 μM) for further 24 h. The $IC_{50}$ concentration of Gem in non-targeting control was 0.0360±0.0042 μM, whereas that in HO-1 knockdown cells was 0.0005±0.0001 μM (Fig. 5C) ($p<0.001$), showing that the inhibition of HO-1 sensitizes KKU-100 cells to be highly susceptible to Gem.

## ZnPP induced intracellular ROS formation and mitochondrial dysfunction

From the above experiments, HO-1 inhibition by ZnPP enhanced the susceptibility of CCA cells to the cytotoxic effect of Gem. To explore the underlying mechanisms of enhanced cytotoxicity by the combination of Gem and ZnPP, the intracellular ROS formation was assessed. Treatment with ZnPP alone caused a remarkable increase in ROS formation as early as 3 h. The combination of ZnPP and Gem showed further increase in ROS levels (Fig. 6A). Gem alone showed no effect on ROS formation. To test whether the ROS was indeed responsible to enhance the cytotoxicity of Gem, the superoxide dismutase (SOD)-mimetic compound, Tempol, was used to scavenge $O_2^{\bullet -}$ induced by combined ZnPP and Gem treatment. The concentrations of Tempol to be used in studies were evaluated in a previous experiment which had shown to inhibit ROS formation and produce minimal toxicity. Moreover, it is verified that Tempol (500 μM) does not inhibit HO-1 activity. ZnPP-enhanced cytotoxicity of Gem was abolished by the presence of Tempol (Fig. 6B). Tempol alone has little cytotoxicity to the cells. Since ROS formation is thought to be involved in induction of cell killing in association with mitochondrial pathway, KKU-100 cells were treated with the combination of ZnPP and Gem and the $\Delta\psi_m$ were evaluated using JC-1 assay. Gem treatment alone had no effect on the $\Delta\psi_m$ (Fig. 6 C, inset b & f), whereas ZnPP and the combination of ZnPP with Gem induced the depolarization of $\Delta\psi_m$ as evident by the change of red fluorescent staining in healthy mitochondria (Fig. 6C, inset a & e) to green fluorescent staining in depolarized mitochondria (Fig. 6C, inset c, d, g & h).

## Combination of ZnPP and Gem altered the expression of proteins related to cell proliferation and apoptosis

To investigate further the effects of combined Gem and ZnPP if it was mediated via mitochondrial pathway, cytochrome c, release from the mitochondria in response to pro-apoptotic stimuli, was determined. The combined drug treatment exerted significant increase in levels of cytochrome c protein when compared with the controls. ZnPP or Gem alone did not induce the release (Fig. 7). Since the combined Gem and ZnPP suppressed the tumor cell growth, a protein related to cell proliferation; the $p21^{Cip/WAF1}$ was analyzed by Western blotting. Gem or ZnPP alone did not affect the $p21^{Cip/WAF1}$ protein expression, whereas the combination of Gem and ZnPP caused marked induction of $p21^{Cip/WAF1}$ and was associated with marked antiproliferative effect.

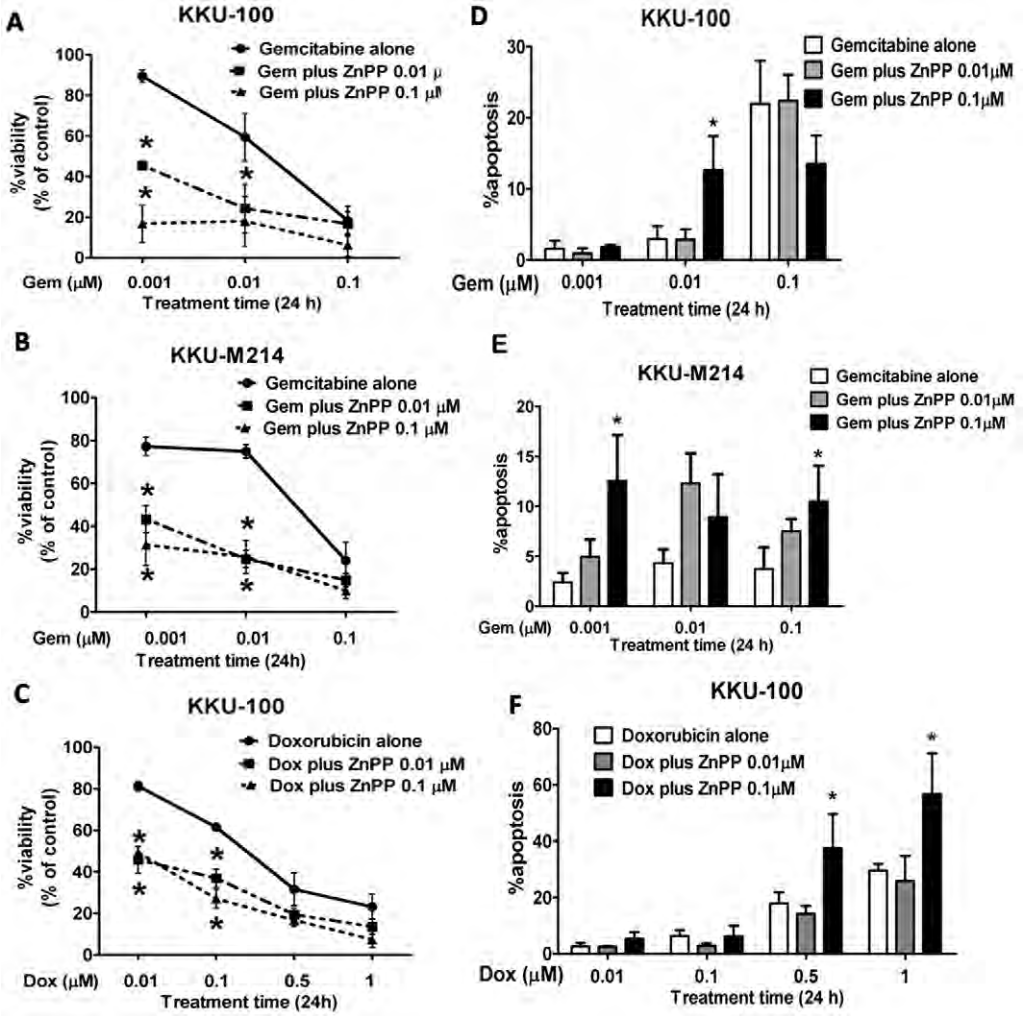


**Figure 3. Inhibition of HO-1 activity enhances the cytotoxic effect of Gem.** KKU-100 and KKU-M214 cells were treated with the varied concentrations (0.001, 0.01 and 0.1 μM) of Gem (A,B,D and E) and (0.01, 0.1, 0.5 and 1 μM) of Dox (C and F) with or without 0.01 and 0.1 μM of ZnPP (HO-1 inhibitor) for 24 h. KKU-100 and KKU-M214 cells were evaluated for cytotoxicity (A,B and C) and apoptosis (D,E and F) by fluorescent dye staining. The cytotoxicity of the drugs are in concentration-response manner, whereas in co-treatment of drug and ZnPP, the concentration-response curves are shifted downward, indicating enhancement of the response to drug combinations. The bars at the right panel show percent of apoptotic cell death when cells were treated with anticancer drugs in combination with various concentrations of ZnPP (0.001–0.1 μM). The bars represent mean±SEM, each from three separated experiments. *, $p<0.05$ vs drug alone (Gem and Dox).
doi:10.1371/journal.pone.0034994.g003

## Discussion

HO-1 has a potent cytoprotective activity against noxious stimuli in inflammatory diseases such as sepsis, inflammatory bowel disease, or in various oxidative injuries [7]. Moreover, HO-1 plays a protective role in normal tissues as well as in cancer cells [22,23]. Our study demonstrated that HO-1 plays a critical role in CCA cells in cytoprotection against anticancer agents, regardless of the basal HO-1 expression levels of the cells. Inhibition of HO-1 by ZnPP or HO-1 siRNA could sensitize CCA cells to the cytotoxicity of anticancer agents, whereas the induction of HO-1 exerted a cytoprotective and drug resistant effects. The sensitization of CCA cells by HO-1 inhibition is probably involved with generation of ROS, which leads to the loss of $\Delta\Psi m$, and initiates apoptotic cell death processes.

Altered expression of drug metabolizing enzymes, such as *UGT1A*, *UGT2B*, *SULT1C* [24], *NAT2* [25] and *GSTO* [26] have been reportedly associated with intrahepatic cholangiocarcinoma in endemic area of liver fluke infection. However, there is still no evidence to establish their roles in protecting cancer cells. Elevated expression of HO-1 has been reported in various human tumors including renal cell carcinoma, prostate tumors, bladder and pancreatic cancers [15,27,28,29], with close association to the disease states. In the present study, HO-1 induction by $SnCl_2$ caused a significant cytoprotection against chemotherapeutic agents regardless of basal HO-1 expression. On the other hand, treatment with anticancer agent also strongly up-regulated HO-1 expression, implying that adaptive defense response in CCA cells is induced to endure the drugs. These results suggest that role of HO-1 in cytoprotection is very critical even in low basal level of HO-1 expression. It should be noted that cytoprotective effect conferred by HO-1 is not specific to Gem but also to Dox and perhaps to some others, in spite of the different mechanisms of actions of these anticancer agents. These results also suggest that the resistance of CCA cells to anticancer agents is, at least in part, due to induction of HO-1. Overall, the inhibition of HO-1 may

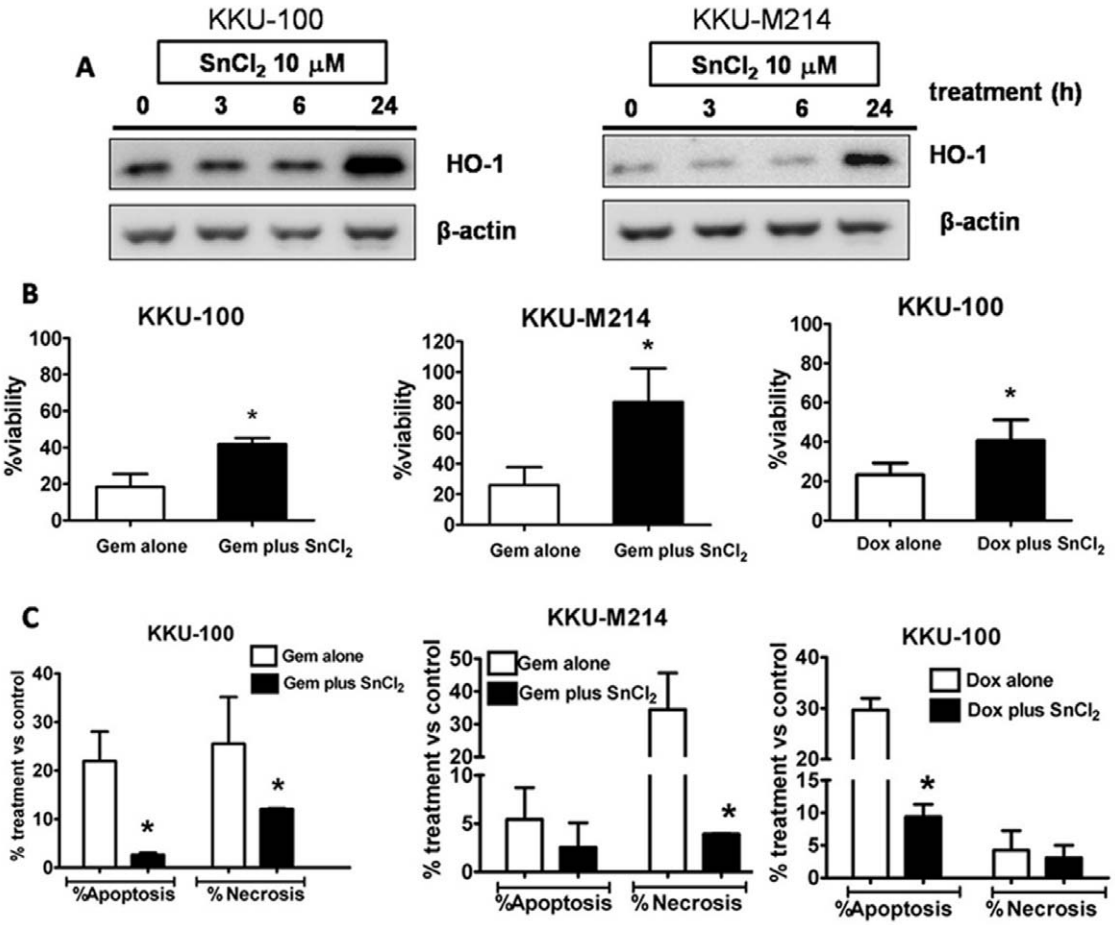


**Figure 4. Induction of HO-1 suppressed the cytotoxicity of Gem and Dox.** (**A**) The time-course of HO-1 induction by $SnCl_2$ (10 μM) in KKU-100 and KKU-M214 cells. The cells were cultured for overnight and exposed to $SnCl_2$ for 3, 6 and 24 h before whole cell lysates were collected and HO-1 protein was determined by the Western blotting, using β-actin; as loading control. The HO-1 protein expression in KKU-100 and KKU-M214 cells is relative stable during the first 6 h of exposure to $SnCl_2$, whereas high HO-1 expression is evident during 6 to 24 h. The cytotoxicity of Gem (0.1 μM) and Dox (0.5 μM) with or without $SnCl_2$ (10 μM) was determined in both cell lines after incubation for 24 h. The cell viability (**B**), apoptotic and necrotic cells (**C**) were evaluated by fluorescent dye staining. Data represent mean±SEM, each from three separated experiments. *, $p<0.05$ vs drug alone.
doi:10.1371/journal.pone.0034994.g004

overcome the intrinsic as well as acquired resistance to chemotherapeutic agents.

Subsequently in this study, we investigated further as to how HO-1 inhibition induces the sensitization in CCA cells to anticancer agents. HO-1 possesses an indirect antioxidant effects probably via generation of biliverdin/bilirubin, carbon monoxide, and other oxidative stress responses [11,30]. Bilirubin is a potent antioxidant by recycling between biliverdin and bilirubin during the catalytic cycle of oxidation and reduction [11]. Inhibition of HO-1 by ZnPP resulted in significant increase in ROS formation [17,23,29]. Our results showed that ZnPP caused marked increase in ROS levels in KKU-100 cells, whereas Gem treatment alone did not induce ROS. Moreover, combination of ZnPP and Gem enhanced more ROS production than ZnPP alone. Our study further verified that ROS is essential for the chemosensitizing effect, as scavenging of ROS by Tempol virtually abolished the sensitizing effect of ZnPP. Moreover, these results imply that inhibition of HO-1 increases the oxidative stress, where ROS may be derived from the metabolism of the cells themselves [7,30].

The loss of $\Delta\psi_m$ is regarded as an early event of mitochondrial dysfunction. It is apparent that a small change in mitochondrial permeability transition (MPT) could depolarize the mitochondria, whilst increasing number of MPT leads to necrosis and apoptosis [31]. The increase of ROS production in ZnPP treated groups was associated with the loss of $\Delta\psi_m$. Our recent study on chemopreventive effect of curcumin has demonstrated a temporal relationship of ROS formation, depolarization of mitochondria and induction of apoptosis [32]. An inducer such as ROS may attack and modify membrane proteins of MPT pores leading to the aggregation of misfolded proteins creating regulated PT pores [31]. In this circumstance, the cells are in a state of highly susceptible to further attack by inducers of MPT. Role of ROS induced by ZnPP in relation to mitochondrial function and induction of apoptotic cell death is needed further clarification.

Alternatively, inhibition of HO-1 activity results in an increase accumulation of protoporphyrin in mitochondria [33] and this lead to depolarization of $\Delta\psi_m$ and sensitize MPT to cytotoxic agents. Protoporphyrin IX has been suggested to be a ligand of peripheral benzodiazepine receptor, a component of MPT pores, thereby sensitizes MPT [34,35]. The present study showed that only the combination of ZnPP and Gem enhanced cell killing effect, whilst ZnPP alone at sub-micromolar concentrations caused

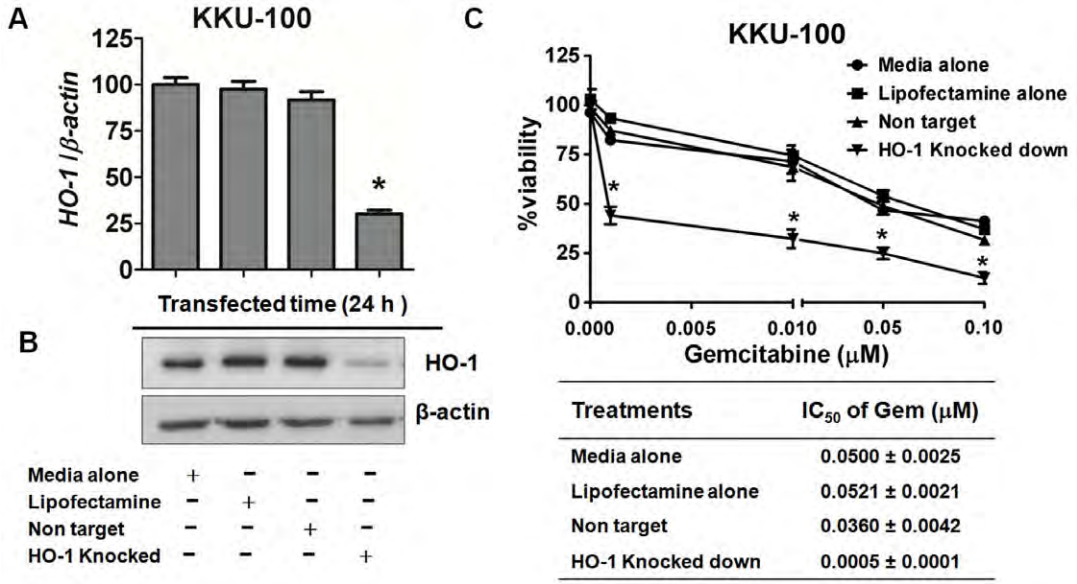


| Treatments | $IC_{50}$ of Gem (μM) |
|---|---|
| Media alone | 0.0500 ± 0.0025 |
| Lipofectamine alone | 0.0521 ± 0.0021 |
| Non target | 0.0360 ± 0.0042 |
| HO-1 Knocked down | 0.0005 ± 0.0001 |

**Figure 5. Knockdown of HO-1 by siRNA sensitized KKU-100 cells to Gem.** The mRNA (A) and protein (B) levels of HO-1expression in KKU-100 cells are shown. KKU-100 cells were transfected with siRNA against HO-1 for 24 h and total RNA was prepared and analyzed by reverse transcription-PCR. In similar experiments, cell lysates were collected and HO-1 was determined by the Western blotting in KKU-100 cells, using β-actin, as loading control. (**C**) The cytotoxicity and IC50 of Gem in knocked down KKU-100 cells was determined. After transfection for 24 h, KKU-100 cells were treated with varied concentrations of Gem (0.001, 0.01, 0.05 and 0.1 μM) for another 24 h. The cell viability was evaluated by fluorescent dye staining. Data represent mean±SEM, each from three separated experiments. *, $p<0.05$ vs non target knocked down cells.
doi:10.1371/journal.pone.0034994.g005

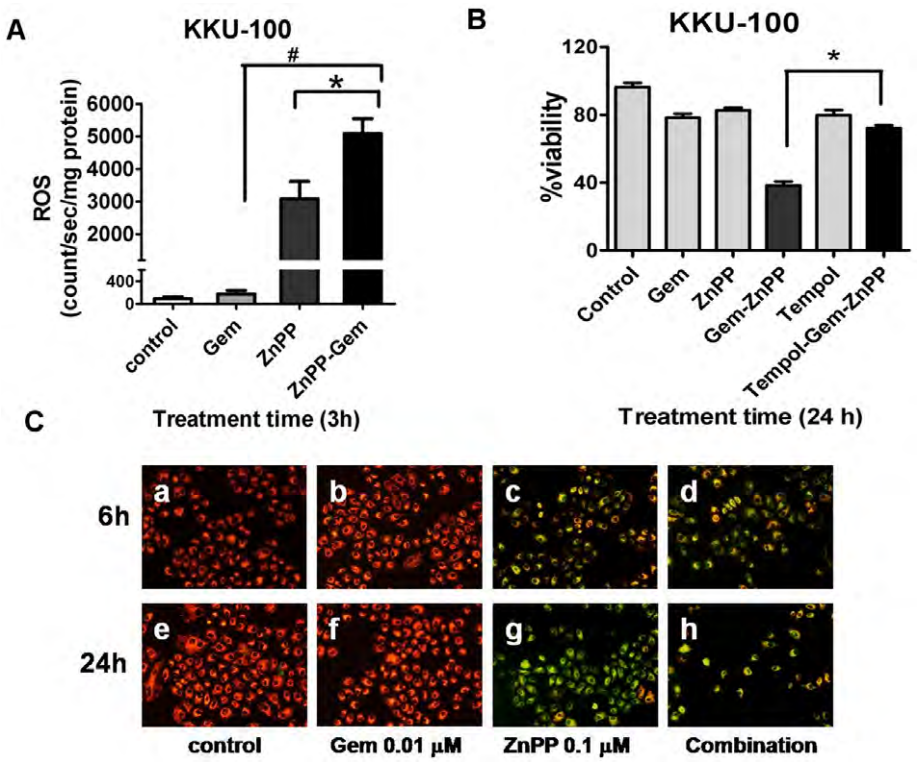


**Figure 6. ZnPP induced the intracellular reactive oxygen generation, depolarization of mitochondrial transmembrane potential and cytotoxicity.** (**A**) The generation of ROS induced by ZnPP (0.1 μM) and combination of ZnPP and Gem (0.01 μM) for 3 h in KKU-100 cells as measured by lucigenin-enhanced chemiluminescent method. *, $p<0.05$ vs ZnPP alone and $^{\#}$, vs Gem alone. (**B**) The ROS scavenger, Tempol (500 μM), inhibited cytotoxicity of the combination of ZnPP (0.1 μM) and Gem (0.01 μM) in KKU-100 cells The cell viability was evaluated by fluorescent dye staining. *, $p<0.05$ vs the combination of ZnPP and Gem. Data represent mean±S.E.M., each from three independent experiments. (**C**) The induction of depolarization of the mitochondrial transmembrane potential ($\Delta\psi_m$) using JC-1 fluorescent probe, in KKU-100 cells after treatment with Gem+/−ZnPP for 6 h (a,b,c, &d) and 24 h (e,f,g & h). The healthy mitochondria, JC-1 forms J-aggregates and display strong red fluorescent signal, whereas the depolarized mitochondria, JC-1 exists as monomers and show green fluorescent signal.
doi:10.1371/journal.pone.0034994.g006

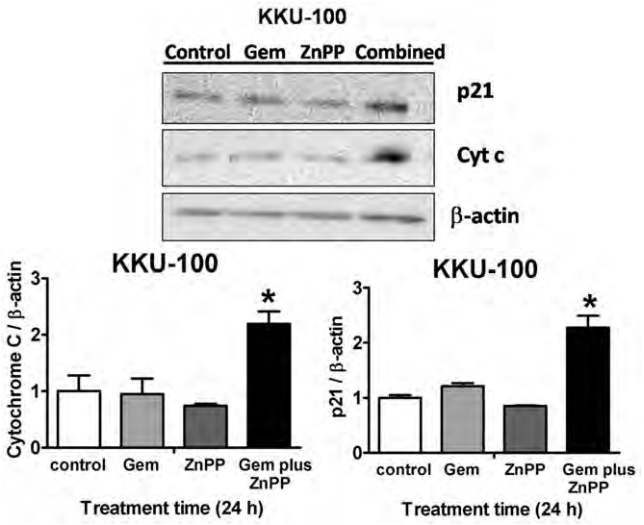


**Figure 7. Alteration of expression of proteins related to cell proliferation and apoptosis.** The Western blots of p21 and cytochrome c protein expression in KKU-100 cells after treatment with Gem (0.01 μM)+/−ZnPP (0.1 μM) for 24 h. The levels of p21 and cytochrome c were normalized with β-actin as a loading control. The bars are mean±SEM, each from three independent experiments. *$p<0.05$ vs untreated controls.
doi:10.1371/journal.pone.0034994.g007

the release of ROS in association with loss of $\Delta\psi_m$, but this was still insufficient to induce cell death. Our study is in agreement with recent reports, ZnPP alone shows no effect on MPT, however ZnPP in combination with triiodothyronine induced oxidative stress, MPT opening and apoptotic cell death [18]. Furthermore, effect of protoporphyrin IX at nanomolar range in enhanced rotenone-induced cytotoxicity is demonstrated to be due to MPT opening, because the effects were inhibited by cyclosporine A, an inhibitor of MPT [35].

The sensitizing effect is consistent with present experiment in that no increased release of cytochrome c by ZnPP or Gem alone, whereas the drug combination increased release of cytochrome c. It is noted that Gem alone may not exert cytotoxic effect via mitochondrial pathway, as Gem did not induce changes of $\Delta\psi_m$ and cytochrome c levels. Gem is known to induce cell cycle arrest and apoptosis by p53-dependent and independent pathways. [36]. Our study observed that combination of ZnPP and Gem induced an increased level of the protein p21, which is a p53-dependent downstream gene product, and a potent cyclin-dependent kinase inhibitor. Gem or ZnPP alone did not exert any significant changes in p21. It is probable that induction of mitochondrial dysfunction induces p21 accumulation [37]. This is consistent with a strong antiproliferation effect of Gem and ZnPP combination.

In summary, HO-1 plays an important role in cytoprotection in both low and high HO-1 expressing CCA cells. Inhibition of HO-1 induced ROS formation, which may initiate the loss of $\Delta\psi_m$ and sensitizes CCA cells to a cytotoxic effect of anticancer agents. Thus, targeted suppression of HO-1 may be a strategy to overcome drug resistance in cholangiocarcinoma chemotherapy.

## Acknowledgments

Valuable suggestions on the manuscript of Prof. Yukifumi Nawa of Faculty of Medicine, Khon Kaen University are gratefully acknowledged.

## Author Contributions

Conceived and designed the experiments: SK VK AP. Performed the experiments: SK AP LS. Analyzed the data: SK VK AP LS. Contributed reagents/materials/analysis tools: UK BB. Wrote the paper: SK VK.

## References

1. Sripa B, Pairojkul C (2008) Cholangiocarcinoma: lessons from Thailand. Curr Opin Gastroenterol 24: 349–56.
2. Shin HR, Oh JK, Masuyer E, Curado MP, Bouvard V, et al. (2010) Epidemiology of cholangiocarcinoma: an update focusing on risk factors. Cancer Sci 101: 579–85.
3. Blechacz B, Gores GJ (2008) Cholangiocarcinoma: advances in pathogenesis, diagnosis, and treatment. Hepatology 48: 308–21.
4. Patel T (2011) Cholangiocarcinoma–controversies and challenges. Nat Rev Gastroenterol Hepatol 8: 189–200.
5. Malhi H, Gores GJ (2006) Cholangiocarcinoma: Modern advances in understanding a deadly old disease. Journal of Hepatology 45: 856–67.
6. Hezel AF, Zhu AX (2008) Systemic therapy for biliary tract cancers. Oncologist 13: 415–23.
7. Ryter SW, Alam J, Choi AM (2006) Heme oxygenase-1/carbon monoxide: from basic science to therapeutic applications. Physiol Rev 86: 583–650.
8. Doi K, Akaike T, Fujii S, Tanaka S, Ikebe N, et al. (1999) Induction of haem oxygenase-1 nitric oxide and ischaemia in experimental solid tumours and implications for tumour growth. Br J Cancer 80: 1945–54.
9. Nuhn P, Kunzli BM, Hennig R, Mitkus T, Ramanauskas T, et al. (2009) Heme oxygenase-1 and its metabolites affect pancreatic tumor growth in vivo. Mol Cancer 8: 37.
10. Boutros C, Zegdi R, Lila N, Cambillau M, Fornes P, et al. (2007) Carbon monoxide can prevent acute lung injury observed after ischemia reperfusion of the lower extremities. J Surg Res 143: 437–42.
11. Ryter SW, Kim HP, Nakahira K, Zuckerbraun BS, Morse D, et al. (2007) Protective functions of heme oxygenase-1 and carbon monoxide in the respiratory system. Antioxid Redox Signal 9: 2157–73.
12. Jozkowicz A, Was H, Dulak J (2007) Heme oxygenase-1 in tumors: is it a false friend? Antioxid Redox Signal 9: 2099–117.
13. Was H, Cichon T, Smolarczyk R, Rudnicka D, Stopa M, et al. (2006) Overexpression of heme oxygenase-1 in murine melanoma: increased proliferation and viability of tumor cells, decreased survival of mice. Am J Pathol 169: 2181–98.
14. Kuroda H, Takeno M, Murakami S, Miyazawa N, Kaneko T, et al. (2010) Inhibition of heme oxygenase-1 with an epidermal growth factor receptor inhibitor and cisplatin decreases proliferation of lung cancer A549 cells. Lung Cancer 67: 31–6.
15. Miyake M, Fujimoto K, Anai S, Ohnishi S, Nakai Y, et al. (2010) Clinical significance of heme oxygenase-1 expression in non-muscle-invasive bladder cancer. Urol Int 85: 355–63.
16. Miyazaki T, Kirino Y, Takeno M, Samukawa S, Hama M, et al. (2010) Expression of heme oxygenase-1 in human leukemic cells and its regulation by transcriptional repressor Bach1. Cancer Sci 101: 1409–16.
17. Nowis D, Bugajski M, Winiarska M, Bil J, Szokalska A, et al. (2008) Zinc protoporphyrin IX, a heme oxygenase-1 inhibitor, demonstrates potent antitumor effects but is unable to potentiate antitumor effects of chemotherapeutics in mice. BMC Cancer 8: 197.
18. Giris M, Erbil Y, Depboylu B, Mete O, Turkoglu U, et al. (2010) Heme oxygenase-1 prevents hyperthyroidism induced hepatic damage via an antioxidant and antiapoptotic pathway. J Surg Res 164: 266–75.
19. Buranrat B, Prawan A, Kukongviriyapan U, Kongpetch S, Kukongviriyapan V (2010) Dicoumarol enhances gemcitabine-induced cytotoxicity in high NQO1-expressing cholangiocarcinoma cells. World J Gastroenterol 16: 2362–70.
20. Buranrat B, Prawan A, Sripa B, Kukongviriyapan V (2007) Inflammatory cytokines suppress arylamine N-acetyltransferase 1 in cholangiocarcinoma cells. World J Gastroenterol 16: 6219–25.
21. Buranrat B, Prawan A, Kukongviriyapan U, Kongpetch S, Kukongviriyapan V (2010) Dicoumarol enhances gemcitabine-induced cytotoxicity in high NQO1-expressing cholangiocarcinoma cells. World J Gastroenterol 16: 2362–70.
22. Correa-Costa M, Semedo P, Monteiro AP, Silva RC, Pereira RL, et al. (2010) Induction of heme oxygenase-1 can halt and even reverse renal tubule-interstitial fibrosis. PLoS One 5: e14298.
23. Fang J, Sawa T, Akaike T, Akuta T, Sahoo SK, et al. (2003) In vivo antitumor activity of pegylated zinc protoporphyrin: targeted inhibition of heme oxygenase in solid tumor. Cancer Res 63: 3567–74.
24. Jinawath N, Chamgramol Y, Furukawa Y, Obama K, Tsunoda T, et al. (2006) Comparison of gene expression profiles between Opisthorchis viverrini and non-Opisthorchis viverrini associated human intrahepatic cholangiocarcinoma. Hepatology 44: 1025–38.
25. Prawan A, Kukongviriyapan V, Tassaneeyakul W, Pairojkul C, Bhudhisawasdi V (2005) Association between genetic polymorphisms of

CYP1A2, arylamine N-acetyltransferase 1 and 2 and susceptibility to cholangiocarcinoma. Eur J Cancer Prev 14: 245–50.
26. Marahatta SB, Punyarit P, Bhudisawasdi V, Paupairoj A, Wongkham S, et al. (2006) Polymorphism of glutathione S-transferase omega gene and risk of cancer. Cancer Lett 236: 276–81.
27. Goodman AI, Choudhury M, da Silva JL, Schwartzman ML, Abraham NG (1997) Overexpression of the heme oxygenase gene in renal cell carcinoma. Proc Soc Exp Biol Med 214: 54–61.
28. Maines MD, Abrahamsson PA (1996) Expression of heme oxygenase-1 (HSP32) in human prostate: normal, hyperplastic, and tumor tissue distribution. Urology 47: 727–33.
29. Berberat PO, Dambrauskas Z, Gulbinas A, Giese T, Giese N, et al. (2005) Inhibition of heme oxygenase-1 increases responsiveness of pancreatic cancer cells to anticancer treatment. Clin Cancer Res 11: 3790–8.
30. Gozzelino R, Jeney V, Soares MP (2010) Mechanisms of cell protection by heme oxygenase-1. Annu Rev Pharmacol Toxicol 50: 323–54.
31. Kim JS, He L, Lemasters JJ (2003) Mitochondrial permeability transition: a common pathway to necrosis and apoptosis. Biochem Biophys Res Commun 304: 463–70.
32. Suphim B, Prawan A, Kukongviriyapan U, Kongpetch S, Buranrat B, et al. (2010) Redox modulation and human bile duct cancer inhibition by curcumin. Food Chem Toxicol 48: 2265–72.
33. Ohgari Y, Miyata Y, Chau TT, Kitajima S, Adachi Y, et al. (2011) Quinolone compounds enhance delta-aminolevulinic acid-induced accumulation of protoporphyrin IX and photosensitivity of tumour cells. J Biochem 149: 153–60.
34. Azarashvili T, Grachev D, Krestinina O, Evtodienko Y, Yurkov I, et al. (2007) The peripheral-type benzodiazepine receptor is involved in control of Ca2+-induced permeability transition pore opening in rat brain mitochondria. Cell Calcium 42: 27–39.
35. Pastorino JG, Simbula G, Gilfor E, Hoek JB, Farber JL (1994) Protoporphyrin IX, an endogenous ligand of the peripheral benzodiazepine receptor, potentiates induction of the mitochondrial permeability transition and the killing of cultured hepatocytes by rotenone. J Biol Chem 269: 31041–6.
36. Tolis C, Peters GJ, Ferreira CG, Pinedo HM, Giaccone G (1999) Cell cycle disturbances and apoptosis induced by topotecan and gemcitabine on human lung cancer cell lines. Eur J Cancer 35: 796–807.
37. Li CH, Tzeng SL, Cheng YW, Kang JJ (2005) Chloramphenicol-induced mitochondrial stress increases p21 expression and prevents cell apoptosis through a p21-dependent pathway. J Biol Chem 280: 26193–9.

RESEARCH ARTICLE

# NQO1 Expression Correlates with Cholangiocarcinoma Prognosis

**Benjaporn Buranrat[1,5], Siri Chau-in[2,4], Auemduan Prawan[1,4], Anucha Puapairoj[3,4], Pornsilp Zeekpudsa[1,4], Veerapol Kukongviriyapan[1,4]***

## Abstract

**Cholangiocarcinoma (CCA) is a rare type of liver cancer with a very poor prognosis. The prevalence of CCA is markedly variable with the highest incidence in the northeast Thailand, followed by other parts of Southeast Asia and China. Currently, there is still no reliable biomarker for diagnosis or treatment. NADPH-quinone oxidoreductase 1 (NQO1) is a xenobiotic metabolizing enzyme detoxifying chemical stressors and antioxidants, thereby providing cytoprotection in normal tissues. However, NQO1 is over-expressed in some cancers, suggesting roles in carcinogenesis and tumor progression. In this study, we examined NQO1 activity in surgical specimens from CCA patients and found much higher values than in the adjacent normal tissues. Immunohistochemical analysis revealed strong staining in tumor epithelial elements, whereas the non-tumor bile ducts and liver parenchyma were weakly stained. *NQO1* mRNA expression in tumor tissues was widely varied among 43 patients. A significant association was observed between high level of *NQO1* expression and short overall survival time by the Cox proportional hazard ratio of 2.40, $p<0.05$. By histological classification, non-papillary adenocarcinoma was an independent predictor for poor prognosis with the hazard ratio of 2.79, $p<0.05$. *NQO1* expression may serve as a prognostic biomarker for the CCA.**

**Keywords:** NADPH-quinone oxidoreductase 1-drug metabolizing enzyme antioxidant-cytoprotection

*Asian Pacific J Cancer Prev,* **13**, 131-136

## Introduction

Cholangiocarcinoma (CCA) is a malignant neoplasm originating from the bile duct epithelium. Although CCA is a rare cancer worldwide, the incidence and mortality rates have grown up in the US, United Kingdom, Japan and Australia (Patel, 2011). The incidence of this cancer is very high in regions of northeast Thailand, Cambodia, and Laos, where the prevalence of liver fluke infection is very high (Sripa and Pairojkul, 2008; Kamsa-ard et al., 2011). *Opisthorchis viverrini* infection is one of the important risk factors of CCA probably through chronic inflammation-induced oxidative stress and nitrosative stress (Coussens and Werb, 2002; Pinlaor et al., 2004), since chronic inflammation predisposes to several types of cancers. Activated inflammatory cells release a variety of inflammatory cytokines such as IL-1β, IFN–γ, TNF-α and inflammatory mediators, including nitric oxide and prostaglandin E2 which act as tumor promoters (Dijkstra et al., 2004; Ohshima et al., 2005). CCA is an aggressive malignancy characterized by the resistance to the current chemotherapy and radiotherapy in vast majority of cases (Patel, 2011). Diagnosis of CCA is very difficult because of the nonspecific clinical manifestations and the lack of appropriate biomarkers (Khan et al., 2005; Patel, 2011). Complete surgical excision with negative tumor margin, solitary lesion, absence of lymph node involvement, and lack of vascular invasion are the best predictors for long term survival (Khan et al., 2005). However, current predictors of pathological and operative staging strategies do not accurately predict long-term prognosis of CCA patients. The other markers for diagnosis or treatment such as serum markers of CA 19-9 and CEA are of very limited value (Patel, 2011).

NAD(P)H:quinone oxidoreductase-1 (*NQO1*) is a ubiquitous flavoprotein that functions as an antioxidant enzyme (Siegel et al., 2004). The enzyme catalyzes two electron reduction of quinones to hydroquinones, thus avoids a one electron reduction and associated redox cycling which generates reactive oxygen species (ROS) (Dinkova-Kostova, 2010). Functions of NQO1 include xenobiotic detoxification, superoxide scavenger and the maintenance of endogenous antioxidant vitamins (Siegel et al., 2004). The antioxidant role of NQO1 was suggested by evidences such that the disruption of *NQO1* gene (Radjendirane et al., 1998) or genetic polymorphism increased the risk of chemical-induced toxicity and cancers (Saldivar et al., 2005; Yang et al., 2012). Several

*[1]Departments of Pharmacology, [2]Surgery, [3]Pathology, Faculty of Medicine, [4]Liver Fluke and Cholangiocarcinoma Research Center, Khon Kaen University, [5]Faculty of Medicine, Mahasarakham University, Thailand *For correspondence: veerapol@kku.ac.th*

lines of evidences indicate that cancer chemoprevention afforded by regular intake of dietary phytochemicals involves with induction of the phase II enzymes including NQO1 (Surh et al., 2008). It is conceivable that NQO1 plays an important role in protecting normal cells against oxidative injury and carcinogenesis.

Over-expression of *NQO1* mRNA in tumor tissue compared to the surrounding normal tissue was reported in liver cancer (Cresteil and Jaiswal, 1991), lung cancer (Kolesar et al., 2002), pancreatic cancer (Logsdon et al., 2003), and over-expression of NQO1 detected by immunohistochemistry in breast, ovary, thyroid, adrenal, colorectal and bladder was also observed (Siegel and Ross, 2000). These circumstantial evidences suggest that over-expression of NQO1 may confer cytoprotection for tumor cells against oxidative stress and cause cells resistant to anticancer agents (Danson et al., 2004). The treatment of CCA based on targeting NQO1 has been shown to be a potential strategy to overcome the resistance in CCA (Buranrat et al., 2010). In this study we analyzed *NQO1* expression in CCA tumor and apparently normal adjacent tissues and examined whether *NQO1* expression could be a prognostic marker of CCA in association with the overall survival.

## Materials and Methods

*Subjects*

Subjects were patients admitted at Sringarind Hospital, Faculty of Medicine, Khon Kaen University for the treatment of cholangiocarcinoma. All patients have been diagnosed and confirmed by histopathological examination. Their average age was (mean±SD) 56.1±9.4 years, with 27 males and 16 females. Their survival time ranged from 36 days to 1,120 days, at which time some subjects were still alive. In this study, nine patients (22.5%) received adjuvant chemotherapy after surgery. Tumor tissues were collected from surgical resection of tumor mass for histopathological examination and other tissue samples were kept in liquid nitrogen before uses for extraction of RNA and enzymatic assay.

*Tissue samples*

Forty-three tissue sections from the specimen bank of the Liver Fluke and Cholangiocarcinoma Research Center, Faculty of Medicine, Khon Kaen University. The study protocol was approved by the Khon Kaen University Ethics Committee for Human Research. Written informed consent was obtained from all patients. Among forty three samples, thirty samples were available as the pair of tumorous and non-tumorous tissues. Samples of the same tissue section were used for assays of NQO1 activity and total mRNA. Patients who died within 2 weeks after operation were excluded from this study.

*Immunohistochemistry*

CCA tissue sections were cut from archival paraffin blocks. Sections were deparaffinized in xylene and rehydrated through descending alcohol series to distilled water. Endogenous peroxidase activity was eliminated by placing sections in 3% hydrogen peroxide for 30 min. Sections were rinsed in PBS for 10 min and then blocked in 5% milk in PBST for 20 min. Immunohistochemistry analysis of NQO1 was performed using mouse monoclonal IgG against NQO1 (sc-32793, Santa Cruz, CA, USA) 1:100 dilution for an overnight at 4°C, followed by Immunodetection with Envision system-HRP labeled polymer anti-mouse (Dako) for 1 hr. Sections were counterstained with hematoxylin, and photographed.

*NQO1 activity in tissues*

Tissues was thawed, cut into small pieces in ice-cold 1.15% (w/v) KCl in 0.1 M phosphate buffer pH 7.4 and homogenized with Utra-Turrax homogenizer. Homogenates were centrifuged at 100,000 g at 4°C for 60 min. Finally, supernatant was collected for the cytosol fraction and the microsomal pellet was resuspended by homogenizing the pellet in the same buffer. Cytosol and microsomal fractions were preserved with 20% (v/v) glycerol. Aliquots of samples were stored at -70°C until use.

NQO1 activity was measured according to the previously described method (Prochaska and Santamaria, 1988) with slight modifications (Prawan et al., 2009). Cytosol samples were assayed by coupling reaction using menadione and MTT (3-(4,5-dmethylthiazol-2-yl)-2,5-diphenyltetrazolium bromide, a tetrazole) as the substrate. Tissue cytosol was added to reaction mixture containing with Tris 25 mM, pH 7.4, bovine serum albumin 67 mg/mL, 0.015% tween-20, 50 $\mu$M FAD, 1 mM glucose-6-phosphate (G6P), 30 μM NADP, 2 unit/mL G6P-dehydrogenase, 0.03 mg/mL MTT and 0.24 μM menadione. The assay was performed in the presence and absence of 50 $\mu$M dicoumarol. The enzyme activity was measured as a rate-kinetics at a wavelength of 620 nm, and the readings were made at 30 second intervals for 5 min. The initial velocity of dicoumarol-suppressible kinetics was calculated as the NQO1 activity using the extinction coefficient of formazan of MTT of 11,300 $M^{-1}$ $cm^{-1}$.

*RNA preparation and reverse transcription-polymerase chain reaction*

Total RNA was extracted from tumor tissues using Trizol reagent following the manufacturer's instruction. Total RNA (1 $\mu$g) was reverse-transcribed in 20 $\mu$L containing 0.5 $\mu$g of oligo$(dT)_{15}$ primer, 20 U of RNasin® ribonuclease inhibitor and 200 U of ImProm-II™ reverse trancriptase in 10xPCR buffer, 3 mmol/L $MgCl_2$, and 1 mmol/L dNTPs. The first-strand cDNA was synthesized at condition of 42°C for 60 min. The reverse transcription products were served as a template for real-time PCR. PCR amplification was performed using specific primers for the *NQO1* using beta-actin as an internal control. The PCR primer sequences were: *NQO1*; forward primer: 5' GGC AGA AGA GCA CTG ATC GTA 3', *NQO1*; reverse primer: 5' TGA TGG GAT TGA AGT TCA TGG C 3', GenBank accession number BC007659.2, with the expected amplicon size of 159 bp, beta-actin; forward primer: 5' TGC CAT CCT AAA AGC CAC 3', beta-actin; reverse primer: 5' TCA ACT GGT CTC AAG TCA GTG 3', GenBank accession number NM_001101.3 with amplicon size of 290 bp. The real-time PCR, based

on SYBR Green, was carried out in a final volume of 20 $\mu$L containing 1x SYBR Green master mix, 0.5 $\mu$mol/L of each NQO1 or beta-actin primers. Thermal cycling was performed for each gene in duplicate on cDNA samples in 96-wells reaction plate using the ABI 7500 Sequence Detection system (Applied Biosystems). The negative control, set up by substituting the template with deionized $H_2O$ and that routinely had a high Ct value which represented the lower detection limit, was included in the experimental runs. Real-time PCR was conducted with the following cycling conditions: 95°C for 10 min, followed by 40 cycles of 95°C for 15 s, 55°C for 30 s and 72°C for 45 s. Assay was performed in triplicate. The relative expression ratio (R) of the target genes was calculated based on the efficiency (E) and CT deviation and expressed as the ratio to the reference gene. The corresponding real time PCR efficiencies were calculated according to the equation $E=10^{[-1/slope]}$. All data were analyzed using Sequence Detector Software Version 1.4 (Applied Biosystems).

*Statistical analysis*

Data are expressed as mean±SD. Student's t-test was used to determine significant differences between tumor and normal tissues. The level of significance was preset at $p<0.05$. Cross tabulations were analyzed with the chi-square test for association of *NQO1* mRNA expression and the pathological features of patients. The Kaplan-Meier survival curves were generated for patients who having high and low expression of *NQO1* mRNA, histological types of papillary type and other. Hazard ratios and p-values for comparisons of patients having high and low *NQO1* expression were calculated based on multivariate Cox proportional hazards model, adjusting for their age, sex, histological types, tumor residue and metastasis. The analyses were conducted by using Stata software version 7.0.

## Results

*Characteristics of patients*

Characteristics of subjects are shown in Table 1. There were 8 long survivors, and 6 out of 8 patients had a papillary type CCA by histopathology. Patients in this series were initially evaluated as the candidates for complete excision. However, only 18 (42%) patients were proven to have been achieved complete resection with negative margin (R0) by histopathology, while all the others have extensive invasion and tumor residue at the surgical margin.

*NQO1 activity and immunohistochemical localization in CCA tissue*

NQO1 activity in tumor tissues was much higher than that in non-tumor adjacent tissues ($p<0.001$) (Figure 1). The median and 25% and 75% percentiles of NQO1 activities were 14.9, 1.0 and 20.8 nmol/min/mg protein for tumor tissues and 0.81, 0.44 and 1.21 nmol/min/mg protein for normal tissues. There was no association between NQO1 activity and survival time or *NQO1* mRNA expression. The immunohistochemical staining in tumor


**Figure 1. Activity of NQO1 in Tissues from Normal and Tumor Sections of CCA Patients.** Surgical liver specimens from CCA patients were sectioned for tumor and adjacent normal tissues. Tissues were homogenized for preparation of cytosolic fraction to determine NQO1 activity by the enzymatic coupling assay. All samples were performed in triplicate assay. Small horizontal bars on the right side of the plots represent the percentiles of 25th, 50th and 75th

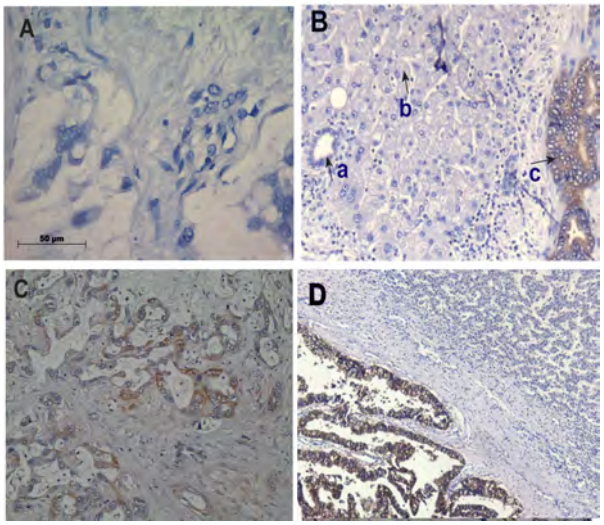


**Figure 2. Immunohistochemical Staining of NQO1 in CCA Sections.** A) The negative control of NQO staining. B) The non-tumor tissue stained very weakly with NQO1, a: non-tumor bile duct, b: liver parenchyma, and c: bile duct tumor stained strongly with NQO1. C) The well-differentiated adenocarcinoma type. D) The papillary type. (Original magnification of x40 for A & C, and 10X for B & D)

**Table 1. The Characteristics of CCA Patients in this Study and in Relation to *NQO1* Expression Levels**

| Characteristics | | No. | *NQO1* expression Low | *NQO1* expression High | p-value |
|---|---|---|---|---|---|
| Age (year±SD) | 56±9 | 43 | 57.5±7.0 | 53.0±13.4 | 0.15 |
| Gender | Female | 16 | 10 | 6 | 0.5 |
| | Male | 27 | 20 | 7 | |
| Status | Death | 35 | 24 | 11 | 0.72 |
| | Alive | 8 | 6 | 2 | |
| Gross type | Mass forming | 24 | 17 | 7 | 0.98 |
| | Periductal infiltrating | 17 | 12 | 5 | |
| | Intraductal growth | 1 | 0 | 1 | |
| Histological type | Papillary | 22 | 16 | 6 | 0.66 |
| | Non-papillary | 21 | 14 | 7 | |
| | Well-differentiated | 16 | | | |
| | Moderately-differentiated | 3 | | | |
| | Poorly-differentiated | 2 | | | |
| Metastasis | Present | 14 | 9 | 5 | 0.69 |
| | Not establish | 27 | 19 | 8 | |
| Surgical margin | R0 | 18 | 13 | 5 | 0.77 |
| | Not R0 | 25 | 17 | 8 | |

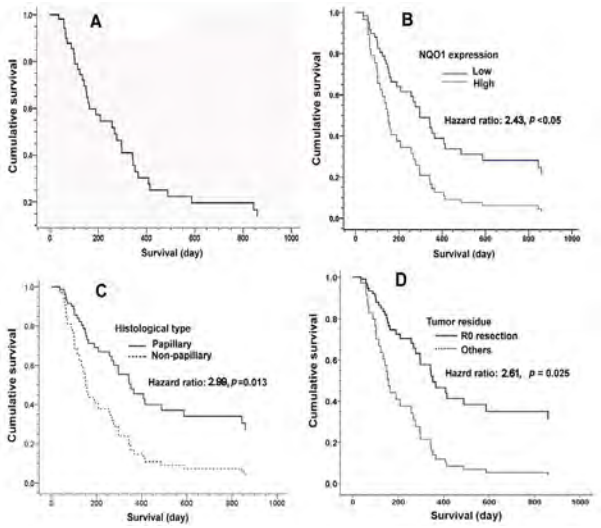


**Figure 3. Cumulative Survival Curves for Intrahepatic Cholangiocarcinoma.** A) The survival function at mean of covariates. B) Survival function stratified by the levels of *NQO1* mRNA expression. C) Survival function stratified by histological. D) Survival function type stratified by surgical margin. Tumor tissues from surgical sections of cholangiocarcinoma patients were prepared for total RNA and analyzed for *NQO1* mRNA by reverse-transcription and real-time PCR. All samples were performed in triplicate assay. Patients with high *NQO1* mRNA expression group or histology of non-papillary type or surgical margin showing tumor residue had worse overall survival

**Table 2. Multivariate Analysis by COX Proportional Hazards**

| Variable | | Hazard ratio | 95%CI | p-value |
|---|---|---|---|---|
| Age | <57 | 1 | | |
| | ≥57 | 2.74 | 1.23-6.07 | 0.013 |
| Gender | Female | 1 | | |
| | Male | 1.02 | 0.49-2.42 | 0.84 |
| Histological types | Papillary | 1 | | |
| | Non-papillary | 2.99 | 1.39-6.42 | 0.005 |
| Metastasis | Presence | 1 | | |
| | No evidences | 1.25 | 0.56-2.79 | 0.58 |
| Surgical margin | R0 | 1 | | |
| | Not R0 | 2.61 | 1.11-6.14 | 0.027 |
| *NQO1* mRNA expression | Low | 1 | | |
| | High | 2.43 | 1.12-5.28 | 0.025 |

and non-tumor areas are shown in Figure 2. The normal issue showed liver parenchyma and small bile ducts only weakly stained with NQO1 in cytosol (Figure 2B). NQO1 is strongly stained in tumors with tubular type as well as papillary type of adenocarcinoma (Figure 2C and D).

*NQO1 expression and association with clinicopathologic variables*

Expression levels of *NQO1* mRNA were measured by reverse-transcription real-time PCR. Subjects at the forth quartile of *NQO1* expression were assigned to high expression group (13 subjects) and the rest were low expression group (30 subjects). There was no significant correlation between the level of *NQO1* and the histological type of tumors, and evidence of metastasis (Table 1). The age of patients between *NQO1* high and low groups was also of no difference.

*Survival time analysis*

The median survival time of the patients in this series was 267 days with 95%CI of 131-403 days. Using Kaplan-Meier and log-rank analysis, the median survival time of CCA patients with the high and low expression of *NQO1* were of 149.0 days (95%CI: 102-196 days) and 342.0 days 95%CI: 228-456 days), respectively. The median survival time of the patients having papillary and non-papillary types by histology were 297 (95%CI: 219-375 days) and 157 day (95%CI: 98-352 days, respectively. In the univariate analysis, none of variables was a significant predictor for survival.

The multivariate Cox proportional hazard analysis was performed in patients to explore the impact of *NQO1* expression after adjusting for age, gender, histological type, metastasis and presence of tumor residue. The levels of *NQO1* expression, histological type, gender and tumor residue at surgical margin were significant predictors of the survival time of CCA patients (Figure 3). CCA patients with low expression of *NQO1* have longer survival than who have high expression, with the hazard ratio of 2.43 ($p<0.05$). The prognosis of patients having papillary adenocarcinoma was better than the patients having other histological types of CCA with the hazard ratio of over 2.99 (Table 2). The patients with residual tumor (surgical margin positive) were at risk with the hazard ratio of 2.61 when compared with complete excision of tumor.

## Discussion

NQO1 functions as xenobiotic metabolizing and antioxidant in normal cells. *NQO1* gene is one of the down-stream genes regulated by Nrf2-antioxidant-response-element (Nrf2-ARE) signaling pathway, which is an important target for cancer chemoprevention of various phytochemicals (Surh et al., 2008). However, in certain circumstances, NQO1 also functions to protect tumor cells, as it is over-expressed in some cancers (Cresteil and Jaiswal, 1991; Kolesar et al., 2002; Danson et al., 2004). Our results revealed that *NQO1* expression by immunohistochemical staining and NQO1 activity in tumor tissues were significantly higher than the normal adjacent tissues. *NQO1* mRNA expression in tumor tissue can be an independent predictor of long-term survival.

In this study, NQO1 activity was very high in CCA tumor tissues compared to the normal liver tissue. There was a wide variation in the activity of tumors, whereas there was much less in normal tissues. However, there was lack of correlation between the activity and mRNA expression of *NQO1*. The high expression might not directly represent the activity observed. Alternatively, *NQO1* expression may represent the activity of Nrf2-ARE signaling system, where the pathway could regulate a number of downstream genes including *NQO1* and other antioxidant genes where they provide cytoprotection and resistance to stress (Kensler and Wakabayashi, 2010).

In a previous study, Strassburg et al. (2002) reported the expression of NQO1 and NQO2 in bile duct tumor was comparable to that of normal bile duct tissues. In contrast to our study, high NQO1 immunohistochemical staining was observed in CCA tissues, whereas surrounding

tissues including normal bile ducts and liver parenchyma were very weakly stained. Since Strassburg et al. (2002) observed in only four CCA patients and use of gall bladder as the representative normal biliary tissues. The small sample size with different control specimen might cause the differences in results.

Recently Wakai et al. (2011) reported that the loss of NQO1 expression evaluated by immunohistochemical technique was associated with the poor prognosis of intrahepatic CCA. This report is in contrast with our finding where low *NQO1* expression is associated with longer survival than the high expression. The discrepancy of findings may be due to the different study populations. CCA patients in our report were from the Northeast region of Thailand where liver fluke infection is probably the most important causative agent of CCA (Green et al., 1991; IARC, 1994). On the other hand, Wakai et al. (2011) studied on Japanese patients where opisthorchiasis is not a risk factor. Related to this, Jinawath et al. (2006) reported that liver fluke-associated and non-liver fluke associated intrahepatic CCA showed significantly different gene expression profiles in such that, xenobiotic metabolizing enzyme genes were over-expressed in Thai CCA patients, whereas growth factor signaling genes were over expressed in Japanese patients (Jinawath et al., 2006). A larger population is deemed necessary to clarify an association of *NQO1* and the prognosis of CCA. It also highlights the need to evaluate the biomarkers under relevant circumstances.

Apart from *NQO1,* the present results revealed that histological type of CCA tissue could be a significant and independent predictor associated with prognosis of the patients; i.e. the patients having papillary type have better prognosis than those having non-papillary type. Our result is in agreement with the previous report in CCA patients of Thailand (Subimerb et al., 2010). Histological type and *NQO1* expression are independent parameters of patients'survival, as the histological type is not correlated with *NQO1* expression level (Table 1). Residual tumor after surgical operation is usually regarded as the predictor of poor survival after surgery. The complete excision of tumor with surgical margin negative (R0) is associated with long-term survival (Guglielmi et al., 2009). Our study is consistent with the concept of patients without R0 excision are at higher risk than those with R0 operation.

In summary, NQO1 acting as xenobiotic metabolizing and antioxidant enzyme was over-expressed in the majority of CCA. Since NQO1 is over-expressed in some other tumors, this enzyme may provide protection to cancer cells. The high expression of *NQO1* was associated with poor prognosis. Histology of tumors of papillary type and complete surgical removal of tumor mass were significantly associated with good prognosis. Further study with larger population is necessary to clarify the inconsistency among the reports.

## Acknowledgements

This work was supported by the Thailand Research Fund, the National Research University Project and the Office of the Higher Education Commission through SHeP-GMS of Khon Kaen University, and a grant-in-aid from the Faculty of Medicine, Khon Kaen University.

We wish to acknowledge the support of the Khon Kaen University Publication Clinic, Research and Technology Transfer Affairs, Khon Kaen University, for their assistance.

## References

Buranrat B, Prawan A, Kukongviriyapan U, Kongpetch S, Kukongviriyapan V (2010). Dicoumarol enhances gemcitabine-induced cytotoxicity in high *NQO1*-expressing cholangiocarcinoma cells. *World J Gastroenterol,* **16**, 2362-70.

Coussens LM, Werb Z (2002). Inflammation and cancer. *Nature,* **420**, 860-7.

Cresteil T, Jaiswal AK (1991). High levels of expression of the NAD(P)H:quinone oxidoreductase (*NQO1*) gene in tumor cells compared to normal cells of the same origin. *Biochem Pharmacol,* **42**, 1021-7.

Danson S, Ward TH, Butler J, Ranson M (2004). DT-diaphorase: a target for new anticancer drugs. *Cancer Treat Rev,* **30**, 437-49.

Dijkstra G, Blokzijl H, Bok L, et al (2004). Opposite effect of oxidative stress on inducible nitric oxide synthase and haem oxygenase-1 expression in intestinal inflammation: anti-inflammatory effect of carbon monoxide. *J Pathol,* **204**, 296-303.

Green A, Uttaravichien T, Bhudhisawasdi V, et al (1991). Cholangiocarcinoma in north east Thailand. A hospital-based study. *Trop Geogr Med,* **43**, 193-8.

Guglielmi A, Ruzzenente A, Campagnaro T, et al (2009). Intrahepatic cholangiocarcinoma: prognostic factors after surgical resection. *World J Surg,* **33**, 1247-54.

IARC (1994). Infection with liver flukes (*Opisthorchis viverrini, Opisthorchis felineus* and *Clonorchis sinensis*). *IARC Monogr Eval Carcinog Risks Hum,* **61**, 121-75.

Jinawath N, Chamgramol Y, Furukawa Y, et al (2006). Comparison of gene expression profiles between *Opisthorchis viverrini* and non-*Opisthorchis viverrini* associated human intrahepatic cholangiocarcinoma. *Hepatology,* **44**, 1025-38.

Kamsa-ard S, Wiangnon S, Suwanrungruang K, et al (2011). Trends in liver cancer incidence between 1985 and 2009, Khon Kaen, Thailand: cholangiocarcinoma. *Asian Pac J Cancer Prev,* **12**, 2209-13.

Kensler TW, Wakabayashi N (2010). Nrf2: friend or foe for chemoprevention? *Carcinogenesis,* **31**, 90-9.

Khan SA, Thomas HC, Davidson BR, Taylor-Robinson SD (2005). Cholangiocarcinoma. *Lancet,* **366**, 1303-14.

Kolesar JM, Pritchard SC, Kerr KM, et al (2002). Evaluation of *NQO1* gene expression and variant allele in human NSCLC tumors and matched normal lung tissue. *Int J Oncol,* **21**, 1119-24.

Logsdon CD, Simeone DM, Binkley C, et al (2003). Molecular profiling of pancreatic adenocarcinoma and chronic pancreatitis identifies multiple genes differentially regulated in pancreatic cancer. *Cancer Res,* **63**, 2649-57.

Ohshima H, Tazawa H, Sylla BS, Sawa T (2005). Prevention of human cancer by modulation of chronic inflammatory processes. *Mutat Res,* **591**, 110-22.

Patel T (2011). Cholangiocarcinoma--controversies and challenges. *Nat Rev Gastroenterol Hepatol,* **8**, 189-200.

Pinlaor S, Hiraku Y, Ma N, et al (2004). Mechanism of NO-mediated oxidative and nitrative DNA damage in hamsters infected with *Opisthorchis viverrini*: a model of inflammation-mediated carcinogenesis. *Nitric Oxide,* **11**,

175-83.

Prawan A, Buranrat B, Kukongviriyapan U, Sripa B, Kukongviriyapan V (2009). Inflammatory cytokines suppress NAD(P)H:quinone oxidoreductase-1 and induce oxidative stress in cholangiocarcinoma cells. *J Cancer Res Clin Oncol,* **135**, 515-22.

Prochaska HJ, Santamaria AB (1988). Direct measurement of NAD(P)H:quinone reductase from cells cultured in microtiter wells: a screening assay for anticarcinogenic enzyme inducers. *Anal Biochem,* **169**, 328-36.

Radjendirane V, Joseph P, Lee YH, et al (1998). Disruption of the DT diaphorase (*NQO1*) gene in mice leads to increased menadione toxicity. *J Biol Chem,* **273**, 7382-9.

Saldivar SJ, Wang Y, Zhao H, et al (2005). An association between a *NQO1* genetic polymorphism and risk of lung cancer. *Mutat Res,* **582**, 71-8.

Siegel D, Gustafson DL, Dehn DL, et al (2004). NAD(P) H:quinone oxidoreductase 1: role as a superoxide scavenger. *Mol Pharmacol,* **65**, 1238-47.

Siegel D, Ross D (2000). Immunodetection of NAD(P) H:quinone oxidoreductase 1 (*NQO1*) in human tissues. *Free Radic Biol Med,* **29**, 246-53.

Sripa B, Pairojkul C (2008). Cholangiocarcinoma: lessons from Thailand. *Curr Opin Gastroenterol,* **24**, 349-56.

Strassburg A, Strassburg CP, Manns MP, Tukey RH (2002). Differential gene expression of NAD(P)H:quinone oxidoreductase and NRH:quinone oxidoreductase in human hepatocellular and biliary tissue. *Mol Pharmacol,* **6**1, 320-5.

Subimerb C, Pinlaor S, Khuntikeo N, et al (2010). Tissue invasive macrophage density is correlated with prognosis in cholangiocarcinoma. *Mol Med Report,* **3**, 597-605.

Surh YJ, Kundu JK, Na HK (2008). Nrf2 as a master redox switch in turning on the cellular signaling involved in the induction of cytoprotective genes by some chemopreventive phytochemicals. *Planta Med,* **74**, 1526-39.

Wakai T, Shirai Y, Sakata J, et al (2011). Prognostic significance of *NQO1* expression in intrahepatic cholangiocarcinoma. *Int J Clin Exp Pathol,* **4**, 363-70.

Yang FY, Guan QK, Cui YH, et al (2012). NAD(P)H quinone oxidoreductase 1 (*NQO1*) genetic C609T polymorphism is associated with the risk of digestive tract cancer: a meta-analysis based on 21 case-control studies. *Eur J Cancer Prev,* **21**, 432-41.

มหาวิทยาลัยขอนแก่น

หนังสือฉบับนี้ให้ไว้ เพื่อแสดงว่า

**โครงการวิจัยเรื่อง:** การศึกษาเปรียบเทียบการแสดงออกและการทำงานของเอนไซม์ต้านอนุมูลอิสระและเอนไซม์กำจัดพิษระหว่างเนื้อเยื่อตัดปรกติและเนื้อเยื่อตับที่เป็นมะเร็งจากผู้ป่วยมะเร็งท่อน้ำดี

(The comparison of expression and activity of antioxidant enzymes and xenobiotic detoxifying enzymes between normal tissues and tumor tissues from cholangiocarcinoma patients)

**ผู้วิจัย:** นางสาวเบญจพร บุราณรัตน์ และคณะ

**หน่วยงานที่สังกัด:** ภาควิชาเภสัชวิทยา คณะแพทยศาสตร์ มหาวิทยาลัยขอนแก่น

ได้ผ่านการรับรองจากคณะกรรมการจริยธรรมการวิจัยในมนุษย์มหาวิทยาลัยขอนแก่น โดยยึดหลักเกณฑ์ตามคำประกาศเฮลซิงกิ (Declaration of Helsinki) และแนวทางการปฏิบัติการวิจัยทางคลินิกที่ดี (ICH GCP)

ให้ไว้ ณ วันที่ 6 สิงหาคม พ.ศ. 2550

(รองศาสตราจารย์จิราภรณ์ ศรีนัครินทร์)

ประธานคณะกรรมการจริยธรรมการวิจัยในมนุษย์มหาวิทยาลัยขอนแก่น

*ลำดับที่* 3.4 06: 8/2550

*เลขที่*: HE500606

คณะกรรมการจริยธรรมการวิจัยในมนุษย์มหาวิทยาลัยขอนแก่น
สำนักงาน: 123 ถนนมิตรภาพ อ.เมือง จ.ขอนแก่น 40002
โทร. (043) 363723, (043) 363749 โทรสาร (043) 363749

Institutional Review Board Number; IRB00001189
Federal Wide Assurance; FWA00003418

Naunyn-Schmiedeberg's Arch Pharmacol (2013) 386:1009–1016
DOI 10.1007/s00210-013-0906-8

ORIGINAL ARTICLE

# Phenethyl isothiocyanate induces apoptosis of cholangiocarcinoma cells through interruption of glutathione and mitochondrial pathway

**Ornanong Tusskorn · Auemduan Prawan · Laddawan Senggunprai · Upa Kukongviriyapan · Veerapol Kukongviriyapan**

Received: 28 April 2013 / Accepted: 26 July 2013 / Published online: 15 August 2013
© Springer-Verlag Berlin Heidelberg 2013

**Abstract** Phenethyl isothiocyanate (PEITC) is a natural isothiocyanate with anticancer activity against many drug-resistant cancer cells. A body of evidence suggests that PEITC enhances oxidative stress leading to cancer cell death. Cholangiocarcinoma (CCA) is an aggressive bile duct cancer with resistance to chemotherapeutic drugs. PEITC rapidly kills KKU-100 CCA cells with concurrent induction of cellular glutathione depletion, superoxide formation, and loss of mitochondrial transmembrane potential. The loss was associated with increased Bax and decreased Bcl-xl proteins followed by the release of cytochrome c and the activation of caspase-9 and -3. Although TEMPOL could prevent superoxide formation, it did not prevent the disruption of glutathione (GSH) redox, mitochondrial dysfunction, and cell death. On the other hand, *N*-acetylcysteine could prevent the events and cell death. It was concluded that disruption of GSH redox but not superoxide formation may be an initial step leading to mitochondrial injury. PEITC could be a promising chemopreventive agent for CCA.

**Keywords** Phenethyl isothiocyanate · Cancer chemoprevention · Cholangiocarcinoma · Mitochondrial dysfunction · Glutathione

O. Tusskorn · A. Prawan · L. Senggunprai · V. Kukongviriyapan (✉)
Department of Pharmacology, Faculty of Medicine, Khon Kaen University, Khon Kaen, Thailand 40002
e-mail: veerapol@kku.ac.th

A. Prawan · L. Senggunprai · V. Kukongviriyapan
Liver Fluke and Cholangiocarcinoma Research Center, Khon Kaen University, Khon Kaen, Thailand

U. Kukongviriyapan
Department of Physiology, Faculty of Medicine, Khon Kaen University, Khon Kaen, Thailand

## Abbreviations

| | |
|---|---|
| BSO | Buthionine sulfoximine |
| TEMPOL | 4-hydroxy-TEMPO |
| CCA | Cholangiocarcinoma |
| PEITC | Phenethyl isothiocyanate |
| GSH | Glutathione |
| GSSG | Glutathione disulfide |
| $\Delta\Psi_m$ | Mitochondrial transmembrane potential |
| NAC | *N*-acetyl-L-cysteine |
| ROS | Reactive oxygen species |
| SRB | Sulforhodamine B |
| JC-1 | 5,5′,6,′-Tetrachloro-1,1′,3,3′-tetraethylbenzimidazolyl-carbocyanine iodide |
| MOMP | Mitochondrial outer membrane permeabilization |

## Introduction

Isothiocyanates (ITCs) are hydrolysis products of a group of naturally occurring thioglucoside and glucosinolate compounds which are found in cruciferous vegetables and others including broccoli, cauliflower, cabbage, brassicas, watercress, and kale (Cheung and Kong 2010). The ITCs rather than their parent compounds, the glucosinolates, are highly active. The ITCs including phenethyl isothiocyanate (PEITC), sulforaphane, and allyl isothiocyanate are very effective antioxidants and potent suppressors of tumor growth (Hayes et al. 2008). The compounds possess dual effects of antioxidant activity and also generation oxidative stress. The antioxidant is demonstrated by the radical scavenging activity and indirectly by induction of the expression of antioxidant and cytoprotective enzymes, whereas

the oxidative stress is generated via several cellular mechanisms (Cheung and Kong 2010). The antitumor activities in vitro and in vivo confer a collective activity so-called cancer chemoprevention (Keum et al. 2003; Khor et al. 2008; Xiao et al. 2010). Several epidemiological studies have suggested that dietary intake of cruciferous vegetables is inversely related to the development of cancer (Chan et al. 2005). PEITC, an isothiocyanate, found abundantly in cruciferous vegetables has been shown effectively inhibit the growth of cancers of prostate, colon, lung, and leukemic cells (Chiao et al. 2004; Cheung et al. 2008; Mi et al. 2011b). Clinical trials of PEITC on the treatment of lung cancer and leukemia are currently undertaken (www.clinicaltrials.gov).

The cancer chemopreventive effects of PEITC are expressed via several cell signaling pathways at multiple levels. The induction of reactive oxygen species (ROS) formation plays a pivotal role in oxidation of cellular redox-sensitive molecules and disruption of the mitochondrial function leading to the death of leukemic and prostate cancer cells (Xiao et al. 2010; Kluza et al. 2011). However, PEITC-mediated apoptosis of HepG2 or multiple myeloma cells was suggested to be independent of ROS formation (Rose et al. 2003; Mi et al. 2011a). It is interesting to note that PEITC mediates apoptotic cell death of various drug-resistant cancer cells including imatinib-, Gleevec-, and fludarabine-resistant leukemic cells and prostate cancer (Trachootham et al. 2008; Mukherjee et al. 2009; Kluza et al. 2011). Moreover, the effects of PEITC on multiple steps of cancer growth make this compound highly versatile and promising candidate for cancer chemoprevention and chemotherapy.

Bile duct cancer or cholangiocarcinoma (CCA) is a highly malignant adenocarcinoma originating from the cholangiocytes (Patel 2011). CCA is a rare type of cancer worldwide; however, CCA is the most common type of liver cancer in some regions in Asia, particularly the Mekong Basin subregion, where the incidence of CCA is highest in the world (Sripa et al. 2012). In the Western countries, the incidence and the mortality rate of intrahepatic CCA are reportedly increasing at an alarming rate (Khan et al. 2005; Patel 2011). The prognosis of CCA patients is very poor because most patients are already in the advanced stage at diagnosis. Chemotherapy and radiotherapy show modest benefit for prolonged overall survival in patients with unresected CCA (Hezel and Zhu 2008). Currently, there is no standard regimen of chemotherapy for CCA (Patel 2011). Despite of the many recent advances in cancer chemotherapy, management of CCA is still an immense challenge, and several strategies in sensitizing resistant CCA cells to respond to chemotherapeutic drugs have been attempted (Buranrat et al. 2010; Kongpetch et al. 2012).

The cancer chemopreventive effect of PEITC in CCA is still unknown. In this study, we examined the inhibitory effect of PEITC on KKU-100, a CCA cell line derived from human tumor tissue with poorly differentiated adenocarcinoma. To elucidate the possible mechanisms of the effects of PEITC on CCA cells, ROS formation, glutathione (GSH) redox stress, and mitochondrial function were evaluated for PEITC-treated CCA cells. The results show that the PEITC-mediated killing of CCA cells was not associated with the generation of superoxide anion. The disruption of GSH redox may be an important step eliciting mitochondrial dysfunction, a common pathway leading to cell death.

## Materials and methods

### Chemicals and reagents

PEITC, 4-hydroxy-TEMPO (TEMPOL), *N*-acetyl-L-cysteine (NAC), dihydroethidium (DHE), sulforhodamine B (SRB), and buthionine sulfoximine (BSO) were obtained from Sigma Chemical Co. (St. Louis, MO, USA). 1-Methyl-2-vinylpyridinium triflate (M2VP) was obtained from Fluka Chemical (Buch, Switzerland). 5,5′,6,′-Tetrachloro-1,1′,3,3′-tetraethylbenzimidazolyl-carbocyanine iodide (JC-1) was obtained from Clayman Chemical (Ann Arbor, MI, USA). Caspase-9 substrate I (Ac-LEHD-AFC), granzyme B substrate II caspase 8 (Z-IETD-AFC), and glutathione monoethyl ester (GSH-MEE) were purchased from Calbiochem (EMD Millipore, Billerica, MA, USA). EnzCheck® Caspase-3 Assay kit#1 was purchased from Molecular Probes (Eugene, OR, USA). Antibodies used for immunoblotting were from Santa Cruz Biotechnology (Sandiego, CA, USA).

### Cell cultures

A human CCA cell line, KKU-100 established in our institute (Sripa et al. 2005), were grown in Ham's F12 medium supplemented with 4 mM L glutamine, 1 mM sodium pyruvate, 12.5 mM *N*-2-hydroxyethylpiperazine-*N*′-2-ethanesulfonic acid (HEPES; pH 7.3), 100 U/mL penicillin, 100 μg/mL streptomycin sulfate, and 10 % fetal calf serum and maintained under 5 % $CO_2$ in air at 37 °C. The cells were subcultured every 2–3 days before cultured cell confluence using 0.25 % trypsin–EDTA, and the medium was changed after overnight incubation.

### Cytotoxicity assay

CCA cells were seeded onto 96-well culture plates at a density of 7,500 cells/well. After an overnight culture, the serum-free medium was replaced with an addition of PEITC, and the cells were cultured for various time intervals. The cytotoxicity was examined by the SRB assay. In brief, cultured cells were fixed with ice-cold trichloroacetic acid and stained with 0.4 % SRB in 1 % acetic acid for 30 min. Excess dye was removed by rinsing several times with 1 % acetic acid, and protein-bound dye was dissolved with 10 mM Tris base solution for determination of

absorbance with a microplate reader with filter wavelength of 570 nm.

To determine if cells have undergone apoptosis, cultured cells were stained with fluorescent dyes as previously described (Buranrat et al. 2010; Suphim et al. 2010). In brief, the cells were washed once with phosphate-buffered saline (PBS) and stained with acridine orange and ethidium bromide (AO/EB) in PBS with the trace amount of hemoglobin. The cells were examined using a Nikon Eclipse TS100 inverted microscope with the excitation and emission filters of 480 and 535 nm, respectively. The number of viable, apoptotic, and necrotic cells which were stained with green fluorescence with intact nuclei, green fluorescence with the appearance of cell shrinkage, nuclear condensation and fragmentation, and bright orange fluorescence, respectively, were enumerated. The apoptotic cells were calculated as the percent apoptotic cells over a total number of cells in the same area.

### Assays for ROS and glutathione

Intracellular ROS generation was measured by cell-permeable fluorescent probe, DHE, staining, which is specific for superoxide anion. Briefly, $5 \times 10^4$ cells were seeded in 96 black well plates and cultured overnight. Then, the medium was removed, and the cells were washed with PBS and were treated with PEITC, 25 μM DHE with or without 2 mM NAC or 0.5 mM TEMPOL in serum-free medium and kept under an atmosphere of 5 % $CO_2$ at 37 °C for 90 min. The fluorescence intensity was read and quantified in a Gemini XPS fluorescent plate reader with excitation and emission wavelength of 518 and 605 nm, respectively.

Glutathione was assayed by the method previously described (Suphim et al. 2010) using M2VP as a glutathione scavenger. In brief, cell lines were trypsinized and washed three times with cold PBS, and cell suspensions were reacted with M2VP (1 mM) for determination of GSSG. Another aliquot of cell suspension was used for the assay of total GSH. The cultured media were collected, centrifuged, and supernatants were saved for total GSH assay.

### Measurement of mitochondrial transmembrane potential

The dissipation of the mitochondrial electrochemical potential gradient is known as an early event in apoptosis. The assay of mitochondrial transmembrane potential ($\Delta\Psi_m$) was performed according to the previously described method (Kongpetch et al. 2012) using the cationic, lipophilic dye, JC-1 staining. The cells were seeded in 96 black well plates at the density of $1 \times 10^4$ cells/well and cultured overnight before treatment with PEITC at varied concentrations for 3 and 24 h. Images were captured by a fluorescence microscope with excitation wavelength of 485 nm and long-pass emission wavelength of 535 nm. JC-1 forms J-aggregates in healthy mitochondrial matrix, which can be visualized as red fluorescence. In depolarized mitochondria, JC-1 effluxes to the cytoplasm and exists as monomers with green fluorescence. The shift of red to green fluorescence is an indicative of depolarization of $\Delta\Psi_m$.

### Western blot analysis

Whole cell lysates were prepared as described previously (Buranrat et al. 2010). The protein was electrophoretically separated on 10 % SDS–polyacrylamide gel and was transferred to polyvinylidene difluoride (PVDF) membranes by semidry blotting. The PVDF membranes were blocked with 5 % (*w*/*v*) skimmed milk powder in PBS and incubated overnight at 4 °C with primary antibodies including rabbit polyclonal IgG against cytochrome c (sc-13560), Bax (sc-493) and AIF (sc-5586), and mouse monoclonal IgG against Bcl-xl (sc-8392) and β-actin (sc-1616). The primary antibody was removed, and the blots were incubated with the respective horseradish peroxidase-conjugated secondary antibodies (goat anti-mouse or anti-rabbit IgG). The blots were incubated with ECL substrate solution. The densities of bands of specific cytochrome c, Bcl-xl, Bax, AIF, and β-actin were visualized and captured by ImageQuant™ 400.

### Measurements of caspase activities

After treatment with PEITC for 3 and 6 h, the cultured cells were trypsinized, washed in PBS, and adjusted to $10^6$ cells for each reaction. Cell pellets were stored frozen at −80 °C for analysis at a later time. Cell pellet was lysed with the cell lysis buffer and incubated on ice for 10 min. After centrifugation to pellet the cellular debris, the supernatant was transferred to individual microplate wells and processed according to the manufacturers' instructions using Ac-LEHD-AFC as caspase-9 substrate, Z-IETD-AFC as caspase-8 substrate, and Z-DEVD-AMC as caspase-3 substrate. The fluorescent signals were read using Gemini XPS fluorescent plate reader with the excitation and emission wavelengths of 400 and 505 nm, respectively, to assess caspase-9 and -8 activities, and 340 and 440 nm, respectively to caspase-3 activity.

### Statistical analysis

All results were presented as the mean±SEM. Comparison between control and treated group performed with student's *t* test or ANOVA with student–Newman–Keuls test where appropriate. The level of significance was set at $p<0.05$.

## Results

### PEITC induced cytotoxicity and depletion of GSH

To examine the cytotoxic effect of PEITC, KKU-100 cells were exposed to various concentrations (0.3, 1, 3, 10, and 30 μM) of PEITC for 24 and 48 h (Fig. 1a). The viability of CCA cells reduced rapidly after exposure to PEITC in a dose–response manner and the percentage of cytotoxicity at 48 h was not significantly different from that at 24 h. The IC50 values were not different between 24 and 48 h of incubation (inset, Fig. 1a). Moreover, PEITC induced apoptosis very rapidly within the first 3 h and in a dose-dependent manner (Fig.1b). In contrast, PEITC induced only few number of necrotic cell death at every time points (data not shown).

As cellular GSH is the major cellular redox buffer, the mechanism of PEITC-induced cytotoxicity was suggested to be associated with disturbance of GSH (Trachootham et al. 2008). GSH in KKU-100 cells was decreased rapidly within the first 3 h and continuously suppressed through 24 h of incubation (Fig. 1c). The efflux of total GSH from the cells into the medium was also determined to observe how oxidative stress was handled by CCA cells. Total GSH levels in the medium were increased with time of incubation and concordant with the decrease of cellular GSH levels (Fig. 1c).

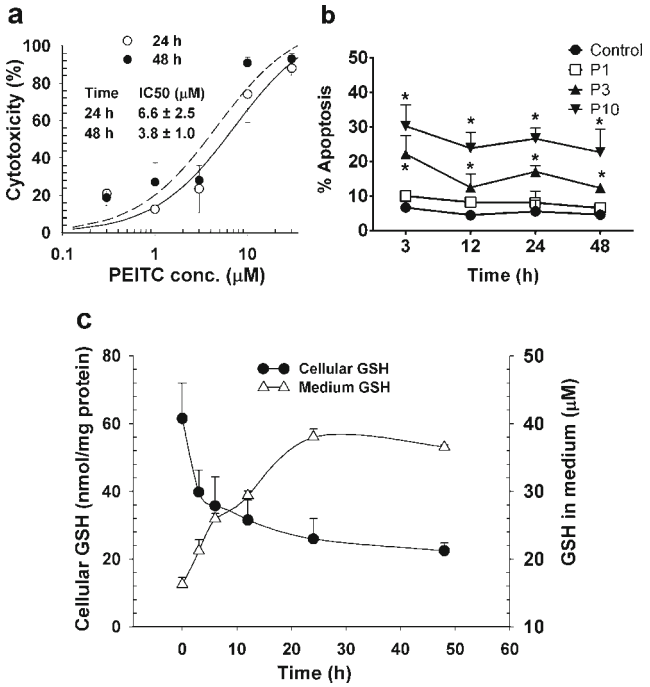


**Fig. 1** PEITC induced cytotoxicity and GSH depletion. KKU-100 cells were incubated with various concentrations (0.3, 1, 3, 10, 30 μM) of PEITC for 24 and 48 h before the cytotoxicity of the cells was determined by SRB assay (**a**) and the number of apoptotic cells was assessed by AO/EB method at 24 h of incubation (**b**). GSH levels were measured in cell pellet as intracellular GSH (**c**) and in the medium as efflux from the cells. Each value represents the mean ± SEM of three experiments. Significantly different from controls, *$p<0.05$

### Effects of antioxidants on PEITC-induced ROS formation and GSH depletion

As PEITC suppressed cell growth and induced cell death in association with oxidative stress manifested as GSH depletion, we evaluated whether the GSH redox stress was causally related with the formation of superoxide anion by using TEMPOL, a superoxide scavenging agent and NAC, a thiol antioxidant and redox reagent. Treatment of 3 or 10 μM of PEITC rapidly induced an increase of fluorescent signals of superoxide formation within 90 min (Fig. 2a). Co-treatment of the cells with PEITC and 0.5 mM TEMPOL or 2 mM NAC almost completely suppressed PEITC-induced ROS formation in the cells. Treatment with NAC or TEMPOL alone did not change the basal ROS levels when compared with controls. GSH in the cells was determined after concurrent treatment of PEITC with TEMPOL or NAC. The PEITC (10 μM) suppressed the cellular GSH after incubation for 3 h. It was only NAC that could completely stabilize GSH levels when cells were treated with PEITC (Fig. 2b). The treatment of TEMPOL could not protect losses of cellular GSH and even induced loss at low concentration of PEITC.

### Protective effect of TEMPOL and NAC on PEITC-induced cytotoxicity

To evaluate whether the cytotoxicity of PEITC was associated with the superoxide and GSH redox stress, KKU-100 cells were concurrently treated with PEITC and TEMPOL or NAC. The presence of TEMPOL could not suppress the cytotoxic effects of PEITC at any incubation periods, i.e., 3, 24, and 48 h. Rather, the concurrent treatment with TEMPOL tended to exacerbate the cytotoxic effect of PEITC at 24–48 h of incubation (Fig. 3, upper panel). On the other hand, NAC significantly prevented the cytotoxicity of PEITC (Fig. 3, upper panel) in association with the protection of cellular GSH (Fig. 2b).

### PEITC-induced depolarization of mitochondrial transmembrane potential

To elucidate the underlying mechanisms of PEITC-induced cytotoxicity in relation to oxidative stress, the effect of PEITC treatment on mitochondrial function was investigated. The mitochondrial transmembrane potential ($\Delta\Psi_m$) was determined by JC-1 assay in cells treated with PEITC for 3 and 24 h. In control cells, mitochondria predominantly exhibited red fluorescence indicating the intact $\Delta\Psi_m$ (Fig. 3a, lower panel). PEITC rapidly depolarized $\Delta\Psi_m$ as revealed by green fluorescence staining. The depolarization of $\Delta\Psi_m$ was apparent within the first 3 h of PEITC treatment and persisted up to 24 h. When cells were concurrently treated with PEITC and antioxidants, NAC but not TEMPOL showed protective effect

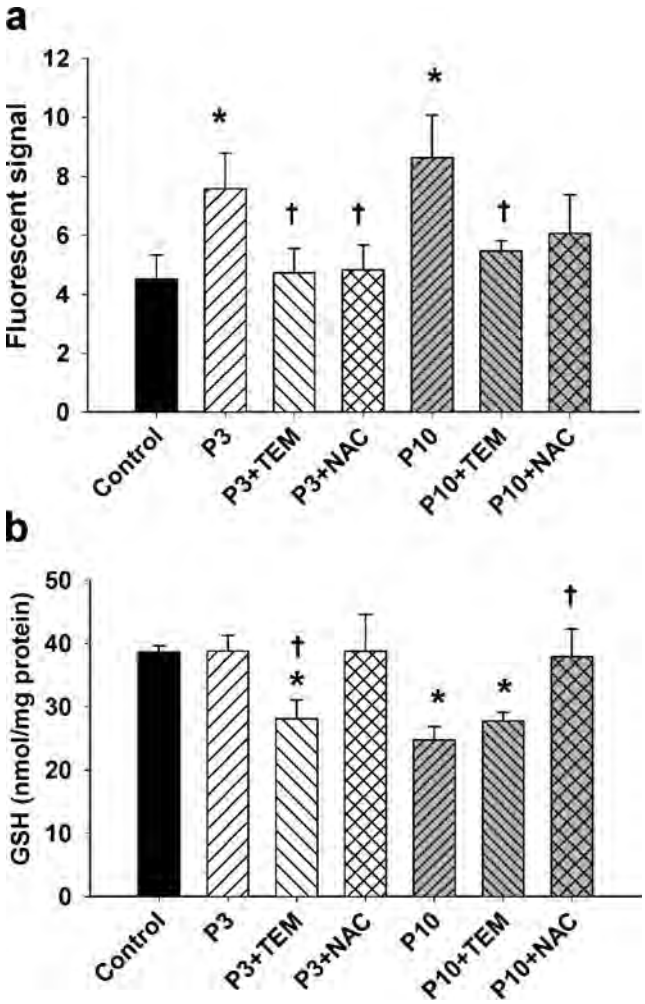


**Fig. 2** Effect of antioxidants on superoxide formation and GSH levels KKU-100 cells were incubated with PEITC at indicated concentrations [3 and 10 μM, shown as P3 and P10] with or without TEMPOL (TEM; 0.5 mM) or *N*-acetyl-L-cysteine (NAC; 2 mM) for 90 min. Superoxide formation was quantified by dihydroethidium fluorescent method (**a**). The effects of TEMPOL and NAC on PEITC-induced reduction of cellular GSH were determined after incubation for 3 h (**b**). Each bar represents the mean ± SEM of three experiments. Significantly different from controls, *$p<0.05$ and significantly different from PEITC treatment, †$p<0.05$

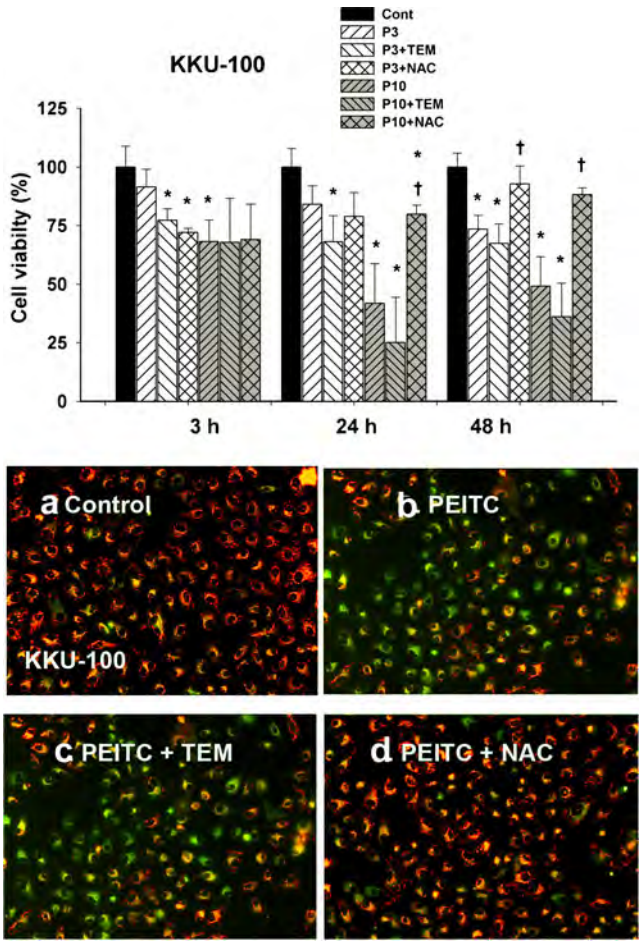


**Fig. 3** Effects of antioxidants on cytotoxicity and changes in mitochondrial transmembrane potential KKU-100 cells were incubated with PEITC at indicated concentrations [P3 and P10 (μM)] with or without TEMPOL (TEM) (0.5 mM) or NAC (2 mM) for 3, 24, and 48 h. The cytotoxicity was assayed by SRB method (bar graph in upper panel). Each *bar* represents the mean ± SEM of three experiments. Significantly different from control, *$p<0.05$ and significantly different from PEITC-treated group, †$p<0.05$. The $\Delta\Psi_m$ was assessed using JC-1 staining method after the cells were treated with PEITC for 24 h. Fluorescent images were captured by a fluorescence microscope. The experiment was done twice with similar results. The representative images from one experiment are shown (images in lower panel)

on the $\Delta\Psi_m$ (Fig. 3c, d). Treatment with TEMPOL or NAC alone did not affect $\Delta\Psi_m$ (data not shown). The changes in $\Delta\Psi_m$ were correlated well with the cytotoxicity of PEITC.

## Effects of GSH replenishment and GSH depletion

Since there was a relationship between GSH depletion and cell death, we further evaluated whether depletion of GSH by PEITC was an important cause of cell death. For this purpose, the cultured cells were treated with BSO (0.5 mM), an inhibitor of GSH synthesis. Treatment with BSO caused a rapid depletion of cellular GSH (data not shown) but did not induce any cytotoxic effect after incubation for 24 h (Fig. 4a). However, BSO strongly potentiated PEITC-induced cytotoxicity. The result indicates that GSH depletion alone is insufficient to cause cell death. To demonstrate if the protective effect of NAC is related to GSH redox regulation, the cells were treated with GSH-MEE, a cell-permeable GSH concurrent with high concentration of PEITC to cause massive cell death. Treatment with GSH-MEE could almost completely prevent cell death (Fig. 4b).

## Effects of PEITC on cytochrome c, Bcl-2 proteins, and caspase activity

The involvement of mitochondria in PEITC-induced cytotoxicity was examined further. After PEITC treatment for 3 and

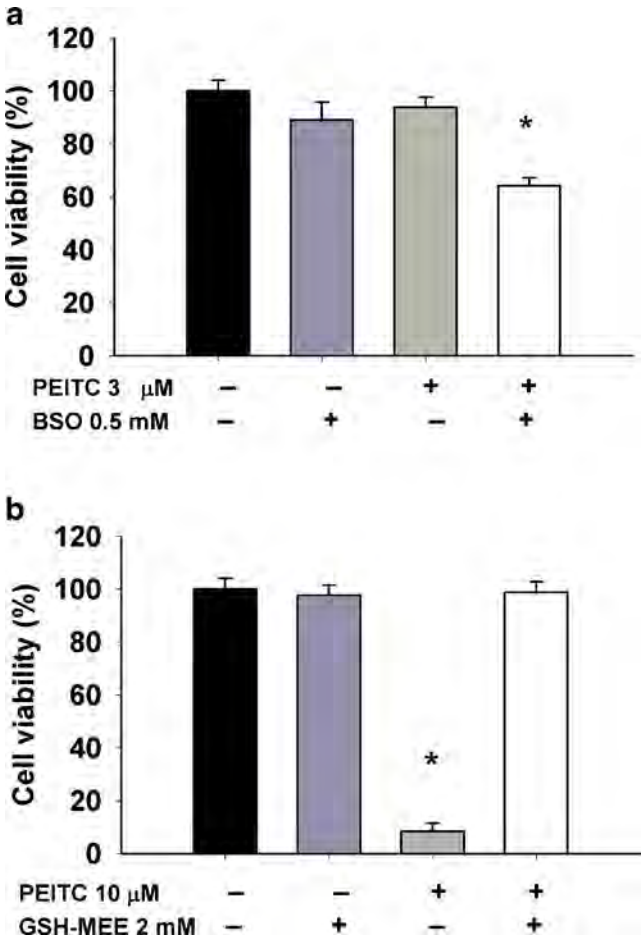


**Fig. 4** Effects of GSH replenishment and GSH depletion on PEITC-induced cytotoxicity. Cultured cells of KKU-100 cells were treated with combination of PEITC and buthionine sulfoximine (BSO) for 24 h (**a**) or PEITC with glutathione monoethyl ester (GSH-MEE) (**b**). Analysis of cell death was performed by fluorescent staining method. Each *bar* represents the mean ± SEM of three experiments. Significantly different from controls, *$p<0.05$

6 h, the remarkable release of cytochrome c was observed (Fig. 5, left panel) along with the increases in AIF and Bax levels, while Bcl-xl expression was suppressed.

Along with the cytochrome c release, the activation of caspases was observed. PEITC treatment activated caspase-9 and -3, but not caspase 8, in KKU-100 cells (Fig. 5, right panel).

## Discussion

PEITC is a natural compound of isothiocyanate group. It has been advocated as a chemopreventive agent for leukemia, pancreatic, prostate, and lung cancers (Mi et al. 2007; Hayes et al. 2008; Trachootham et al. 2008; Xiao et al. 2010). The mechanism of actions of PEITC is multifaceted, including ROS formation, interacting with redox signaling and mitochondrial proteins, leading to oxidative stress and mitochondrial damage (Cheung et al. 2008; Kluza et al. 2011; Mi et al. 2011b). Although CCA is a malignant tumor highly resistant to chemotherapy (Eckel and Schmid 2007; Hezel and Zhu 2008), PEITC potently inhibited CCA cell growth and induced apoptosis. The ROS was generated by PEITC, but it does not seem to play a critical role in the induction of cell death. On the other hand, GSH depletion and oxidative stress seem to increase cellular redox stress and alter expression of Bcl-xl and Bax protein expressions with subsequently initiating an intrinsic mitochondrial cell death pathway leading to the release of cytochorome c, activation of caspase enzymes, and ensuing cell death.

PEITC-induced GSH depletion in association with cell death is consistently observed in various tumor cells (Lee et al. 2002; Hayes et al. 2008; Trachootham et al. 2008). GSH depletion might be caused by the increased ROS formation. Alternatively, GSH depletion by PEITC may be caused by rapid adduction of GSH. The PEITC adducts efflux from the cells via multidrug resistance-associated protein 2 (MRP2), whereas PEITC could reversibly be hydrolyzed and retaken up into the cells to generate a wasting cycle of GSH (Hayes et al. 2008). This was consistent with the observed rapid increase of GSH efflux into the medium. However, GSH depletion itself could not induce cell death, as BSO, which could deplete GSH by large, did not induce cell death. However, depletion of GSH may sensitize the cells to the other concurrent effect of PEITC leading to cell death. This is consistent with our results that NAC and GSH-MEE can almost completely abolish cytotoxicity of PEITC. Because NAC is not an efficient radical scavenging agent (Parasassi et al. 2010), it serves as a precursor for GSH synthesis. More importantly, GSH and NAC have been shown to play critical roles in modulating a number of redox-sensitive enzymes, where these proteins involve in cellular signaling for survival and cell death (Lee et al. 2012). It is probable that PEITC may exert multiple effects probably via redox stress in induction of cell death.

In these studies, TEMPOL, a superoxide scavenger (Krishna et al. 1996), abolished superoxide anion without cytoprotective effect. The role of ROS in PEITC-induced cell death may be cell type-specific because PEITC caused cell death of chronic lymphocytic and chronic myelogenous leukemic cells in a ROS-dependent manner (Trachootham et al. 2008; Xiao et al. 2010). On the other hand, PEITC and its electrophilic adducts may cause oxidative stress by interacting with an active cysteine thiol moiety of vital cellular molecules, particularly redox regulating and signaling regulating proteins such as thioredoxin, 14-3-3 protein, and HSP where those proteins are ultimately involved in the regulation of cell death

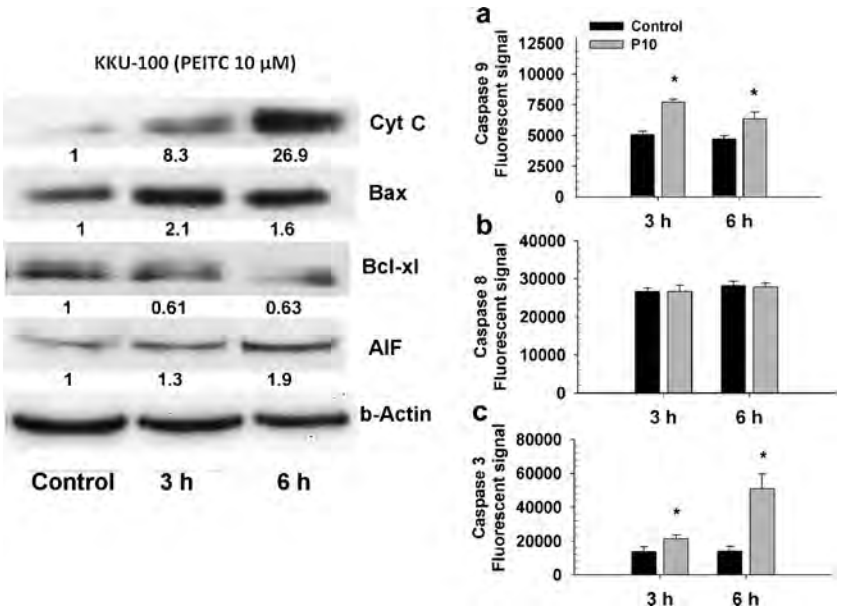


**Fig. 5** PEITC induced the release of cytochrome c and Bcl2 proteins, and activation of caspases KKU-100 cells were treated with PEITC (10 μM) for 3 and 6 h. The cytosol protein was analyzed for cytochrome c, Bax, Bcl-xl, and AIF by Western immunoblotting using β-actin as loading control. Values beneath images indicated the relative protein intensity as a ratio of the treatment to the corresponding vehicle-treated control. Each experiment was done at least twice with similar results, and the representative bands from one experiment are shown (images at left panel). The total cell lysates were assayed for caspase activities using specific fluorogenic substrates (bar graph at right panel), caspase-9 (**a**), caspase-8 (**b**), and caspase-3 (**c**). Each *bar* represents the mean ± SEM of three experiments. Significantly different from corresponding controls, $*p<0.05$

(Mi et al. 2011b). Our results suggested a mechanistic dissociation between superoxide production and cellular redox disturbance, in the regulation of cell death.

Cellular GSH redox plays important roles in the complex process of apoptosis involving with Bcl2 family proteins where Bcl2 proteins modulate the mitochondrial permeability transition (MPT) and the activity of mitochondrial complexes (Xiao et al. 2010). The mode of action of PEITC to CCA cells, which is common to some tumor cells, may be an induction of mitochondrial damage (Xiao et al. 2010; Kluza et al. 2011). The mitochondrial dysfunction is evidenced by the loss of $\Delta\Psi_m$ which is closely related to the cytotoxic effect of PEITC. The MPT pore is a protein pore that is formed in the inner membrane of mitochondria under certain stimuli. The opening of the MPT pores leads to the loss of proton gradient across the inner membrane rendering mitochondria into a depolarized state while increasing the number of MPT pores leads to apoptosis and necrosis (Kim et al. 2003). As NAC prevented the loss of $\Delta\Psi_m$ and protected cell death, this suggests that redox stress may be an early event leading to mitochondrial damage, whereas NAC may alleviate the redox stress.

In the present study, the release of cytochrome c and AIF via mitochondrial outer membrane paralleled with the altered levels of Bax and Bcl-xl. Bax is a multidomain proapoptotic Bcl2 family protein which forms the mitochondrial outer membrane permeabilization (MOMP) upon activation (Chipuk and Green 2008). The release of cytochrome c resulted in the activation of caspase enzymes in KKU-100 cells. AIF, a caspase-independent effector of apoptosis, is located in the inner membrane of mitochondria and released upon induction of apoptosis (Norberg et al. 2010). AIF is activated by oxidative modifications and proteolysis. The release of AIF from mitochondria is regulated by Bcl2 proteins including Bcl-xl and Bax to form MOMP (Norberg et al. 2010). It is noted that, caspase-8 activity remained unchanged, suggesting that the induction of apoptosis of KKU-100 cells by PEITC may be primarily mediated through the intrinsic mitochondrial pathway.

In summary, PEITC induced ROS-independent oxidative stress, GSH depletion, and alteration of Bcl2 proteins leading to mitochondrial dysfunction and cell death. The exact mechanism of alteration of GSH affecting the changes in Bcl2 proteins remains to be elucidated. PEITC is a useful chemopreventive agent where it provides multiple modes of actions to inhibit CCA cells.

**Acknowledgments** This work was supported by the Thailand Research Fund (BRG5480011), the Office of the Higher Education Commission through SHeP-GMS of Khon Kaen University, grant-in-aid from Faculty

of Medicine, Khon Kaen University, and a scholarship from the Office of the Higher Education Commission to Ornanong Tusskorn. Valuable suggestions on the manuscript of Prof. Yukifumi Nawa of Faculty of Medicine, Khon Kaen University are gratefully acknowledged.

**Conflict of interest** The authors declare that there are no conflicts of interest.

## References

Buranrat B, Prawan A, Kukongviriyapan U, Kongpetch S, Kukongviriyapan V (2010) Dicoumarol enhances gemcitabine-induced cytotoxicity in high NQO1-expressing cholangiocarcinoma cells. World J Gastroenterol 16:2362–2370

Chan JM, Wang F, Holly EA (2005) Vegetable and fruit intake and pancreatic cancer in a population-based case–control study in the San Francisco bay area. Cancer Epidemiol Biomarkers Prev 14:2093–2097

Cheung KL, Khor TO, Yu S, Kong AN (2008) PEITC induces G1 cell cycle arrest on HT-29 cells through the activation of p38 MAPK signaling pathway. AAPS J 10:277–281

Cheung KL, Kong AN (2010) Molecular targets of dietary phenethyl isothiocyanate and sulforaphane for cancer chemoprevention. AAPS J 12:87–97

Chiao JW, Wu H, Ramaswamy G, Conaway CC, Chung FL, Wang L, Liu D (2004) Ingestion of an isothiocyanate metabolite from cruciferous vegetables inhibits growth of human prostate cancer cell xenografts by apoptosis and cell cycle arrest. Carcinogenesis 25:1403–1408

Chipuk JE, Green DR (2008) How do BCL-2 proteins induce mitochondrial outer membrane permeabilization? Trends Cell Biol 18:157–164

Eckel F, Schmid RM (2007) Chemotherapy in advanced biliary tract carcinoma: a pooled analysis of clinical trials. Br J Cancer 96:896–902

Hayes JD, Kelleher MO, Eggleston IM (2008) The cancer chemopreventive actions of phytochemicals derived from glucosinolates. Eur J Nutr 47(Suppl 2):73–88

Hezel AF, Zhu AX (2008) Systemic therapy for biliary tract cancers. Oncologist 13:415–423

Keum YS, Owuor ED, Kim BR, Hu R, Kong AN (2003) Involvement of Nrf2 and JNK1 in the activation of antioxidant responsive element (ARE) by chemopreventive agent phenethyl isothiocyanate (PEITC). Pharm Res 20:1351–1356

Khan SA, Thomas HC, Davidson BR, Taylor-Robinson SD (2005) Cholangiocarcinoma. Lancet 366:1303–1314

Khor TO, Cheung WK, Prawan A, Reddy BS, Kong AN (2008) Chemoprevention of familial adenomatous polyposis in Apc(Min/+) mice by phenethyl isothiocyanate (PEITC). Mol Carcinog 47:321–325

Kim JS, He L, Lemasters JJ (2003) Mitochondrial permeability transition: a common pathway to necrosis and apoptosis. Biochem Biophys Res Commun 304:463–470

Kluza J, Jendoubi M, Ballot C, Dammak A, Jonneaux A, Idziorek T, Joha S, Dauphin V, Malet-Martino M, Balayssac S, Maboudou P, Briand G, Formstecher P, Quesnel B, Marchetti P (2011) Exploiting mitochondrial dysfunction for effective elimination of imatinib-resistant leukemic cells. PLoS One 6:e21924

Kongpetch S, Kukongviriyapan V, Prawan A, Senggunprai L, Kukongviriyapan U, Buranrat B (2012) Crucial role of heme oxygenase-1 on the sensitivity of cholangiocarcinoma cells to chemotherapeutic agents. PLoS One 7:e34994

Krishna MC, Russo A, Mitchell JB, Goldstein S, Dafni H, Samuni A (1996) Do nitroxide antioxidants act as scavengers of O2-. or as SOD mimics? J Biol Chem 271:26026–26031

Lee S, Kim WH, Jung HY, Yang MH, Kang GH (2002) Aberrant CpG island methylation of multiple genes in intrahepatic cholangiocarcinoma. Am J Pathol 161:1015–1022

Lee Y, Kim YJ, Choi YJ, Lee JW, Lee S, Chung HW (2012) Enhancement of cisplatin cytotoxicity by benzyl isothiocyanate in HL-60 cells. Food Chem Toxicol 50:2397–2406

Mi L, Gan N, Chung FL (2011a) Isothiocyanates inhibit proteasome activity and proliferation of multiple myeloma cells. Carcinogenesis 32:216–223

Mi L, Hood BL, Stewart NA, Xiao Z, Govind S, Wang X, Conrads TP, Veenstra TD, Chung FL (2011b) Identification of potential protein targets of isothiocyanates by proteomics. Chem Res Toxicol 24:1735–1743

Mi L, Wang X, Govind S, Hood BL, Veenstra TD, Conrads TP, Saha DT, Goldman R, Chung FL (2007) The role of protein binding in induction of apoptosis by phenethyl isothiocyanate and sulforaphane in human non-small lung cancer cells. Cancer Res 67:6409–6416

Mukherjee S, Bhattacharya RK, Roy M (2009) Targeting protein kinase C (PKC) and telomerase by phenethyl isothiocyanate (PEITC) sensitizes PC-3 cells towards chemotherapeutic drug-induced apoptosis. J Environ Pathol Toxicol Oncol 28:269–282

Norberg E, Gogvadze V, Vakifahmetoglu H, Orrenius S, Zhivotovsky B (2010) Oxidative modification sensitizes mitochondrial apoptosis-inducing factor to calpain-mediated processing. Free Radic Biol Med 48:791–797

Parasassi T, Brunelli R, Costa G, De Spirito M, Krasnowska E, Lundeberg T, Pittaluga E, Ursini F (2010) Thiol redox transitions in cell signaling: a lesson from *N*-acetylcysteine. ScientificWorldJournal 10:1192–1202

Patel T (2011) Cholangiocarcinoma—controversies and challenges. Nat Rev Gastroenterol Hepatol 8:189–200

Rose P, Whiteman M, Huang SH, Halliwell B, Ong CN (2003) beta-Phenylethyl isothiocyanate-mediated apoptosis in hepatoma HepG2 cells. Cell Mol Life Sci 60:1489–1503

Sripa B, Brindley PJ, Mulvenna J, Laha T, Smout MJ, Mairiang E, Bethony JM, Loukas A (2012) The tumorigenic liver fluke Opisthorchis viverrini—multiple pathways to cancer. Trends Parasitol 28:395–407

Sripa B, Leungwattanawanit S, Nitta T, Wongkham C, Bhudhisawasdi V, Puapairoj A, Sripa C, Miwa M (2005) Establishment and characterization of an opisthorchiasis-associated cholangiocarcinoma cell line (KKU-100). World J Gastroenterol 11:3392–3397

Suphim B, Prawan A, Kukongviriyapan U, Kongpetch S, Buranrat B, Kukongviriyapan V (2010) Redox modulation and human bile duct cancer inhibition by curcumin. Food Chem Toxicol 48:2265–2272

Trachootham D, Zhang H, Zhang W, Feng L, Du M, Zhou Y, Chen Z, Pelicano H, Plunkett W, Wierda WG, Keating MJ, Huang P (2008) Effective elimination of fludarabine-resistant CLL cells by PEITC through a redox-mediated mechanism. Blood 112:1912–1922

Xiao D, Powolny AA, Moura MB, Kelley EE, Bommareddy A, Kim SH, Hahm ER, Normolle D, Van Houten B, Singh SV (2010) Phenethyl isothiocyanate inhibits oxidative phosphorylation to trigger reactive oxygen species-mediated death of human prostate cancer cells. J Biol Chem 285:26558–26569

Naunyn-Schmiedeberg's Arch Pharmacol (2013) 386:1017
DOI 10.1007/s00210-013-0914-8

ERRATUM

# Erratum to: Phenethyl isothiocyanate induces apoptosis of cholangiocarcinoma cells through interruption of glutathione and mitochondrial pathway

**Ornanong Tusskorn · Auemduan Prawan · Laddawan Senggunprai · Upa Kukongviriyapan · Veerapol Kukongviriyapan**

Published online: 12 September 2013
© Springer-Verlag Berlin Heidelberg 2013

**Erratum to: Naunyn-Schmiedeberg's Arch Pharmacol DOI 10.1007/s00210-013-0906-8**

The Figure 3 entitled "Effects of antioxidants on cytotoxicity and changes in mitochondrial transmembrane potential" in the original publication has some mistake. The inset C was mistaken, as it was the same picture as inset b.

The corrected figure is as shown below:

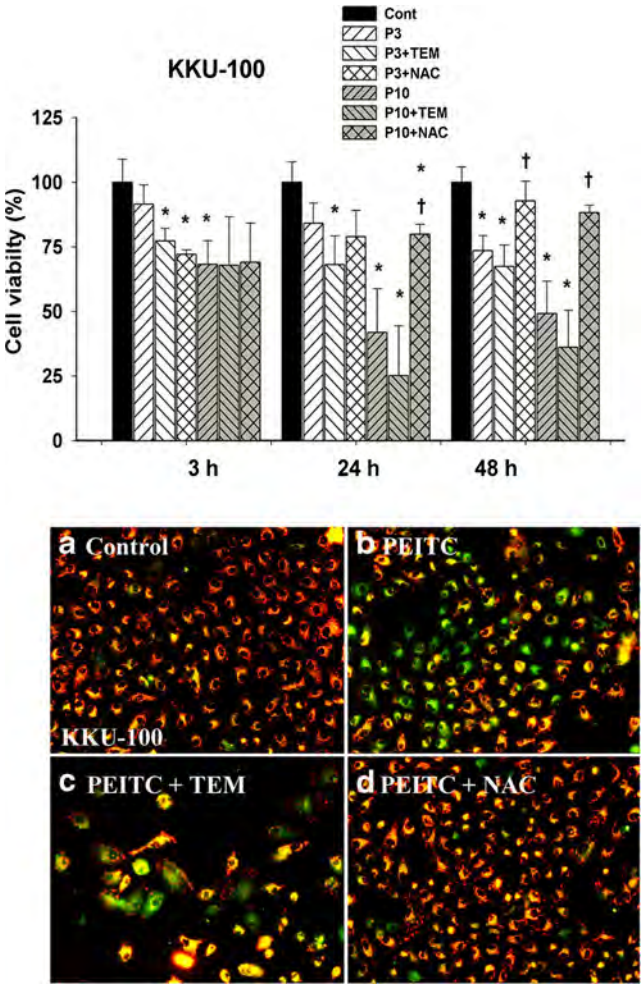


The online version of the original article can be found at: http://dx.doi.org/10.1007/s00210-013-0906-8.

O. Tusskorn · A. Prawan · L. Senggunprai · V. Kukongviriyapan (✉)
Department of Pharmacology, Faculty of Medicine, Khon Kaen University, Khon Kaen, Thailand 40002
e-mail: veerapol@kku.ac.th

A. Prawan · L. Senggunprai · V. Kukongviriyapan
Liver Fluke and Cholangiocarcinoma Research Center, Khon Kaen University, Khon Kaen, Thailand

U. Kukongviriyapan
Department of Physiology, Faculty of Medicine, Khon Kaen University, Khon Kaen, Thailand

BMC Cancer

RESEARCH ARTICLE Open Access

# Phenethyl isothiocyanate induces calcium mobilization and mitochondrial cell death pathway in cholangiocarcinoma KKU-M214 cells

Ornanong Tusskorn[1], Laddawan Senggunprai[1,2], Auemduan Prawan[1,2], Upa Kukongviriyapan[3] and Veerapol Kukongviriyapan[1,2*]

## Abstract

**Background:** Phenethyl isothiocyanate (PEITC) is a cancer chemopreventive agent from cruciferous vegetables. Cholangiocarcinoma (CCA) is a chemo-resistant cancer with very poor prognosis. We evaluated the effects of PEITC on induction of apoptotic cell death in relation to cellular glutathione (GSH) and mitochondrial function of a CCA cell line, KKU-M214.

**Methods:** Cytotoxic effects of PEITC on a CCA cell line, KKU-M214, and a reference cell line, Chang cells were evaluated. To delineate mechanisms of cell death, the following parameters were measured; GSH and superoxide levels as the oxidative status parameters, apoptosis related proteins levels using Western blotting. Cellular free calcium level and mitochondrial transmembrane potential were also measured.

**Results:** PEITC induced apoptotic cell death of both KKU-M214 and Chang cells. After PEITC treatment, both cells showed decrease of Bcl-xl and increase of Bax levels. While KKU-M214 cells released AIF, Chang cells released cytochrome c, with subsequent activation of caspase 3 and 9, upon PEITC treatment. PEITC induced superoxide formation in both cells, although it seemed not play a role in cell death. PEITC caused GSH redox stress in different ways in two cell types, because *N*-acetylcysteine (NAC) prevented redox stress in Chang but not in KKU-M214 cells. The loss of mitochondrial transmembrane potential was induced by PEITC concurrent with GSH stress, but was not a primary cause of cell death. The rapid increase of free calcium level in cytosol was associated with cell death in both cell lines. These events were prevented by NAC in Chang cells, but not in KKU-M214 cells.

**Conclusion:** PEITC induced cell death KKU-M214 cells and Chang cells via increase of cellular calcium mobilization and activation of mitochondrial cell death pathway. The effects of PEITC on the redox stress was mediated via different ways in CCA and Chang cells because NAC could prevent redox stress in Chang cells, but not in KKU-M214 cells. The multiple effects of PEITC may be useful for the development of novel chemotherapy for CCA.

**Keywords:** Phenethyl isothiocyanate, Anticancer, Cholangiocarcinoma, Mitochondrial transmembrane potential, GSH redox, Intracellular calcium

* Correspondence: veerapol@kku.ac.th
[1]Department of Pharmacology, Faculty of Medicine, Khon Kaen University, Mitraparb Road, Khon Kaen 40002, Thailand
[2]Liver Fluke and Cholangiocarcinoma Research Center, Khon Kaen University, Khon Kaen 40002, Thailand
Full list of author information is available at the end of the article

BioMed Central

© 2013 Tusskorn et al.; licensee BioMed Central Ltd. This is an open access article distributed under the terms of the Creative Commons Attribution License (http://creativecommons.org/licenses/by/2.0), which permits unrestricted use, distribution, and reproduction in any medium, provided the original work is properly cited.

## Background

Cholangiocarcinoma (CCA) is a malignancy originating from the bile ducts, usually adenocarcinomatous, and is the second common primary liver cancer [1]. CCA is a rare cancer worldwide, but the most common form of liver cancer in Mekong subregion countries, including northeastern Thailand, Cambodia, Vietnam and Laos [2]. In the Western countries, the incidence and the mortality rate of intrahepatic CCA have risen steeply and steadily over the last decades [3]. In spite of tremendous efforts to improve the treatment, CCA is still notoriously difficult in diagnosis and treatment [3]. Most of CCA patients are already in the advanced stage at diagnosis, and the radical surgery is not feasible. Chemotherapy and radiotherapy could not improve the survival of patients with unresectable CCA [3]. Despite of recent advances in chemotherapy for many cancers, management of CCA with chemotherapeutic drugs and biologic agents has so far been unsatisfied. The development of appropriate new chemotherapeutic drugs and new approaches for the treatment of chemo-resistant cancer like CCA should be of the high priority.

Isothiocyanates (ITCs) are the hydrolysis products of a group of naturally occurring thioglucoside and glucosinolate compounds found in cruciferous vegetables [4]. Among ITCs, phenethyl isothiocyanate (PEITC), sulforaphane and benzyl isothiocyanate are known to have potent biological activities. Recent epidemiological studies showed that intake of ITCs reduced the risk of certain cancers, such as pancreatic and lung cancers [5,6]. PEITC can suppress tumor cells growth, and induce apoptosis and cell cycle arrest [7]. Dietary intake of PEITC strongly inhibited tumorigenesis in various animal models such as a prostate cancer xenografted model [8], colon and lung tumors in transgenic mice models [9,10]. The effects of PEITC on tumor cells are multifaceted including induction of reactive oxygen species (ROS) formation, depolarization of mitochondrial transmembrane potential ($\Delta\Psi_m$) [11,12], activation of c-Jun N-terminal kinase (JNK) and p38 kinase-mediated apoptotic pathway [7,13], and induction of hyper-expression of death receptor-5 mediated caspase 8 activation [14]. PEITC also can depress pro-survival signaling pathways of NF-κB and PI3K/Akt [15], as PEITC inhibits IKK, IκB and Akt phosphorylation leading to inhibit cell proliferation and apoptosis.

The selective cytotoxic effects of ITCs on various cell types have less frequently been reported. PEITC, benzyl ITC and sulforaphane showed the same ranges of $IC_{50}$ values to MCF-7 breast cancer cells and MCF-12A, the non-cancer mammary epithelial cells, and also to HK-2 kidney cells [16]. The selective toxicity of anticancer agents on the major organs may be the primary concern in cancer chemotherapy. Although some functional distinction between cancer and normal cells such as oxidative status have been suggested [17,18], it is yet to be translated into an effective strategy to eliminate cancer cells while spare normal cells.

The effects of PEITC on multiple steps of cancer growth make this compound highly versatile and promising candidate in cancer chemoprevention and chemotherapy. However, the exact mechanisms of its chemopreventive effects are not fully understood. For the better understanding of the anticancer mechanisms of PEITC, we evaluated the effects of PEITC on a bile duct cancer cell line, KKU-M214 in relation to GSH redox stress and mitochondrial function. In this study, HeLa [Chang liver] cells were used as the reference because our previous study showed that oxidative stress caused the suppression of glutathione (GSH) redox in this cell line [19].

## Methods

### Cell cultures

Human CCA cell line, KKU-M214 established in our institute and human HeLa [Chang liver] cells were both kindly provided by Prof. Banchob Sripa, Department of Pathology, Faculty of Medicine, Khon Kaen University. Cells were grown in Ham's F12 medium supplemented with 12.5 mM N-2-hydroxyethylpiperazine-N'-2-ethanesulfonic acid (HEPES; pH 7.3), 100 U/mL penicillin, 100 μg/mL streptomycin sulfate and 10% fetal calf serum and maintained under 5% $CO_2$ in air at 37°C as described previously [20]. The cells were subcultured every 2–3 days before confluence of the cells using 0.25% trypsin–EDTA, and the medium was changed after an overnight incubation.

### Cytotoxicity assay

KKU-M214 and Chang liver cells were seeded onto 96-well culture plates at a density of 7,500 cells/well. After an overnight culture, the serum-free medium was replaced with the media containing PEITC, and the cells were cultured for various time intervals. The cytotoxicity was examined by the sulphorhodamine B (SRB) assay. In brief, cultured cells were washed once with phosphate-buffered saline (PBS), fixed with 100 μl of ice-cold trichloroacetic acid for 1 h, and stained with 50 μl of 0.4% SRB in 1% acetic acid for 30 min. The cells were then rinsed several times with 1% acetic acid, and protein-bound dye was dissolved with 200 μl of 10 mM Tris base solution. The absorbance was determined using a microplate reader with the filter wavelength of 540 nm.

To determine cells undergone apoptosis, cultured cells were stained with fluorescent dyes as previously described with modifications [20,21]. In brief, the medium was removed after PEITC treatment and the cells were stained with acridine orange and ethidium bromide (AO/EB) in PBS. The cells were examined using a Nikon Eclipse TS100 inverted microscope with the excitation

and long-pass emission filters of 480 nm and 535 nm, respectively. The fluorescent images were taken at 2 predetermined areas in each well with triplicate wells per concentration using a Nikon Coolpix digital camera. The number of viable, apoptotic, and necrotic cells, which were stained with green fluorescence with intact nuclei, green fluorescence with the appearance of cell shrinkage, nuclear condensation and fragmentation, and bright orange fluorescence, respectively, were enumerated. The apoptotic cells were calculated as the percent apoptotic cells over a total number of cells in the same area.

### Measurement of ROS

Intracellular ROS generation was measured using a cell-permeable fluorescent probe, dihydroethidium (DHE). Briefly, $5 \times 10^4$ cells were seeded in 96 black well plates and cultured overnight. Then, the medium was removed and the cells were washed with phosphate buffered saline (PBS). They were then treated with PEITC and 25 μM DHE with or without 2 mM *N*-acetyl-L-cysteine (NAC) or 0.5 mM 4-hydroxy-TEMPO (TEMPOL), in serum-free medium and kept in 5% $CO_2$ atmosphere at 37°C for 90 min. The fluorescence intensity was read and quantified in a Gemini XPS fluorescent plate reader with the excitation and emission wavelength of 518 nm and 605 nm, respectively.

### Glutathione assay

Total glutathione was measured essentially according to Tietze's method [22]. Glutathione disulfide (GSSG) was assayed by the method previously described [21] using 1-methyl-2 vinyl-pyridinium trifate (M2VP) as a glutathione scavenger. Cultured cells were trypsinized and washed three times with cold PBS. Cell suspensions were reacted with M2VP (1 mM) to determine GSSG. Aliquots of untreated cell suspensions were used for the assay of total GSH. Protein concentration was assayed using the Bradford's dye binding method.

### Calcium mobilization assay

Intracellular calcium level was measured using an assay kit (FluoForte® Calcium Assay, Enzo Life Sciences, PA, USA). In brief, KKU-M214 and Chang cells were grown on 96 well plates at the density of 10,000 cells/well and treated with 3 and 10 μM PEITC with/without 2 mM of NAC for 1 h. Then, the media were removed and FluoForte® dye-loading solution was added according to the manufacturer's instruction. The plate was incubated at 37°C for 30 min and the fluorescent staining was analyzed under a fluorescent microscope with the excitation and emission wavelengths of 485 nm and 535 nm, respectively. Images of the cultured cells were captured and the integrated optical density (IOD) of each image was analyzed by using the Image-Pro Plus (Media Cybernetics) software.

### Measurement of mitochondrial transmembrane potential

The dissipation of the mitochondrial electrochemical potential gradient is known as an early event leading to apoptosis. To measure the change in mitochondrial transmembrane potential ($\Delta\Psi_m$), cells were seeded in 96 black well plates at the density of 10,000 cells/well and cultured overnight before treatment with various concentrations of PEITC for 3 and 24 h. The assay was performed according to the method described previously [23] using the cationic, lipophilic dye, 5,5′,6,′-tetrachloro-1,1′,3,3′tetraethylbenzimidazolyl carbocyanine iodide (JC-1) (Clayman Chemical) staining with some modifications. The cultured plate was centrifuged at 1,000 rpm for 5 min at room temperature and the cultured medium was removed, loaded with JC-1 dye for 20 min, washed by centrifugation, incubated in the assay buffer and $\Delta\Psi_m$ was analyzed under a fluorescent microscope with the excitation wavelength of 485 nm and emission wavelength of 535 nm. JC-1 forms J-aggregates in healthy mitochondrial matrix, which can be visualized as red fluorescence. In depolarized mitochondria, JC-1 effluxes to the cytoplasm and exists as monomers with green fluorescence. The shift of red to green fluorescence is an indicative of the depolarization of $\Delta\Psi_m$.

### Western blot analysis

Whole cell lysates were prepared as described previously [21]. PEITC-treated and control cells were washed with PBS, collected, and lysed with cell lysis buffer at 4°C with vigorous shaking. After centrifugation at 12,000 g for 30 min, the supernatant was collected and stored at −80°C until use. The protein samples (30 μg protein/sample) were electrophoretically separated on 10% SDS–polyacrylamide gel (SDS-PAGE). The proteins were transferred to polyvinylidene difluoride (PVDF) membranes by semi-dry blotting at 10 V for 40 min. The PVDF membranes were blocked for 2 h at 4°C with 5% (w/v) skimmed milk powder in PBS containing 0.1% Tween-20. The PVDF membrane was incubated overnight at 4°C with primary antibodies including rabbit polyclonal IgG against cytochrome c (sc-13560, Santa Cruz BioTechnology, 1:1000 dilution), mouse monoclonal IgG against Bcl-xl (sc-8392, 1:500 dilution), rabbit polyclonal IgG against Bax (sc-493,1:1000 dilution), rabbit polyclonal IgG against AIF (sc-5586, 1:500 dilution), rabbit polyclonal IgG against p53 (sc-6243, 1:500 dilution), goat polyclonal IgG against β-actin (sc-1616 HRP, 1:2500 dilution), in PBS containing 0.1% Tween-20. The primary antibody was removed and the membranes were extensively washed with PBS/Tween-20. The membranes were then incubated for 2 h at 4°C with 1:5,000 dilution of respective horseradish peroxidase-conjugated secondary antibodies (goat anti-mouse or anti-rabbit IgG). After removal of the secondary antibody and PBS buffer washings, the blotted membranes were

incubated with ECL substrate solution (ECL™ Prime Western Blotting Detection Reagent). The densities of the specific cytochrome c, Bcl-xl, Bax, AIF, p53 and β-actin bands were visualized and captured using ImageQuant™ 400 (GE Healthcare).

### Measurements of caspase activities

#### *Caspase 8 and 9*

After treatment with PEITC for 3 and 6 h, the cultured cells were trypsinized, and adjusted to $10^6$ cells for each reaction. Cell pellet was lysed with cell lysis buffer on ice for 10 min, centrifuged, and then 50 μl of the supernatant was transferred to individual black microplate wells. The sample in each well was mixed with 50 μl of 2x reaction buffer (containing 10% glycerol; 0.5 mM EDTA; 20 mM HEPES, pH 7.0; DTT 10 mM) and fluorogenic Ac-LEHD-AFC, a caspase 9 substrate (50 μM) or Z-IETD-AFC (EMD Millipore), a caspase 8 substrate (50 μM). Reaction mixtures were incubated for 8 h at 37°C in dark and fluorescent signals were read using the Gemini XPS fluorescent plate reader with the excitation and emission wavelengths of 400 and 505 nm, respectively.

#### *Caspase 3*

Cell lysates were prepared as above and mixed with the reaction buffer (containing 0.2% CHAPS; 4 mM EDTA; 20 mM PIPES, pH 7.4; DTT 10 mM and 0.2 mM Z-DEVD-AMC), EnzCheck® Caspase-3 Assay kit#1 (Molecular Probe). Reaction mixtures were incubated for 1 h at 30°C in dark and fluorescent signals were read using the Gemini XPS fluorescent plate reader with the excitation and emission wavelengths of 342 and 441 nm, respectively.

### Statistical analysis

All the results were presented as the mean ± SEM. Statistical comparison between control and treated group was performed using Student's t-test or One-way ANOVA with Student-Newmann-Keuls post-hoc test, where appropriate. The level of significance was set at $p < 0.05$.

## Results

### Cytotoxic effects of PEITC on CCA and Chang cells

KKU-M214 and Chang cells were exposed to PEITC at the indicated concentrations and the cytotoxicity of PEITC was assessed at 24 and 48 h. Viability of both cell lines was reduced rapidly after exposure to PEITC and the percent cytotoxicity remained similar level after 24 and 48 h incubation (Figure 1). The $IC_{50}$ values were not different between 24 and 48 h of incubation (2.99 ± 0.87 and 3.25 ± 0.19 μM), respectively, for KKU-M214 (Figure 1A), and (3.46 ± 0.20 and 3.39 ± 0.75 μM) for Chang cells (Figure 1B). KKU-M214 was apparently more sensitive to PEITC than Chang cells, especially at 24 h of incubation.

### PEITC-induced apoptosis in relation to apoptosis-associated proteins expression

Induction of apoptotic cell death by PEITC was examined for KKU-M214 and Chang cells. PEITC induced apoptosis of both cell lines very rapidly within 3 h in a dose dependent manner (Figure 2A & B). In contrast, PEITC did not induce necrotic cell death at any time points examined (data not shown). The induction of apoptotic cell death was associated with changes in apoptotic proteins, *i.e.*, decrease of Bcl-xl and increase of Bax protein expression within 3 h. PEITC induced cytochrome c release in Chang cells but not in KKU-M214 cells. Conversely, AIF was markedly increased in KKU-M214 cells but not in Chang cells. Bcl-2 protein expression is known to be regulated partly by p53, but, in this study, no significant changes in p53 protein expression were observed at 3 h (Figure 2C) in spite of significant changes in Bcl-xl, Bax and other apoptogenic proteins in both cells.

### PEITC-induced cell death via caspase-dependent and -independent pathways

As the increase of AIF and cytochrome c levels are known to be involved in the intrinsic death pathway, their downstream caspase activities in mitochondrial pathway were evaluated along with caspase-8 extrinsic pathways. The effects of PEITC on caspase 3, 8 and 9 activities in both cell lines were measured at 3 and 6 h after treatment. Caspase-8 activity was unaltered in both cell lines (Figure 3A & B). While caspase-3 and −9 activities in KKU-M214 cells were unchanged after PEITC treatment, they were significantly increased in PEITC-treated Chang cells (Figure 3C-F).

### PEITC-induced glutathione depletion

Previous reports [11,12] suggested that cytotoxicity of PEITC is related to oxidative stress. As GSH is a major cellular antioxidant, we investigated the effect of PEITC on cellular GSH levels. After exposure to PEITC, both KKU-M214 and Chang cells rapidly lost cellular GSH in a dose-dependent manner as early as 3 h of incubation (Figure 4A & C). In KKU-M214 cells, GSH levels returned to, or rose up even higher than, the control level at 24 h. GSH /GSSG ratio in KKU-M214 cells was initially reduced and then returned to the control level by 24 h (Figure 4B). After treatment with 10 μM PEITC, only very few KKU-M214 cells were left alive at 24 h, then it was not possible to determine the levels of GSH. In contrast to the rapid recovery of KKU-M214 cells, PEITC-mediated depletion of GSH levels and depressed

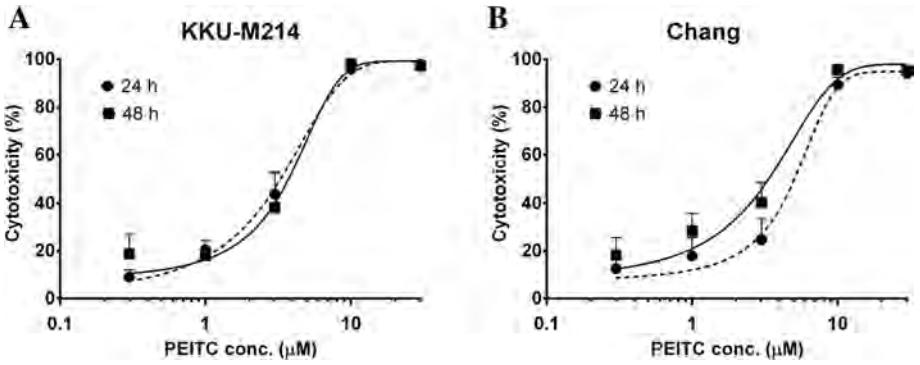


**Figure 1 Cytotoxic effects of PEITC on KKU-M214 and Chang cells.** Cells were incubated with various concentrations from 0.3 to 30 μM PEITC for 24 and 48 h. The cytotoxicity of PEITC in KKU-M214 **(A)** and Chang cells **(B)** was examined by SRB assay. Each value represents the mean ± SEM of three experiments.

GSH redox ratios in Chang cells persisted even at 24 h of incubation (Figure 4C & D).

### Effects of antioxidants on PEITC-induced oxidative stress

Since the results given above, PEITC treatment induced GSH depletion in both cell lines, we examined whether this depletion was associated with the formation of reactive oxygen species (ROS). We examined also the role of antioxidants on GSH depletion and ROS formation. For this purpose, we used TEMPOL, a ROS scavenging agent, and NAC, a thiol modifier. As shown in Figure 5A and B, the basal level of superoxide in KKU-M214 cells was approximately 2-fold higher than that in Chang cells.

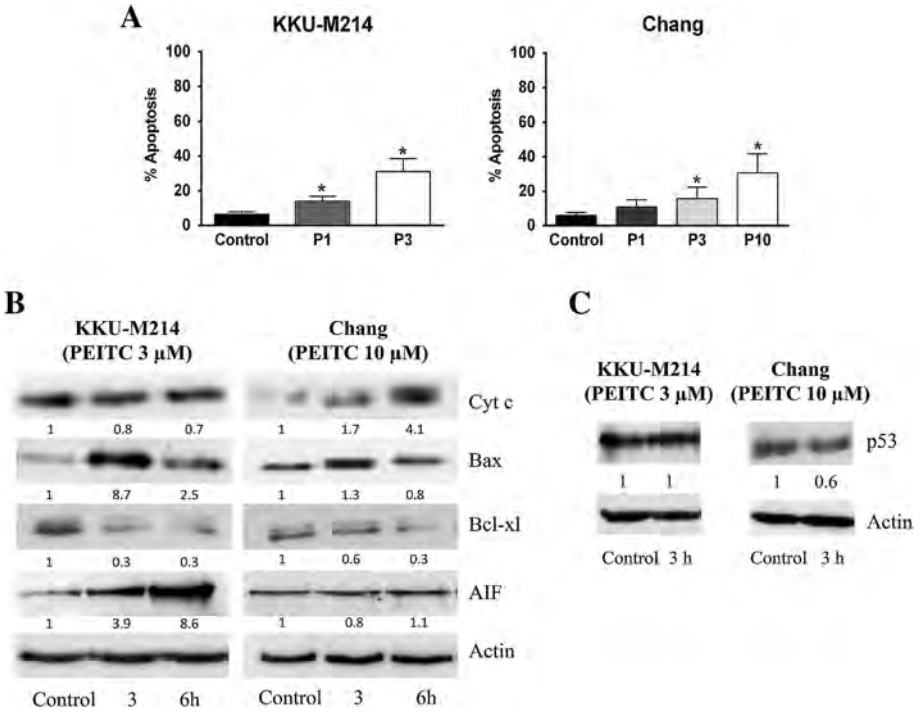


**Figure 2 PEITC-induced apoptosis and release of proapoptogenic proteins.** KKU-M214 and Chang cells were treated with PEITC 1, 3 or 10 μM (P1, P3 or P10, respectively) for 3 or 6 h. The number of apoptotic cells was assessed by AO/EB method at 3 h of incubation **(A)**. Each bar represents the mean ± SEM of three experiments. Significantly different from control, $*p < 0.05$. Immunoblot analysis was performed using 30 μg of protein and cytochrome c, Bax, Bcl-xl, AIF and p53 were detected by specific antibodies. β-actin was used as loading control **(B & C)**. Value indicates the relative protein intensity as a ratio to the corresponding vehicle-treated control. Each experiment was done at least twice with similar results, and the representative bands from one experiment are shown.

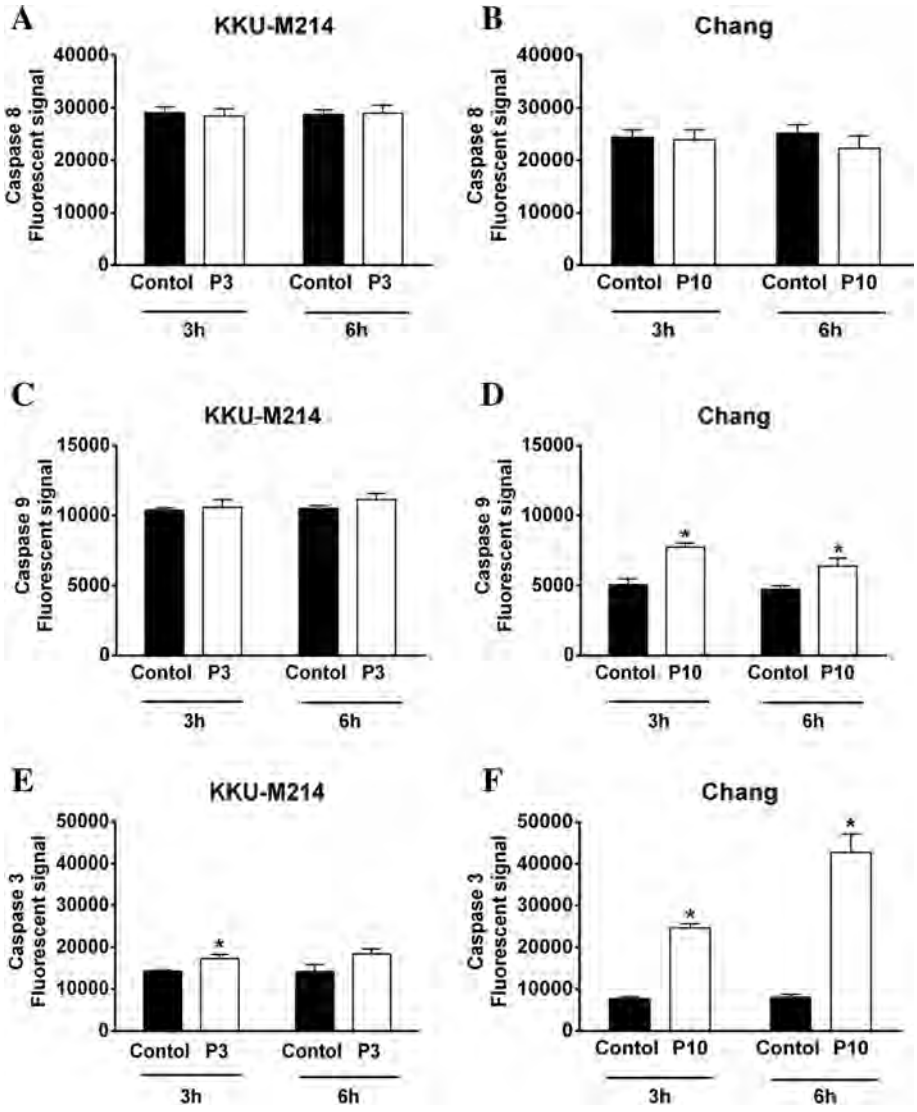


**Figure 3 Activation of caspases by PEITC.** Cells were treated with 3 or 10 μM of PEITC (P3, P10), for 3 and 6 h. Caspase-3 **(E & F)**, caspase-8 **(A & B)** and caspase-9 **(C & D)** activities were determined by incubating the cell lysates with fluorogenic substrates specific for each caspase enzyme. Each bar represents the mean ± SEM of three experiments. Significantly different from corresponding controls, *$p < 0.05$.

Treatment of the cells with 3 and 10 μM PEITC caused significant increase of ROS in Chang cells, but only slight increase in KKU-M214 cells. Co-treatment of the cells with PEITC and 0.5 mM TEMPOL or 2 mM NAC completely normalized the ROS levels in both cell lines (Figure 5A & B). Moreover, treatment of NAC also largely prevented PEITC-induced losses of GSH in both cell lines at 3 h (Figure 5C & D) and this protective effect persisted up to 48 h of incubation (data not shown). However, TEMPOL, which could completely neutralize ROS, could only partially prevented GSH depletion in both cell lines.

### PEITC-induced intracellular calcium mobilization

Oxidative stress is known to trigger the release of $Ca^{2+}$ from some intracellular $Ca^{2+}$ storages, particularly from the endoplasmic reticulum, resulting in the increase of cytosolic and mitochondrial $Ca^{2+}$, which initiates cell death [24]. We examined the effects of PEITC on intracellular $Ca^{2+}$ mobilization in KKU-M214 and Chang cells. As shown in Figures 6A & B, PEITC induced rapid $Ca^{2+}$ mobilization into cytosol within the first 1 hour of incubation, which was visualized by $Ca^{2+}$ fluorescent probe in KKU-M214 and Chang cells. NAC, a thiol modifier, could not inhibit $Ca^{2+}$ flux into cytosol in KKU-M214 cells (Figure 6C), but could completely

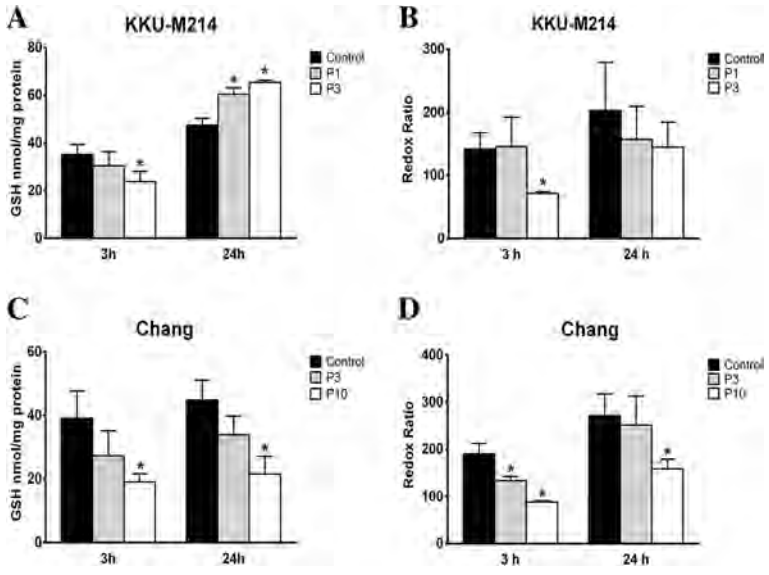


**Figure 4 Effect of PEITC on intracellular GSH and redox ratio.** KKU-M214 **(A & B)** and Chang cells **(C & D)** were incubated with PEITC 1, 3 or 10 μM (P1, P3 or P10, respectively) for 3 and 24 h. Total GSH contents were measured from cell pellets as intracellular GSH **(A & C)**, and GSH and GSSG ratios **(B & D)** were determined for GSH redox ratio. Each bar represents the mean ± SEM of three experiments. Significantly different from control, $*p < 0.05$.

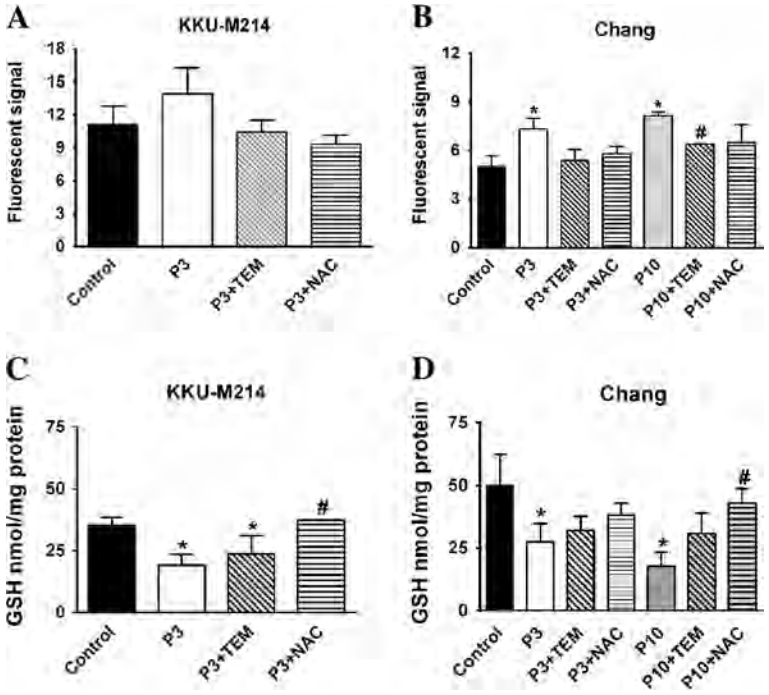


**Figure 5 Effect of PEITC on ROS production and GSH depletion.** KKU-M214 **(A & C)** and Chang cells **(B & D)** were incubated with PEITC at indicated concentrations 3 and 10 μM (P3 & P10) with or without TEMPOL (0.5 mM TEM) or NAC (2 mM). ROS formation was quantified by dihydroethidium method after incubation for 90 min **(A & B)** and cellular GSH **(C & D)** was assayed at 3 h after incubation. Each bar represents the mean ± SEM of three experiments. Significantly different from control, $*p < 0.05$, and significantly different from PEITC treated group, $\#p < 0.05$.

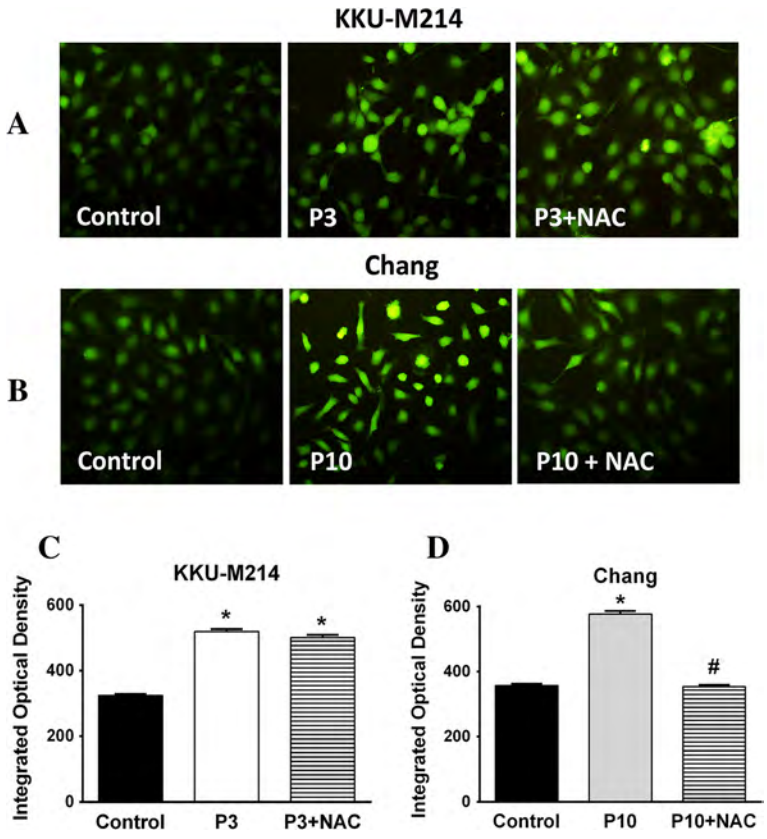


**Figure 6 PEITC induced the mobilization of intracellular $Ca^{2+}$ .** Cultured cells were treated with 3 or 10 μM of PEITC (P3 or P10) with NAC (2 mM) for 1 h. The mobilization of $Ca^{2+}$ into cytosol was analyzed by fluorescence staining using Fluoforte dye with excitation and emission wavelength of 485 and 535 nm, respectively. Representatives of images in each condition are shown **(A & B)**. The integrated optical density (IOD) of fluorescence in each condition was analyzed **(C & D)** from 10 images of two experiments. Each bar represents the mean ± SEM. Significantly different from control, *$p < 0.05$ and significantly different from PEITC treated group, #$p < 0.05$.

inhibit $Ca^{2+}$ flux into cytosol in Chang cells (Figure 6D). This underlines the causal relationship between calcium flux and oxidative stress.

### PEITC-induced depolarization of the mitochondrial transmembrane potential

Since PEITC induced apoptotic cell death via Bcl-2 protein family and other apoptogenic proteins, it is likely that the cytotoxicity of PEITC would be associated with the mitochondrial pathway. We examined the effect of PEITC on mitochondrial integrity by measuring the $\Delta\Psi_m$ using JC-1 fluorescent assay. In untreated control cells, mitochondria predominantly exhibited red fluorescence due to accumulation of J-aggregates representing the intact $\Delta\Psi_m$. PEITC treatment rapidly depolarized $\Delta\Psi_m$ as shown by the green fluorescence of JC-1 monomeric forms present in the cytosol (Figure 7). The effect was apparent within the first 1 hour of incubation and sustained up to 24 h in both cells. The images of the cells treated with PEITC for 3 h are shown in Figure 7. The effects of TEMPOL and NAC on the PEITC-induced $\Delta\Psi_m$ changes were evaluated. As was expected, TEMPOL did not prevent the depolarization of $\Delta\Psi_m$ in both cell lines. In contrast, NAC completely protected PEITC-induced mitochondrial depolarization in Chang cells, but this protective effect was not apparent in KKU-M214 cells, despite that GSH in KKU-M214 cells was well maintained by NAC.

### Effect of cyclosporine on PEITC-induced cell death

Since the depolarization of $\Delta\Psi_m$ may be resulted from the opening of the mitochondrial permeability transition (MPT) pores, we examined whether the opening of MPT was the primary effect of PEITC to induce cell death. The results show that cyclosporine (Cs) (Sandimmune, Novartis), a potent MPT inhibitor, could prevent the losses of $\Delta\Psi_m$ (data not shown), but could not prevent cell death in both cell types (Figure 8A & B). These results suggested that the loss of $\Delta\Psi_m$ was not a critical event and might be secondary to the recruitment of Bcl-2 protein members (Figure 2).

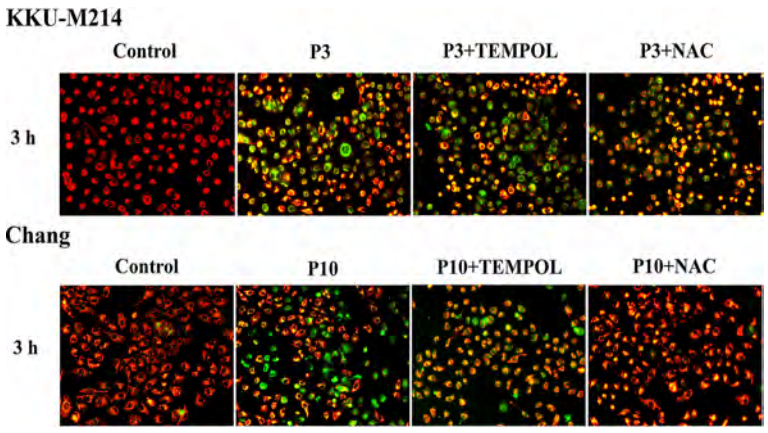


**Figure 7 PEITC-induced depolarization of the mitochondrial transmembrane potential.** Cells were treated with 3 or 10 μM (P3 or P10) of PEITC with TEMPOL (0.5 mM TEM) or NAC (2 mM NAC) for 3 h. The change in $\Delta\Psi_m$ was examined using JC-1 staining method. Fluorescent images were captured by fluorescence microscopy with the excitation wavelength of 485 nm and the emission wavelength of 535 nm. The experiments were performed twice with similar results, representative images from one experiment were shown.

### Effect of antioxidants on PEITC-induced cytotoxicity

It is apparent from the results given above that PEITC affected differently on KKU-M214 and Chang cells over the induction of GSH redox stress, protection of $Ca^{2+}$ efflux into cytosol and the protection to the loss of $\Delta\Psi_m$ by NAC. Therefore, the protective effects of antioxidants, TEMPOL or NAC, on PEITC-induced cytotoxicity were assessed. Figure 8 (C & D) shows that, co-treatment of the cells with PEITC and TEMPOL apparently could not protect cell death in both cell types, which was consistent with the results of the inefficacy of TEMPOL to prevent depolarization of $\Delta\Psi_m$ changes. Rather, treatment with TEMPOL exacerbated cell death in KKU-M214 cells (Figure 8C). NAC, which was unable to prevent the loss of $\Delta\Psi_m$ nor the $Ca^{2+}$ mobilization in cytosol in KKU-M214 cells, also could not protect PEITC-induced cell death. In contrast to the inefficacy to KKU-M214 cells, NAC almost fully protected Chang cells from the cytotoxic effect of PEITC at any time points examined after incubation (Figure 8D).

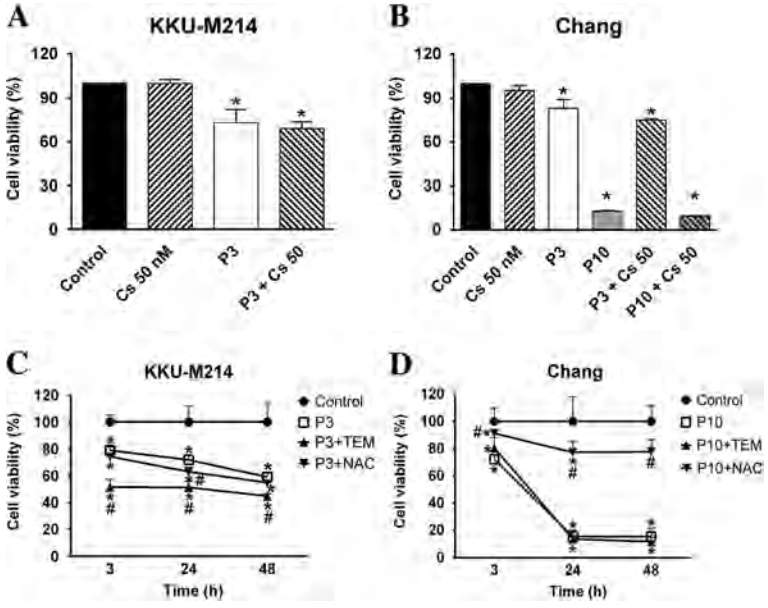


**Figure 8 Effects of Cs, NAC and TEMPOL on PEITC-induced cell death.** Cells were treated with 3 or 10 μM of PEITC (P3 or P10) in combination with Cs (cyclosporine) (50 nM) for 24 h **(A** and **B)**. Another experiments, cells were treated with NAC (2 mM) or TEMPOL (0.5 mM, TEM) for 3, 24 and 48 h **(C** and **D)**. Cell viability was assayed. Each bar or each value represents the mean ± SEM of three experiments. Significantly different from control group, *$p < 0.05$. and significantly different from PEITC treated group, #$p < 0.05$.

## Discussion

The chemopreventive properties of dietary cruciferous vegetables are well recognized from the results of epidemiological and experimental studies [5,6,9]. PEITC, one of the most promising ITCs, has been extensively studied *in vivo* and *in vitro*, information of its effects on CCA cells is lacking. Many strategies to enhance therapeutic outcomes in CCA treatment have been studied. For example, addition of biologic agents to block various kinase enzymes, or to suppress cytoprotective enzymes; NQO1 and HO-1 in CCA cells could increase the susceptibility of CCA to chemotherapeutic drugs [1,20,23]. In the present study, we demonstrated that PEITC could inhibit CCA cell growth and rapidly induce apoptosis. PEITC exerts different effects on KKU-M214 and Chang liver cells over cellular GSH redox and the release of mitochondrial apoptogenic molecules. The different cytoprotective effect of NAC on PEITC-induced cell death of the two cell types may reflect that the intracellular targets of PEITC are different in KKU-M214 and Chang liver cells.

Previous studies showed that PEITC induced cell death via several different mechanisms depending on cell types. Induction of cell death was associated with activation of c-Jun-N-terminal kinase (JNK) in DU145 but not in LnCaP cells [13] or with formation of ROS in PC3 and LnCaP, but was independent of ROS in HepG2 and multiple myeloma cells [12,25,26]. In this study, cytotoxic effects of PEITC were explored using a CCA cell line, KKU-M214 cells and Chang liver cells, since most chemotherapeutic agents have little selectivity over cancer cells from normal host cells. Our findings of the lack of selective toxicity of PEITC over CCA and Chang cells is consistent with the previous reports that various ITC killed cancer cells and non-cancer cells at the same order of concentration [16].

Present study showed that PEITC could induce apoptosis of both KKU-M214 and Chang liver cell lines in association with the decreased Bcl-xl and increased Bax expressions. It is known that p53 plays an important role in physically and functionally interacting with Bcl-2 family members for their translocation to mitochondria [27]. However, in the present study, the changes of the Bcl-2 protein members were not associated with p53 expression. This may imply that the apoptotic signal from PEITC to mitochondria is not transmitted via p53 pathway. Alternatively, stress signals provoked by PEITC may induce Bcl-2 family proteins via TNF family receptors, endoplasmic reticulum stress pathway or others [14,28]. It has been shown that PEITC sensitized HN22 oral carcinoma cells to DR5-mediated extrinsic death pathway [14]. We measured caspase 8 and 9 activities, which represent the initiator caspases of the extrinsic and intrinsic death signaling pathways, respectively. From the results of this study, PEITC-induced cell death appeared to be associated only with the intrinsic mitochondrial pathway, as there was no change in the caspase 8 activity after PEITC treatment.

In the present study, the cytotoxicity of PEITC was mediated via caspase-independent and caspase-dependent pathways for KKU-M214 and Chang cells, respectively. AIF is released from mitochondria and translocated to the nucleus where it fulfills the lethal function. Similar to cytochrome c, AIF play an important role in mitochondrial respiratory chain and is required for cell survival [29]. However, AIF is not a widespread cell death effector and its contribution to the execution of cell death is dependent upon the cell type, as well as the insulting signals [29]. PEITC induced AIF release in U2 OS sarcoma [11] and KKU-M214 cells in the present study. On the other hand, PEITC induced cytochrome c release in many cancer cells including MCF7, a breast cancer cell line [30], HT29, a colon cancer cell line [30], PC3, a prostate cancer cell line [12] and Chang cells in the present study. Our results showed that PEITC exerts its effects via AIF or cytochrome c depending on the cell types.

One of the prominent effects of PEITC is the induction of oxidative stress in cancer cells, which is characterized by ROS formation, GSH depletion and protein oxidation [11,12]. Our results only partially concurred with those previous reports. In the present study, PEITC induced GSH depletion in both KKU-M214 and Chang cells. However, PEITC induced ROS formation and GSH redox stress only in Chang cells but not in KKU-M214 cells (at least at 24 h of incubation). PEITC-induced cytotoxicity on Chang cells was associated with the depression of cellular GSH redox, as the replenishment of GSH by NAC could protect from cell killing by PEITC. This suggests PEITC-induced cell death of Chang cells may be via GSH redox stress. On the other hand, KKU-M214 cells seemed to handle PEITC-induced GSH redox stress rather well, because GSH levels were restored to the control level, or overshoot higher than controls at 24 h. Moreover, the treatment with NAC did not prevent PEITC-induced cell death of KKU-M214 cells. It is, therefore, the main mechanism of PEITC-induced cytotoxicity in KKU-M214 may be not by GSH redox stress. Although the cytotoxicity of PEITC against KKU-M214 and Chang cells was not much different in terms of the potency and efficacy, the underlining mechanism of the expression of cytotoxicity of PEITC on those two cells was obviously different because of the opposing results of the protective effect of NAC. It is, therefore, important to investigate further whether CCA tissues in the patients have the similar characteristics as the tumor cell responses to PEITC, before implementing NAC as an adjuvant.

PEITC is known to induce ROS formation, which is assumed to be a main mechanism of cell killing action

of PEITC on some tumor cells [11,12,17]. However, in this study, ROS was not causally related to GSH depletion or induction of cell death of KKU-M214 and Chang cells. Treatment with TEMPOL, which could completely normalize the superoxide to the background level, could not prevent cell death of both types of cells. Our results were consistent with the previous report of the failure of using various radical scavengers to prevent PEITC-induced cell death [26]. These results suggest that the mechanism of PEITC to induce cell death may be unique. The possible mechanisms of PEITC could be such as, modifications of redox-sensitive proteins or forming electrophiles attracting some critical proteins [31].

Oxidative stress can trigger the mobilization of $Ca^{2+}$ into cytosol, where endoplasmic reticulum is the important $Ca^{2+}$ storage [24]. We observed a rapid flux of $Ca^{2+}$ into cytosol shortly after PEITC treatment. The rapid increase of cytosolic $Ca^{2+}$ may cause elevation of mitochondrial $Ca^{2+}$ and decrease of $Ca^{2+}$ in endoplasmic reticulum, and such imbalance of $Ca^{2+}$ may trigger a variety of cascades leading to cell death. The lack of protective effect of NAC on cytosol $Ca^{2+}$ flux in KKU-M214 cells suggests that PEITC may exert the effect on the release of $Ca^{2+}$ by cellular stress other than the GSH redox system. On the other hand, in Chang cells, GSH redox disturbance may be primarily involved in cytosolic $Ca^{2+}$ flux.

In the present study, an increase of cytosolic $Ca^{2+}$ was accompanied with the rapid loss of $\Delta\Psi_m$. The depolarization of $\Delta\Psi_m$ is resulted from the opening of MPT pores, which is formed in the inner membrane of mitochondria [32]. The opening of MPT pores leads to diminish of ATP synthesis and ensuing cell death. However, present study showed that cyclosporine, a MPT pore inhibitor could not prevent PEITC-induced cell death, although it could prevent losses of the $\Delta\Psi_m$. This may imply that the depolarization of $\Delta\Psi_m$ is probably an associated event of PEITC treatment, but is not a direct effect leading to cell death. Taken all these together, mitochondria may not be a primary target of the increase of cytosolic $Ca^{2+}$ flux for initiation of cell death. Instead, the increased cytosol $Ca^{2+}$ may initiate the death signals in the cytosol by activation of a variety of $Ca^{2+}$-sensitive enzymes, such as calpain, leading to the cleavage and targeting of Bax to mitochondria [24] to activate the mitochondrial cell death pathway.

Our study revealed that PEITC induces up-regulation of Bax and down regulation of Bcl-xl. The formation of Bax pore and mitochondrial outer membrane permeabilization (MOMP) upon activation may be the critical event leading to the release of proapoptogenic proteins, cytochrome c and AIF, and ensuing cell death [33]. The mechanisms of the induction of cytosol $Ca^{2+}$ mobilization and activation of Bcl-2 proteins by PEITC remain to be elucidated. Since the precise mechanisms of PEITC-induced cell death of KKU-M214 cells remain unclear, further study is needed to explore novel mechanisms of the expression of cytotoxicity of PEITC.

## Conclusion

In conclusion, the present results show that PEITC induced apoptosis of CCA cells and Chang cells. This process may involve induction of oxidative stress and triggering of $Ca^{2+}$ flux, which leads to mitochondrial cell death mechanisms. Effect of PEITC on redox status of GSH may be not important for cell killing for CCA cells but it is important for maintaining cell functions in Chang cells. The different effect of PEITC on different cell types was clearly shown by the cytoprotection response to antioxidant, NAC. More study is needed using several CCA cell lines over the response to PEITC. Taken together, the present results highlighted different responses of the cells to PEITC, which may facilitate the new approaches in the study of PEITC for drug development for the treatment of CCA.

#### Abbreviations

CCA: Cholangiocarcinoma; Cs: Cyclosporine; GSH: Glutathione; GSSG: Glutathione disulfide; JC-1: 5,5′,6,′-tetrachloro- 1,1′,3,3′ tetraethylbenzimidazolyl carbocyanine iodide; JNK: c-Jun-N-terminal kinase; NAC: N-acetylcysteine; PEITC: Phenethyl isothiocyanate; ROS: Reactive oxygen species; SRB: Sulphorhodamine B; $\Delta\Psi_m$: Mitochondrial transmembrane potential.

#### Competing interests

The authors declare that they have no competing interests.

#### Authors' contributions

VK designed the study. OT performed the experiments. VK and OT analyzed the data. VK, OT, LS, AP and UK interpreted the results. OT, VK, and LS wrote the manuscript. All authors read and approved the final manuscript.

#### Acknowledgements

This work was supported by the Thailand Research Fund (BRG5480011), the Office of the Higher Education Commission through SHeP-GMS of Khon Kaen University, Grant-in-Aid from Faculty of Medicine, Khon Kaen University, and a scholarship from the Office of the Higher Education Commission to Ornanong Tusskorn. Valuable comments on the manuscript of Prof. Yukifumi Nawa of Faculty of Medicine, Khon Kaen University are gratefully acknowledged.

#### Author details

[1]Department of Pharmacology, Faculty of Medicine, Khon Kaen University, Mitraparb Road, Khon Kaen 40002, Thailand. [2]Liver Fluke and Cholangiocarcinoma Research Center, Khon Kaen University, Khon Kaen 40002, Thailand. [3]Department of Physiology, Faculty of Medicine, Khon Kaen University, Khon Kaen 40002, Thailand.

Received: 8 August 2013 Accepted: 26 November 2013
Published: 5 December 2013

#### References

1. Patel T: **Cholangiocarcinoma–controversies and challenges.** *Nat Rev Gastroenterol Hepatol* 2011, **8**:189–200.
2. Sripa B, Pairojkul C: **Cholangiocarcinoma: lessons from Thailand.** *Curr Opin Gastroenterol* 2008, **24**:349–356.

3. Khan SA, Davidson BR, Goldin RD, Heaton N, Karani J, Pereira SP, Rosenberg WM, Tait P, Taylor-Robinson SD, Thillainayagam AV, *et al*: **Guidelines for the diagnosis and treatment of cholangiocarcinoma: an update.** *Gut* 2012, **61:**1657–1669.
4. Cheung KL, Kong AN: **Molecular targets of dietary phenethyl isothiocyanate and sulforaphane for cancer chemoprevention.** *AAPS J* 2010, **12:**87–97.
5. Chan JM, Wang F, Holly EA: **Vegetable and fruit intake and pancreatic cancer in a population-based case–control study in the San Francisco bay area.** *Cancer Epidemiol Biomarkers Prev* 2005, **14:**2093–2097.
6. Lam TK, Ruczinski I, Helzlsouer KJ, Shugart YY, Caulfield LE, Alberg AJ: **Cruciferous vegetable intake and lung cancer risk: a nested case–control study matched on cigarette smoking.** *Cancer Epidemiol Biomarkers Prev* 2010, **19:**2534–2540.
7. Cheung KL, Khor TO, Yu S, Kong AN: **PEITC induces G1 cell cycle arrest on HT-29 cells through the activation of p38 MAPK signaling pathway.** *AAPS J* 2008, **10:**277–281.
8. Chiao JW, Wu H, Ramaswamy G, Conaway CC, Chung FL, Wang L, Liu D: **Ingestion of an isothiocyanate metabolite from cruciferous vegetables inhibits growth of human prostate cancer cell xenografts by apoptosis and cell cycle arrest.** *Carcinogenesis* 2004, **25:**1403–1408.
9. Khor TO, Cheung WK, Prawan A, Reddy BS, Kong AN: **Chemoprevention of familial adenomatous polyposis in Apc (Min/+) mice by phenethyl isothiocyanate (PEITC).** *Mol Carcinog* 2008, **47:**321–325.
10. Yang YM, Conaway CC, Chiao JW, Wang CX, Amin S, Whysner J, Dai W, Reinhardt J, Chung FL: **Inhibition of benzo (a) pyrene-induced lung tumorigenesis in A/J mice by dietary N-acetylcysteine conjugates of benzyl and phenethyl isothiocyanates during the postinitiation phase is associated with activation of mitogen-activated protein kinases and p53 activity and induction of apoptosis.** *Cancer Res* 2002, **62:**2–7.
11. Wu CL, Huang AC, Yang JS, Liao CL, Lu HF, Chou ST, Ma CY, Hsia TC, Ko YC, Chung JG: **Benzyl isothiocyanate (BITC) and phenethyl isothiocyanate (PEITC)-mediated generation of reactive oxygen species causes cell cycle arrest and induces apoptosis via activation of caspase-3, mitochondria dysfunction and nitric oxide (NO) in human osteogenic sarcoma U-2 OS cells.** *J Orthop Res* 2011, **29:**1199–1209.
12. Xiao D, Powolny AA, Moura MB, Kelley EE, Bommareddy A, Kim SH, Hahm ER, Normolle D, Van Houten B, Singh SV: **Phenethyl isothiocyanate inhibits oxidative phosphorylation to trigger reactive oxygen species-mediated death of human prostate cancer cells.** *J Biol Chem* 2010, **285:**26558–26569.
13. Xiao D, Choi S, Lee YJ, Singh SV: **Role of mitogen-activated protein kinases in phenethyl isothiocyanate-induced apoptosis in human prostate cancer cells.** *Mol Carcinog* 2005, **43:**130–140.
14. Huong LD, Shin JA, Choi ES, Cho NP, Kim HM, Leem DH: **Cho SD: beta-Phenethyl isothiocyanate induces death receptor 5 to induce apoptosis in human oral cancer cells via p38.** *Oral Dis* 2012, **18:**513–519.
15. Kim JH, Xu C, Keum YS, Reddy B, Conney A, Kong AN: **Inhibition of EGFR signaling in human prostate cancer PC-3 cells by combination treatment with beta-phenylethyl isothiocyanate and curcumin.** *Carcinogenesis* 2006, **27:**475–482.
16. Tseng E, Scott-Ramsay EA, Morris ME: **Dietary organic isothiocyanates are cytotoxic in human breast cancer MCF-7 and mammary epithelial MCF-12A cell lines.** *Exp Biol Med (Maywood)* 2004, **229:**835–842.
17. Trachootham D, Alexandre J, Huang P: **Targeting cancer cells by ROS-mediated mechanisms: a radical therapeutic approach?** *Nat Rev Drug Discov* 2009, **8:**579–591.
18. Chaiswing L, Zhong W, Oberley TD: **Distinct Redox Profiles of Selected Human Prostate Carcinoma Cell Lines: Implications for Rational Design of Redox Therapy.** *Cancers (Basel)* 2011, **3:**3557–3584.
19. Prawan A, Buranrat B, Kukongviriyapan U, Sripa B, Kukongviriyapan V: **Inflammatory cytokines suppress NAD (P) H:quinone oxidoreductase-1 and induce oxidative stress in cholangiocarcinoma cells.** *J Cancer Res Clin Oncol* 2009, **135:**515–522.
20. Buranrat B, Prawan A, Kukongviriyapan U, Kongpetch S, Kukongviriyapan V: **Dicoumarol enhances gemcitabine-induced cytotoxicity in high NQO1-expressing cholangiocarcinoma cells.** *World J Gastroenterol* 2010, **16:**2362–2370.
21. Suphim B, Prawan A, Kukongviriyapan U, Kongpetch S, Buranrat B, Kukongviriyapan V: **Redox modulation and human bile duct cancer inhibition by curcumin.** *Food Chem Toxicol* 2010, **48:**2265–2272.
22. Tietze F: **Enzymic method for quantitative determination of nanogram amounts of total and oxidized glutathione: applications to mammalian blood and other tissues.** *Anal Biochem* 1969, **27:**502–522.
23. Kongpetch S, Kukongviriyapan V, Prawan A, Senggunprai L, Kukongviriyapan U, Buranrat B: **Crucial role of heme oxygenase-1 on the sensitivity of cholangiocarcinoma cells to chemotherapeutic agents.** *PLoS One* 2012, **7:**e34994.
24. Hajnoczky G, Csordas G, Das S, Garcia-Perez C, Saotome M, Sinha Roy S, Yi M: **Mitochondrial calcium signalling and cell death: approaches for assessing the role of mitochondrial Ca2+ uptake in apoptosis.** *Cell Calcium* 2006, **40:**553–560.
25. Mi L, Gan N, Chung FL: **Isothiocyanates inhibit proteasome activity and proliferation of multiple myeloma cells.** *Carcinogenesis* 2011, **32:**216–223.
26. Rose P, Whiteman M, Huang SH, Halliwell B: **Ong CN: beta-Phenylethyl isothiocyanate-mediated apoptosis in hepatoma HepG2 cells.** *Cell Mol Life Sci* 2003, **60:**1489–1503.
27. Vaseva AV, Moll UM: **The mitochondrial p53 pathway.** *Biochim Biophys Acta* 2009, **1787:**414–420.
28. Rong Y, Distelhorst CW: **Bcl-2 protein family members: versatile regulators of calcium signaling in cell survival and apoptosis.** *Annu Rev Physiol* 2008, **70:**73–91.
29. Hangen E, Blomgren K, Benit P, Kroemer G, Modjtahedi N: **Life with or without AIF.** *Trends Biochem Sci* 2010, **35:**278–287.
30. Lee JW, Cho MK: **Phenethyl isothiocyanate induced apoptosis via down regulation of Bcl-2/XIAP and triggering of the mitochondrial pathway in MCF-7 cells.** *Arch Pharm Res* 2008, **31:**1604–1612.
31. Mi L, Hood BL, Stewart NA, Xiao Z, Govind S, Wang X, Conrads TP, Veenstra TD, Chung FL: **Identification of potential protein targets of isothiocyanates by proteomics.** *Chem Res Toxicol* 2011, **24:**1735–1743.
32. Kim JS, He L, Lemasters JJ: **Mitochondrial permeability transition: a common pathway to necrosis and apoptosis.** *Biochem Biophys Res Commun* 2003, **304:**463–470.
33. Chipuk JE, Green DR: **How do BCL-2 proteins induce mitochondrial outer membrane permeabilization?** *Trends Cell Biol* 2008, **18:**157–164.

doi:10.1186/1471-2407-13-571
**Cite this article as:** Tusskorn *et al.*: Phenethyl isothiocyanate induces calcium mobilization and mitochondrial cell death pathway in cholangiocarcinoma KKU-M214 cells. *BMC Cancer* 2013 **13**:571.

**Submit your next manuscript to BioMed Central and take full advantage of:**

- **Convenient online submission**
- **Thorough peer review**
- **No space constraints or color figure charges**
- **Immediate publication on acceptance**
- **Inclusion in PubMed, CAS, Scopus and Google Scholar**
- **Research which is freely available for redistribution**

Submit your manuscript at
www.biomedcentral.com/submit

BioMed Central

REVIEW

# Genetic Polymorphism of Drug Metabolizing Enzymes in Association with Risk of Bile Duct Cancer

**Veerapol Kukongviriyapan**

## Abstract

**Cholangiocarcinoma (CCA) is the most common cancer in endemic areas of liver fluke infection. Although the liver fluke is recognized as a carcinogenic agent in cholangiocarcinogenesis, other factors may play important roles in bringing about the high prevalence of the cancer in populations of this region. Drug metabolizing enzymes (DME) are essential for detoxification of toxic and carcinogenic chemicals. Moreover, DME can play an alternative role by activating chemicals to more toxic metabolites. The large variation of DME activity among individuals is partly due to polymorphism of the genes encoding enzymes. Defective or variant alleles of DME genes may modify the risk of cancer in those who are exposeed to carcinogenic agents. The focus in this review is on DME genes which have been reported to be associated with CCA risk. These include *CYP1A2*, arylamine-N-acetyltransferase-1 (*NAT1*) and *NAT2*, NADPH-quinone oxidorecutase-1 (*NQO1*), glutathione-S-transferase M1 (*GSTM1*), *GSTT1*, *GSTO1* and methylenetetrahydrofolate reductase (*MTHFR*). Mutant alleles which have been reportedly associated with an increased risk include *CYP1A2*1F*, *GSTT1 null*, *GSTO1* and *MTHFR 677C>T*, whereas, slow *NAT2* and *NQO1*2* decrease risk and *NAT1* variants and *GSTM1 null* have no effect. These genes modify the risk of cancer potentially by interaction and exposure with certain environmental conditions, thereby altering the metabolism of causative agents.**

**Keywords:** Pharmacogenetics - drug metabolizing enzymes - cholangiocarcinoma - *CYP1A2* - glutathione-S-transferase

*Asian Pacific J Cancer Prev,* **13**, 7-15

## Introduction

Cancer resulting from exposure to chemicals in the environment is well established. A long list of human carcinogenic chemicals is reported by various world authorities, such as the International Agency for Research on cancer (IARC), Globally Harmonized System and the American Conference of Governmental Industrial Hygienists (ACGIH) or WHO. The discovery of chemical carcinogenesis in modern time was described by an eminent English surgeon, Sir Percivall Pott in 1775 over the occurrence of cancer of the scrotum in chimney sweeps. His report suggested that the occupational exposure to soot since their childhood period was the causative agent of cancer (Klaassen, 2007). The socio-economic conditions and child labor during the industrial revolution in England were important factors relating to incidence of the cancer, as this cancer in chimney sweeps did not happen in the European continent. Other occupational and environmental exposure to chemicals in relation to cancers have been emerging, for instance, aromatic hydrocarbons, aromatic and heterocyclic amines, and also various natural products, such as mycotoxins, aflatoxins and plant toxins such as cycasin (Loeb and Harris, 2008).

Epidemiological studies provide the first clues and evidence of carcinogenicity of chemicals which are supported by laboratory studies using various *in vitro* and *in vivo* models. It has been estimated that about 75% of carcinogenic chemicals required metabolic activation to reactive electrophilic intermediates, such as benzo[a] pyrene, β-naphthylamine or IQ to be mutagenic and carcinogenic, whereas only 25% are directly carcinogenic, such as TCDD (Nebert and Dalton, 2006). Indeed, a number of complex metabolic pathways are involved in metabolic activation and metabolic detoxification of carcinogenic chemicals. The reactions are conducted largely by a drug metabolizing enzyme (DME) system which is made up of phase I, and phase II enzymes. Phase I enzymes catalyze oxidation, reduction and hydrolysis of xenobiotics resulting in formation of a functional group (-OH, -NH2, -SH, or -COOH), whereas phase II enzymes involve conjugation reactions including glucuronidation, acetylation, sulfation and methylation of chemicals producing more water-soluble metabolites readily for renal and biliary excretion (Parkinson, 1996).

*Department of Pharmacology, Faculty of Medicine, Liver Fluke and Cholangiocarcinoma research Center, Khon Kaen University, 40002, Thailand *For correspondence: veerapol@kku.ac.th*

## Roles of Drug Metabolizing Enzymes in Cancer

DME play important roles in metabolic activation of procarcinogenic compounds including phase I enzymes, for instance some CYP isoforms, such as CYP1A1, 1A2, 2E1, 2A6 and 2A13. A number of the phase II enzymes namely, arylamine-*N*-acetyltransferases (NAT), sulfotransferases (SULT), glutathione-S-transferases (GST) and UDP-glucuronosyl-transferases (UGT) may also participate in metabolic activation of particular carcinogenic compounds. Some DME act predominately as drug detoxifying enzymes include, GSTs, NADPH-quinone oxidoreductase-1 (NQO1), UGTs, epoxide hydrolase (EHs). It has been noted that the role of DME in metabolic activation or detoxification is not absolute, but depending on type of compounds and metabolic pathways.

Examples of carcinogenic chemicals and roles of DME in activation are shown in Table 1. The activation of reactive metabolites usually involves the formation of unstable electrophilic groups by oxidation or reduction by CYPs. CYP1A1, and 1B1 which participate in metabolic activation of polycyclic aromatic hydrocarbons, such as benzo[a]pyrene yielding epoxide intermediates and those epoxides are further converted to dihydrodiol and then to highly reactive epoxide derivatives by epoxide hydrolase and CYP2B1, respectively (Parkinson, 1996) (Table 1). Alternatively, CYP1A2 carries out the *N*-hydroxylation of arylamines and heterocyclic amines food mutagens; MeIQ or PhIP, and reactions follow with *O*-esterification by acetate or sulfate via transferase enzymes, i.e. NAT and SULT, resulting in unstable electrophilic intermediates (Kim and Guengerich, 2005). Moreover, CYP1A2 also metabolizes aflatoxin B1 to the reactive epoxides. CYP2E1 mainly metabolizes small aliphatic and aromatic molecules such as ethanol, vinyl halides, aniline, *N*-nitrosomethylamine and yields strong electrophilic compounds. The tobacco-specific nitrosamines, i.e. 4-(methylnitrosamino)-1-(3-pyridyl)-1-butanone (NNK) and *N*''-nitrosonornicotine (NNN) are activated to their carcinogenic metabolites by hepatic CYP2E1, 2A6 and lung CYP2A13. CYP2A13 is not expressed in the liver but expressed in the lung and is highly efficient in metabolizing NNN, NNK and aflatoxin B1. The reactive electrophiles react rapidly with nucleophilies in the vicinity; e.g. nucleic acids, proteins and lipids, forming adducts, causing the lost of functional molecules and leading to cytotoxicity, cell death or cell transformation. A schematic of possible events in metabolic activation and detoxification of reactive metabolites, which lead to cell injury, cell death, transformation and carcinogenesis, is shown in Figure1.

## Drug Metabolizing Enzymes and Cholangiocarcinogenesis

Cancers of the bile duct in populations of northeast Thailand, and neighboring countries are associated with liver fluke infection (Kurathong et al., 1985; IARC, 1994). An animal model of opischorchiasis-induced cholangiocarcinoma suggests that the concurrent exposure to carcinogens with liver fluke infection may be necessary to enhance the carcinogenesis process of cholangiocarcinoma (Thamavit et al., 1978). Carcinogenic agents identified in relation to cancer in this region so far include nitroso compounds, tobacco, mycotoxins, heterocyclic amines from food mutagens, ethanol and hepatitis viruses (Srivatanakul et al., 1991b; Mitacek et al., 2008; Shin et al., 2010). *N*-nitrosodimethylamine (NDMA) induces liver damage and liver cancer, however, when administered in liver fluke-infected hamster, NDMA

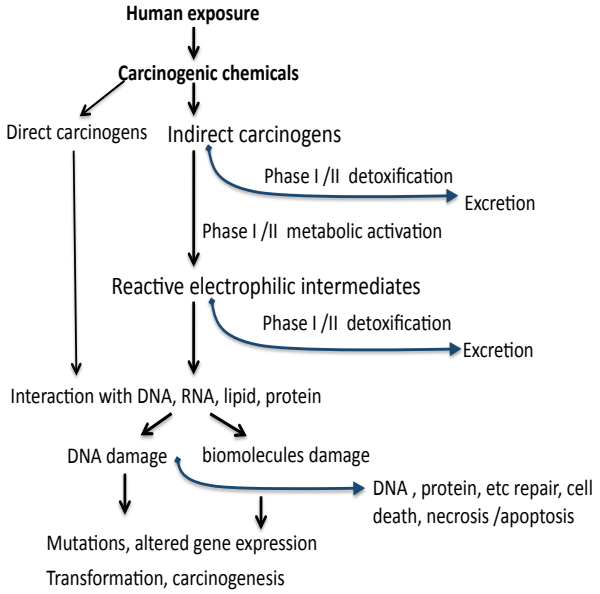


**Figure 1. Sequence of Events in Metabolic Transformation of Chemicals Leading to Cell Death, Transformation and Carcinogenesis**

**Table 1. Carcinogenic Agents, Cancer Sites and Enzymes in Metabolic Pathways**

| Chemical | Cancer sites | Activating enzymes | Reference |
|---|---|---|---|
| 1. Polycyclic aromatic hydrocarbons (PAH); benzo[a]pyrene, dibenz[a,h]anthracene, chrysene, 3-methylcholanthrene | Lung, skin, bladder | CYP1A1, 1B1, EHs | Shimada,2006; coal tar, tobacco; Irigaray and Belpomme, 2010 |
| 2. Polyhalogenated aromatic hydrocarbon; dioxins, polychlorinated biphenyls (PCBs) | Liver, biliary tract | CYP1A1, 1B1 | Shimada, 2006; Irigaray and Belpomme, 2010 |
| 3. Heterocyclic amines: food mutagens; MeIQ, PhIP, arylamnes: benzidine, 2-naphthylamine, 2-aminofluorene | Colon, bladder | CYP1A2, 1A1, 1B1, NQO1, NAT1, NAT2, SULTs | Williams et al., 2001; Suzuki et al., 2008 |
| 4. Nitroso compounds: N-nitrosodimethylamine (NDMA) | Liver | CYP2E1, CYP2A6, | Kushida et al., 2000 |
| 5. Tobacco-specific: NNN, NNK | Lung | CYP2A13, NQO1, EHs | Wang et al., 2003; Zhu et al., 2006 |
| 6. Mycotoxins; aflatoxins, | Liver, lung | CYP1A2, CYP3A4, | Guengerich et al., 1998; Chen et al., 2006 |

specifically induces cholangiocarcinoma (Thamavit et al., 1978). NDMA was found to be a food contaminant in region of the high prevalence of liver fluke infection. Moreover, subjects with liver fluke infection showed much higher endogenous nitrosation rate than subjects without liver fluke infection, as assessed by ingestion of proline and measurement of nitrosation product of N-nitrosothioproline (Srivatanakul et al., 1991a). It is possible that endogenous nitrosation may be another source of formation of mutagenic nitroso-compounds. NDMA and other nitro-compounds, aflatoxins, and many other agents are required for metabolic activation to yield ultimate reactive carcinogenic compounds. It has been suggested that metabolic capacity of DME in individuals may contribute to susceptibility to toxic responses of carcinogenic agents.

## Genetic polymorphism of drug metabolizing enzymes

It is well-known that there is considerable individual variation in activity of DME and the variation may be accountable for individual susceptibility to toxic chemicals. It is apparent that variability in gene encoding DME often affect outcome to a large extent in drug efficacy and toxicity (Eichelbaum et al., 2006). Most genes exist in many physical forms or alleles, and those alleles differ in certain nucleotides positions (or single nucleotide polymorphism: SNP) on coding and non-coding regions of the genes. The presence of several forms or polymorphism of DME genes result in a variation of DME activity or phenotype polymorphism. Phenotypes of DME in individuals may be classified as: 1. absent or very low enzymatic activity, which are designated as Slow metabolizers, resulting from the presence of the severe defective alleles including gene deletion, nonsense, frame shift or missense mutations in both alleles, 2. Intermediate metabolizers, the presence of only one active allele, 3. Rapid metabolizers, the presence of two active alleles, and 4. Ultra-rapid metabolizers, the presence of multiple copy of active alleles. Frequency of allelic variants of given genes could vary widely resulting in inter-individual variation in a population and variation among populations in susceptibility to toxic chemicals and carcinogenesis. Allele frequency of important alleles of DME among populations is shown in Table 2.

## Polymorphism of DME and Cholangiocarcinoma

Epidemiological studies have shown that liver fluke infection is a major risk factor in cholangiocarcinoma. However, as not all subjects with liver fluke infection develop cancer, some individuals may be more susceptible to develop this disease. The individual susceptibility has been related to polymorphism in DME genes. As exposure to carcinogenic compounds is probably related to cancer risk, genetic polymorphism of DME genes may contribute to individual susceptibility. Candidate DME genes have been identified based on the discovery of tumor-specific mutations through genotyping of CCA patients. Epidemiological studies and meta-analyses have revealed several tumor susceptible genes and identified associated risk factors of tumor development (Prawan et al., 2005; Ko et al., 2006; Marahatta et al., 2006; Songserm et al., 2012). The susceptibility genes are usually weakly associated with cancer or have low penetrance in causing cancer.

Environmental factors may also play crucial part in carcinogenesis. Non-genetic factors associated with increased cancer risk include consumption of food contaminated with liver fluke (*Opisthorchis viverrini*), HBV or HCV infection, alcoholic drinking, processed meat, whereas consumption of vegetables and fruits decreased the risk. Following is a discussion of polymorphism of DME genes in association with the risk of CCA.

*Polymorphism of CYP1A1/2 and CYP1B1*

CYP1A1 and CYP1B1 participated in reactions of substrate molecules of planar shape, such as PAH found in tobacco smoking, pollutants from combustion of fossil fuel. The heterocyclic amines, food mutagens formed during the pyrolysis of creatine, amino acids and proteins such as AIAs, IQ, MeIQ, MeIQx and PhIP, and aromatic amines, such as naphthylamine and benzidine are metabolized by CYP1A2. All have been shown to be carcinogenic in animals. *CYP1A2* is expressed in the liver, while *CYP1A1* and *CYP1B1* are expressed at

**Table 2. Polymorphism of DME Genes in Populations. Allelic Variants of Some DME Genes and their Association with Phenotypic Characteristics, and Allele Frequency in Various Populations**

| Gene | Variant alleles | Phenotype activity | Variant allele frequency (%) | | | |
|---|---|---|---|---|---|---|
| | | | Thai | Chinese | Caucasian | African |
| *CYP1A2* | *CYP1A2**1F | Higher inducibility | 72.3 | 67 | 72.3 | 61 |
| *CYP2A6* | *CYP2A6*4,*7, *9,*10* | Absence or reduced | 41 | 37.3 | 15.5 | 25.6 |
| *NAT2* | *NAT2*5, *6, *7* | Slow acetylation | 56.7 | 49 | 75 | 63 |
| *NAT1* | *NAT1**3,**10,*11,*14* | Unchanged | 49.6 | 50 | 21 | 51.5 |
| *NQO1* | *NQO1*2* | Reduced activity | 58.7 | 41.4 | 18 | 16 |
| *GSTM1* | *GSTM1 null* | Absence | 67.2 | 44 | 53.5 | 26.1 |
| *GSTT1* | *GSTT1 null* | Absence | 39.2 | 51 | 17.5 | 22 |
| *GSTO1* | *GSTO1**A140D | Unchanged | 13 | 17 | 33.4 | 8.1 |
| *MTHFR* | *MTHFR* C677T | Reduced activity | 31.1 | 32.8 | 42 | 13 |

*Data from; Kukongviriyapan et al., 2003a; Kukongviriyapan et al., 2003b; Prawan et al., 2005; Marahatta et al., 2006; Peamkrasatam et al., 2006; Ginsberg et al., 2009; Chutinet et al., 2012; Songserm et al., 2012

extra-hepatic tissues (Landi et al., 1999). All these CYPs are highly inducible by PAHs, some drugs and many phytochemicals via Ah receptor (Landi et al., 1999). To date, at least 11 allelic variants and several subvariants have been described in *CYP1A1* gene (www.cypalleles.ki.se/, access date Aug 16, 2012).

There are at least 133 SNPs described for *CYP1A1* and 23 are nonsynonymous mutations, however, for most their effect is not known. Some of SNPs in *CYP1A1* i.e 2455 A>G, *CYP1A1*2B*, and *2C, have been suggested to influence the inducibility. About 10% of the Caucasian population has a highly inducible form of the *CYP1A1*, that might present risk to individuals with high inducibility for tobacco smoke-induced lung cancer (Nakachi et al., 1993). In smokers with 2455A>G SNP, more PAH-DNA adducts were observed in white blood cells compared with smokers without SNP. Apart from lung cancer, *CYP1A1*1* is associated with breast cancer risk in individuals who are exposed to polychlorinated biphenyls, known as potent *CYP1A1* inducers, by increased metabolism forming reactive hydroxylated metabolites (Moysich et al., 1999; Modugno et al., 2003). However, there is still no reports concerning *CYP1A1* polymorphism and cholangiocarcinoma.

For *CYP1A2*, its expression is distinct from *CYP1A1*, and the enzymes have considerable overlapping substrate specificity. A number of SNPs are observed on the 5' flanking region in introns and exons, however, no common alleles have been described that cause any important change in gene expression and enzymatic activity. *CYP1A2*1C*, **1F* and **1K* are alleles that have received much interest, in that *CYP1A2*1F* is suggested to be highly inducible and *CYP1A2*1C*, **1K* to be reduced in activity (Nakajima et al., 1999). However, there are still many conflicting reports over the inducibility phenotype of *CYP1A2*1F*. This may be partly because that only SNP -163C>A in *CYP1A2*1F* is also present in haplotypes with SNPs -739C>T and 729C>T in *CYP1A2*1K*, where this allele is suggested to be a reduced activity allele (www.cypalleles.ki.se/, access date Aug 16, 2012). Allele frequency of *CYP1A2*1F* is relatively high in most populations, i.e. about 60-70%. In Thai populations, the frequency has been reported to be 72% (Prawan et al., 2005). Furthermore, our study reported that the male population with wild type *CYP1A2*1A* genotype had lower risk of developing CCA when compared with males who carried the *CYP1A2*1F*/**1F* genotype with odds ratio of 0.28: 95% CI: 0.08-0.94. Individuals with wild type genotype also have lower risk of breast cancer when compared with -163A/A, which is consistent with the observation of lower plasma estrogen levels in premenopausal women with -163C/C genotype (Le Marchand et al., 2005a). A significant effects of *CYP1A2*1F* or combination of *CYP1A2*1F* and *NAT1*10* or **11* on the increased risk for pancreatic cancer was observed among non-smokers (Li et al., 2006). Similarly, light smokers with *CYP1A2**1 and *NAT2* slow acerylator genotypes were at the highest risk of lung cancer (Osawa et al., 2007). The high inducibility of *CYP1A2* genotype may confer cancer risk in individuals who are exposed to carcinogenic chemicals.

*Polymorphism of arylamine-N-acetyltransferases*

Arylamine-*N*-acetyltransferases (NATs) are phase II enzyme genes that catalyze the transfer of acetyl group to various substrates including endogenous compounds, drugs and food mutagens. There are 2 isoforms of enzymes encoded from 2 different but related genes, i.e. *NAT1* and *NAT2* (Sim et al., 2008). Individuals who carry defective *NAT2* genotypes or slow acetylators are likely to develop peripheral neuropathy when use of isoniazid for the treatment of tuberculosis. Other adverse drug reactions with use of sulfasalazine and hydrazine were observed. *NAT1* is composed of at least 20 alleles with various subvariants (http://louisville.edu/medschool/pharmacology/consensus-human-arylamine-n-acetyltransferase-gene-nomenclature/). *NAT1*3, *10, *11* common genotypes do not cause any consistent changes in enzymatic activity when compared with the

**Table 3. Polymorphism of DME and Association with Risk of CCA and Other Cancers**

| Gene | Variant allele | CCA risk | Other cancer risk | References |
|---|---|---|---|---|
| *CYP1A2* | *CYP1A2*1F* (-163C>A) | ↑(male)* | ↑ panceas (smokers) ↑lung, breast (non-smokers) | Prawan et al., 2005; Li et al., 2006; Osawa et al., 2007; |
| *NAT2* | Slow acetylators | ↓ | ↑bladder (smokers), ↓colon, ↑HCC (non viral hepatitis) | Garcia-Closas et al., 2005; Agundez, 2008; Walker et al., 2009 |
| *NAT1* | Variant alleles | ↔ | ↑ panceas (smokers), ↑bladder (slow *NAT2*+smokers), ↔colon, ↔HCC | Prawan et al., 2005; Li et al., 2006; Agundez, 2008; |
| *NQO1* | *NQO1*2* (609C>T) | ↓ | ↑breast, ↑colon (Caucasian), ↓bladder, ↓lung | Menzel et al., 2004; Zeekpudsa et al., 2009; Yang et al., 2012; Yu et al., 2012 |
| *GSTM1* | *GSTM1 null* | ↔ ↑ (Ov+ve) | ↑HCC, ↑colon, ↑lung, ↑bladder (combination with *GSTT1 null*), ↑prostate, ↔breast | Egan et al., 2004; Honjo et al., 2005; White et al., 2008; Mo et al., 2009; Economopoulos and Sergentanis, 2010; Safarinejad et al., 2011; Li et al., 2012 |
| *GSTT1* | *GSTT1 null* | ↑↔ | ↑HCC, ↑ panceas, ↔colon (Caucasian), ↔prostate, ↔breast | |
| *GSTO1* | *GSTO1**A140D | ↑ | ↑ breast (advanced), ↑bladder (high As exposure), ↑ALL, ↑HCC | Marahatta et al., 2006; Pongstaporn et al., 2009; Escobar-Garcia et al., 2012; |
| *MTHFR* | *MTHFR 677C>T* | ↑ (raw fish intake) | ↓Colon, ↑ panceas (Caucasian), | Le Marchand et al., 2005b; Ko et al., 2006; Mazaki et al., 2011; Songserm et al., 2012 |

wild type *NAT1*4* (Sim et al., 2008). On the other hand, there are at least 18 alleles of *NAT2* and 27 alleles of *NAT1* reported to date. The defective *NAT2* alleles consist of several SNPs forming SNP haplotypes designated as *NAT2*5, *6* and **7*. These are common defective alleles in most populations. Asian populations, including Thais, have lower frequencies of slow acetylator genotype and phenotype when compared with Caucasian and African populations, i.e. about 20-35% vs 60% and 40%, respectively (Kukongviriyapan et al., 2003a). The major defective alleles in Asian populations are *NAT2*6* and **7*, while those found in Caucasians and Africans are *NAT2*5* and **6*. The important *NAT1* allele, *NAT1**10, has been reported to have prevalence of 43.8% in Asian populations including Thais at about 40-50%, whereas that in white Caucasians is about 20% (Kukongviriyapan et al., 2003b) (Table 2).

Polymorphism of *NAT2* was reported to be associated with risk of CCA, in which some slow acetylator genotypes, i.e. *NAT2*6* and **7* are at lower risk (OR: 0.26, 95%CI: 0.15-0.44). However, *NAT1*10* is not associated with cancer risk (Kukongviriyapan et al., 2003b). Further epidemiological studies in larger populations and environmental exposure to identify putative carcinogenic chemicals in relation to *NAT2* metabolism may be beneficial to reduce the risk of CCA in populations in this region.

Moreover, slow acetylators of *NAT2* have been shown to be associated with increased risk of bladder cancer among smokers, but not of those with *NAT1* (Garcia-Closas et al., 2005). On the other hand, rapid acetylator genotypes are at increased risk of colon cancer among smokers and individuals who consumed red meat (Walker et al., 2009). A study in patients with hepatocellular carcinoma who were not related to viral hepatitis showed a minor, but relevant association with slow *NAT2* status (Agundez, 2008). It is noted that an association of risk of various cancers with *NAT2* is strongly modified by environmental exposure, particularly, heterocyclic amines and aromatic amines from food and occupational chemicals.

*Polymorphism of NADPH-quinone oxidoreductase-1*

NADPH-quinone oxidoreductase-1 (NQO1) is the cytosolic enzyme that catalyzes the two-electron reduction of nitroaromatic, quinones and quinine-imines, to hydroquinones, thereby promoting detoxification and preventing the formation of reactive oxygen species. Moreover, NQO1 also plays a role in regenerating antioxidant forms of ubiquinone and tocopherol (vitamin E) after free radical attack (Dinkova-Kostova and Talalay, 2010). NQO1, a highly inducible enzyme, is regulated by the Nrf2-ARE signaling pathway suggesting important functions as an antioxidant and cytoprotection in the defense of oxidative stress and prevention of cancer. This is consistent with recent studies showing that defective in *NQO1* gene is associated with increased risk of cancers (Yang et al., 2012). Using immunohistochemisty, NQO1 staining is found in vascular endothelium in most tissues, i.e. respiratory, colon, and breast epithelium, thyroid follicle, and weakly expressed in the liver, bile duct and myocardium (Siegel and Ross, 2000). Interestingly, NQO1 is found highly expressed in various solid tumors, i.e. thyroid, breast, colon and lung suggesting its role in carcinogenesis, probably by conferring cytoprotection for tumors (Siegel and Ross, 2000). CCA tissues also showed high activity of NQO1, when compared with normal liver tissues (Buranrat et al., 2012). It is reasonable to suggest that inhibition of NQO1 is a novel approach to enhance anticancer agent sensitivity in cancers (Buranrat et al., 2010).

Polymorphism of human *NQO1* gene is constituted from more than 300 SNPs (http://www.genecards.org/cgi-bin/carddisp.pl?gene=*NQO1*). The most common allele is *NQO1*2*, a nonsynonymous mutation at 609C>T (P187S) which causes reduced activity due to a rapid degradation of the mutant protein (Siegel et al., 1999). Allele frequency of *NQO1* among Asian populations is relatively high i.e. 50%, and low in Caucasian and African populations, i.e. 18% and 16%, respectively (Table 2). Carriers of *NQO1*2* allele are at greater risk of cancers of the gastrointestinal tract as compared to ones who carry *NQO1*1*, the wild type allele (Yang et al., 2012) which is similar to breast cancer (Menzel et al., 2004). On the other hand, our preliminary study in patients with cancers of the bile duct suggested that *NQO1 609T* allele was associated with lower risk of CCA (Zeekpudsa et al., 2009), in the other words, 609C wild type genotype presented a risk of CCA (adjusted odds ratio: 2.57 (95% CI: 1.39-4.74) and the risk was even higher in patients who also carried null alleles of *GSTT1* genotype. The increased risk of cancers in wild type *NQO1* genotype might suggest a role in metabolic activation of carcinogenic agents in exposed populations.

*Polymorphism of glutathione-S-transefrases*

Human glutathione-S-transferase (GST) enzymes have been discovered as over 16 cytosolic isoforms. They are divided into 7 main classes, α (alpha, GSTA), κ (kappa GSTK), μ (mu, GSTM), ω (omega, GSTO), π (Pi, GSTP), θ (theta, GSTT), and ζ (zeta, GSTZ). Moreover, there are also mitochobndrial and microsomal forms (now designated as MAPEG). Cytosolic and mitochondrial GST share some similarity in their structure, but not with MAPEG. Cytosolic GSTs represent the largest family and are of interest to biomedical research, because they are relevant to several drug targets including anticancer agents, and environmental toxicants, carcinogens and by-products of oxidative stress (Hayes et al., 2005).

The GSTs play central role in xenobiotic detoxification, resulting more water-soluble conjugates facilitating excretion via the MRP efflux pumps or undergo further metabolism to mercapturic acid derivatives (Hayes et al., 2005). Metabolism by GSTs, thereby, confers cellular protection from environmental and oxidative stress, yet is also implicated in resistance to anticancer agents. Drug resistant tumor cell lines have been shown to have over expression of GST genes, which leads to an increase of drug-glutathione conjugation with subsequent excretion (Lo and Ali-Osman, 2007). Apart from catalyzing GSH conjugation reactions for chemicals, GSTs also function as ligand-binding proteins with cellular protein, such as JNK, ASK, PKC in cell signaling, apoptosis and drug

sensitivity (Lo and Ali-Osman, 2007). The polymorphism of GST isoforms that has been reported in association with cholangiocarcinoma included *GSTM, GSTO* and *GSTT*.

*GSTM* subfamily consists of 5 isoforms (M1- M5).The *GSTM1* is the most studied isoform, where loss of function is ascribed to a homozygous deletion of this gene resulting in the *GSTM1 null* or *GSTM1*0* allele. The *GSTM null* has been reported to be associated with various cancer risk (Hayes et al., 2005). The allele frequency of *GSTM1*0* in Thais is about 67% (Table 2) whereas in other populations it is lower. Additionally, *GSTT* consists of two subfamilies: *GSTT1* and *GSTT2*. Polymorphisms exist within both genes particularly, the gene deletion type, *GSTT1**0 or *GSTT1 null*. A number of reports implicated *GSTT1 null* and GSTM null in association with risk of various cancers. In a meta-analysis of hepatocellular carcinoma, a study suggested that a small excessive risk of liver cancer in individuals with *GSTM1 null* and possibly with *GSTT1 null* genotypes as well (White et al., 2008). In a study of lung cancer, *GSTM1* genotype was associated with cancer risk and smoking may enhance a greater risk of cancer (Li et al., 2012). In an analysis of 42 studies in colorectal cancer, *GSTM1 null* allele exhibited a small excessive risk of colorectal cancer (pooled odds ratio 1.15, 95%CI: 1.06-1.25) in Caucasian but not Chinese populations a similar result to *GSTT1 null* that exhibited increased cancer risk in Caucasian population with pooled odds ratio 1.31, 95%CI: 1.12-1.54 (Economopoulos and Sergentanis, 2010). In contrast, a large population study previously showed that *GSTM1 null* and *GSTT1 null* or the combination did not present risk of breast cancer (Egan et al., 2004). In a case-control study in an endemic area of liver fluke infection in northeast Thailand, genetic polymorphism of *GSTM1* and *GSTT1* alone did not present a risk for CCA. However, elevated serum anti-*Opischorchis viverrini* (liver fluke) indicating previous liver fluke infection was correlated with an increase in CCA risk (adjusted odds ratio 10.3, 95% CI: 1.31-81.63) and the risk was even amplified in subjects with *GSTM1 null* genotype with adjusted odds ratio 23.5, 95%CI:3.33-97.40 (Honjo et al., 2005).

The omega class of GST contains 2 members, *GSTO1* and *GTSO2*. Substrates of GSTO do not usually overlap with other classes of GSTs. The enzymes act as small stress response proteins involved in redox regulation and possess dehydroascorbate reductase activity (Schmuck et al., 2005). No synonymous mutations on *GSTO1* causes amino acid change of A140D and E208K, but these polymorphisms do not alter specific activity of the recombinant enzyme. *GSTO1-1* may play important roles in arsenic metabolism and non-enzymatic effects, in that polymorphism of *GSTO1-A140D* and *E208K* are associated with higher expression of IL-1, IL-8, TGF-β and Apaf-1 which, thereby, could increase risk of inflammatory diseases (Escobar-Garcia et al., 2012). *GSTO1* polymorphism has been suggested to be associated with increased risk of chronic obstructive pulmonary diseases, acute lymphoblastic leukemia (Pongstaporn et al., 2009), hepatocellular carcinoma and breast cancer (Marahatta et al., 2006). *GSTO1 A140D* polymorphism has been suggested to a risk factor for cholangiocarcinoma in endemic areas of liver fluke infection (Marahatta et al., 2006).

*Polymorphism of Methylenetetrahydrofolate reductase*

The enzyme methylenetetrahydrofolate reductase (MTHFR) plays a central role in folate metabolism, by regulation of the synthesis of thymidylate and purines, and supply of methyl groups for the synthesis of methionine and DNA methylation (Powers, 2005). Polymorphism of *MTHFR* gene at *677C>T* generates a change of amino acid from alanine to valine resulting in a thermolabile enzyme with decreased activity. The defective allele frequency in Thais is comparable with other Asian and European populations (Table 2) (Chutinet et al., 2012; Songserm et al., 2012). The second common mutation in coding region of *MTHFR* is *1298A>C*, which causes a glutamic acid to alanine substitution with decreased enzymatic activity. The prevalence of this allele in Thai populations is 28.1% (Songserm et al., 2012). The polymorphism of *MTHFR* in coding region causing decreased *MTHFR* activity has been suggested to be associated with increased homocysteine levels and abnormal DNA methylation, an important epigenic feature of DNA, which is associated with a number of diseases, including, hypertension, neuro-behavioral abnormalities and cancers (Powers, 2005; Cheng et al., 2010; Kim et al., 2012). It should be noted that the levels of folate and homocysteine are strong modifying factors of the diseases, as low folate and hyperhomocysteinaemia are known to be causally related to cancers and cardiovascular diseases (Powers, 2005; Kim et al., 2012).

The common *MTHFR 677C>T* allele was investigated in a large case-control study in association with colorectal cancer. The TT genotype was associated with decreased risk with adjusted odds ratio 0.77, 95%CI: 0.58-1.03, especially at high levels of folate and low levels of ethanol intake (Le Marchand et al., 2005b; Powers, 2005). In contrast, *MTHFR 677C>T* or T genotype had a tendency to have a higher risk to develop pancreatic cancer, especially in the condition of depletion of folate, vitamin B6, B12 (Mazaki et al., 2011). An analysis for CCA risk in Thai popluations, showed that *MTHFR 677TT* and *1298TT* genotypes alone did not present significant risk, however, the risk was significantly elevated in individuals with high intake of raw fresh water fish, which are at risk of liver fluke infection, and other meat products (Songserm et al., 2012). The study suggested that the gene-environment interaction plays crucial part in cancer risk. In a study in Korean populations, which is not an endemic area of liver fluke infection, *MTHFR* and thymidylate synthase enhancer region (TSER) polymorphisms were analyzed. A combination of *MTHFR 677CC* with *TSER 2R(+)* genotype had a higher risk for developing CCA compared to *MTHFR 677CC* with *TSER3R* genotype (odds ratio 5.4, 95%CI: 1.2-23.5) (Ko et al., 2006). The studies suggest that *MTHFR* may be a risk modifier of environmental exposure to toxic agents.

## Conclusion

Cumulating evidence illustrates an association of genetic polymorphism of drug metabolizing genes with

risk of developing cancer of the bile duct. The frequency of important allelic variants of various DME genes in high risk populations of the northeast Thailand is similar to most Asian populations. The mutant alleles may encode defective enzymes, which alter the metabolism of carcinogenic chemicals probably due to environmental exposure with subsequent modifations of the risk of CCA. Polymorphism of DME is similar to other cancer susceptible genes in that these genes generally present only a small excessive risk, however, the risk is modified by environmental exposure. The well recognized and important environmental factor is liver fluke infection, which causes chronic inflammation of the biliary tract. However, liver fluke alone may not trigger cancer. Other causative agents, which may be affected by various DME, are yet to be identified. Alcohol, tobacco, nitroso compounds, raw fresh water fish, fermented meat and mycotoxins are among chemicals/substances possibly related to tumor development. Comprehensive studies of the complex interactions of genes and the environment are required to better understand the nature of chemical exposure and impact of genetic polymorphism in individual settings.

## Acknowledgement

Research works were supported by grant-in-aid from Khon Kaen University and Thailand Research Fund. We wish to acknowledge the support of the Khon Kaen University Publication Clinic, Research and Technology Transfer Affairs, Khon Kaen University, for their assistance.

## References

Agundez JA (2008). Polymorphisms of human N-acetyltransferases and cancer risk. *Curr Drug Metab*, **9**, 520-31.

Buranrat B, Chau-in S, Prawan A, Puapairoj A, Kukongviriyapan V (2012). *NQO1* expression is correlated with the prognosis of cholangiocarcinoma. *Asian Pac J Cancer Prev,* **13**, 127-32.

Buranrat B, Prawan A, Kukongviriyapan U, Kongpetch S, Kukongviriyapan V (2010). Dicoumarol enhances gemcitabine-induced cytotoxicity in high *NQO1*-expressing cholangiocarcinoma cells. *World J Gastroenterol*, **16**, 2362-70.

Chen X, Wang H, Xie W, et al (2006). Association of *CYP1A2* genetic polymorphisms with hepatocellular carcinoma susceptibility: a case-control study in a high-risk region of China. *Pharmacogenet Genomics*, **16**, 219-227.

Cheng DM, Jiang YG, Huang CY, et al (2010). Polymorphism of *MTHFR* C677T, serum vitamin levels and cognition in subjects with hyperhomocysteinemia in China. *Nutr Neurosci*, **13**, 175-82.

Chutinet A, Suwanwela NC, Snabboon T, et al (2012) Association between genetic polymorphisms and sites of cervicocerebral artery atherosclerosis. *J Stroke Cerebrovasc Dis*, **21**, 379-85.

Dinkova-Kostova AT, Talalay P (2010). NAD(P)H:quinone acceptor oxidoreductase 1 (*NQO1*), a multifunctional antioxidant enzyme and exceptionally versatile cytoprotector. *Arch Biochem Biophys*, **501**, 116-23.

Economopoulos KP, Sergentanis TN (2010). *GSTM1*, *GSTT1*, *GSTP1*, *GSTA1* and colorectal cancer risk: a comprehensive meta-analysis. *Eur J Cancer*, **46**, 1617-31.

Egan KM, Cai Q, Shu XO, et al (2004). Genetic polymorphisms in *GSTM1*, *GSTP1*, and *GSTT1* and the risk for breast cancer: results from the Shanghai Breast Cancer Study and meta-analysis. *Cancer Epidemiol Biomarkers Prev*, **13**, 197-204.

Eichelbaum M, Ingelman-Sundberg M, Evans WE (2006). Pharmacogenomics and individualized drug therapy. *Annu Rev Med*, **57**, 119-37.

Escobar-Garcia DM, Del Razo LM, Sanchez-Pena LC, et al (2012). Association of glutathione S-transferase Omega 1-1 polymorphisms (A140D and E208K) with the expression of interleukin-8 (IL-8), transforming growth factor beta (TGF-beta), and apoptotic protease-activating factor 1 (Apaf-1) in humans chronically exposed to arsenic in drinking water. *Arch Toxicol*, **86**, 857-68.

Garcia-Closas M, Malats N, Silverman D, et al (2005). *NAT2* slow acetylation, *GSTM1 null* genotype, and risk of bladder cancer: results from the Spanish Bladder Cancer Study and meta-analyses. *Lancet*, **366**, 649-59.

Ginsberg G, Smolenski S, Neafsey P, et al (2009). The influence of genetic polymorphisms on population variability in six xenobiotic-metabolizing enzymes. *J Toxicol Environ Hlth B Crit Rev*, **12**, 307-33.

Guengerich FP, Johnson WW, Shimada T, et al (1998). Activation and detoxication of aflatoxin B1. *Mutat Res*, **402**, 121-8.

Hayes JD, Flanagan JU, Jowsey IR (2005). Glutathione transferases. *Annu Rev Pharmacol Toxicol*, **45**, 51-88.

Honjo S, Srivatanakul P, Sriplung H, et al (2005). Genetic and environmental determinants of risk for cholangiocarcinoma via *Opisthorchis viverrini* in a densely infested area in Nakhon Phanom, northeast Thailand. *Int J Cancer*, **117**, 854-60.

IARC (1994). Infection with liver flukes (*Opisthorchis viverrini*, Opisthorchis felineus and Clonorchis sinensis). *IARC Monogr Eval Carcinog Risks Hum*, **61**, 121-75.

Irigaray P, Belpomme D (2010). Basic properties and molecular mechanisms of exogenous chemical carcinogens. *Carcinogenesis*, **31**, 135-48.

Kim D, Guengerich FP (2005). Cytochrome P450 activation of arylamines and heterocyclic amines. *Annu Rev Pharmacol Toxicol*, **45**, 27-49.

Kim J, Cho YA, Kim DH, et al (2012). Dietary intake of folate and alcohol, *MTHFR* C677T polymorphism, and colorectal cancer risk in Korea. *Am J Clin Nutr*, **95**, 405-12.

Klaassen CD (2007). Casarett and Doull's Toxicology: The Basic Science of Poisons, 7th ed. Mc-Graw-Hill, New York.

Ko KH, Kim NK, Yim DJ, et al (2006). Polymorphisms of 5,10-methylenetetrahydrofolate reductase (*MTHFR* C677T) and thymidylate synthase enhancer region (TSER) as a risk factor of cholangiocarcinoma in a Korean population. *Anticancer Res*, **26**, 4229-33.

Kukongviriyapan V, Prawan A, Tassaneyakul W, Aiemsa-Ard J, Warasiha B (2003a). Arylamine N-acetyltransferase-2 genotypes in the Thai population. *Br J Clin Pharmacol*, **55**, 278-81.

Kukongviriyapan V, Prawan A, Warasiha B, Tassaneyakul W and Aiemsa-ard J (2003b) Polymorphism of N-acetyltransferase 1 and correlation between genotype and phenotype in a Thai population. Eur J Clin Pharmacol 59:277-281.

Kurathong S, Lerdverasirikul P, Wongpaitoon V, Pramoolsinsap C, Kanjanapitak A, Varavithya W, Phuapradit P, Bunyaratvej S, Upatham ES and Brockelman WY (1985) *Opisthorchis viverrini* infection and cholangiocarcinoma. A prospective, case-controlled study. Gastroenterology 89:151-156.

Kushida H, Fujita K, Suzuki A, et al (2000). Metabolic

activation of N-alkylnitrosamines in genetically engineered Salmonella typhimurium expressing CYP2E1 or CYP2A6 together with human NADPH-cytochrome P450 reductase. *Carcinogenesis*, **21**, 1227-32.

Landi MT, Sinha R, Lang NP, Kadlubar FF (1999). Chapter 16. Human cytochrome P4501A2. *IARC Sci Pub*, **148**, 173-95.

Le Marchand L, Donlon T, Kolonel LN, Henderson BE, Wilkens LR (2005a) Estrogen metabolism-related genes and breast cancer risk: the multiethnic cohort study. *Cancer Epidemiol Biomarkers Prev*, **14**, 1998-2003.

Le Marchand L, Wilkens LR, Kolonel LN, Henderson BE (2005b). The *MTHFR* C677T polymorphism and colorectal cancer: the multiethnic cohort study. *Cancer Epidemiol Biomarkers Prev*, **14**, 1198-203.

Li D, Jiao L, Li Y, et al (2006). Polymorphisms of cytochrome P4501A2 and *N*-acetyltransferase genes, smoking, and risk of pancreatic cancer. *Carcinogenesis*, **27**, 103-111.

Li W, Yue W, Zhang L, et al (2012). Polymorphisms in *GSTM1*, *CYP1A1*, CYP2E1, and CYP2D6 are associated with susceptibility and chemotherapy response in non-small-cell lung cancer patients. *Lung*, **190**, 91-8.

Lo HW, Ali-Osman F (2007). Genetic polymorphism and function of glutathione S-transferases in tumor drug resistance. *Curr Opin Pharmacol*, **7**, 367-74.

Loeb LA, Harris CC (2008). Advances in chemical carcinogenesis: a historical review and prospective. *Cancer Res*, **68**, 6863-72.

Marahatta SB, Punyarit P, Bhudisawasdi V, Paupairoj A, Wongkham S, Petmitr S (2006). Polymorphism of glutathione S-transferase omega gene and risk of cancer. *Cancer Lett*, **236**, 276-81.

Mazaki T, Masuda H, Takayama T (2011). Polymorphisms and pancreatic cancer risk: a meta-analysis. *Eur J Cancer Prev*, **20**, 169-83.

Menzel HJ, Sarmanova J, Soucek P, et al (2004). Association of *NQO1* polymorphism with spontaneous breast cancer in two independent populations. *Br J Cancer*, **90**, 1989-94.

Mitacek EJ, Brunnemann KD, Suttajit M, et al (2008). Geographic distribution of liver and stomach cancers in Thailand in relation to estimated dietary intake of nitrate, nitrite, and nitrosodimethylamine. *Nutr Cancer*, **60**, 196-203.

Mo Z, Gao Y, Cao Y, Gao F, Jian L (2009). An updating meta-analysis of the *GSTM1*, *GSTT1*, and GSTP1 polymorphisms and prostate cancer: a HuGE review. *Prostate*, **69**, 662-88.

Modugno F, Knoll C, Kanbour-Shakir A, Romkes M (2003). A potential role for the estrogen-metabolizing cytochrome P450 enzymes in human breast carcinogenesis. *Breast Cancer Res Treat*, **82**, 191-7.

Moysich KB, Shields PG, Freudenheim JL, et al (1999). Polychlorinated biphenyls, cytochrome P4501A1 polymorphism, and postmenopausal breast cancer risk. *Cancer Epidemiol Biomarkers Prev*, **8**, 41-4.

Nakachi K, Imai K, Hayashi S, Kawajiri K (1993). Polymorphisms of the *CYP1A1* and glutathione S-transferase genes associated with susceptibility to lung cancer in relation to cigarette dose in a Japanese population. *Cancer Res*, **53**, 2994-9.

Nakajima M, Yokoi T, Mizutani M, et al (1999) Genetic polymorphism in the 5'-flanking region of human *CYP1A2* gene: effect on the *CYP1A2* inducibility in humans. *J Biochem*, **125**, 803-8.

Nebert DW, Dalton TP (2006). The role of cytochrome P450 enzymes in endogenous signalling pathways and environmental carcinogenesis. *Nat Rev Cancer*, **6**, 947-60.

Osawa Y, Osawa KK, Miyaishi A, et al (2007). *NAT2* and *CYP1A2* polymorphisms and lung cancer risk in relation to smoking status. *Asian Pac J Cancer Prev*, **8**, 103-8.

Parkinson A (1996). Biotransformation of xenobiotics, in Casarett and Doull's Toxicology: The basic science of poisons (Kalaassen CD ed) pp 113-186, McGraw-Hill, New York.

Peamkrasatam S, Sriwatanakul K, Kiyotani K, et al (2006). *In vivo* evaluation of coumarin and nicotine as probe drugs to predict the metabolic capacity of CYP2A6 due to genetic polymorphism in Thais. *Drug Metab Pharmacokinet*, **21**, 475-84.

Pongstaporn W, Pakakasama S, Sanguansin S, Hongeng S, Petmitr S (2009). Polymorphism of glutathione S-transferase Omega gene: association with risk of childhood acute lymphoblastic leukemia. *J Cancer Res Clin Oncol*, **135**, 673-8.

Powers HJ (2005). Interaction among folate, riboflavin, genotype, and cancer, with reference to colorectal and cervical cancer. *J Nutr*, **135**, 2960-6.

Prawan A, Kukongviriyapan V, Tassaneeyakul W, Pairojkul C, Bhudhisawasdi V (2005). Association between genetic polymorphisms of *CYP1A2*, arylamine N-acetyltransferase 1 and 2 and susceptibility to cholangiocarcinoma. *Eur J Cancer Prev*, **14**, 245-50.

Safarinejad MR, Safarinejad S, Shafiei N (2011). Association of genetic polymorphism of glutathione S-transferase (*GSTM1*, *GSTT1*, GSTP1) with bladder cancer susceptibility. *Urol Oncol*, **10**, 1016.

Schmuck EM, Board PG, Whitbread AK, et al (2005). Characterization of the monomethylarsonate reductase and dehydroascorbate reductase activities of Omega class glutathione transferase variants: implications for arsenic metabolism and the age-at-onset of Alzheimer's and Parkinson's diseases. *Pharmacogenet Genomics*, **15**, 493-501.

Shimada T (2006). Xenobiotic-metabolizing enzymes involved in activation and detoxification of carcinogenic polycyclic aromatic hydrocarbons. *Drug Metab Pharmacokinet*, **21**, 257-76.

Shin HR, Oh JK, Masuyer E, et al (2010). Epidemiology of cholangiocarcinoma: an update focusing on risk factors. *Cancer Sci*, **101**, 579-85.

Siegel D, McGuinness SM, Winski SL, Ross D (1999). Genotype-phenotype relationships in studies of a polymorphism in NAD(P)H:quinone oxidoreductase 1. *Pharmacogenetics*, **9**, 113-21.

Siegel D, Ross D (2000). Immunodetection of NAD(P) H:quinone oxidoreductase 1 (*NQO1*) in human tissues. *Free Radic Biol Med*, **29**, 246-53.

Sim E, Lack N, Wang CJ, et al (2008). Arylamine N-acetyltransferases: structural and functional implications of polymorphisms. *Toxicology*, **254**, 170-83.

Songserm N, Promthet S, Sithithaworn P, et al (2012). Risk factors for cholangiocarcinoma in high-risk area of Thailand: role of lifestyle, diet and methylenetetrahydrofolate reductase polymorphisms. *Cancer Epidemiol*, **36**, 89-94.

Srivatanakul P, Ohshima H, Khlat M, et al (1991a). Endogenous nitrosamines and liver fluke as risk factors for cholangiocarcinoma in Thailand. *IARC Sci Pub*, **105**, 88-95.

Srivatanakul P, Parkin DM, Jiang YZ, et al (1991b). The role of infection by *Opisthorchis viverrini*, hepatitis B virus, and aflatoxin exposure in the etiology of liver cancer in Thailand. A correlation study. *Cancer*, **68**, 2411-7.

Suzuki H, Morris JS, Li Y, et al (2008). Interaction of the cytochrome P4501A2, SULT1A1 and NAT gene polymorphisms with smoking and dietary mutagen intake in modification of the risk of pancreatic cancer. *Carcinogenesis*, **29**, 1184-91.

Thamavit W, Bhamarapravati N, Sahaphong S, Vajrasthira S, Angsubhakorn S (1978). Effects of dimethylnitrosamine on

induction of cholangiocarcinoma in *Opisthorchis viverrini*-infected Syrian golden hamsters. Cancer Res 38:4634-4639.

Walker K, Ginsberg G, Hattis D, et al (2009). Genetic polymorphism in N-Acetyltransferase (NAT): Population distribution of *NAT1* and *NAT2* activity. *J Toxicol Environ Hlth B Crit Rev*, **12**, 440-72.

Wang H, Tan W, Hao B, et al (2003). Substantial reduction in risk of lung adenocarcinoma associated with genetic polymorphism in CYP2A13, the most active cytochrome P450 for the metabolic activation of tobacco-specific carcinogen NNK. *Cancer Res*, **63**, 8057-61.

White DL, Li D, Nurgalieva Z, El-Serag HB (2008) Genetic variants of glutathione S-transferase as possible risk factors for hepatocellular carcinoma: a HuGE systematic review and meta-analysis. *Am J Epidemiol*, **167**, 377-89.

Williams JA, Stone EM, Fakis G, et al (2001). N-Acetyltransferases, sulfotransferases and heterocyclic amine activation in the breast. *Pharmacogenetics*, **11**, 373-88.

Yang FY, Guan QK, Cui YH, et al (2012). NAD(P)H quinone oxidoreductase 1 (*NQO1*) genetic C609T polymorphism is associated with the risk of digestive tract cancer: a meta-analysis based on 21 case-control studies. *Eur J Cancer Prev*, **21**, 42-1.

Yu H, Liu H, Wang LE, Wei Q (2012). A functional *NQO1* 609C>T polymorphism and risk of gastrointestinal cancers: a meta-analysis. *PLoS One*, **7**, 30566.

Zeekpudsa P, Prawan A, Kukongviriyapan V, Bhudhisawasdi V (2009). Genetic polymorphism of NAD(P) H-quinone reductase-1 in Thais and its association with cholangiocarcinoma, in 3rd Asian Pacific Regional Meeting International Society for the Study of Xenobiotics p 75, Bangkok, Thailand.

Zhu LR, Thomas PE, Lu G, et al (2006). CYP2A13 in human respiratory tissues and lung cancers: an immunohistochemical study with a new peptide-specific antibody. *Drug Metab Dispos*, **34**, 1672-6.

Journal of Experimental & Clinical Cancer Research

RESEARCH Open Access

# Suppression of NAD(P)H-quinone oxidoreductase 1 enhanced the susceptibility of cholangiocarcinoma cells to chemotherapeutic agents

Ponsilp Zeekpudsa[1,3], Veerapol Kukongviriyapan[1,3], Laddawan Senggunprai[1,3], Banchob Sripa[2,3] and Auemduan Prawan[1,3*]

## Abstract

**Background:** Cholangiocarcinoma (CCA) is highly resistant to most of the known chemotherapeutic treatments. NAD(P)H-quinone oxidoreductase 1 (NQO1) is an antioxidant/detoxifying enzyme recently recognized as an important contributor to chemoresistance in some human cancers. However, the contribution of NQO1 to chemotherapy resistance in CCA is unknown.

**Methods:** Two CCA cell lines, KKU-100 and KKU-M214, with high and low NQO1 expression levels, respectively, were used to evaluate the sensitivity to chemotherapeutic agents; 5-fluorouracil (5-FU), doxorubicin (Doxo), and gemcitabine (Gem). NQO1 and/or p53 expression in KKU-100 cells were knocked down by siRNA. NQO1 was over-expressed in KKU-M214 cells by transfection with pCMV6-XL5-NQO1 expression vector. CCA cells with modulated NQO1 and/or p53 expression were treated with chemotherapeutic agents, and the cytotoxicity was assessed by SRB assay. The mechanism of enhanced chemosensitivity was evaluated by Western blot analysis.

**Results:** When NQO1 was knocked down, KKU-100 cells became more susceptible to all chemotherapeutic agents. Conversely, with over-expression of NQO1 made KKU-M214 cells more resistant to chemotherapeutic agents. Western blot analysis suggested that enhanced chemosensitivity was probably due to the activation of p53-mediated cell death. Enhanced susceptibility to chemotherapeutic agents by NQO1 silencing was abolished by knockdown of p53.

**Conclusions:** These results suggest that inhibition of NQO1 could enhance the susceptibility of CCA to an array of chemotherapeutic agents.

**Keywords:** NAD(P)H-quinone oxidoreductase 1 (NQO1), Cholangiocarcinoma (CCA), 5-fluorouracil (5-FU), Doxorubicin (Doxo), Gemcitabine (Gem), p53

## Background

Cholangiocarcinoma (CCA) is a malignant cancer arising from neoplastic transformation of cholangiocytes, the epithelial cells lining of intrahepatic and extrahepatic bile duct [1,2]. The incidence of CCA is extremely high in northeastern Thailand [3,4]. The most important risk factor is the liver fluke (*Opisthorchis viverrini*) infection [5,6]. Several lines of studies have shown that the incidence and mortality rates of intrahepatic CCA are increasing worldwide [2,7]. The prognosis is generally poor because most patients present at advanced disease and early diagnosis is difficult [7]. Curative surgical resection is considered the most effective treatment, but most cases are inoperable at the time of diagnosis [7]. Unfortunately, chemotherapeutic agents are modestly effective on CCA and drug resistance is the major obstacle in the treatment. Multiple mechanisms are assumed to be involved in drug resistance; *e.g.*, alteration of drug metabolizing enzymes, efflux transporters, cytoprotective enzymes or derangement of intracellular signaling system [8]. It is an urgent need to search for novel treatments for CCA.

* Correspondence: peuamd@kku.ac.th
[1]Department of Pharmacology, Faculty of Medicine, Khon Kaen University, Khon Kaen 40002, Thailand
[3]3Liver Fluke and Cholangiocarcinoma Research Center, Khon Kaen University, Khon Kaen, Thailand
Full list of author information is available at the end of the article

BioMed Central

© 2014 Zeekpudsa et al.; licensee BioMed Central Ltd. This is an Open Access article distributed under the terms of the Creative Commons Attribution License (http://creativecommons.org/licenses/by/2.0), which permits unrestricted use, distribution, and reproduction in any medium, provided the original work is properly cited. The Creative Commons Public Domain Dedication waiver (http://creativecommons.org/publicdomain/zero/1.0/) applies to the data made available in this article, unless otherwise stated.

NAD(P)H-quinone oxidoreductase 1 (NQO1 or DT-diaphorase, EC 1.6.99.2) is a drug metabolizing enzyme. Its over-expression has been observed in many cancers of the liver, thyroid, breast, colon, and pancreas [9,10]. NQO1 is a flavoprotein mainly expressed in cytosol, catalyzing an obligate two-electron reduction of a broad range of substrates, particularly quinines, quinone-imines, nitro and azo compounds as the most efficient substrates [11-15]. NQO1 has several functions including xenobiotic detoxification, superoxide scavenging, and modulation of p53 proteasomal degradation [12]. Chronic inflammation suppresses NQO1 expression [16] and may increase susceptibility to cell injury. Increasing number of evidences suggest that up-regulation of NQO1 at the early process of carcinogenesis may provide cancer cells a growth advantage [17,18]. Since NQO1 is also an antioxidant enzyme, it may protect cancer cells by removing free radicals and making cells more resistant to anticancer agents, particularly to oxidative stress inducers.

Recently, a role of NQO1 in cancer chemotherapy has been demonstrated by several groups. Inhibition of NQO1 by a pharmacological inhibitor, dicoumarol, suppressed urogenital and pancreatic cancer cell growth and also potentiated cytotoxicity of cisplatin and doxorubicin [19,20]. Significant association was observed between high NQO1 expression in CCA tissue and short survival [21]. We have recently demonstrated that dicoumarol potentiated gemcitabine-induced cytotoxicity on CCA cells with high NQO1 activity [22]. The chemosensitizing effect was associated with oxidative stress and induction of p53 protein [20]. However, dicoumarol could exert several effects apart from inhibition of NQO1, such as suppression of JNK and NF-κB pathways, and potentiation of apoptosis induced by TNF-α in HeLa cells [23]. The exact mechanism of the chemosensitizing effect conferred by suppression of NQO1 still remains unclear. The importance of NQO1 on modulation of p53 is also conflicting [22,24].

In the present study, we validate the role of NQO1 in cytoprotection, and then demonstrate that suppression of NQO1 potentiates antitumor activity of chemotherapeutic agents. These results suggest the crucial role of NQO1 in cancer cells. NQO1 may be a potential target molecule to enhance the susceptibility of tumor cells to chemotherapeutic agents.

## Methods

### Human cell line cultures and chemotherapeutic agents

Two human CCA cell lines, KKU-100 and KKU-M214, were developed from tumor tissues of CCA patients at the Srinagarind Hospital, Faculty of Medicine, Khon Kaen University. Liver Chang cells and normal bile duct epithelial cells, MMNK1, were also used in this study. CCA cells and normal cells were routinely cultured in Ham's F12 media, supplemented with 4 mmol/L L-glutamine, 12.5 mmol/L N-2-hydroxyethylpiperazine-N'-2-ethanesulfonic acid (HEPES), at pH 7.4, 100 U/mL penicillin, 100 μg/mL streptomycin sulfate, and 10% fetal bovine serum (FBS) in a humidified atmosphere containing 5% $CO_2$ at 37°C. The media was renewed every 2–3 days. After the cells became confluent, cells were trypsinized with 0.25% trypsin-EDTA and subcultured in the same media. Some aliquots of cells were transferred to freezing medium containing 10% DMSO and stored at −80°C for subsequent use.

Chemotherapeutic agents were selected on the basis of the frequent usage for CCA, gastrointestinal tract cancers and solid tumors. These included 5-fluorouracil (5-FU) dissolved in DMSO (100 mM), doxorubicin HCl (Boryung Pharm, Seoul, South Korea: Doxo) dissolved in DMSO (100 mM), and gemcitabine (Gemzar, Eli Lilly, IN, USA: Gem) dissolved in phosphate-buffered saline (PBS: 137 mM NaCl, 2.7 mM KCl, 10 mM $Na_2HPO_4$, 2 mM $KH_2PO_4$, pH 7.4). They were added to the culture media without FBS to make final concentrations indicated in the "Results" section and incubated for a designated period of time.

### Transient transfection of NQO1 and/or p53 small interfering RNA (NQO1 and/or p53 siRNA)

Pre-designed NQO1 siRNA (siGENOME SMARTpool siRNA #M-005133-02-0020), p53 siRNA (siGENOME SMARTpool siRNA #M-003329-03-0005), and control siRNA (siGENOME non-targeting siRNA #D-001210-02-20) were purchased from Thermo Scientific. In this study, NQO1 siRNA and p53 siRNA were the pooled siRNAs, each is composed of four different sequences of siRNA, targeting for NQO1 and p53, respectively. For transfection of the siRNA, $1.5\times10^5$ KKU-100 cells were plated in 6-well plates and grown in Ham's F12 medium supplemented with FBS, without antibiotics. The cells were transfected with 50 or 100 pmole of the siRNA for 6 hr using 0.4 or 2 μL of Lipofectamine™ 2000 reagent (Invitrogen, Calsbad, CA, USA) in 500 μL of Ham's F12 medium without FBS and antibiotics. After transfection, the cells were added with 1.5 mL of Ham's F12 medium supplemented with FBS, without antibiotics, and incubated further for 24-48 hr. The efficiency of the NQO1 knockdown by transient transfection was determined by gene expression with reverse transcription real-time polymerase chain reaction (RT-qPCR) using specific primers, NQO1 activity assay, and Western blotting analysis.

For cytotoxicity assay, CCA cells were seeded onto 96-well cultured plates with FBS, without antibiotics at a density of $5 \times 10^3$ cells/well for an overnight. The cells were transfected with 3 pmole of the siRNA for 6 hr using 0.06 μL of Lipofectamine™ 2000 reagent in 100 μL of Ham's F12 medium without FBS and antibiotics. After

6 hr, the cells were added 100 μL of Ham's F12 medium supplemented with FBS, without antibiotics, and incubated for 48 hr. The cells were then incubated with chemotherapeutic agents in serum free medium for additional 24 hr.

### Transfection of NQO1 vector into CCA cells

A plasmid encoding human wild-type NQO1 in pCMV6-XL5 (4,707 bp) was purchased from Origene Technologies (#SC119599; Rockville, MD). The insert cDNA (1,120 bp) contained the complete NQO1 coding sequence (NM_000903.2). For transfection of the pCMV6-XL5-NQO1 or pCMV6-XL5, as a negative control vector, KKU-M214 at a density of $5\times10^5$ cells were plated in 6-well plates and grown overnight. At 70-80% confluent condition, cells were transfected with 2.5 μg of pCMV6-XL5-NQO1 or pCMV6-XL5 for 24 hr using Lipofectamine® LTX and Plus™ reagent (Invitrogen) protocol as directed by the manufacturer in 2 mL of Ham's F12 medium without FBS and antibiotics. Then the cells were collected for Western blot analysis and enzymatic assay. The empty vector control was prepared by cutting the NQO1 insert site from pCMV6-XL5-NQO1 plasmid at the *Eco*RI and *Xbal*I site. The bearing vector was ligated with oligonuclotide (non-coding sequence) and cloned into *E. coli* (JM109). The empty vector control was purified and the presence of vector was confirmed by restriction digestion and run it on 2% agarose gel.

For cytotoxicity assay, KKU-M214 cells were seeded onto 96-well cultured plates at a density of $7.5 \times 10^3$ cells/well for an overnight, the cells were transfected with 100 ng of pCMV6-XL5-NQO1 or pCMV6-XL5 using Lipofectamine® LTX and Plus™ reagent for 24 hr. The cells were then incubated with chemotherapeutic agents in serum free medium for additional 24 hr (Doxo) or 48 hr (5-FU and Gem), since it was the optimal incubation time for each drug.

### NQO1 enzyme activity assay

NQO1 assay was performed according to the method described previously [20]. Cells were seeded at $7.5 \times 10^3$ cells/well in flat-bottomed 96-well cultured plates overnight. After cells were cultured for the designated time, cells were lysed with 50 μL solution containing 0.8% digitonin and agitated on a shaker at room temperature for 10 min. Twenty-five microliter of 0.55% dicoumarol was added into culture wells designated as baseline activity, while the corresponding paired wells were added with distilled water (DW) designated as the test activity wells. After that, all wells were added with 200 μL of reaction mixture (the following stock solution was prepared for each set of assay: 7.5 mL of 0.5 M Tris–HCl (pH 7.4), 100 mg of bovine serum albumin (BSA), 1 mL of 1.5% Tween-20 solution, 0.1 mL of 7.5 mM FAD, 1 mL of 150 mM glucose-6-phosphate, 100 μL of 50 mM β-NADP, 275 unit of yeast glucose-6-phosphate dehydrogenase, 45 mg of MTT, and DW to a final volume of 150 mL and menadione (1 μL of 50 mM menadione dissolved in acetonitrile per milliliter of reaction mixture) was added just before the mixture is dispensed into the microtiter plates. A blue color developed and the plates were placed into a microplate reader with filter wavelength of 620 nm and readings were made at 0.5 min interval for about 10 min. The rate of increase of the optical readings with times represents the activity of the reaction. Using the extinction coefficient of MTT formazan of 11,300 $M^{-1}$ $cm^{-1}$ at 610 nm and correction for the light path of the microplate, NQO1 activity was expressed as nmol/min/mg protein.

### Cytotoxicity or SRB assay

Cytotoxicity testing is used to evaluate the effects of chemotherapeutic agents. In brief, CCA cells were seeded onto 96-well cultured plates at a density of $7.5 \times 10^3$ cells/well overnight, then media was renewed with fresh media containing test compound and further incubated for the indicated times. Assay was performed at the end-point of treatment to determine amount of protein remaining in each well. Media was discarded and replaced with 100 μL of ice-cold 10% trichloroacetic acid (TCA) and placed in 4°C for at least 1 hr. Then TCA was removed and wells were carefully rinsed with deionized (DI) water for 5 times. After 10 min of air drying, 50 μL of 0.4% sulforhodamine B (SRB) in 1% acetic acid was added for 30 min. Cells were rinsed 3–4 times with 1% acetic acid and air dried for 1 hr at room temperature. Finally, adhered cells were solubilized with 200 μL of 10 mM Tris base and plates were shaken for 20 min before absorbance reading with a microplate reader with filter wavelength of 540 nm.

### Real-time polymerase chain reaction (real-time PCR or qPCR)

CCA cells were seeded in 6-well plates at the density of $1.5\times10^5$ cells/well. Total RNA was extracted from CCA cell lines using TRIzol® reagent following the manufacturer's instructions (Invitrogen). Total RNA was isolated using a previously described method [20]. Total RNA (1 μg) was reverse transcribed in a 20 μL reaction mixture, containing 0.5 μg of oligo(dT)15 primer, 20 U of RNasin® ribonuclease inhibitor, and 200 U of ImProm-II™ reverse transcriptase in 1× PCR buffer, 3 mmol/L $MgCl_2$, and 1 mmol/L dNTPs. The first-strand cDNA was synthesized at conditions of 42°C for 60 min. The reverse transcription products served as templates for real-time PCR. PCR amplification was performed using specific primers for the NQO1, wild type p53 and the internal control using β-actin. The primer sequences were

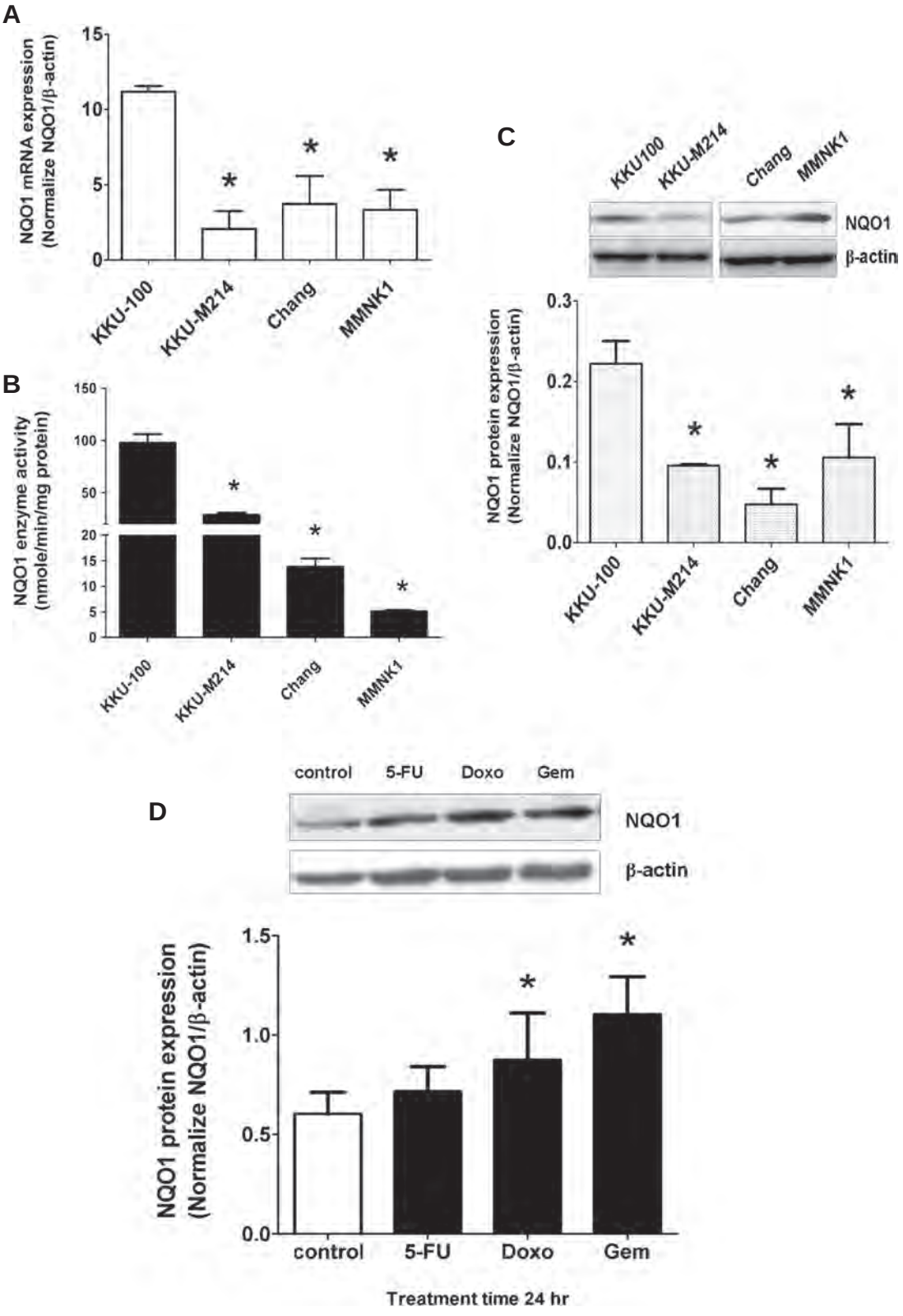


**Figure 1** (See legend on next page.)

(See figure on previous page.)
**Figure 1 Basal level of NQO1 mRNA, protein expression, and enzyme activity of CCA cells and NQO1 protein induction by chemotherapeutic agents (5-FU, Doxo, and Gem). (A)** Basal NQO1 mRNA expression in CCA cell lines (KKU-100 and KKU-M214) and two other cell lines (Chang and MMNK1 cells) analyzed by qPCR. The bars represent relative mRNA expression of NQO1 normalized with β-actin as internal control. *$p < 0.05$ vs KKU-100 cells. **(B)** Basal NQO1 enzyme activity analyzed by enzymatic methods. *$p < 0.05$ vs KKU-100 cells. **(C)** Basal NQO1 protein expression analyzed by Western Blot analysis using β-actin as internal control. Representative images of NQO1 and β-actin are shown in the top panel of the figure. *$p < 0.05$ vs KKU-100 cells. **(D)** Effect of chemotherapeutic agents on NQO1 protein expression in KKU-100 cells. Cells were exposed to 5-FU (3 μM), Doxo (0.1 μM), and Gem (0.1 μM) for 24 hr. Data represent mean ± SEM, each from three separated experiments. *$p < 0.05$ vs the untreated control.

as follows: 1) NQO1 (NM_000903.2): forward primer 5'-GGCAGAAGAGCACTGATCGTA-3' and reverse primer 5'-TGATGGGATTGAAGTTCATGGC-3'; 2) wild type p53 (NM_005256778.1) [25]: forward primer 5'-ATGGAGGAGCCGCAGTCAGATCC-3' and reverse primer 5'-TTCTGTCTTCCCGGACTGAGTCTGACT-3'; 3) β-actin: forward primer 5'-TGCCATCCTAAAAGCCAC-3' and reverse primer 5'-TCAACTGGTCTCAAGTCAGTG-3'. The real-time fluorescence PCR, based on EvaGreen® dye, was carried out in a final volume of 20 μL containing 1x SsoFast™ EvaGreen® supermix (#172-5200; Bio-Rad, CA, USA), 0.5 μmol/L of each NQO1 or wild type p53, and 0.25 μmol/L of β-actin primer. Thermal cycling was performed for each gene in duplicate on cDNA samples in 96-well reaction plates using the ABI 7500 Sequence Detection system (Applied Biosystems). A negative control was also included in the experimental runs. The negative control was set up by substituting the template with DI water. Real-time PCR was conducted with the following cycling conditions: 95°C for 3 min, followed by 40 cycles of 95°C for 15 s and 60°C for 31 s. To verify the purity of the products, a melting curve analysis was performed after each run. Upon completion of 40 PCR amplification cycles, there was a dissociation step of ramping temperature from 60°C to 95°C steadily for 20 min, while the fluorescence signal was continually monitored for melting curve analysis. The concentration of PCR product was calculated on the basis of established standard curve derived from serial dilutions of the positive control for NQO1, wild type p53 and β-actin in the CCA cell lines.

### Western blot analysis

After treatment with chemotherapeutic agents, CCA cells were washed with PBS, collected, and lysed at 4°C with 1x cell lysis buffer with 1 mmol/L dithiothreitol and 0.1 mmol/L phenylmethylsulfonyl fluoride (PMSF) with vigorous shaking. After centrifugation at 12,000 *g* for 30 min, supernatant was collected and stored at −80°C until use. Thirty microgram of the protein samples were mixed with 5x loading-dye buffer, heated at 90°C for 10 min, and proteins were then separated by electrophoresis in 10% SDS-polyacrylamide gel. Proteins were transferred to polyvinylidene difluoride (PVDF) membranes at 180 mA for 1 hr. The PVDF membranes were blocked for 1 hr at room temperature with 5% (w/v) skim milk powder in PBS with 0.1% Tween-20. PVDF membrane was incubated overnight at 4°C with primary antibodies diluted with PBS/Tween-20. The antibodies purchased from Santa Cruz BioTechnology, Inc. (California, USA) were: rabbit polyclonal IgG Bax (1:2500) (#sc-493), rabbit polyclonal IgG cyclin D1 (1:1000) (#sc-718), rabbit polyclonal IgG p21 (1:500) (#sc-56335), mouse polyclonal IgG p53 (1:500) (#sc-98), and mouse monoclonal IgG β-actin (1:2500) (#sc-1616). The rabbit polyclonal IgG NQO1 (1:2500) (#ab34173) was purchased from Abcam (Cambridge, MA, USA). The primary antibody was then removed and the blots were extensively washed with PBS/Tween-20. Blots were then incubated for 2 hr at room temperature with the secondary antibody horseradish peroxidase-labeled goat anti-mouse IgG (#sc-2005) or goat anti-rabbit IgG (#sc-2004) at 1:5000 dilutions in PBS. After removal of the secondary antibody and extensive washing in PBS/Tween-20, the blots were incubated in the ECL substrate solution (Amersham™ ECL™ prime Western Blotting detection reagent; GE Healthcare, Piscataway, NJ, USA). Densities of the specific bands of Bax, cyclin D1, p21, p53, NQO1 and β-actin were visualized and captured by ImageQuant™ LAS4000 (GE Healthcare).

### Statistical analysis

Data were expressed as mean ± SEM of triplicate assays from three independent experiments. An analysis of variance with repeated measurement was used to determine significant differences between each experimental group. The level of significance was set at $p < 0.05$.

## Results

### NQO1 expression in CCA cells is constitutively high and increased further by chemotherapeutic agents

We first examined the NQO1 expression in two CCA cell lines, KKU-100 and KKU-M214, and two other cell lines (liver Chang cells and bile duct epithelial MMNK1 cells). KKU-100 cells showed the highest expression in NQO1 mRNA, protein and enzymatic activity (Figure 1A-C). Chang and MMNK1 cell lines showed relatively low

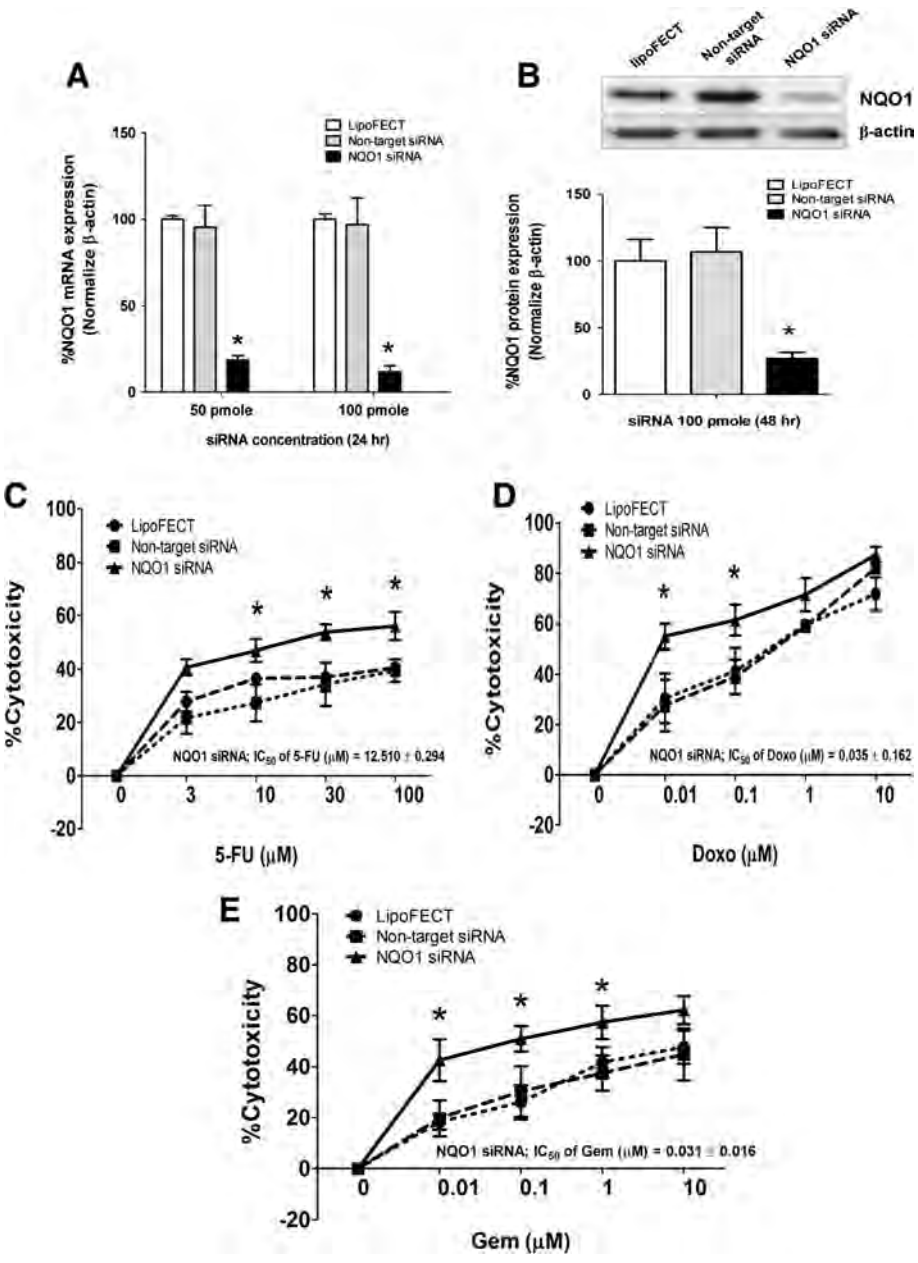


**Figure 2 Knockdown of NQO1 by siRNA sensitized KKU-100 cells to chemotherapeutic agents. (A-B)** Effect of NQO1 siRNA on mRNA and protein levels of NQO1 in KKU-100 cells. Cells were transfected with the pooled siRNA against NQO1 gene for 24 hr and 48 hr. Data represent mean ± SEM, each from three separated experiments. *$p < 0.05$ vs the non-targeting siRNA transfected cells. **(C-E)** Cytotoxicity of chemotherapeutic agents on NQO1 siRNA transfected KKU-100 cells. Forty-eight hour after transfection, cells were treated with varied concentration of chemotherapeutic agents; 5-FU, Doxo, and Gem for another 24 hr as described in the "Methods" section. The cytotoxicity was evaluated by SRB assay. Data represent mean ± SEM, each from three separated experiments. *$p < 0.05$ vs the non-targeting siRNA transfected cells.

enzymatic activity. KKU-100 and KKU-M214 cells were used in the subsequent study as the representative of the high and low NQO1 expressing cells, respectively. To examine whether chemotherapeutic agents could induce the antioxidative stress response by induction of NQO1, KKU-100 was treated with 3 μM of 5-FU, 0.1 μM of Doxo, and 0.1 μM of Gem for 24 hr. The results showed that NQO1 protein expression was increased after treatment with Doxo and Gem, but not 5-FU (Figure 1D).

### NQO1 gene silencing sensitizes CCA cells to chemotherapeutic agents

To verify the possibility that NQO1 can modulate the susceptibility of CCA cells to chemotherapeutic agents,

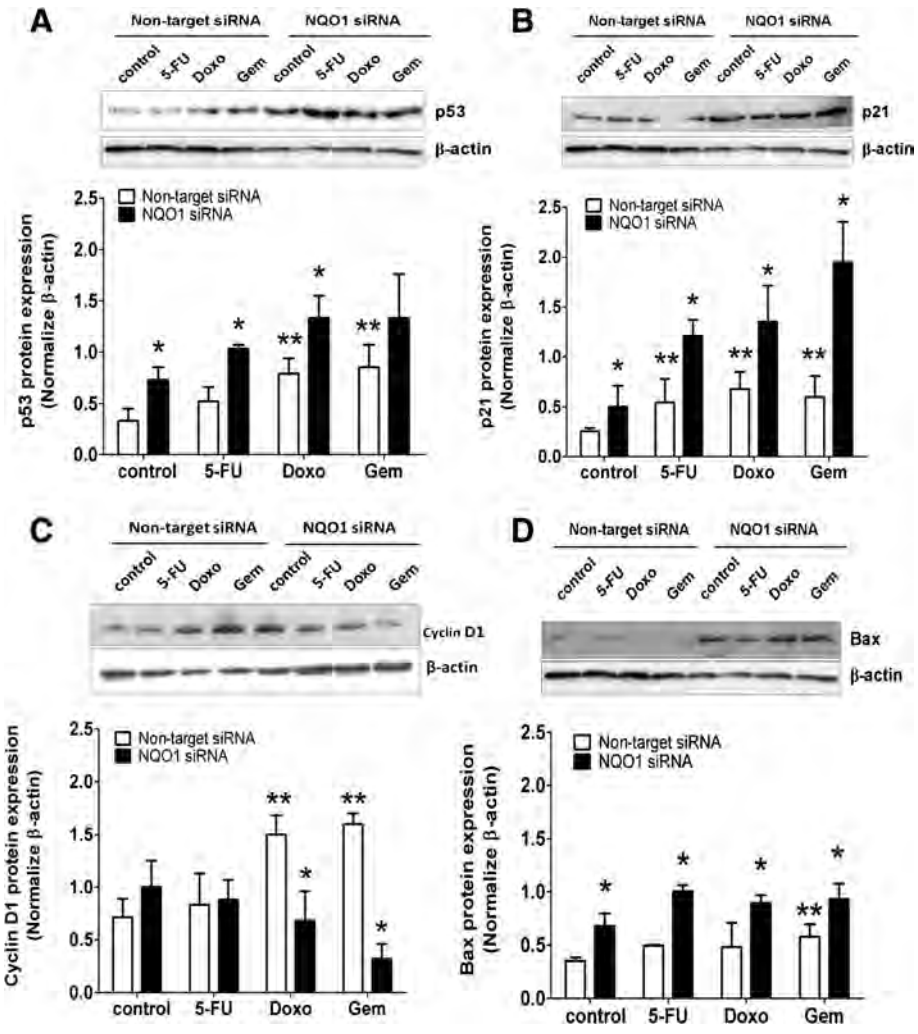


**Figure 3 Altered expressions of proteins related to cell proliferation and apoptosis pathways. A-D**, Expressions of proteins related to cell proliferation and apoptosis pathways. KKU-100 with NQO1 knocked down cells were exposed to chemotherapeutic agents; 5-FU (3 μM), Doxo (0.1 μM), and Gem (0.1 μM) for 24 hr. Whole cell lysates were prepared after indicated treatment and Western blot analysis was conducted using anti-p53 **(A)**, -p21 **(B)**, -cyclin D1 **(C)**, -Bax **(D)** and -β-actin antibodies. The relative bars that were normalized with β-actin as a loading control of each band is shown below the Western blot images. Data represent mean ± SEM, each from three separated experiments. *$p < 0.05$ vs the treated non-targeting knocked down cells. **$p < 0.05$ vs the untreated non-targeting knocked down cells.

NQO1 expression was knocked down by using a siRNA method. KKU-100 cells were used in the study, because the recent study has shown that the high NQO1 expressing cells, KKU-100 cells, are sensitized by dicoumarol to the cytotoxicity of chemotherapeutic agents, while the low expressing cells are not [22]. The results showed that NQO1 mRNA expression was suppressed by siRNA more than 80% at 24 hr (Figure 2A). The protein expression levels (Figure 2B) and enzymatic activity (data not shown) were also suppressed moderately at 24 hr (data not shown) and about 80% at 48 hr after the siRNA transfection. The further experiment was performed after transfection for 48 hr.

Then, we examined the susceptibility of NQO1-knockdown-KKU-100 cells to various chemotherapeutic agents. NQO1 siRNA treatment alone did not alter significantly the cell viability compared with that of KKU-100 cells treated with non-target siRNA. By NQO1-knockdown, KKU-100 cells became more sensitive to the cytotoxic effect of 5-FU, Doxo, and Gem (Figure 2C-E). The chemosensitizing effect was remarkable especially at the low concentrations of the chemotherapeutic agents.

### NQO1-knockdown and chemotherapeutic agent treatment induce p53 and altered expression of cell death pathway proteins

To explore the possible mechanisms of chemosensitizing effect of NQO1-knockdown, we examined the expression levels of cell death-related proteins in NQO1-knockdown-KKU-100 cells. Western blot analyses revealed that Doxo and Gem treatment alone increased p53 levels (Figure 3A).

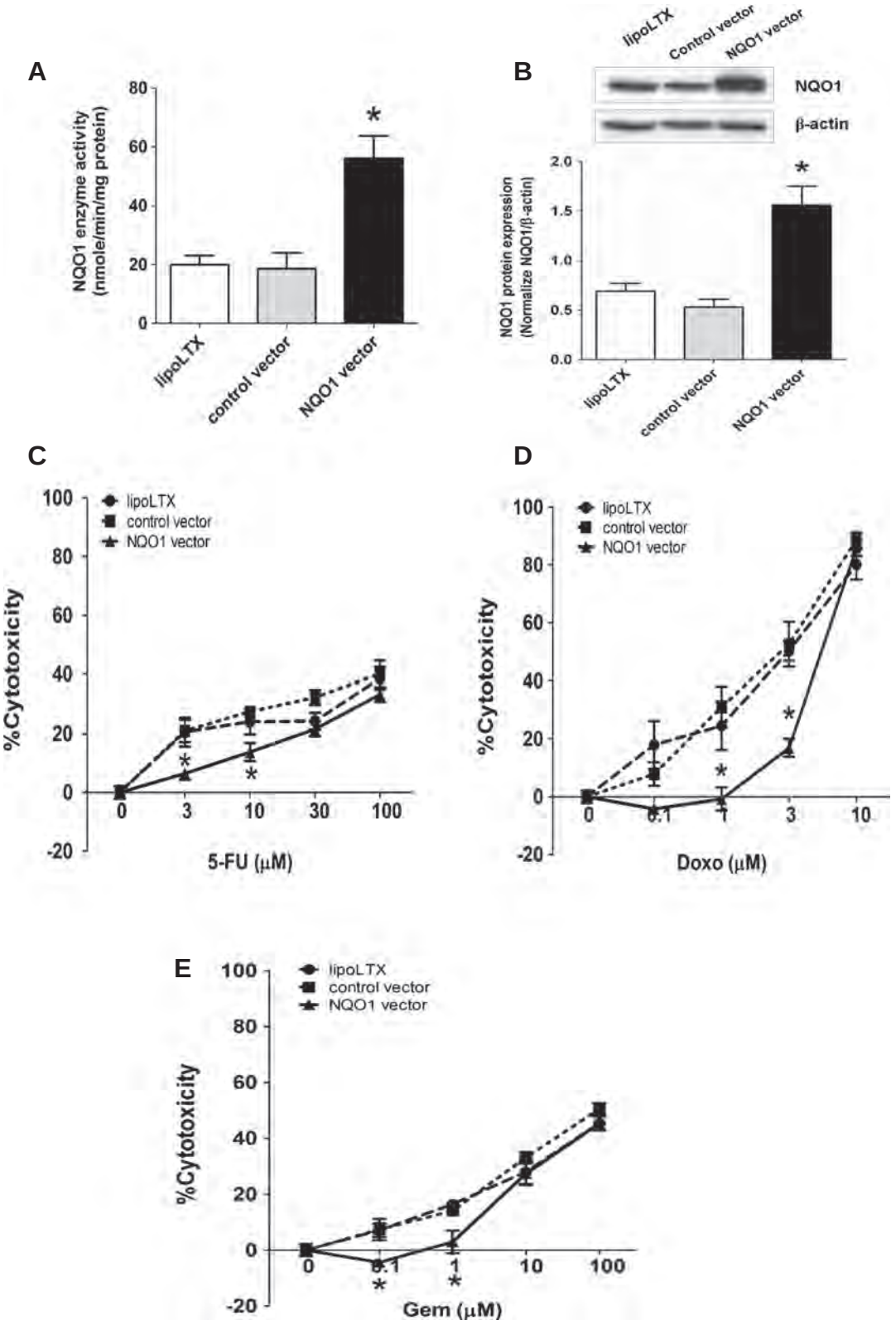


**Figure 4** (See legend on next page.)

(See figure on previous page.)
**Figure 4 Effects of NQO1 over-expression on the susceptibility of KKU-M214 cells to chemotherapeutic agents (5-FU, Doxo, and Gem).** **A-B**, Effect of NQO1 over-expression on mRNA and protein levels of NQO1 in KKU-M214 cells. The pCMV6-XL5-NQO1 (wild type NQO1) or pCMV6-XL5 (control vector) was transfected to KKU-M214 for 24 hr. The whole cells were collected for NQO1 enzyme activity assay **(A)** and Western blot analysis **(B)**. The data represent mean ± SEM, each from three experiments. *$p < 0.05$ vs the control vector transfected cells. **(C-E)** Cytotoxicity of chemotherapeutic agents on NQO1 over-expressed KKU-M214 cells. Twenty-four hour after transfection, cells were incubated with chemotherapeutic agents for additional 24 hr (Doxo) and 48 hr (5-FU and Gem). The cytotoxicity was evaluated by SRB assay. Data represent mean ± SEM, each from three separated experiments. *$p < 0.05$ vs the control vector transfected cells.

When NQO1-knockdown-KKU-100 cells were treated with chemotherapeutic agents, p53 level was enhanced further by all 3 agents (Figure 3A). Then, we examined the expression levels of some p53 downstream proteins, i.e. p21, cyclin D1, and Bax protein. Similar to p53, p21 and Bax were over-expressed by the drug treatments (Figure 3B, 3D). In contrast, in the NQO1 knockdown cells, treatment with chemotherapeutic agents strongly suppressed the cyclin D1 level (Figure 3C). In the non-target siRNA transfected KKU-100 cells, Doxo and Gem, but not 5-FU, treatments increased cyclin D1 expression (Figure 3C).

### Over-expression of NQO1 in CCA cells induces drug resistance against chemotherapeutic agents

Since KKU-M214 cells naturally express relatively low level of NQO1, effects of NQO1 over-expression by transient transfection with NQO1 expression vector on the susceptibility of cells to chemotherapeutic agents was evaluated. After transfection, the NQO1 enzyme activity in the transfected cells was elevated approximately 2.5-fold and the NQO1 protein level was 2.25-fold higher than the control vector (Figure 4A-B), indicating that NQO1 construct was efficiently expressed in KKU-M214 cells. Then, NQO1-over-expressed KKU-M214 cells were exposed to 5-FU and Gem for 48 hr, and to Doxo for 24 hr. The results showed that the cytotoxicity of 5-FU, Doxo, and Gem were markedly decreased for NQO1-over-expressed KKU-M214 cells (Figure 4C-E), indicating the protective effect of NQO1.

### Over-expression of NQO1 suppresses chemotherapeutic agents-induced p53 and protein expression in the cell death pathway

Previous experiment showed that NQO1-knockdown increased p53 and apoptogenic protein expression. The results of this experiment showed that over-expression of NQO1 in KKU-M214 cells strongly suppressed the chemotherapeutic agents-induced increased expression of p53, p21, and Bax (Figure 5A-B & D). On the other hand, over-expression of NQO1 enhanced Doxo- and Gem-induced cyclin D1 expression (Figure 5C).

### Knockdown of p53 abolishes the chemosensitizing effect of NQO1 silencing

Since the results given above showed that the knockdown and over-expression of NQO1 enhanced and suppressed, respectively, the chemotherapeutic agent-mediated cytotoxicity in association with the altered expression of p53, p53 apparently play a role in the expression of the cytotoxic effect of those anti-cancer agents. To validate the role of p53, we prepared the double knockdown of NQO1 and p53 in KKU-100 cells. The efficiency of NQO1 and p53 knockdown was more than 80% (Figure 6A). As is shown above, NQO1-knockdown increased the susceptibility of KKU-100 cells to chemotherapeutic agents. Conversely, p53-knockdown markedly reduced cytotoxic effect of all tested chemotherapeutic agents compared with chemotherapeutic agents alone (Figure 6B-D). Interestingly, in the double knockdown experiment, the cytotoxic potentiation effect of NQO1 gene silencing was totally diminished by the simultaneous knockdown of p53. The cytotoxic effects of chemotherapeutic agents on double knockdown cells were similar to those on p53 knockdown cells. These results strongly suggest that the cytotoxic effects of all 3 chemotherapeutic agents on CCA cells were dependent on p53 expression and NQO1 is probably the upstream modulator of p53.

## Discussion

We previously showed that the survival time of CCA patients with high NQO1 mRNA expression was shorter than patients having CCA with low NQO1 expression [21], suggesting the possible role of NQO1 in CCA progression. We also demonstrated that inhibition of NQO1 in high NQO1 expressing cell line, KKU-100, enhanced the cytotoxic effect of chemotherapeutic agents, but not in the low NQO1 expressing cells, i.e. KKU-M214 [22]. In the present study, the role of NQO1 was validated by knockdown of NQO1 expression in KKU-100 cells and over-expression of NQO1 in KKU-M214 cells. Knockdown of NQO1 enhanced the cytotoxic effect of 5-FU, Doxo and Gem, whereas over-expression of NQO1 protected the cells from chemotherapeutic agents. The suppression of NQO1 expression was associated with up-regulation of p53, p21, and Bax proteins, while over-expression

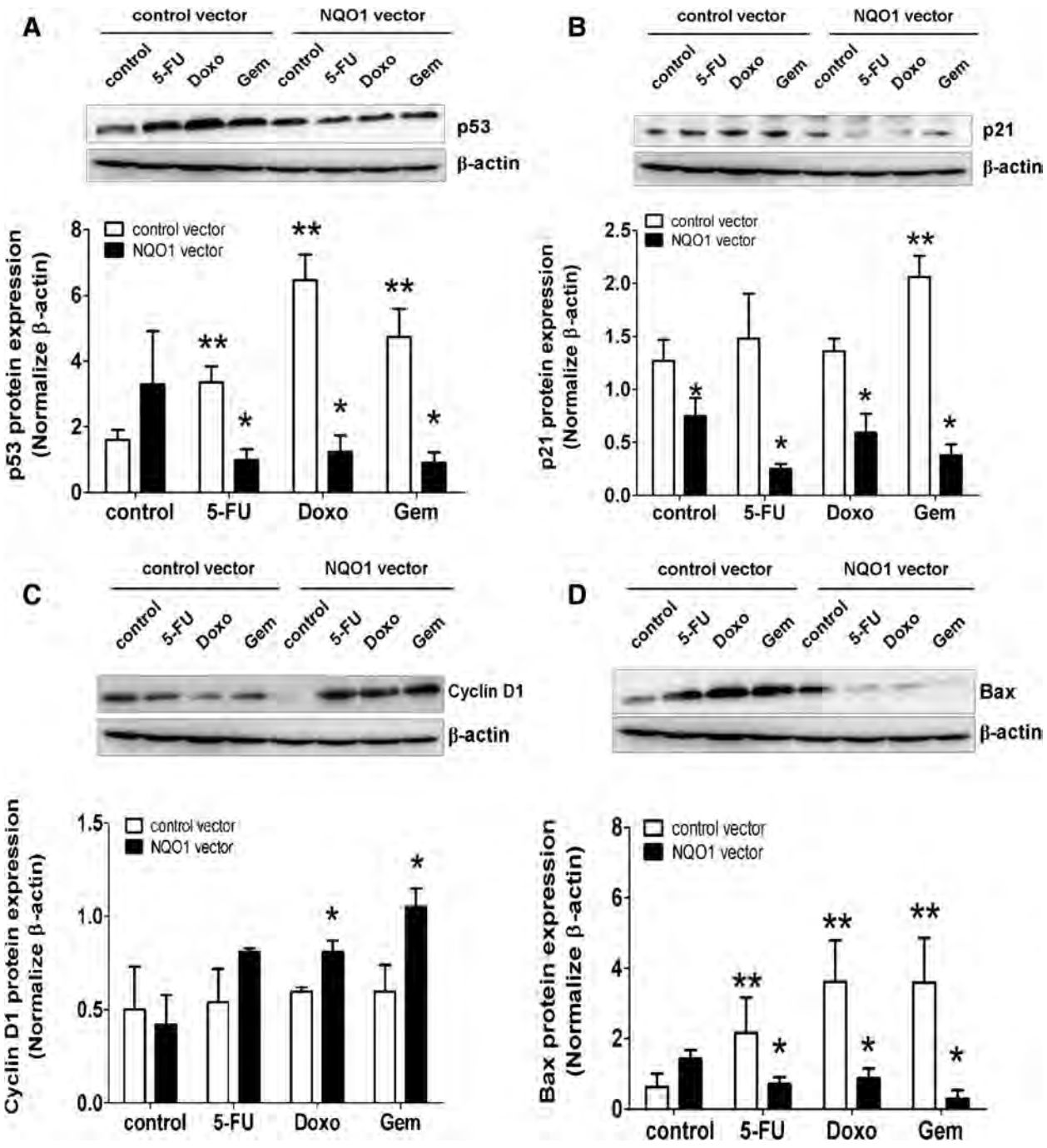


**Figure 5 NQO1 over-expression attenuates the p53 pathway in KKU-M214 cells. A-D**, Western blots of p53 **(A)**, p21 **(B)**, cyclin D1 **(C)**, and Bax **(D)** protein in KKU-M214-NQO1 over-expressed cells after treatment with 5-FU 3 μM (48 hr), Doxo 0.1 μM (24 hr), and Gem 0.1 μM (48 hr). The relative bars that were normalized with β-actin of each band are shown below the Western blot images. *$p < 0.05$ vs the treated control vector transfected cells. **$p < 0.05$ vs the untreated control vector transfected cells.

was associated with down-regulation of those proteins. The role of NQO1 in cell viability became significant when NQO1 knockdown KKU-100 cells exposed to chemotherapeutic agents. It should be noted that NQO1 plays an important role in cell viability especially at severe stress condition in CCA cells. The role of p53 was verified by p53 and NQO1 gene silencing with siRNA. The potentiation effect of NQO1 gene silencing on the cytotoxicity of chemotherapeutic agents was inhibited by p53 knockdown. Thus, the sensitizing effect of NQO1 is likely to be mediated via p53.

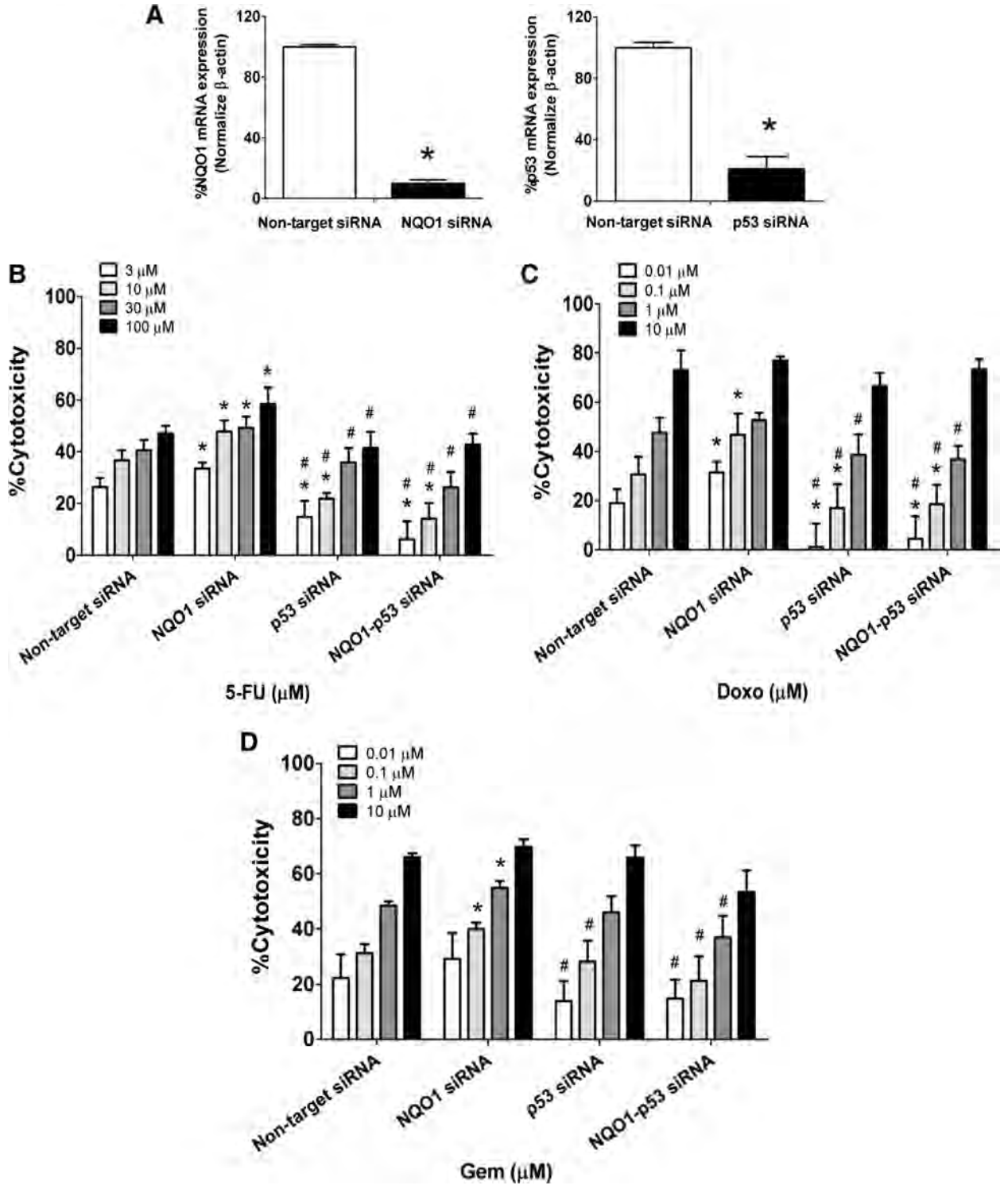


**Figure 6 Double knockdown of NQO1 and p53 by siRNA altered KKU-100 cells to chemotherapeutic agents. (A)** Effect of co-transfected NQO1 and p53 siRNA in KKU-100 cells. Cells were transfected with the pooled siRNA against NQO1 and p53 for 24 hr. The bars represent relative expression of NQO1 and p53 normalized with β-actin as internal control. **(B-D)** After co-transfection, cells were treated with varied concentrations of chemotherapeutic agents; 5-FU, Doxo, and Gem for another 24 hr as described in the "Methods" section. The cytotoxicity was evaluated by SRB assay. Data represent mean ± SEM, each from three separated experiments. *$p < 0.05$ vs the non-targeting knocked down cells and $^{\#}p < 0.05$ vs NQO1 knocked down cells.

Inhibition of NQO1 by dicoumarol suppressed cancer cell growth and potentiated the cytotoxicity of chemotherapeutic agents [19,20]. Chemotherapeutic agents such as Doxo and Gem induced over-expression of NQO1 in CCA cells. This may be a cellular adaptive response to oxidative stress and cytotoxicity [13] and may confer the cytoprotective effect to the cells. The biological role of NQO1 in CCA was validated in this study and found to be consistent with our recent report in that suppression of NQO1 enhances the cytotoxic effect of many chemotherapeutic agents and the activation of mitochondrial death pathway [22]. On the other hand, over-expression of NQO1 in KKU-M214 cells suppressed the cytotoxic effect of chemotherapeutic agents. The results indicated the protective effect of NQO1 from chemotherapy in CCA. Taken together, this may provide a possibility to combine NQO1 inhibitor together with chemotherapy as a novel treatment strategy for CCA. However, to apply this information to CCA patients, several critical studies are requested to confirm the *in vivo* relevance of these findings. For example, the synergistic role of NQO1 inhibition in chemotherapy of CCA should be further validated in animal models. This could be carried out in our future study.

The mechanism of NQO1-mediated chemosensitization was further explored. Previous reports suggested that NQO1 modulates p53 expression by interfering with 20S proteasome-mediated degradation of p53 [24]. Inhibition of NQO1 by dicoumarol suppressed p53 protein levels and induced cell death [24]. In contrast, dicoumarol at non-cytotoxic concentrations, but sufficient to inhibit NQO1 enzyme activity, enhanced p53 protein levels [22]. Present results show that the suppression of NQO1 increased p53 expression.

Tumor protein p53 and Bcl family proteins regulate mitochondrial outer membrane permeabilization (MOMP) [26]. Our results showed that the increase of p53 was associated with increased p21 and Bax levels. Both p21 and Bax are p53-dependent downstream gene products. The p21 is a potent cyclin-dependent kinase inhibitor and its expression is associated with the strong antiproliferative effect as was seen in the present study. Bax is a multidomain proapoptotic Bcl2 family. It translocates into the mitochondrial outer membrane and forms Bax pores leading to the release of proapoptotic proteins and ensuing cell death [27]. p53 is a tumor suppressor gene that responded to DNA damage or oxidative stress by inducing growth arrest or apoptotic cell death [28,29]. Our results showed that knockdown of p53 inhibited the chemosensitizing effect, which was induced by knockdown of NQO1 in KKU-100 cells. This indicates that the sensitizing effect of NQO1 knockdown is mediated via p53 pathway. It is also noted that KKU-100 cells expressed both the wild type full length p53 as well as the splicing variant of truncated p53 protein [30]. Interestingly, our results showed that the potentiation effect of NQO1 gene silencing on the cytotoxicity of chemotherapeutic agents can occur even in cancer cells with high expression ratio of mutant p53/wild type p53. It is yet to determine the chemosensitizing effect of NQO1 suppression on cells expressing the other mutated p53. As some CCA patients express high NQO1 [20], targeting the NQO1 by suppressing the activity or expression could be a strategy to overcome drug resistance of cancer and enhancing the efficacy of chemotherapeutic agents.

## Conclusions

In summary, NQO1 plays an important role in cytoprotection of cancer cells and modulates the sensitivity of chemotherapeutic agents, particularly in the high NQO1 expressing CCA cells. NQO1 is a potential molecular target for enhancing the antitumor activity of chemotherapeutic agents.

#### Abbreviations

NQO1: NAD(P)H-quinone oxidoreductase 1; CCA: Cholangiocarcinoma; 5-FU: 5-fluorouracil; Doxo: Doxorubicin; Gem: Gemcitabine; siRNA: Small interfering RNA; SRB: Sulforhodamine B; p53: Tumor protein 53.

#### Competing interests

The authors declare that they have no competing interests.

#### Authors' contributions

Conceived and designed: PZ AP VK. Performed the experiments: PZ AP LS BS. Analyzed the data: PZ AP VK. Wrote the paper: PZ AP VK. All authors read and approved the final manuscript.

#### Acknowledgments

This work was supported by the Thailand Research Fund (RMU5380027), the National Research University Project and the Office of Higher Education Commission through SHeP-GMS of Khon Kaen University, the Liver Fluke and Cholangiocarcinoma Research Center, grant-in-aid from Faculty of Medicine (I 56108), Khon Kaen University, and a scholarship from the Office of the Higher Education Commission to Ponsilp Zeekpudsa. Valuable suggestions on the manuscript of Prof. Yukifumi Nawa of Faculty of Medicine, Khon Kaen University are gratefully acknowledged.

#### Author details

[1]Department of Pharmacology, Faculty of Medicine, Khon Kaen University, Khon Kaen 40002, Thailand. [2]Department of Pathology, Faculty of Medicine, Khon Kaen University, Khon Kaen, Thailand. [3]Liver Fluke and Cholangiocarcinoma Research Center, Khon Kaen University, Khon Kaen, Thailand.

Received: 24 September 2013 Accepted: 21 January 2014
Published: 24 January 2014

#### References

1. Lazaridis KN, Gores GJ: **Cholangiocarcinoma.** *Gastroenterology* 2005, **128:**1655–1667.
2. Patel T: **Cholangiocarcinoma.** *Nat Clin Pract Gastroenterol Hepatol* 2006, **3:**33–42.
3. Sripa B, Pairojkul C: **Cholangiocarcinoma: lessons from Thailand.** *Curr Opin Gastroenterol* 2008, **24:**349–356.
4. Sriplung H, Sontipong S, Martin N, Wiangnon S, Vootiprux V, Cheirsilpa A, Kanchanabat C, Khuhaprema T: **Cancer incidence in Thailand, 1995–1997.** *Asian Pac J Cancer Prev* 2005, **6:**276–281.
5. Kurathong S, Lerdverasirikul P, Wongpaitoon V, Pramoolsinsap C, Kanjanapitak A, Varavithya W, Phuapradit P, Bunyaratvej S, Upatham ES, Brockelman WY: **Opisthorchis viverrini infection and cholangiocarcinoma. A prospective, case-controlled study.** *Gastroenterology* 1985, **89:**151–156.

6. Thamavit W, Bhamarapravati N, Sahaphong S, Vajrasthira S, Angsubhakorn S: **Effects of dimethylnitrosamine on induction of cholangiocarcinoma in Opisthorchis viverrini-infected Syrian golden hamsters.** *Cancer Res* 1978, **38:**4634–4639.
7. Khan SA, Thomas HC, Davidson BR, Taylor-Robinson SD: **Cholangiocarcinoma.** *Lancet* 2005, **366:**1303–1314.
8. Fodale V, Pierobon M, Liotta L, Petricoin E: **Mechanism of cell adaptation: when and how do cancer cells develop chemoresistance?** *Cancer J* 2011, **17:**89–95.
9. Logsdon CD, Simeone DM, Binkley C, Arumugam T, Greenson JK, Giordano TJ, Misek DE, Kuick R, Hanash S: **Molecular profiling of pancreatic adenocarcinoma and chronic pancreatitis identifies multiple genes differentially regulated in pancreatic cancer.** *Cancer Res* 2003, **63:**2649–2657.
10. Siegel D, Ross D: **Immunodetection of NAD(P)H:quinone oxidoreductase 1 (NQO1) in human tissues.** *Free Radic Biol Med* 2000, **29:**246–253.
11. Chao C, Zhang ZF, Berthiller J, Boffetta P, Hashibe M: **NAD(P)H:quinone oxidoreductase 1 (NQO1) Pro187Ser polymorphism and the risk of lung, bladder, and colorectal cancers: a meta-analysis.** *Cancer Epidemiol Biomarkers Prev* 2006, **15:**979–987.
12. Cullen JJ, Hinkhouse MM, Grady M, Gaut AW, Liu J, Zhang YP, Weydert CJ, Domann FE, Oberley LW: **Dicumarol inhibition of NADPH: quinone oxidoreductase induces growth inhibition of pancreatic cancer via a superoxide-mediated mechanism.** *Cancer Res* 2003, **63:**5513–5520.
13. Jaiswal AK: **Regulation of genes encoding NAD(P)H: quinone oxidoreductases.** *Free Radic Biol Med* 2000, **29:**254–262.
14. Long DJ 2nd, Waikel RL, Wang XJ, Perlaky L, Roop DR, Jaiswal AK: **NAD(P)H: quinone oxidoreductase 1 deficiency increases susceptibility to benzo(a)pyrene-induced mouse skin carcinogenesis.** *Cancer Res* 2000, **60:**5913–5915.
15. Ross D, Kepa JK, Winski SL, Beall HD, Anwar A, Siegel D: **NAD(P)H: quinone oxidoreductase 1 (NQO1): chemoprotection, bioactivation, gene regulation and genetic polymorphisms.** *Chem Biol Interact* 2000, **129:**77–97.
16. Prawan A, Buranrat B, Kukongviriyapan U, Sripa B, Kukongviriyapan V: **Inflammatory cytokines suppress NAD(P)H:quinone oxidoreductase-1 and induce oxidative stress in cholangiocarcinoma cells.** *J Cancer Res Clin Oncol* 2009, **135:**515–522.
17. Kolesar JM, Pritchard SC, Kerr KM, Kim K, Nicolson MC, McLeod H: **Evaluation of NQO1 gene expression and variant allele in human NSCLC tumors and matched normal lung tissue.** *Int J Oncol* 2002, **21:**1119–1124.
18. Cresteil T, Jaiswal AK: **High levels of expression of the NAD(P)H: quinone oxidoreductase (NQO1) gene in tumor cells compared to normal cells of the same origin.** *Biochem Pharmacol* 1991, **42:**1021–1027.
19. Matsui Y, Watanabe J, Ding S, Nishizawa K, Kajita Y, Ichioka K, Saito R, Kobayashi T, Ogawa O, Nishiyama H: **Dicoumarol enhances doxorubicin-induced cytotoxicity in p53 wild-type urothelial cancer cells through p38 activation.** *BJU Int* 2010, **105:**558–564.
20. Watanabe J, Nishiyama H, Matsui Y, Ito M, Kawanishi H, Kamoto T, Ogawa O: **Dicoumarol potentiates cisplatin-induced apoptosis mediated by c-Jun N-terminal kinase in p53 wild-type urogenital cancer cell lines.** *Oncogene* 2006, **25:**2500–2508.
21. Buranrat B, Chau-In S, Prawan A, Puapairoj A, Zeekpudsa P, Kukongviriyapan V: **NQO1 expression correlates with cholangiocarcinoma prognosis.** *Asian Pac J Cancer Prev* 2012, **13**(Suppl):131–136.
22. Buranrat B, Prawan A, Kukongviriyapan U, Kongpetch S, Kukongviriyapan V: **Dicoumarol enhances gemcitabine-induced cytotoxicity in high NQO1-expressing cholangiocarcinoma cells.** *World J Gastroenterol* 2010, **16:**2362–2370.
23. Cross JV, Deak JC, Rich EA, Qian Y, Lewis M, Parrott LA, Mochida K, Gustafson D, Vande Pol S, Templeton DJ: **Quinone reductase inhibitors block SAPK/JNK and NFkappaB pathways and potentiate apoptosis.** *J Biol Chem* 1999, **274:**31150–31154.
24. Asher G, Lotem J, Cohen B, Sachs L, Shaul Y: **Regulation of p53 stability and p53-dependent apoptosis by NADH quinone oxidoreductase 1.** *Proc Natl Acad Sci USA* 2001, **98:**1188–1193.
25. Dhar SK, Xu Y, Chen Y, St Clair DK: **Specificity protein 1-dependent p53-mediated suppression of human manganese superoxide dismutase gene expression.** *J Biol Chem* 2006, **281:**21698–21709.
26. Chao DT, Korsmeyer SJ: **BCL-2 family: regulators of cell death.** *Annu Rev Immunol* 1998, **16:**395–419.
27. Chipuk JE, Fisher JC, Dillon CP, Kriwacki RW, Kuwana T, Green DR: **Mechanism of apoptosis induction by inhibition of the anti-apoptotic BCL-2 proteins.** *Proc Natl Acad Sci USA* 2008, **105:**20327–20332.
28. Chipuk JE, Green DR: **Dissecting p53-dependent apoptosis.** *Cell Death Differ* 2006, **13:**994–1002.
29. Zheng C, Jia W, Tang Y, Zhao H, Jiang Y, Sun S: **Mesothelin regulates growth and apoptosis in pancreatic cancer cells through p53-dependent and -independent signal pathway.** *J Exp Clin Cancer Res* 2012, **31:**84.
30. Nutthasirikul N, Limpaiboon T, Leelayuwat C, Patrakitkomjorn S, Jearanaikoon P: **Ratio disruption of the 133p53 and TAp53 isoform equilibrium correlates with poor clinical outcome in intrahepatic cholangiocarcinoma.** *Int J Oncol* 2013, **42:**1181–1188.

doi:10.1186/1756-9966-33-11
**Cite this article as:** Zeekpudsa *et al.*: Suppression of NAD(P)H-quinone oxidoreductase 1 enhanced the susceptibility of cholangiocarcinoma cells to chemotherapeutic agents. *Journal of Experimental & Clinical Cancer Research* 2014 **33**:11.

**Submit your next manuscript to BioMed Central and take full advantage of:**

- **Convenient online submission**
- **Thorough peer review**
- **No space constraints or color figure charges**
- **Immediate publication on acceptance**
- **Inclusion in PubMed, CAS, Scopus and Google Scholar**
- **Research which is freely available for redistribution**

Submit your manuscript at
www.biomedcentral.com/submit

BioMed Central

**Modulation of heme oxygenase-1 increases sensitivity of cholangiocarcinoma cells to radiation and chemotherapy**

Sarinya Kongpetch[1,3], Choon Kiat Ong [2], Waraporn Chan-On[2†], Ee Yan Siew[2], Auemduan Prawan[1,3], Laddawan Senggunprai[1,3], Upa Kukongviriyapan[4], Bin Tean Teh[2*], Veerapol Kukongviriyapan [1,3b]*

S. Kongpetch, A. Prawan, L.Senggunprai, V.Kukongviriyapan
Department of Pharmacology, Faculty of Medicine and Liver Fluke & Cholangiocarcinoma Research Center, Khon Kaen University, Thailand 40002

U. Kukongviriyapan
Department of Physiology, Faculty of Medicine, Khon Kaen University, Thailand 40002

C.K.Ong, W.Chan-On, E.Y.Siew[†], B.T.Teh.
Laboratory of Cancer Epigenome, National Cancer Centre of Singapore, Singapore
([†] Present address: Faculty of Medical Technology, Mahidol University, Thailand)

[*]**Corresponding author:**

Bin Tean Teh: E-mail: teh.bin.tean@singhealth.com.sg

Veerapol Kukongviriyapan : E-mail: veerapol@kku.ac.th

SK: sarinyako@kku.ac.th, CKO: abelong@gmail.com, WC: wara_ae@yahoo.com, EYS: siew.ee.yan@gmail.com, AP: peuamd@kku.ac.th, LS: laddas@kku.ac.th, UK: upa_ku@kku.ac.th, BTT: teh.bin.tean@singhealth.com.sg, VK: veerapol@kku.ac.th

**Abstract**

**Purpose** Cholangiocarcinoma (CCA) is the deadliest form of liver cancer. It is highly resistant chemotherapy and radiotherapy. Heme oxygenase-1 (HO-1) plays important roles in tumor growth, migration and angiogenesis. However, its therapeutic role in cholangiocarcinoma is not known. We aimed to study the roles of HO-1 in sensitivity to gamma irradiation and chemotherapeutic agent.

**Methods** Human cholangiocarcinoma cells were subjected to gamma irradiation and HO-1 knockdown by siRNA or shRNA. Cell migration, clonogenic assay and cell cycle distribution were analyzed. Effect of inhibition of HO-1 on gemcitabine-mediated tumor suppression was evaluated in nude mice xenografted with CCA cells. DNA double-strand breaks, proteins involving in cell proliferation, cell cycle and angiogenesis were analyzed by immunocytofluorescence, Western immunoblotting and immunohistochemistry.

**Results** The knockdown of HO-1 expression, strongly suppressed cell migration and enhanced the sensitivity of CCA cells to gamma irradiation by diminishing colony forming ability and increased DNA double strand breaks. The anti-proliferative effect was attributable to G2-M cell cycle arrest which was further enhanced by combining irradiation. Suppression of HO-1 by Zn-protoporphyrin enhanced the cytotoxicity of CCA cells to gemcitabine was validated in CCA xenografts. The drug combination almost completely arrested tumor growth whereas single agent only retarded it. Tumor inhibition was associated with greater decrease in expression of Ki67, CD31 and enhanced in p53 and p21 immunohistochemical staining.

**Conclusions** Taken together, our results indicated the synergistic role of HO-1 inhibition in radiotherapy and chemotherapy of CCA a worthy strategy that warrants further investigation in the treatment of CCA.

**Keywords**: Heme oxygenase-1, Cholangiocarcinoma, Chemosensitization, Radiosensitization, Cytoprotection, zinc protoporphyrin

## Introduction

**C**holangiocarcinoma (CCA) is one of the most devastating malignancies, because the majority of cases develop without clinical symptoms, and thus making the diagnosis of CCA very difficult. Prognosis of CCA is extremely poor because treatment outcomes and survival of the patients have only slightly improved in the past several decades (Khan et al. 2005). The complete tumor resection with negative pathological margins (R0 resection) is the only effective option to prolong survival with the five-year survival rate of 20-44%, but the recurrence of cancer is common which can occur in up to 63% within 2 year (Farges et al. 2011; Skipworth et al. 2011). Nonetheless, most of patients are already in the advanced stage of the disease at diagnosis thus making radical surgery not possible and prognosis of the unresectable or incomplete (R1) resection is extremely poor (Farges et al. 2011). Chemotherapy and radiotherapy may be the options left for most patients (Khan et al. 2012). The most accepted chemotherapy with gemcitabine-base has documented a median overall survival of only 11 months. Experiences in radiotherapy of CCA in adjuvant and neoadjuvant settings are very limited and there is currently no evidence to support the routine use of radiotherapy for unresectable disease (Khan et al. 2012; Skipworth et al. 2011). It is, therefore, there is an urgent need for a more effective treatment approach to improve survival and quality of life of these patients (Butthongkomvong et al. 2013; Patel 2011). Targeting the prosurvival mechanisms in cancer cells could be a strategy to overcome resistance to chemotherapy and radiotherapy. Antioxidant and cytoprotective proteins such as HO-1 and NQO1 could be such targets (Buranrat et al. 2010; Na and Surh 2014; Zeekpudsa et al. 2014).

Heme oxygenase-1(HO-1) is a microsomal enzyme catalyzing the first rate-limiting step in degradation of heme, leading to equimolar production of biliverdin, carbon monoxide (CO) and free iron. HO-1 can be induced in response to cellular stress, oxidative stimuli, hypoxia and during tumor growth (Prawan et al. 2005). More importantly, HO-1 is found to be over-expressed in various cancer types including prostate cancer, hepatoma, pancreatic cancer and lymphosarcoma (Jozkowicz et al. 2007). These cancers express a high level of HO-1 and the over-expression of this enzyme may provide growth advantages and render resistance to chemotherapeutic agents such as cisplatin, doxorubicin and gemcitabine (Gueron et al. 2009; Maines and Abrahamsson 1996; Nuhn et al. 2009). HO-1 plays a role in tumor growth, neoangiogenesis and cytoprotection of tumors against the attack of oxidative insults from

chemotherapy and radiotherapy, probably due to its anti-oxidative and anti-apoptotic activities (Berberat et al. 2005; Hirai et al. 2007; Kongpetch et al. 2012). Thus, suppression of HO-1 activity may be a strategy to increase the chemosensitivity and radiosensitivity of tumors. We recently have shown that the inhibition of HO-1 in CCA cell lines by HO-1 siRNA or by pharmacological inhibitor, zinc protoporphyrin IX (ZnPP) resulted in an remarkable reduction of the IC50 of CCA cells to gemcitabine (Kongpetch et al. 2012). Moreover, ellagic acid inhibits prostate cancer cells in association with downregulation of HO-1 (Vanella et al. 2013).

In the present study, the effects of HO-1 suppression on tumor cell growth, cell cycle progression and sensitivity to radiation and chemotherapeutic agents were examined by using HO-1 knockdown CCA cells with high and low basal HO-1 levels. We further evaluated and examined the effects of combined therapy of gemcitabine and ZnPP using an *in vivo* model.

## Materials and methods

### Cell lines and cell cultures

The human cholangiocarcinoma (CCA) cell lines; KKU-100, KKU-M055, KKU-M214, KKU-M213, and KKU-M139 were kindly provided by Dr. Banchob Sripa, Department of Pathology, Faculty of Medicine, Khon Kaen University. Cell lines were established, characterized, and derived from CCA tissues which are classified histologically as follows: poorly differentiated adenocarcinom (KKU-100, M055), well differentiated adenocarcinoma (M214, M213), aquamous cell carcinoma (KKU-M139) (Sirica 2005; Yonglitthipagon et al. 2012). All cell lines were routinely cultured in complete media consisting of Ham's F12 media, supplemented with 10% fetal calf serum, 12.5 mM HEPES, pH 7.3, 100 U/ml penicillin G and 100 μg/ml gentamicin (Tusskorn et al. 2013).

### Cytotoxicity assay

KKU-100 cells were seeded onto 96-well plate at density of 7,500 cells/well for overnight. The cells were treated with varied concentration of ZnPP and gemcitabine (GEM) from 1- 1000 nM for 24 h. For the combination treatment, KKU-100 cells were pretreated with ZnPP for 4 h prior GEM, and incubation was continued for 24 h. The cytotoxicity assay was performed by sulforhodamine B (SRB) assay as previously described (Tusskorn et al. 2013).

**Cell motility, wound healing and clonogenic assays**

KKU-100 and M213 cells with HO-1 knockdown were used in the cell motility and wound healing assays. KKU-100 and M213 cells were transfected with HO-1 siRNA (method as below) for 24 h, then seeded onto a transwell insert in 300 µL of medium. After incubation for 6 h, the filter membrane was cut and placed on the glass slide, covered with the mounting medium with DAPI, and then covered with a cover-slip. The cells migrated across the membrane were enumerated using a fluorescence microscope; Nikon Eclipse Ti.

For wound healing assay, after transfection with HO-1 siRNA for 24 h, KKU-100 and M213 cells were seeded into 24-well plate with density of 150,000 per well in full cultured media to obtain cell confluence of 80-90% on the experimental day. On the next day, cultured cells were scratched with a sterile 200 µL-pipette tip making straight line of wounds. The width of wound outline was recorded under a phase-contrast microscope at 0, 6, 12 and 24 h after scratching the cultured cells.

The clonogenic survival of CCA cells following gamma irradiation was determined by clonogenic assay. The stable knockdown of HO-1, KKU-100 and M214 cells in suspensions at the density of 12,500 cells/mL were irradiated over the dose range of 0-10 Gy. Immediately after irradiation, the cells were seeded at 300 and 200 cells of KKU-100 and M214, respectively, onto a 6-well plate. After 14 days of incubation with renewal of cultured media every other day, the cells were fixed in absolute methanol and stained with 0.25% crystal violet in 2% ethanol. The number of colonies in each well was counted under a Nikon Eclipse Ti microscope (10X).

**Irradiation-induced antiproliferation**

The five CCA cells; KKU-100, M213, M214, M055 and M139 cells were employed to assay of the sensitivity to radiation. Cells in suspensions at the density of 12,500 cells/mL were irradiated at room temperature over the dose range of 0–10 Gy using a Gammacell® 40 Exactor (Nordion Gamma Irradiator®). The cells were seeded at density of 625-1250 cells/well in 96-well plate and incubated for 4 days. Cell proliferation was determined by MTS assay, performed according to the instruction guideline of CellTiter 96® (Promega)

**HO-1 small interfering RNA transfection**

The transfection of HO-1 siRNA was performed using siGENOME SMARTpool of four sequences of siRNA (M-006372-02-0005: Dharmacon) at a final concentration of 200 nM and

lipofectamine 2000 (Invitrogen) according to the manufacturers' instructions. The siGENOME non-targeting siRNA (D-001210-02-05), as a negative control was introduced to the cells using the same protocol as previously described method (Kongpetch et al. 2012).

**Generation of HO-1 stable knocked down by Lentivirus-mediated shRNA transfection**

To generate the lentivirus for transduction, ps-ShRNA-ControlA and ps-ShRNA -HO-1 plasmids were purchased from Santa Cruz and packaged using the ViraPower™ Lentiviral Packaging Mix (Invitrogen) as described by manufacturer. Briefly, 293FT cells were plated at 90% confluence in 10-cm plates and transfected with 3µg of ps-ShRNA-ControlA, or ps-ShRNA -HO-1, 36µL lipofectamine and 9 µg ViraPower™Packaging mixed in 1.5 mL Opti-MEM medium for an overnight. On the third day, medium with specific viral conjugated with ps-ShRNA-controlA or -HO-1, was collected and kept at -80°C before use. To generate stable control and HO-1 knockdown cell, 30,000 cells/well in 12-well plate of KKU-100 and M214 cells were transduced with 1µL of ps-ShRNA-ControlA or ps-ShRNA-HO-1 lentivirus. Positively transduced cells were selected by culturing in media containing 2 µg/ml puromycin B for 3 weeks.

**Reverse transcription real-time polymerase chain reaction**

The five CCA cells; KKU-100, M213, M214, M055 and M139 cells were seeded at the density of $1.5x10^4$ cells/well in 6 well-plates and allowed to grow for 24 h. Total RNA was isolated and the PCR products were generated using a previously described method (Buranrat et al. 2007). The primer sequences were as follows: HO-1: forward, 5'-CTG ACC CAT GAC ACC AAG GAC-3' and HO-1 reverse: 5'-AAA GCC CTA CAG CAA CTG TCG-3', Gen Bank accession number.NM_002133.2, β-actin: forward 5'-AGT GTA GCC CAG GAT GCC CTT-3' and β-actin: reverse, 5'-GCC AAG GTC ATC CAT GAC AAC-3', Gen Bank accession number NM_00246.5. To quantify the relative expression of genes, the relative quantitation was performed by using standard curve method. The amount of HO-1 mRNA was expressed as a ratio to β-actin mRNA.

**Western blot analysis**

Western blot analysis was used to determine the expression levels of HO-1, cyclin A, cyclin B1, cdc2, and β-actin. Cultured cells were washed with PBS, lysed with RIPA buffer containing protease inhibitor cocktail. The protein samples were mixed with SDS loading buffer and subject to separation by electrophoresis in 8-10% SDS-polyacrylamide gel. The protein bands were

blotted onto a PVDF membrane. After blocking with skimmed milk in phosphate buffer saline (PBS), the membrane was incubated overnight at 4°C with primary antibodies of HO-1 (ADI-SPA-895: Enzo Life Sciences), cdc2 p34 (sc-8395: Santa Cruz), cyclinA (sc-751), cyclinB1 (sc-752) and β-actin (A1978: Sigma-Aldrich) in PBS. After washing with PBS containing 0.05% Tween-20, the blots were incubated with the secondary antibodies (170-6515 or 170-6516: Biorad). The protein bands were detected by using an ECL kit (Pierce Biotechnology).

**Immunocytofluorescence for γ- H2AX**

To analyze the irradiation-induced phosphorylated histone protein, γ- H2AX foci in CCA cells were examined by the immunocytofluorescence technique after irradiation as described previously (Chan-On et al. 2009). KKU-100 cells (30,000 cells/well) were seeded on polystyrene treated glass slide, irradiated with gamma ray at the doses of 5 Gy for KKU-100, and incubated for 15 min. Cells were fixed in 3.7% paraformaldehyde in PBS and permeabilized with 0.2% Triton X-100 in PBS. The cultured cells on slides were blocked, stained with anti- γ-H2AX (ab11174: ABCAM) in 0.2% BSA, followed by anti-rabbit IgG conjugated to Alexa-fluor 594 (Molecular Probe: Eugene). The cultured slides were covered with DAPI mounting medium (H1200: VECTASHIELD®, Vector Lab) and examined under a fluorescence microscope (TE-2000E: Nikon). γ-H2AX foci were measured under a 60X -objective lens.

**Flow cytometry for cell cycle analysis**

After the transfection with HO-1 siRNA, cells were irradiated with 5 Gy for KKU-100 and 8 Gy for M214. Then, at the designated times post-irradiation, cells were fixed by resuspending the cells in 3 mL of ice-cold 70% ethanol. The cell pellets were resuspended in 1 mL of PBS containing 0.1% Triton X-100, 20 µg/mL of propidium iodide and 20 µg/mL of RNase incubated at 4°C for 60 minutes in dark chamber, and then analyzed in a FACSCalibur flow cytometer (BD Biosciences).

**Antitumor activity in animal model**

All experimental procedures were performed according to the experimental animal handling standards and study protocol was approved by the Institutional Animal Care and Use Committee (IACUC) (application #2011/SHS/650) SingHealth, Singapore. KKU-100 cells ($2x10^6$) in 200 µL Ham-F12 medium were injected subcutaneously into the dorsal skin of 6-week-old female

Balb/c nude mice (Animal Resource Center, Western Australia) and housed under a specific pathogen-free condition. When tumor grew to the volume about 200 $mm^3$, mice were randomly divided into four groups; control, gemcitabine (Gemzar®, Eli Lilly), ZnPP (Enzo Life Sciences) and the combination of both agents. ZnPP was dissolved in DMSO at the concentration of 100 mg/mL and diluted further in PBS immediately before use. Gem was dissolved in PBS as previously described to the concentration of 10 mg/mL and diluted further in PBS. ZnPP (12.5 mg/kg) and GEM (60 mg/kg) were administered intraperitonially once a week for three weeks (day 0, 7 and 14). In the combined drug treated group, ZnPP was injected 1 hour before Gem injection. Control group was treated with vehicle with the same schedule. Xenograft tumor volume was measured twice a week using electronic calipers and the tumor volume was calculated by the equation; $[L \times W^2]/2$ ($mm^3$), where L = length and W = width. The weight of mice was measured twice a week. The mice were terminated on day 17, and the tumor mass were collected for further analysis.

**Immunohistochemical analysis of tumor tissues**

The tumor tissues from xenografted mice were dissected, weighted and fixed in 10% formaldehyde solution and embedded in paraffin. The sections (3-μm-thick) were deparaffinised, followed by antigen retrieval with autoclave treatment for 10 min in 0.01 M citrate buffer (pH 6.0). Immunohistochemical staining for Ki67, CD31, mdm2, p53 and p21 was performed with a streptavidin-biotin (SAB) complex method using R.T.U. VECTORSTAIN® Universal Quick Kit (PK-7800: VECTOR) according to the manufacturer's instruction. The tissue-sections were incubated with primary antibodies, anti-Ki- 67 (clone MIB-1; Dako) at room temperature for 30 min, anti-CD31 (ab 28364: ABCAM), anti mdm2 (sc-965: Santa Cruz), anti p53 (sc-98) and anti p21 (2946: Cell Signaling Technology) at 4˚C overnight. The IHC-sections were counterstained with haematoxylin and with eosin for H&E staining, and then mounted with DPX Mounting Medium (UN 1866: CellPath). CD31-stained vessels were detected under a Zeiss Axio ScopeA.1 microscope with original magnification 200X. The mean value of the vessel numbers in tumors, were calculated from 10 fields of the three most vascularized areas according to previously described. The areas of mdm2, p21 and p53 positive cell staining were captured under a Nikon DS-Ri1 microscope with original magnification 400X and using Image Pro-plus program to count positive cells. The staining levels of p53 were calculated by the grading of numbers of

positive-cells multiply with the levels of intensity (positive-cell numbers were graded as 0-30=1, 31-60=2, 61-90=3 and 91-120=4 and levels of intensity ranges by 0-4)

**Statistical analysis**

Data were expressed as the mean ± SD. An analysis of variance was used to determine significant differences between each experimental group with Student-Newmann-Keuls post-hoc test. The level of significance was set at $P < 0.05$.

## Results

### HO-1 expression in CCA cells and contribution to cell migration

The expression levels of HO-1 were determined in five CCA cell lines using reverse transcription RT-PCR. KKU-100 cells showed high level of HO-1 mRNA expression, while others cell lines including M213, M214, M139 and M055 have much lower expression levels (Fig. 1A). KKU-100, and M213 and M214 which are representative of high, and low HO-1 expressing cell lines, respectively, were used for further functional studies. To investigate the functional role of HO-1 in CCA, HO-1 knockdown cells using siRNA were subjected to transwell and wound healing assays. The siRNA effectively reduced the HO-1 transcripts in KKU-100 and M213 cells by about 70% and 60%, respectively compared to control (Fig. 1B). HO-1 knockdown CCA cells showed a reduced number of cells migrated through the membrane in transwell chamber compared to control cells (Fig. 1C and 1D). The suppression of cell motility was further supported by wound healing assay, where the HO-1 knockdown CCA cells migrate much slower than the control cells, resulting in almost no closure of the wounds (Fig. 1E). This result suggested HO-1 plays role in cell migration in CCA cells regardless of basal HO-1 expression.

### HO-1 conferred cytoprotection to gamma radiation and DNA repair

HO-1 has been shown to exert prosurvival effect in cancer cells against chemotherapeutic agents (Kongpetch et al. 2012). However, the effect against radiation is not certain. Firstly, we determine the sensitivity of CCA cell lines to gamma irradiation by establishing the median effective dose (IC50) of radiation in antiproliferation (Fig. 2A). There was no clear relationship between the basal levels of HO-1 expression and IC50 doses, although the two lowest HO-1 expression cell lines were the most sensitive cell lines to radiation. Next we studied KKU-100 and M214 cells with stable HO-1 knockdown by transduction with lentiviral-mediated HO-1 shRNA. The knockdown clones were selected where the efficiency of HO-1 knockdown in KKU-100 and M214 cells were about 60% and almost 100%, respectively (Fig. 2B). The control cells and HO-1 knockdown cells of KKU-100 and M214 were exposed to 2.5 or 5.0 Gys of gamma radiation, respectively, and subject to clonogenic assay. The non-irradiated, HO-1 knockdown KKU-100 cells showed a decrease in their ability to form colonies when compared with shRNA control cells, but not observed in M214 cells (Fig. 2C & 2D, left bar groups). The role of HO-1 in colony forming became significant when CCA cells were exposed to gamma

irradiation. The irradiated cells with HO-1 knockdown diminished significantly in their ability to form cancer cell colony, compared to the relevant control cells ($p<0.05$), suggesting that inhibiting of HO-1 sensitize CCA cells to gamma radiation (Fig. 2C & 2D, right bar groups).

To further evaluate the role of HO-1 in the maintenance of genomic stability, the level of phosphorylated histone H2AX (γ-H2AX) formation, a surrogate marker for unrepaired DNA double-strand breaks (DSBs) was determined in HO-1 knockdown and control CCA cells subjected to gamma irradiation. More γ- H2AX foci were observed in HO-1 knockdown KKU-100 cells compared to control, even before exposure to radiation (Fig. 2E) suggesting that HO-1 is associated with genome stability. Moreover, the number of γ- H2AX foci was significantly greater in HO-1 knocked down cells with exposure to gamma radiation when compared to the non-target siRNA control cells (Fig. 2F). The result indicated the suppression of HO-1 is associated with suppression of DNA DSBs repair mechanism.

**Inhibition of HO-1 promoted G2-M arrest in CCA cells after irradiation**

HO-1 is known to regulate cell proliferation and migration, and the silencing of HO-1 expression suppresses cell growth (Berberat et al. 2005; Gueron et al. 2009). In this study, knockdown of HO-1 in both KKU-100 and M214 cells resulted in significant accumulation of cells (~10%) at G2-M phase (Fig. 3A and 3B) suggesting its role in cell cycle progression. However, dramatic G2-M arrest was observed in HO-1 knockdown CCA cells exposed to gamma irradiation (Fig. 3B). The proportion of cells in the G2-M phase in HO-1 knockdown KKU-100 cells was increased from 20% before irradiation to 48 % after the irradiation and that in M214 cells increased from 16% to 56% (Fig. 3B). It was noted that the effects on cell cycle progression by radiation were similar in KKU-100 and M214 cells regardless of their significant difference in basal HO-1 expression.

To characterize the influence of HO-1 in cell cycle progression, proteins of cell cycle regulators involved in G2-M transition were examined by Western immunoblotting. The basal expression levels of cyclin A, B1, and its positive regulator, cdc2, were higher in HO-1 knockdown cells of KKU-100 and M214 cells than in their corresponding control cells. These protein expression was even increased higher when the HO-1 knockdown cells were irradiated (Fig. 3C), supporting the functional role of HO-1 in cell cycle progression.

**Suppression of HO-1 enhanced antitumor response to GEM in vitro and in vivo**

The effect of HO-1 inhibition in relation to GEM-induced cytotoxicity was evaluated *in vitro* and *in vivo*. In the *in vitro* study, the toxicity of ZnPP, as a HO-1 inhibitor, and GEM alone was evaluated in KKU-100 cells. The cytotoxicity of ZnPP and GEM was dose-dependent (Fig. 4A). ZnPP at 10 nM induced cytotoxicity of less than 10%, which was then used in combination with GEM. The drug combination enhanced cytotoxicity, particularly at low concentrations of GEM (Fig. 4B).

The enhanced cytotoxic effect of GEM by ZnPP was further evaluated in nude mice xenografted with KKU-100 cells. The mice were treated with ZnPP or GEM or both in combination. Tumor mass in control mice grew exponentially during the study (Fig. 4C). Treatment with GEM or ZnPP alone for 3 cycles resulted in a partial suppression of tumor growth when compared with non-treatment controls. In contrast, the combination of ZnPP and GEM caused almost complete arrest of tumor growth (Fig. 4C). The treatment with individual agent or in combination for 3 cycles did not cause overt toxicity, as indicated by absence of significant changes in body weight (Fig. 4D). The mean tumor weight (mg) on day 17, three days after the last cycle of treatment, was 772, 427, 300 and 110 mg, for control, ZnPP, GEM and the combination group, respectively (Fig. 4E and 4F).

**Combined GEM and ZnPP treatment suppressed tumor growth via activation of p53 pathway**

We further investigated whether suppression of tumor growth was associated with the inhibition of cell proliferation and angiogenesis of tumor tissues. Tumor tissues extracted from 4 groups of animals were analyzed for the expression of Ki-67 and CD31 by immunohistochemistry. The monotherapy of GEM or ZnPP significantly suppressed the nuclear expression of Ki-67 compared to control group (Fig. 5A). The drug combination further decreased the expression of Ki-67 more than the monotherapy. For the CD31 staining, a representative of microvascular density, tumor tissues from control group showed the highest density of the blood vessels, followed by the ZnPP-alone and GEM-alone groups. Tumors from drug combination group showed the lowest density (Fig. 5B). These results indicated that the drug combination enhanced anti-proliferation and anti-angiogenesis in CCA.

Since the suppression of HO-1 activity by ZnPP enhanced GEM-induced antiproliferation and inhibition of neoangiogenesis, the underlying mechanism was explored. The p53 and its negative regulator, mdm2, and p21 protein expression in tumor tissues were evaluated. The immunohistochemistry showed that the drug combination induced p53 at a higher level than that of single drug treatment (Fig. 6A & 6C). On the other hand, mdm2 was highly expressed in control tissues and was decreased in GEM or ZnPP group and most remarkably decreased in drug combination group (Fig. 6B). Expression of p21 or cyclin-dependent kinase inhibitor 1, was highly expressed in the combination treatment group followed by the single drug treatment groups with the lowest in the control (Fig. 6D). The results demonstrated the effect of ZnPP-enhanced GEM-induced tumor suppression was associated with p53 and downstream protein expression.

**Discussion**

HO-1 confers a powerful cytoprotective effect against various insults in normal tissues (Otterbein et al. 2011; Tsuchihashi et al. 2007). Several lines of evidences have demonstrated that HO-1 plays an important role in tumor growth, anti-apoptosis, angiogenesis, metastasis, and DNA repair response following chemotherapeutic or radiotherapy treatment (Jozkowicz et al. 2007). In this study, we showed the crucial role of HO-1 in radiotherapy and chemotherapy in cholangiocarcinoma that, regardless of it basal expression level.

HO-1 plays an important role in cell proliferation, and the hyperplastic and malignant tissues showed pronounced increase in HO-1 expression (Maines and Abrahamsson 1996) which was associated with cell migration and invasion (Gueron et al. 2009). Role of HO-1 in cancer may be mediated via the Nrf2-HO-1 axis, where it is activated in some cancers (Na and Surh 2014). The present works were consistent with these findings in that HO-1 is necessary for CCA cells proliferation and migration. HO-1 knockdown in both high and low HO-1 expressing cells, i.e. KKU-100 or M213 cells showed diminished ability of migration in transwell and wound healing assays.

The role of HO-1 in cell proliferation under genotoxic stress by gamma irradiation is even more important. In non-radiation condition, knockdown of HO-1 in only the high HO-1

expressing KKU-100 cells could impair the clonogenic survival. However, with gamma radiation, both KKU-100 and M214 cells require HO-1 for colony forming ability. This suggests that HO-1 plays an important role in proliferative ability especially at severe stress condition in CCA cells. Our study is consistent with recent studies in that HO-1 inhibition enhanced the X-ray irradiation in reducing clonogenic survival in A549 cells (Zhang et al. 2011).

The role of HO-1 may be extended to DNA repair system in some cancers (Otterbein et al. 2011) and probably including CCA cells. γ-H2AX is a phosphorylated form of the histone H2AX by action of ATM, ATR and other kinases in the chromatin microenvironment marking the accommodation of adaptor proteins for DNA repair process (Celeste et al. 2003). γ-H2AX foci are therefore used as markers of DNA damage and vanishing of the γ-H2AX foci reflects efficiency of the DNA repair of cells (Ivashkevich et al. 2012; Otterbein et al. 2011). In HO-1 knockdown CCA cells, there was an increased level of γH2AX foci and when cells were irradiated, the foci were markedly increased as compared with control cells (Figure 2E & 2F). Our results were consistent with recent studies that several organs from $Hmox1^{-/-}$ mice had increased γH2AX foci (Otterbein et al. 2011). HO-1 may be important in DNA repair, as HO-1 knockdown resulted in increase in γH2AX foci in association with marked cell cycle derangement, suggesting the role of HO-1 in the interplay of DNA repair mechanism and cell cycle progression in CCA cells.

The antiproliferative effect in CCA cells is associated with cell cycle arrest in that HO-1 knockdown caused a cell cycle arrest at G2-M phase. Gamma irradiation further potentiated the cell cycle arrest. It suggests the important role of HO-1 in regulation of cell cycle progression and DNA repair mechanism, as unrepaired chromosome will result in cell cycle arrest or apoptosis (Jackson 2001). Our study is consistent with the role of HO-1 in cell cycle progression and is even more obvious in cells treated with gamma irradiation. Together these results explained the enhanced antiproliferation of irradiation in HO-1 knockdown cells.

The deregulation of cell cycle was found to be related to the expression of cell cycle related proteins in HO-1 knockdown cells. Western immunoblotting revealed a marked increase in cyclin A and B1 and cdc2 protein expression in both cell lines. Cyclin A is synthesized in late G1 and accumulates during S and G2 phase. Expression of cyclin B, a major activator of cdc2 (Vermeulen et al. 2003), is normally maximal during the G2 to M phase transition and controls passage through the M phase. In normal cells, the mitosis phase is initiated by the cdc2/Cyclin

B1 complex, however, in cancer cells, these proteins are deregulated (Evan and Vousden 2001). In contrast to our results, pectenotoxin-2-induced G2-M arrest was associated with the reduced levels of cdc2, cylcin B1 and cdc25C in MDA-MB-231 cells (Moon et al. 2010). It is, therefore, the alteration of these checkpoint proteins could be variable depending on inducing agents (DiPaola 2002).

In previous reports showed that ZnPP, a HO-1 inhibitor, enhanced the sensitivity of CCA cells to chemotherapeutic agents *in vitro* (Kongpetch et al. 2012). In the present study, we demonstrated that the inhibition of HO-1 activity by ZnPP significantly potentiated the chemotherapeutic effect of GEM *in vivo* using CCA xenograft model. This result was consistent with recent studies using xenografted urothelial tumor, LL/2 lung cancer and pancreatic tumor in mice, where treatment with GEM plus ZnPP resulted in inhibition of tumor growth (Miyake et al. 2010; Nuhn et al. 2009). The drug combination probably inhibits cancer proliferation by interrupting the cell cycle and inhibiting neovascularization by suppression the levels of vascular endothelial growth factor in tumors (Hirai et al. 2007). *In vivo* with mice study, ZnPP or GEM alone suppressed tumor growth with decrease in Ki-67; the regulatory protein for cell cycle and CD31 or PECAM-1which represents microvascular density. The combination of HO-1 inhibitor and GEM strongly decreased of Ki-67 and CD31 expression more than monotherapy. This suggests the enhanced tumor suppression may be from inhibition of cell proliferation and neovascularization.

The mechanism of CCA growth suppression by the drug combination is associated markedly with increased levels of p53 and p21expression in tumor tissues where the monotherapy of ZnPP or GEM did not affect these levels. p21 has been reported as a p53-dependent downstream transcriptional control, and a potent cyclin-dependent kinase inhibitor, inhibiting cell cycle progression and growth (Li et al. 2005). It is noted that GEM or ZnPP alone could only slow down tumor growth, as both treatment did not significantly induce p53 and p21 levels. These present results were consistent with our previous *in vitro* studies , which found increased p21 and cytochrome c expression in the drug combination group compared to drug alone (Kongpetch et al. 2012). The p53 can also cause cell death through the Bcl2 proteins which can induce the intrinsic mitochondrial apoptotic pathway (Galluzzi et al. 2009). Our previous studies showed that the drug combination could induce a massive formation of reactive

oxygen species which was associated with mitochondrial dysfunction triggering cell death in CCA cells (Kongpetch et al. 2012).

It should be noted that animals in ZnPP group or combination group did not show any overt signs of toxicity, because body weight loss, generally a sensitive index of toxicity, was unchanged in all animals. Therefore, it probably allow further optimization of the dosage regimen to maximize the antitumor activity. The strong sensitizing effect of HO-1 inhibition to chemotherapeutic agents may be of relevance in clinical setting where drug resistance is the main cause of failure in cancer chemotherapy.

In summary, inhibition of HO-1 resulted in antiproliferation, and suppression of cytoprotection when it is in combination with anticancer agent (eg. gemcitabine) or gamma radiation in CCA cells. The antiproliferation of HO-1 knockdown is associated with cell cycle arrest. The animal experiment showed the potential tumor suppression effect by using combination of ZnPP plus GEM. This study may provide a novel treatment strategy for CCA by combining HO-1 inhibitor with chemotherapy and radiotherapy.

**Competing interests**

We declare that we have no conflicts of interest.

**Author's contributions**

VK, BTT, CKO, UK designed the study, SK, WCO, EYS performed experiments, SK, CKO, VK, AP, LS analyzed the data and interpreted the results, SK, CKO, VK wrote the manuscript, BTT provided research facilities and critical review. All authors read and approved the final manuscript.

**Acknowledgements**

This study was supported by National Medical Research Council of Singapore, Thailand Research Fund, the National Research University Project and Office of the Higher Education Commission through SHeP-GMS of Khon Kaen University, and the Royal Golden Jubilee Ph.D. Programme (to S.K.).

**References**


Berberat PO et al. (2005) Inhibition of heme oxygenase-1 increases responsiveness of pancreatic cancer cells to anticancer treatment. Clin Cancer Res 11:3790-3798

Buranrat B, Prawan A, Kukongviriyapan U, Kongpetch S, Kukongviriyapan V (2010) Dicoumarol enhances gemcitabine-induced cytotoxicity in high NQO1-expressing cholangiocarcinoma cells. World J Gastroenterol 16:2362-2370

Buranrat B, Prawan A, Sripa B, Kukongviriyapan V (2007) Inflammatory cytokines suppress arylamine N-acetyltransferase 1 in cholangiocarcinoma cells. World J Gastroenterol 16:6219-6225

Butthongkomvong K, Sirachainan E, Jhankumpha S, Kumdang S, Sukhontharot OU (2013) Treatment outcome of palliative chemotherapy in inoperable cholangiocarcinoma in Thailand. Asian Pac J Cancer Prev 14:3565-3568

Celeste A et al. (2003) Histone H2AX phosphorylation is dispensable for the initial recognition of DNA breaks. Nat Cell Biol 5:675-679

Chan-On W et al. (2009) Cholangiocarcinomas associated with long-term inflammation express the activation-induced cytidine deaminase and germinal center-associated nuclear protein involved in immunoglobulin V-region diversification. Int J Oncol 35:287-295

DiPaola RS (2002) To arrest or not to G(2)-M Cell-cycle arrest : commentary re: A. K. Tyagi et al., Silibinin strongly synergizes human prostate carcinoma DU145 cells to doxorubicin-induced growth inhibition, G(2)-M arrest, and apoptosis. Clin Cancer Res 8:3311-3314

Evan GI, Vousden KH (2001) Proliferation, cell cycle and apoptosis in cancer. Nature 411:342-348

Farges O et al. (2011) Influence of surgical margins on outcome in patients with intrahepatic cholangiocarcinoma: a multicenter study by the AFC-IHCC-2009 study group. Ann Surg 254:824-829; discussion 830

Galluzzi L, Blomgren K, Kroemer G (2009) Mitochondrial membrane permeabilization in neuronal injury. Nat Rev Neurosci 10:481-494

Gueron G et al. (2009) Critical role of endogenous heme oxygenase 1 as a tuner of the invasive potential of prostate cancer cells. Mol Cancer Res 7:1745-1755

Hirai K, Sasahira T, Ohmori H, Fujii K, Kuniyasu H (2007) Inhibition of heme oxygenase-1 by zinc protoporphyrin IX reduces tumor growth of LL/2 lung cancer in C57BL mice. Int J Cancer 120:500-505

Ivashkevich A, Redon CE, Nakamura AJ, Martin RF, Martin OA (2012) Use of the gamma-H2AX assay to monitor DNA damage and repair in translational cancer research. Cancer Lett 327:123-133

Jackson SP (2001) Detecting, signalling and repairing DNA double-strand breaks. Biochem Soc Trans 29:655-661

Jozkowicz A, Was H, Dulak J (2007) Heme oxygenase-1 in tumors: is it a false friend? Antioxid Redox Signal 9:2099-2117

Khan SA et al. (2012) Guidelines for the diagnosis and treatment of cholangiocarcinoma: an update. Gut 61:1657-1669

Khan SA, Thomas HC, Davidson BR, Taylor-Robinson SD (2005) Cholangiocarcinoma. Lancet 366:1303-1314

Kongpetch S, Kukongviriyapan V, Prawan A, Senggunprai L, Kukongviriyapan U, Buranrat B (2012) Crucial Role of Heme Oxygenase-1 on the Sensitivity of Cholangiocarcinoma Cells to Chemotherapeutic Agents. PLoS ONE 7:e34994

Li CH, Tzeng SL, Cheng YW, Kang JJ (2005) Chloramphenicol-induced mitochondrial stress increases p21 expression and prevents cell apoptosis through a p21-dependent pathway. J Biol Chem 280:26193-26199

Maines MD, Abrahamsson PA (1996) Expression of heme oxygenase-1 (HSP32) in human prostate: normal, hyperplastic, and tumor tissue distribution. Urology 47:727-733

Miyake M et al. (2010) Inhibition of heme oxygenase-1 enhances the cytotoxic effect of gemcitabine in urothelial cancer cells. Anticancer Res 30:2145-2152

Moon DO, Kim MO, Nam TJ, Kim SK, Choi YH, Kim GY (2010) Pectenotoxin-2 induces G2/M phase cell cycle arrest in human breast cancer cells via ATM and Chk1/2-mediated phosphorylation of cdc25C. Oncol Rep 24:271-276

Na HK, Surh YJ (2014) Oncogenic potential of Nrf2 and its principal target protein heme oxygenase-1. Free Radic Biol Med 67:353-365

Nuhn P et al. (2009) Heme oxygenase-1 and its metabolites affect pancreatic tumor growth in vivo. Mol Cancer 8:37

Otterbein LE, Hedblom A, Harris C, Csizmadia E, Gallo D, Wegiel B (2011) Heme oxygenase-1 and carbon monoxide modulate DNA repair through ataxia-telangiectasia mutated (ATM) protein. Proc Natl Acad Sci U S A 108:14491-14496

Patel T (2011) Cholangiocarcinoma--controversies and challenges. Nat Rev Gastroenterol Hepatol 8:189-200

Prawan A, Kundu JK, Surh YJ (2005) Molecular basis of heme oxygenase-1 induction: implications for chemoprevention and chemoprotection. Antioxid Redox Signal 7:1688-1703

Sirica AE (2005) Cholangiocarcinoma: molecular targeting strategies for chemoprevention and therapy. Hepatology 41:5-15

Skipworth JR, Olde Damink SW, Imber C, Bridgewater J, Pereira SP, Malago M (2011) Review article: surgical, neo-adjuvant and adjuvant management strategies in biliary tract cancer. Aliment Pharmacol Ther 34:1063-1078

Tsuchihashi S, Zhai Y, Bo Q, Busuttil RW, Kupiec-Weglinski JW (2007) Heme oxygenase-1 mediated cytoprotection against liver ischemia and reperfusion injury: inhibition of type-1 interferon signaling. Transplantation 83:1628-1634

Tusskorn O, Prawan A, Senggunprai L, Kukongviriyapan U, Kukongviriyapan V (2013) Phenethyl isothiocyanate induces apoptosis of cholangiocarcinoma cells through

interruption of glutathione and mitochondrial pathway. Naunyn Schmiedebergs Arch Pharmacol 386:1009-1016

Vanella L et al. (2013) Apoptotic markers in a prostate cancer cell line: effect of ellagic acid. Oncol Rep 30:2804-2810

Vermeulen K, Van Bockstaele DR, Berneman ZN (2003) The cell cycle: a review of regulation, deregulation and therapeutic targets in cancer. Cell Prolif 36:131-149

Yonglitthipagon P et al. (2012) Prognostic significance of peroxiredoxin 1 and ezrin-radixin-moesin-binding phosphoprotein 50 in cholangiocarcinoma. Hum Pathol 43:1719-1730

Zeekpudsa P, Kukongviriyapan V, Senggunprai L, Sripa B, Prawan A (2014) Suppression of NAD(P)H-quinone oxidoreductase 1 enhanced the susceptibility of cholangiocarcinoma cells to chemotherapeutic agents. J Exp Clin Cancer Res 33:11

Zhang W, Qiao T, Zha L (2011) Inhibition of heme oxygenase-1 enhances the radiosensitivity in human nonsmall cell lung cancer a549 cells. Cancer Biother Radiopharm 26:639-645

**Figure legends**

**Fig. 1** Expression of HO-1 in CCA cells and effect of HO-1 knockdown on cell migration. **(a)** The basal HO-1 mRNA expression in CCA cells. Total RNA of CCA cells: KKU-100, M213, M214, M055 and M139, were collected and analyzed by real-time PCR. Each bar represents the relative expression of HO-1 normalized with β-actin. **(b)** KKU-100 and M213 were knocked down of HO-1 expression by HO-1 siRNA (si HO-1) or control transfection (si Cont). The efficiency was validated by using real-time PCR**. (c & d)** Cell migration of KKU-100 and M213 cells was performed using a transwell inserts. Representatives of DAPI-staining images of migrated cells, were captured under fluorescence microscope (original magnification 200X). **(d)** The number of colonies of KKU-100 and M213 cells was counted for four fields from each insert (original magnification 100X). Each bar represents the mean±SD of 12 fields from at least three independent experiments. * $p<0.05$ vs controls). **(e)** Wound-healing assay in KKU-100 and M213 cells. Cells were grown into confluence in 24-well plate. Images of four fields from each well were captured (original magnification 100X) and distance of the closing wound was measured.

**Figure 2** HO-1 knockdown enhanced the DNA damage of gamma radiation and formation of γ-H2AX foci. **(a)** The sensitivity (IC50) of five CCA cell lines to gamma irradiation. The IC50 values represent mean±SD. **(b)** KKU-100 and M214 were stably knocked down HO-1 expression by transduction with HO-1 shRNA (sh HO-1) or control vector (sh Cont). The efficiency was validated by using Western blot analysis**. (c & d)** The clonogenic assay of CCA cells with or without irradiation. KKU-100 and M214 cells were irradiated by gamma radiation at the doses of 2.5 Gy and 5 Gy, respectively. Each bar represents the mean±SD, each from three separated experiments. * $p<0.05$ vs controls. **(e)** The representative fluorescent images of γ-H2AX foci (original magnification 600X). KKU-100 cells were transfected with HO-1 siRNA for 24 hr, then the cells were irradiated with gamma ray at 5 Gy. Left panel shows the DAPI staining to the nucleus, the right panel shows the γ- H2AX foci (red), and the merged images in the middle. Presented images are representatives of two independent experiments conducted in duplicate chambers. **(f)** Each bar represents the mean±SD of γ- H2AX foci per cell, each from two separated experiments. *$p<0.05$ vs control knockdown.

**Figure 3** Effect of HO-1 knockdown and irradiation on cell cycle distribution and regulatory proteins in cell cycle. **(a)** The cell cycle histograms represent DNA content using FACS

analysis. KKU-100 and M214 cells were transfected with HO-1 siRNA (si HO-1) or control (si Cont) with or without gamma irradiation at 5 and 8 Gy, respectively. Cells were collected and stained with propidium iodide for flow analysis. **(b)** The tables present the percentage of cells in cell cycle. Each value represents the mean±SD, each from three separated experiments. *$p$<0.05 HO-1 knockdown vs control knockdown, **$p$<0.05 irradiated HO-1 knockdown vs nonirradiated HO-1 knockdown. (**c**) Immunoblots of regulatory proteins in cell cycle. Following the irradiation on wild type or HO-1 knockdown KKU-100 and M214 cells, cell lysates were prepared and analyzed by Western immunobloting for cdc2, cyclin A, cyclin B1 and β-actin as a loading control. The experiment was done twice with similar results, and representative bands from one experiment are shown.

**Figure 4** Inhibition of HO-1 by ZnPP enhances the antitumor effect of GEM *in vitro* and *in vivo*. (**a**) The dose-response cytotoxicity of ZnPP and GEM in KKU-100 cells after incubation for 24 h. **(b)** Enhanced cytotoxicity of GEM by ZnPP. KKU-100 cells with or without pretreatment with ZnPP for 4 h were exposure to GEM for another 24 h. Each bar represents the mean±SD from each three independent experiment. * $p$<0.05 vs GEM alone. (**c**) Time-course of tumor growth on nude mice transplanted with KKU-100 cells. ZnPP, GEM, combination of ZnPP and GEM and saline as vehicle control were administered intraperitoneally on days 0, 7 and 14, when the tumor mass grew to have at least 200 $mm^3$. Each value represents the mean±SEM, each from 7 mice per group. * $p$<0.05 the combination group vs control group; † $p$<0.05 the combination vs ZnPP alone, and ‡ $p$<0.05 the combination vs GEM alone. **(d)** Time-course of body weights of mice during the drug treatments. **(e)** The representative of tumors resected from mice on day 17. **(f)** The tumor weights from each group of treatment on day 17. Each bar represents the mean±SEM each from 7 mice in the group. * $p$<0.05 drug combination vs GEM alone, and ** $p$<0.05 drug combination vs ZnPP alone.

**Figure 5** Immunohistochemistry of Ki-67 and CD31 staining in tumor tissues. **(a)** The tumor tissues from mice treated with various drug regimens were analyzed by H&E staining and immunohistochemical staining for Ki-67 and CD31. Panels a-c: control; d-f: ZnPP alone, g-i: GEM alone; j-l: combination of GEM and ZnPP. Panels a, d, g, j; H&E staining; b, e, h, k for Ki-67 staining; c, f, i,l for CD31 staining (the arrows indicate microvessels). **(b)** Microvascular density as assessed by CD31 staining (original magnification 200X). Each bar represents the

mean±SD, each from 7 mice * $p<0.05$ drug combination vs GEM alone, and ** $p<0.05$ drug combination vs ZnPP alone.

**Figure 6** Immunohistochemistry of mdm2, p53 and p21 staining in tumor tissues. **(a)** The tumor tissues from mice treatment with various drug regimens were analyzed by immunohistochemical staining for mdm2, p53 and p21. Panels a-c: control; d-f: ZnPP alone, g-i: GEM alone; j-l: combination of GEM and ZnPP. Panels a, d, g and j for mdm2 staining; b, e, h and k for p53 staining; c, f, i, and l for p21staining. (original magnification 400X). **(b)** The numbers of mdm2 positive-nuclear staining, **(c)** levels of p53 staining, assessed from the intensity and area of staining and **(d)** the numbers of p21 positive-nuclear staining were shown. Each bar represents the mean±SD, each from 7 mice * $p<0.05$ drug combination vs GEM alone, and ** $p<0.05$ drug combination vs ZnPP alone.

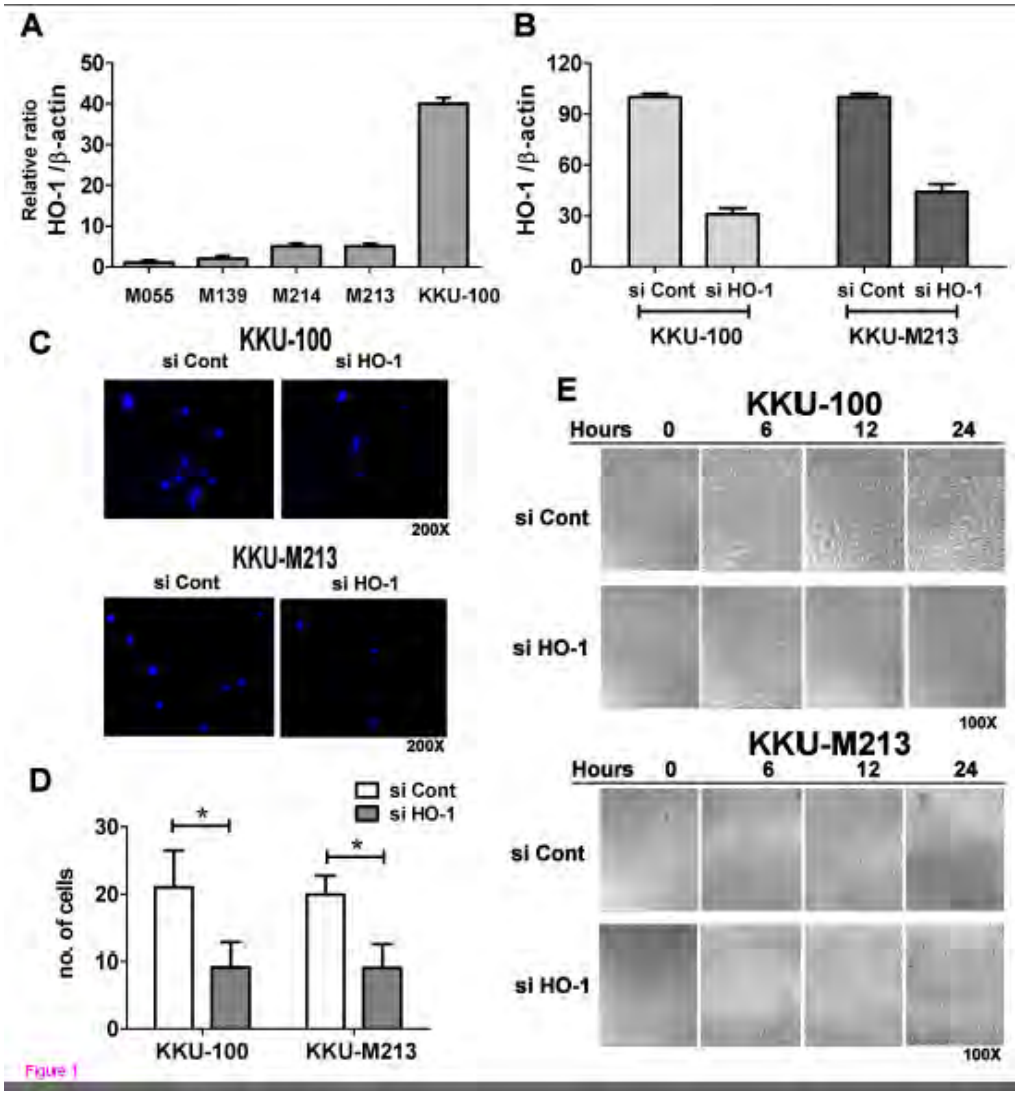
A
Relative ratio HO-1 /β-actin
50
40
30
20
10
0
M055
M139
M214
M213
KKU-100
B
HO-1 /β-actin
120
90
60
30
0
si Cont
si HO-1
si Cont
si HO-1
KKU-100
KKU-M213
C
KKU-100
si Cont
si HO-1
200X
KKU-M213
si Cont
si HO-1
200X
D
si Cont
si HO-1
no. of cells
30
20
10
0
*
*
KKU-100
KKU-M213
E
KKU-100
Hours 0 6 12 24
si Cont
si HO-1
100X
KKU-M213
Hours 0 6 12 24
si Cont
si HO-1
100X
Figure 1

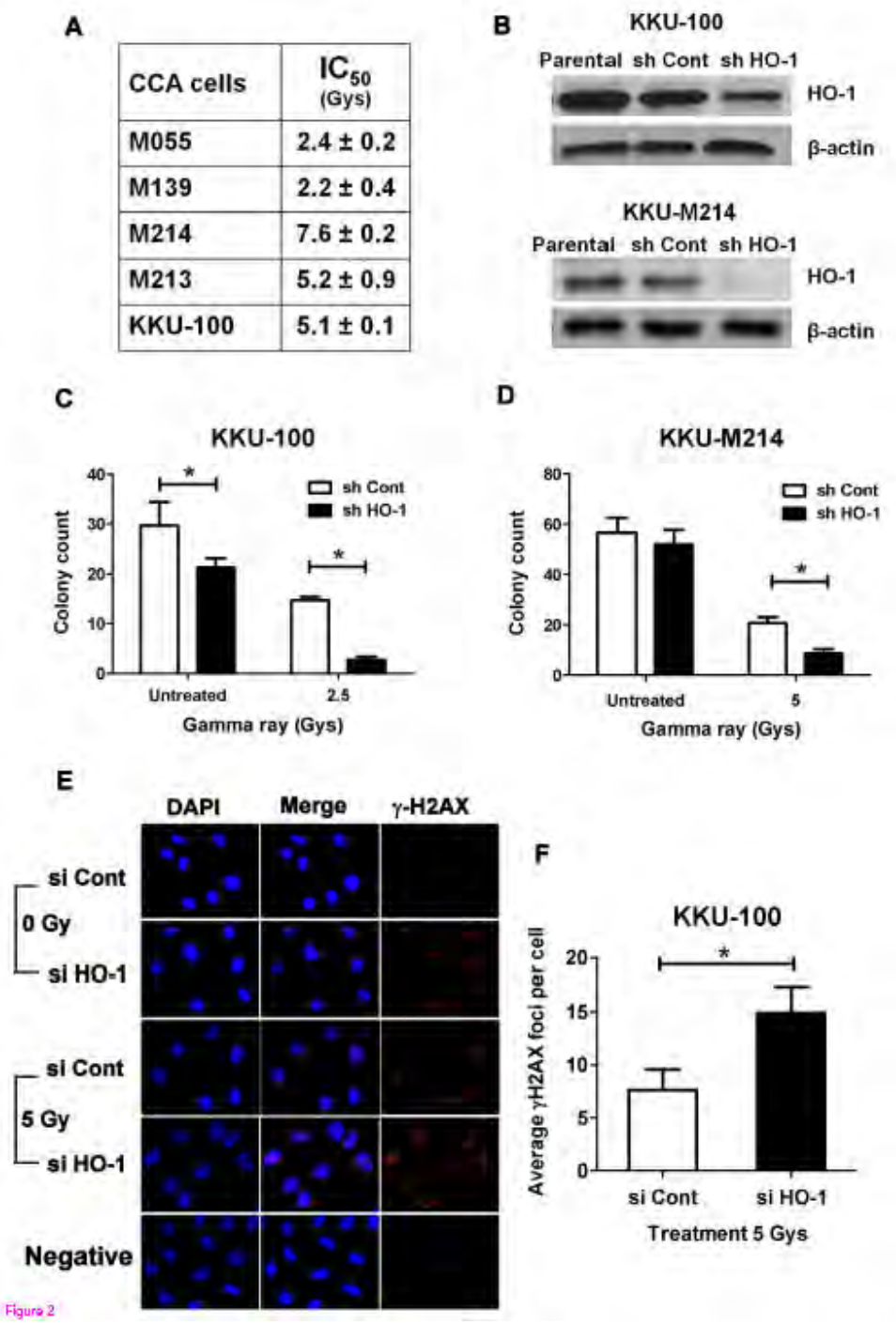
A
CCA cells
IC50 (Gys)
M055
2.4 ± 0.2
M139
2.2 ± 0.4
M214
7.6 ± 0.2
M213
5.2 ± 0.9
KKU-100
5.1 ± 0.1
B
KKU-100
Parental sh Cont sh HO-1
HO-1
β-actin
KKU-M214
Parental sh Cont sh HO-1
HO-1
β-actin
C
KKU-100
Colony count
sh Cont
sh HO-1
Untreated
2.5
Gamma ray (Gys)
D
KKU-M214
Colony count
sh Cont
sh HO-1
Untreated
5
Gamma ray (Gys)
E
DAPI
Merge
γ-H2AX
si Cont
0 Gy
si HO-1
si Cont
5 Gy
si HO-1
Negative
F
KKU-100
Average γH2AX foci per cell
si Cont
si HO-1
Treatment 5 Gys

Figure 2

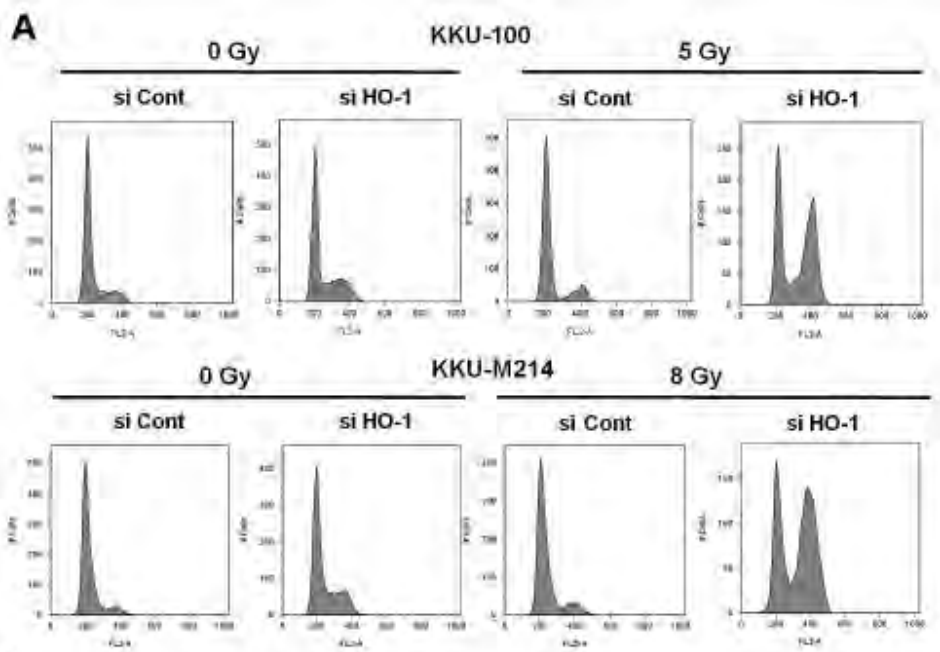


B

| KKU-100 | | Cell Proportion (Mean±SD) | | |
|---|---|---|---|---|
| | | G0-G1 | S | G2-M |
| 0 Gy | si Cont | 83 ± 1.9 | 7 ± 0.3 | 10 ± 1.7 |
| | si HO-1 | 69 ± 1.6 | 11 ± 0.5 | 20 ± 1.5* |
| 5 Gy | si Cont | 83 ± 1.4 | 5 ± 1.0 | 12 ± 0.4 |
| | si HO-1 | 44 ± 1.0 | 8 ± 0.2 | 48 ± 0.9** |

| KKU-M214 | | Cell Proportion (Mean±SD) | | |
|---|---|---|---|---|
| | | G0-G1 | S | G2-M |
| 0 Gy | si Cont | 89 ± 1.2 | 4 ± 0.2 | 7 ± 1.1 |
| | si HO-1 | 73 ± 1.6 | 11 ± 0.4 | 16 ± 2.0* |
| 8 Gy | si Cont | 84 ± 1.1 | 5 ± 0.5 | 11 ± 0.6 |
| | si HO-1 | 36 ± 1.0 | 8 ± 0.8 | 56 ± 2.1** |

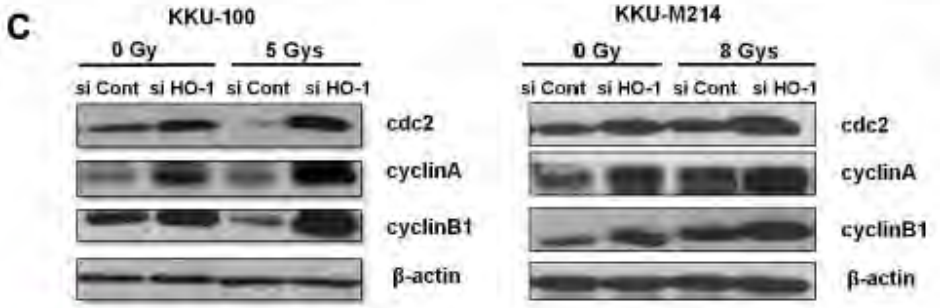


Figure 3

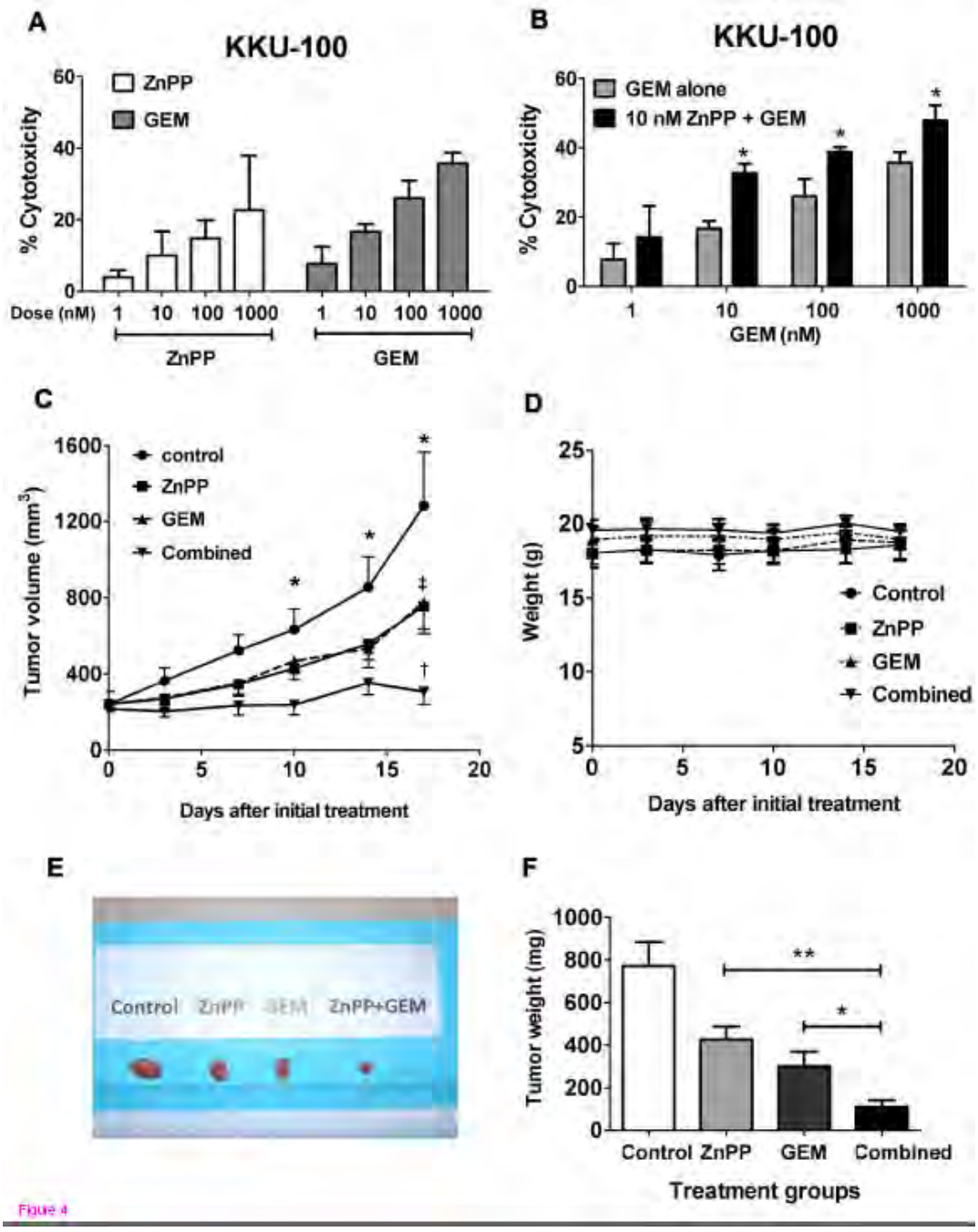
A
KKU-100
ZnPP
GEM
% Cytotoxicity
Dose (nM)
1 10 100 1000 1 10 100 1000
ZnPP
GEM
B
KKU-100
GEM alone
10 nM ZnPP + GEM
% Cytotoxicity
GEM (nM)
C
control
ZnPP
GEM
Combined
Tumor volume (mm3)
Days after initial treatment
D
Control
ZnPP
GEM
Combined
Weight (g)
Days after initial treatment
E
Control
ZnPP
GEM
ZnPP+GEM
F
Tumor weight (mg)
Control ZnPP GEM Combined
Treatment groups

Figure 4

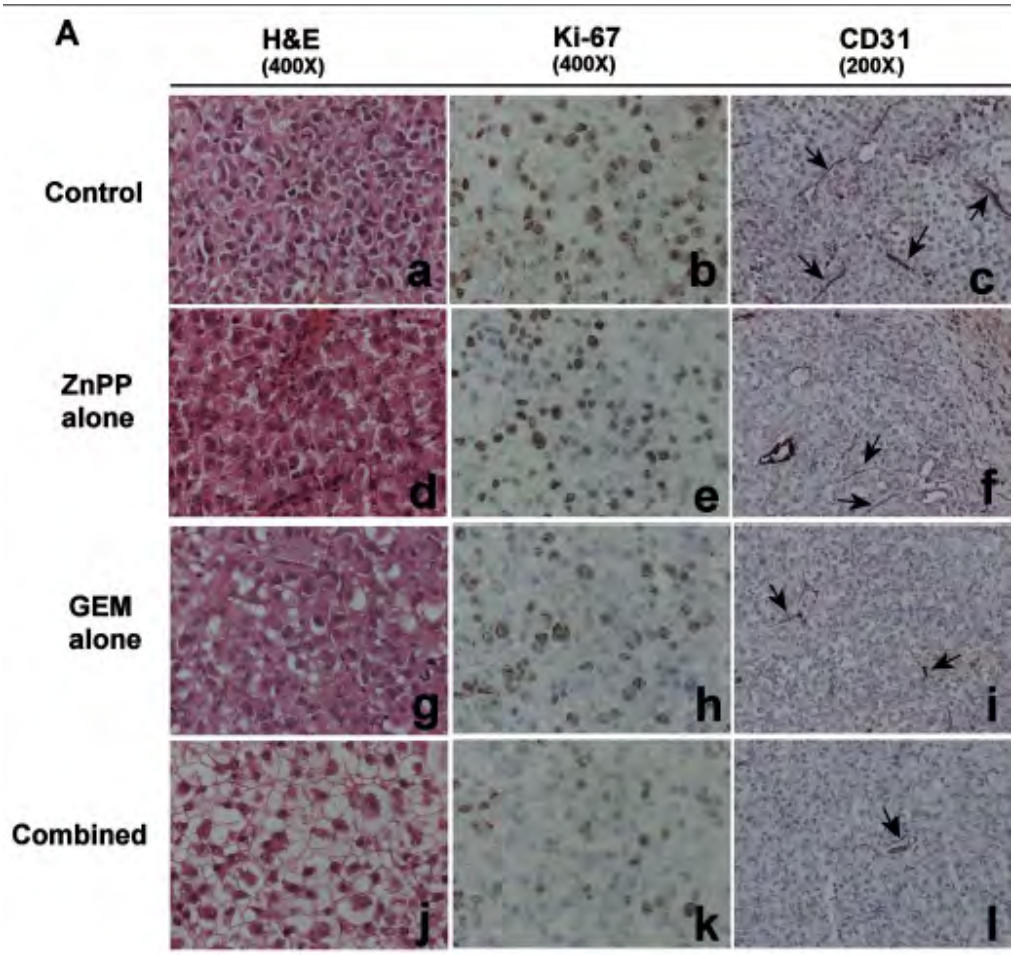
A
H&E
(400X)
Ki-67
(400X)
CD31
(200X)
Control
ZnPP
alone
GEM
alone
Combined
a
b
c
d
e
f
g
h
i
j
k
l
B
Microvascular density
(No. of CD31-stained vessel)
15
10
5
0
**
*
Control
ZnPP
GEM
Combined

Figure 5

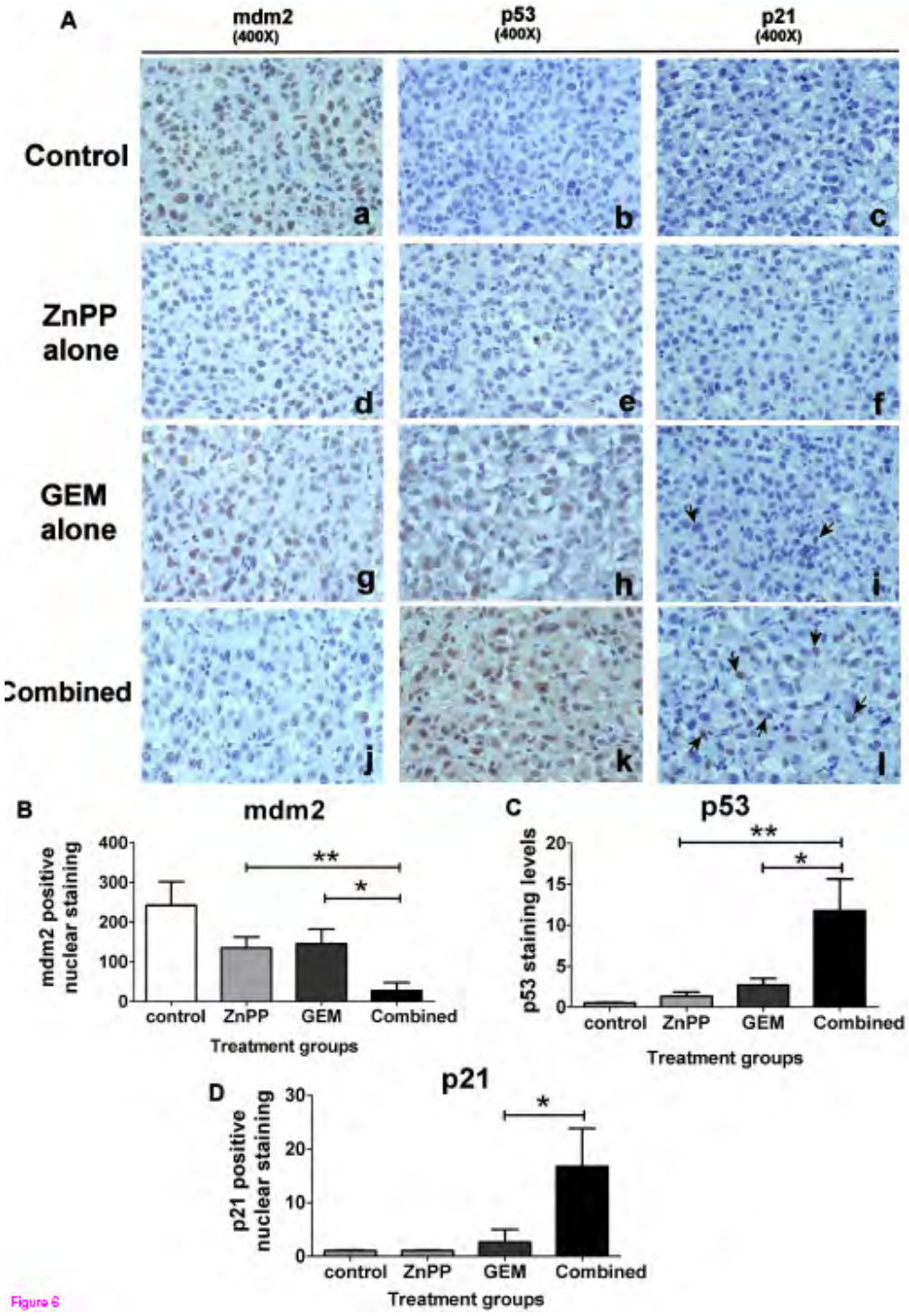
A
mdm2
(400X)
p53
(400X)
p21
(400X)
Control
ZnPP
alone
GEM
alone
Combined
a
b
c
d
e
f
g
h
i
j
k
l
B
mdm2
mdm2 positive
nuclear staining
400
300
200
100
0
**
*
control
ZnPP
GEM
Combined
Treatment groups
C
p53
p53 staining levels
20
15
10
5
0
**
*
control
ZnPP
GEM
Combined
Treatment groups
D
p21
p21 positive
nuclear staining
30
20
10
0
*
control
ZnPP
GEM
Combined
Treatment groups

Figure 6